University of Southampton Research Repository

THE COMPOSITE BEHAVIOUR OF WALLS

INTERACTING WITH FLEXURAL MEMBERS

A Thesis

presented for the Degree of

Doctor of Philosophy

of the

University of Southampton

in the ˉ

Faculty of Engineering and Applied

Science

by

JOHN ROBIN RIDDINGTON

AUGUST 1974

ABSTRACT

FACULTY OF ENGINEERING AND APPLIED SCIENCE

DEPARTMENT OF CIVIL ENGINEERING

Doctor of Philosophy

THE COMPOSITE BEHAVIOUR OF WALLS INTERACTING WITH FLEXURAL MEMBERS

by John Robin Riddington

A study is made of the composite interactive behaviour of wall on beam and infilled frame type structures.

Simple design methods are developed for both types of structure and it is anticipated that these will be included in a new revised version of BS449, the British Standard for structural steelwork design.

Finite element computer programs are developed for the analysis of both types of structure. These programs allow for the automatic generation of separation cracks on the interfaces between the walls and the beams or columns. A listing of these programs is included in the thesis. Using these programs, analytical investigations are made into the composite elastic behaviour of the structures. From the results of the analyses of basic wall on beam structures, formulae are produced for the main design parameters. The results from the analyses of infilled frames are shown to confirm the accuracy of the simple design method for laterally loaded infilled frames. Suggestions are given for including vertical loading in the design method.

Two sets of wall on beam model tests are described. The first set consisted of plaster walls with steel beams. The results from these tests were used in the development of the design method for walls on beams. The second set consisted of an araldite wall with steel beams.

The results from these tests were used to check the accuracy of the finite element computer analyses.

The apparatus design and initial testing for a series of tests to determine diagonal compressive strength of masonry under infill type loading is also described.

Acknowledgements

The author wishes to express his gratitude to the following:

Professor B. Stafford Smith for his encouragement and guidance throughout the period of research;

Dr. P. Lau for his help in the early periods of computer programming;

Mr. D. Owen for his help with the test work;

Dr. H. Barker and Redland Research and Development Ltd. for undertaking the diagonal compression tests;

Mr. G. Weeks and the Building Research Establishment for permission to observe and report the results of their wall on beam tests;

Dr. M.A.H. Khan and Dr. R. Adey for their helpful discussions;

Dr. T. Graves Smith for his administrative help;

The Science Research Council for providing financial support;

Mrs. A. Lampard for neatly typing the thesis.

NOTATION

L	Clear span of beam
h	Height of wall or infill
ℓ	Length of infill
t	Thickness of wall or infill
d	Diagonal length of infill
α	Length of contact
S	Length of beam inbuilding
Z'	Depth of wall below beam
Q	Length of wall past end of span
w	Effective width of infill
θ	Slope of infill diagonal to horizontal
B_B	Breadth of steel section
D_B	Depth of steel section
I	Second moment of area of beam or frame member
Z	Section modulus of beam
Z_s	Section modulus of beam required for self weight
δ	Central beam deflection
δ_s	Specified maximum design deflection
E	Modulus of elasticity of beam or frame member
E_w	Modulus of elasticity of wall
E_I	Modulus of elasticity of infill
ν	Poisson's ratio
μ	Coefficient of friction
W, W_w	Vertical wall load
W_s	Beam self weight plus floor loading

W_{wf} Wall crushing load

H Horizontal load on infilled frame

R Diagonal load on infill

T Tie force in beam

H' Horizontal shear force per unit length

M Moment in beam

M_o Uniformly distributed moment ($WL/8$)

f_b Peak wall compressive stress

f_{bs} Bond shear strength

f_{bu} Compressive strength of plaster

f'_{cd} Diagonal compressive strength of infill material

f'_{dt} Diagonal tensile strength of infill material

f_k Characteristic vertical strength of the infill material

f_s Ultimate shear strength

p_b Permissible compressive stress in wall material

p_{cb} Permissible compressive stress in concrete encasement material

p_{st} Permissible stress in steel beam

τ Peak shear stress on wall-beam interface

τ_{xy} Horizontal shear stress

σ_{dt} Diagonal tensile stress

σ_y Vertical stress

γ_f Partial safety factor for load

γ_m Partial safety factor for the compressive strength of brickwork or blockwork

γ_{mv} Partial safety factor for the shear strength of brickwork

K, K' Relative stiffness parameters ($\sqrt[4]{\dfrac{E_w t L^3}{EI}}$)

λ Relative stiffness parameter ($\sqrt[4]{\dfrac{E_I t}{4EIh}}$)

C Beam self weight parameter ($1 - Z_s/Z$)

B Beam length of contact constant ($K\alpha/L$)

P Percentage difference

x x-direction coordinate

y y-direction coordinate

u x-direction displacement

v y-direction displacement

k_1 Beam tie force parameter (W_w/T)

k_2 Beam sagging moment parameter ($W_w L/M$)

k_3 Beam hogging moment parameter ($W_w L/M$)

$A_1, A_2, \ldots, A_8$ Displacement variables

CONTENTS

CHAPTER   1

GENERAL INTRODUCTION

When wall and frame members are in contact with each other in a
building structure and are subjected to loading, the members tend to
act compositely. The design of these structures has usually either
been based on intuitive of empirical methods, or the effects of the
walls on the behaviour has been ignored completely. For example,
although frames are often infilled with partition walls, it has been
the practice in this country to design the frames for lateral loading
by totally ignoring the stiffening effects of the infill. This has
usually resulted in inefficient designs, with the frames being designed
for the wrong mode of behaviour. Because the infill walls are con-
siderably stiffer in plane than the surrounding frames, the infills
unintentionally pick up a major portion of the horizontal loading with
a consequence that on frequent occasions, unsightly cracks have devel-
oped in the walls. Another example of inefficient design in structures
is that of a wall on a beam. Although this form of structure is fre-
quently found in buildings, the design of these structures has generally
been based on intuitive or empirical design methods. One such intuitive
method, in common use in the past, is that in which the beam is designed
to carry only the wieght of wall above contained within a 60° triangle.

In this thesis, the study of composite behaviour between flexural
members and walls is restricted to walls on beams and infilled frames.
Simple design methods are developed for both of these structures which
take into account composite action. It is anticipated that these

design methods will be included in a new revised version of BS449, the British Standard on structural steelwork design. Finite element programs are developed for the analysis of these structures and are used in an analytical study of their composite elastic behaviour. In addition to the analytical study, model testing was undertaken on wall on beam structures and diagonal compression tests were initiated to determine masonry compressive strength under infill type loading.

CHAPTER 2

WALLS ON BEAMS: INTRODUCTION AND REVIEW

OF PREVIOUS WORK

2.1 Introduction

When a vertically loaded wall is supported by a beam, the wall and beam tend to combine together structurally to form one composite unit. This unit can be considered as a tied arch system with the wall arching between the beam supports and the beam acting as the tie as shown in Fig. 2.1. The vertical loading of the wall on the beam tends to push the beam away from the wall in the mid-span region. In cases of heavy loading, horizontal cracking, or even visible separation of the beam away from the wall can result from this interaction effect. The arching behaviour produces concentrations of vertical and horizontal shear stress in the wall close to the beam supports. The shift towards the supports of the vertical loading on the beam, combined with the hogging effect of the outward thrust of the wall arch, produces a much lower bending moment in the beam, than if the same load were distributed uniformly over the beam span. The horizontal reaction of the arch is resisted by the tying action of the beam, which is therefore subjected to additional axial tensile stresses.

Although walls on beams are very common in structures in this country, the design methods used have usually been intuitive or empirical. A relatively simple design method is developed in this thesis for the design of walls on steel beams. This design method has been developed in association with the British Standards Committee B/20/5 and the method will probably be included in a new revised
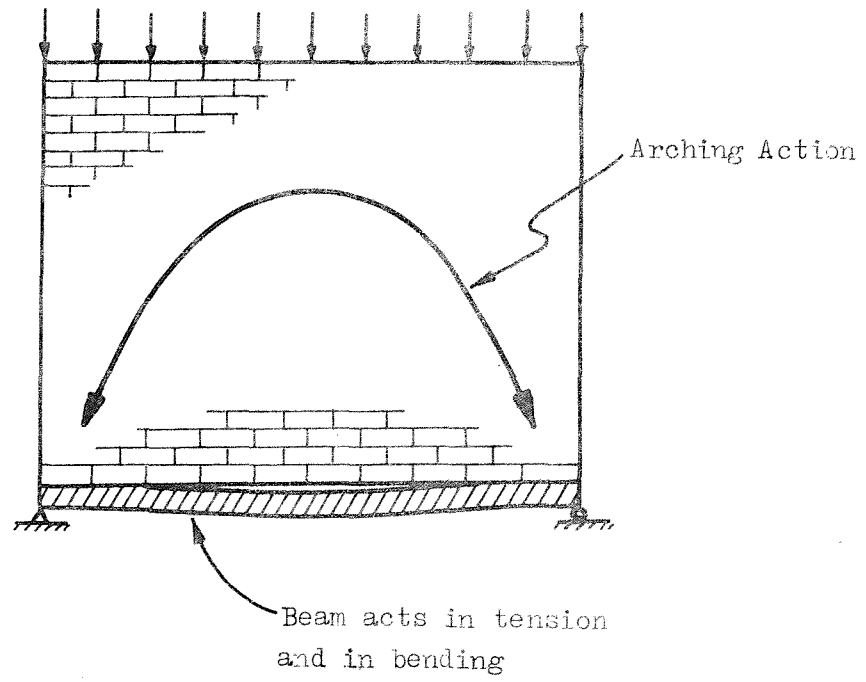
FIG. 2.1   COMPOSITE ACTION OF A WALL ON A BEAM

British Standard on structural steelwork design.

In addition to the development of the design method, a theoretical and experimental investigation was undertaken into the elastic behaviour of walls on beams. For the theoretical investigation, a finite element program was developed which allowed for crack generation on the wall-beam interface.

2.2 Review of previous work

Dischinger[1], in 1932, and Durant and Garwood[2], in 1947, used Fourier series with the theory of bending in deep beams, to analyse wall on beam problems. These approximate analyses indicated that when the wall height exceeded two thirds of the span, the beam moment arm at the centre of span was virtually independent of the wall height.

Wood[3], in 1952, presented the results from tests of brick walls, with and without openings, on simply supported reinforced concrete beams. He also included in this paper, the results from the analysis of simply supported walls, obtained using the relaxation technique. From this work, Wood suggested two methods of design for brick walls in reinforced concrete beams. The first method consisted of calculating the beam reinforcement using an equivalent beam bending moment of WL/100 when door and window openings were absent or occurred at mid-span, and WL/50 when openings occurred near the supports. The second method was intended for use with walls without openings and consisted of calculating the beam reinforcement from the beam tie force which was calculated using an internal moment arm equal to $\frac{2}{3}$ x wall height, but not greater than 0.7 x beam span. Restrictions were imposed for both methods that the wall height should exceed 0.6 x span and that the beam span to depth ratio should be between 15 and 20.

Rosenhaupt[4-6] presented in his Doctor of Science thesis and two papers published in 1962 and 1964, a finite difference solution for the wall on beam problem based on the Airy stress function, as well as the results of a series of full scale tests of masonry walls on reinforced concrete beams. In the analysis, he made the assumption that the bending rigidity of the beam is small enough to be neglected. This has the effect of eliminating the normal stress between the wall

and the beam. The entire load is therefore carried at the bottom corners of the wall, and the exact solution of the problem must contain singularities at these points. Since the finite difference method is used to calculate the vertical wall stress immediately over the support points, the result is inversely proportional to the mesh size. This analysis cannot, therefore, provide any useful information regarding the wall stress concentration and the beam moments.

Coull[7], in 1966, presented an approximate solution for the wall on beam problem, based on minimising the strain energy of the system using the Kantorovich method. In the analysis, the wall stresses are expressed as a power series in the horizontal direction, the coefficients of the series being functions of height only. Coull solved the problem by taking only the first two terms of the power series and in Section 4.3, this is shown to have led to considerable errors in the wall-beam interface region. Using the method, Coull undertook a parameter study on the basic wall on beam problem.

Colbourne[8], in 1969, presented a solution for the wall on beam problem, based on representing the structure by a lattice analogy, and solving the differential equations for the system by the finite difference method. The Poisson's ratio for the structure was taken as zero.

Burhouse[9], in 1969, published the results from a series of ten full scale tests carried out at the Building Research Station. The tests consisted of single leaf brick walls resting on simply supported beams. Both encased steel and reinforced concrete beams were used in the tests. One of the parameters varied in the tests was the wall height to width ratio, and as a result, Burhouse concluded that to prevent the possibility of slipping between the wall and beam, the

wall height to width ratio should exceed 0.6 as was suggested by Wood[3].
In order to obtain analytical values to compare with his experimental
results, Burhouse used Colbourne's[8] method of analysis.

Wood and Simms[10], in 1969, presented a paper detailing a proposed
design method for load bearing brick walls on simply supported beams.
The design method was based on the idea of equivalent beam moments,
first suggested by Wood in 1952[3]. In the design method, the beam
design moment is related to the allowable degree of stress concentration
in the wall. A sliding scale is introduced so that when a wall stress
concentration of $12\frac{1}{2}$ is allowed, the design moment is WL/100, but when
the wall is loaded near its working stress, and no stress concentration
is allowed, the design moment is reduced to WL/8. The present author
has one fundamental objection to this design method. This is that there
is absolutely no evidence that the distribution of stress on the wall–
beam interface is dependent on the level of loading, as is assumed in
this design method. In fact, the results of Wood's own tests, published
in 1952[3], indicate that the form of the vertical stress distribution
along the beam remains virtually unchanged as the stress level increases.

Male and Arbon[11], in 1969, published a paper in which the finite
element method was used to analyse some wall on beam structures. The
basic three node, two degrees of freedom per node, triangular finite
element was used in their program. No crack generation was allowed
for on the wall–beam boundary. The results from only a few analyses
are included in the paper. The problems analysed included the case of
a wall on beam structure resting directly on an elastic soil foundation.

Green[12,13] also used the finite element method to study wall on
beam behaviour. In his program, Green combined quadrilateral, triang-
ular and eccentric beam finite elements. The study was concerned with

the interaction of large shear walls with their supporting frames.
A parameter study was undertaken with variables which included the
beam stiffness, the beam support width and the size and position of
openings in the wall. Perspex models were used to check the accuracy
of the finite element results and to indicate what effective support
width a supporting column was likely to give. From the work, Green
developed a design method for shear walls with and without central
openings, supported by reinforced concrete beams. For the design
method, the effective support width is taken as 0.75 x column width
for external columns and 0.5 x column width for internal columns.
The present author finds these standard values for support width hard to
accept, because intuitively, the effective support width must be depend-
ent upon the flexibility of the column and this is a function of its
length, thickness and end fixidity as well as its width. Green's
assumption, used in the design method that the stiffness of a reinforced
concrete beam is independent of the quantity of reinforcement must also
be approximate.

Yettram and Hirst[14], in 1971, published a paper in which an
approximate method of analysing walls on beams is described. This shear
lag method consists basically of dividing the wall into vertical
stringers which carry all the vertical load, and having these connected
by shear carrying panels. For practical examples, the method requires
a computer to produce a solution.

CHAPTER 3

WALLS ON BEAMS: DEVELOPMENT OF A SIMPLE DESIGN METHOD

3.1 Introduction

This work was undertaken at the instigation of the British Standards Institute Committee B/20/5. A simple design method for the composite action of walls on beams was required for inclusion in a section on composite construction for the revised version of BS 449, the structural steelwork code of practice. The design method was limited to considering steel beams as these were the only beams relevant to this particular code.

The design method went through several major revisions before the final version was reached. This work can, for convenience, be split into four main stages of development, although in fact its development was more gradual with intermediate stages which have not been included here. The first design method produced four formulae for designing the beam against the various limiting conditions. Unfortunately the beam section could only be found from these formulae by trial and error. Additional information became available during the period that the iterative first design method was being transformed into a non-iterative design procedure. This information came from the analytical and experimental research being undertaken concurrently and described in Chapters 4 and 5. The second design method is considerably different from the first method because of this additional information. This second method is a direct, non-iterative design procedure. The third design method is a direct development on the second method, but accounts for beam self weight effects, which were not considered when developing the second method. This third method is again non-

iterative and can be used in the form presented for design work.
The fourth design method is the method finally accepted by the British
Standards Institute Committee. It is again non-iterative and allows
for both beam self weight and beam level loading.

3.2 Development of the first design method

3.2.1 Basic concepts

The extent of the arching effect between a wall and beam and the resultant stress distribution in the wall-beam system is shown in Chapter 4 to be dependent on the relative stiffness of the two components. With changes in beam flexural stiffness, from very stiff to very flexible, so the composite behaviour changes from a uniformly loaded beam in bending to that of a tied arch. The most economical design will be that which gives the lightest beam whilst retaining the wall and beam stresses and beam deflections within the design limits.

When arching occurs, the beam usually separates from the wall in the mid-span region. The shear and vertical stress distribution at the interface of the wall and beam then take the form shown typically in Figs. 3.1(a) and 3.1(b). (These results are from the K = 15, E/E_W = 20, finite element analysis described in Chapter 4). Both of these stress distributions can be approximated by triangular distributions.

The behaviour of a wall resting on a beam is comparable in many respects to that of a beam on an elastic foundation subjected to a concentrated load as shown in Figs. 3.2(a) and 3.2(b). Hetényi[15] derived a relationship for the length of contact α between the beam and the foundation. This can be expressed in terms of a parameter K and a constant B by

$$\frac{\alpha}{L} = \frac{B}{K} \qquad \qquad \ldots \ 3.1$$

where

$$K = \sqrt[4]{\frac{E_W \, t \, L^3}{EI}} \qquad \qquad \ldots \ 3.2$$
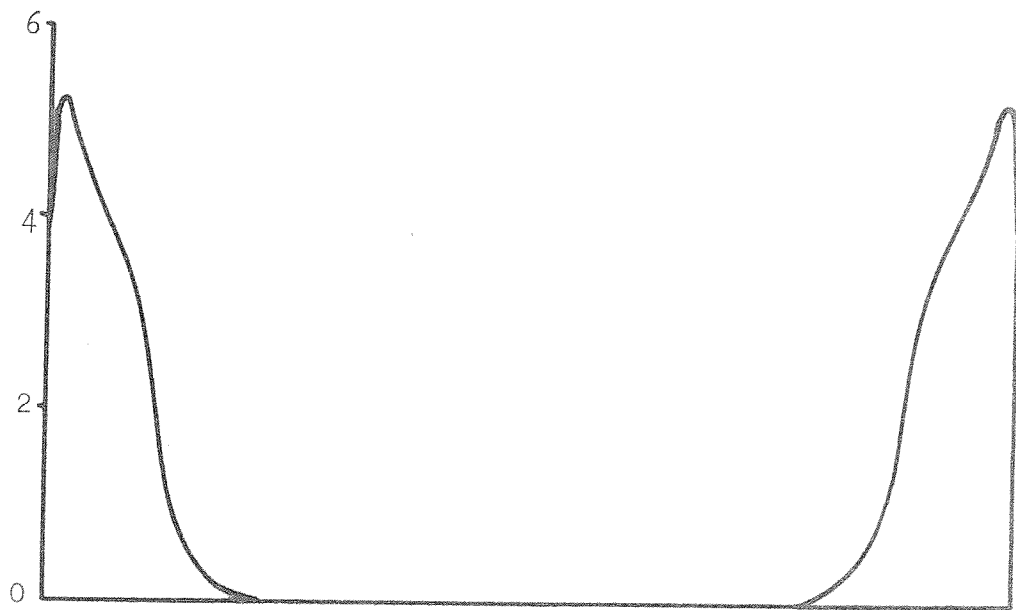
FIG. 3.1(1)   TYPICAL SHEAR STRESS DISTRIBUTION ON WALL-BEAM BOUNDARY
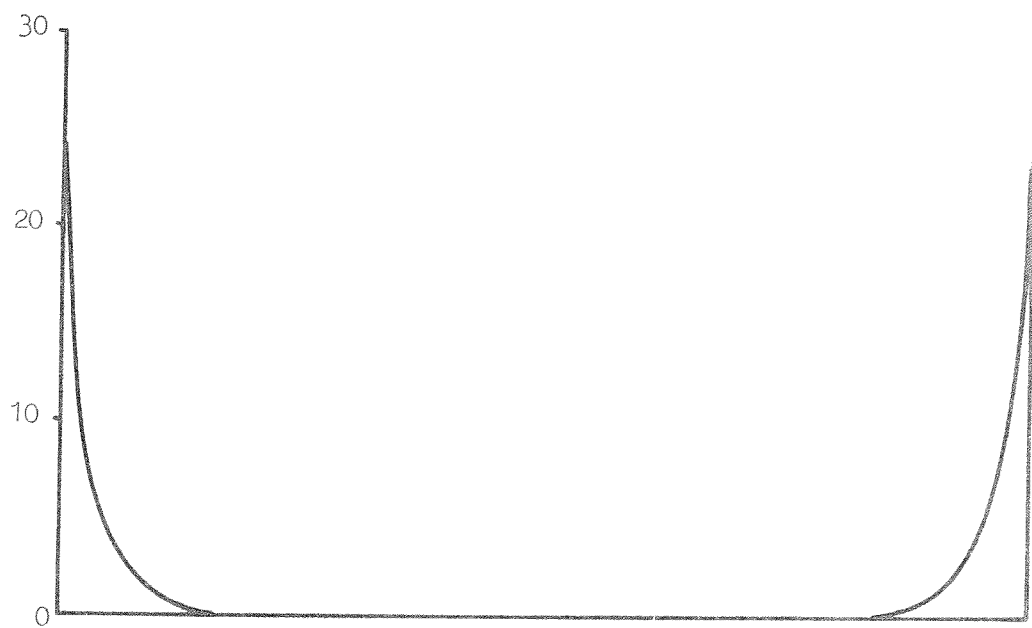
FIG. 3.1(b)   TYPICAL VERTICAL STRESS DISTRIBUTION ON WALL-BEAM BOUNDARY
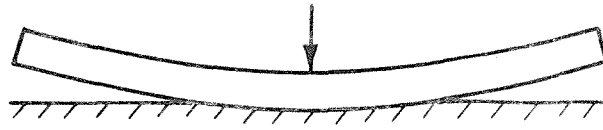
FIG. 3.2(a)   BEAM ON ELASTIC FOUNDATION

FIG. 3.2(b)   WALL ON BEAM

Triangular distribution
of vertical and shear
stress

$\frac{W_w}{4.4}$

$\frac{W_w}{2}$

$\frac{W_w}{2}$

α

L
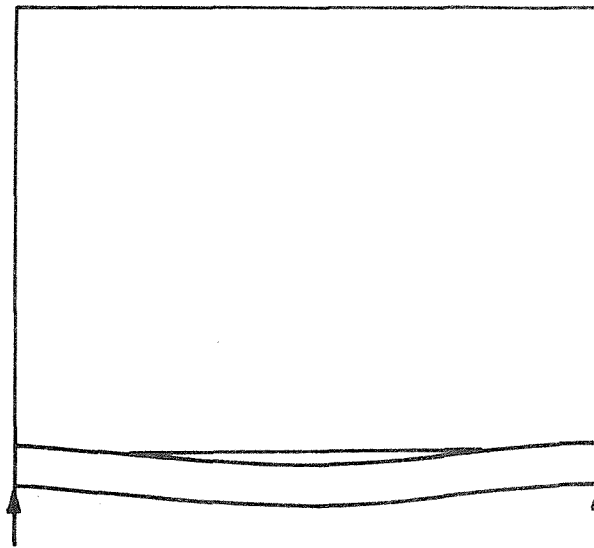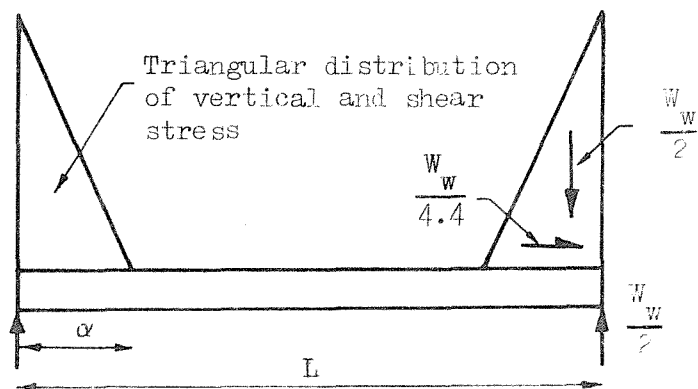
FIG. 3.3   ASSUMED LOADING ON BEAM

in which for the problem currently being considered, E_w and t are the elastic modulus and thickness of the wall, respectively, and EI and L are the flexural rigidity and span of the beam, respectively.

Hetényi calculated the value of β to be $\pi/\sqrt{2}$. Thus Eq. 3.1 becomes

$$\frac{\alpha}{L} = \frac{2.22}{K} \qquad \qquad \ldots \; 3.3$$

It will be noted that the height of the wall has not been included in the parameter K. Green[12] and Burhouse[9] have shown that for wall heights exceeding 0.6L, there are only small variations in the wall stress distribution close to the beam. To have included a height parameter would have complicated the design method considerably. Partly on this account, but also to ensure a high arch and thus avoid any outward slip of the wall on the beam, a restriction is introduced into the design method that the wall height must be greater than 0.6L. In one of Burhouse's tests, where the wall height was 0.33L, slip along the interface occurred.

At this first stage of developing the design method, four possible limiting conditions were considered.
These were:- (a) Bending stress in the beam.

(b) Deflection of the beam.

(c) Bond stresses between the encasement and the beam.

(d) Peak compressive stress in the wall.

3.2.2 Bending stress in the beam

Considering the limiting condition of bending stress in the beam, it was proposed to make the conservative design assumption that the length of contact is 1.5 times that given in Eq. 3.3

i.e. $\dfrac{\alpha}{L} = \dfrac{1.5 \times 2.22}{K} = \dfrac{3.33}{K}$ $\qquad$ . . . 3.4

With the assumed loading as shown in Fig. 3.3, the moment at the centre of the beam is given by

$$M = \dfrac{W_w \, \alpha}{6} = \dfrac{3.33}{6} \dfrac{W_w \, L}{K} \qquad \text{. . . 3.5}$$

Now $\dfrac{M}{Z} \not> P_{st}$, where P_{st} is the permissible stress in the steel beam.

Thus $\dfrac{3.33}{6} \dfrac{W_w \, L}{KZ} \not> P_{st}$ $\qquad$ . . . 3.6

This was approximated to

$$\dfrac{0.5 \, W_w \, L}{KZ} \not> P_{st} \qquad \text{. . . 3.7}$$

It will be noted that when calculating the peak beam stress and deflection, no account has been taken of the tie force and the reverse moment created by the shear force acting on the wall-beam interface. Approximate calculations indicated that the net effect of the tie force and reverse moment, was to reduce both the peak beam stress and the beam deflection. For the sake of simplicity, both the tie force and the reverse moment were excluded from the peak beam stress and deflection calculations.

3.2.3 Deflection of beam

When considering the beam central deflection, the length of contact was taken as that given in Eq. 3.3.

The central deflection, δ, will then be given by

$$\delta \;=\; \frac{W_w\,\alpha}{EI}\left(\frac{L^2}{48} - \frac{\alpha^2}{120}\right) \qquad\qquad \dots\; 3.8$$

Substituting $\alpha = 2.22L/K$ gives

$$\delta \;=\; \frac{W_w L^2}{KEI}\left(\frac{2.22}{48} - \frac{2.22^3}{120K^2}\right) \qquad\qquad \dots\; 3.9$$

The term $\dfrac{2.22^3}{120K^2}$ is relatively small and can be neglected.

Thus

$$\delta \;=\; \frac{0.046\, W_w L^3}{KEI} \qquad\qquad \dots\; 3.10$$

This was approximated to

$$\frac{W_w L^3}{20KEI} \;\not>\; \delta_s \qquad\qquad \dots\; 3.11$$

where δ_s is a specified maximum design deflection.

3.2.4 Bond stresses between encasement and beam

The length of contact assumed for bending would lead to unsafe results if used to predict the bond stresses between the encasement and beam. Therefore, for this case, the conservative assumption was made that the length of contact was two thirds of that given by Eq. 3.3

i.e.

$$\frac{\alpha}{L} \;=\; \frac{0.67 \times 2.22}{K} \;\simeq\; \frac{1.5}{K} \qquad\qquad \dots\; 3.12$$

Wood[10] proposed that the value of the horizontal shear force between the wall and beam was approximately $W_w/4.4$. This value was calculated by assuming a parabolic line of thrust in the wall of height 0.55L. After undertaking a parameter study using the finite element

technique, Green[12] suggested that the value was $W_w/4$. The value of $W_w/4.4$ was adopted for this design method. Wood also recommended that the maximum value for bond stress should be taken as $P_{cb}/20$, where P_{cb} is the permissible compressive strength of the concrete encasement material.

Assuming bond to occur around a beam section perimeter length of $2(B_B + D_B)$ and that the shear stress distribution can be taken as triangular. The limiting condition for bond stress is given by

$$\frac{2 . W_w}{4.4 \times 1.5L \times 2(B_B + D_B)} \not> P_{cb}/20$$

i.e. $$\frac{W_w K}{6.6L(B_B + D_B)} \not> P_{cb}/20 \qquad \ldots \ 3.13$$

This was approximated to

$$\frac{W_w K}{7L(B_B + D_B)} \not> P_{cb}/20 \qquad \ldots \ 3.14$$

3.2.5 Peak compressive stress in the wall

The length of contact assumed for the peak compression stress in the wall was taken as in Eq. 3.12. This value was adopted for the same reason as given in Section 3.2.4 above.

Considering the vertical equilibrium at the wall-beam interface and assuming the triangular stress distribution

$$f_b \, \alpha \, t = W_w \qquad \ldots \ 3.15$$

where f_b is the peak wall stress.

Thus substituting in for α from Eq. 3.12 gives

$$\frac{2}{3} \cdot \frac{W_w K}{Lt} \not> P_b \qquad \qquad \ldots \ 3.16$$

where P_b is the maximum permissible compressive wall stress.

3.2.6 Summary of the design method

Using Eq. 3.2, 3.7, 3.11, 3.14 and 3.16, a beam could be designed, by a method of trial and error, to ensure that it satisfied all the four failure criteria given in Section 3.2.1.

3.3 Development of a second design method

3.3.1 Introduction

The previously described design method was iterative and thus inconvenient to apply. A direct, non-iterative design method was required and this was developed in this second design method.

Also at this time, test information, described in Chapter 5, became available, which led to the modification of some of the assumptions on which the first design method was based.

3.3.2 Modifications caused by additional information

The plaster model tests, the Building Research Establishment tests and the masonry wall on reinforced concrete beam tests described in Sections 5.2, 5.4 and 5.5 respectively indicated that the length of contact assumptions of the first design method were inaccurate. The results from these tests are summarised in Table 3.1. It can be seen that the actual length of contact as represented by the B values is considerably less than the assumed value given by B = 2.22. The difference between the beam on elastic foundation length of contact and the wall on beam length of contact is due to differences in beam support restraint. Considering Fig. 3.2(a), it can be seen that the beam on elastic foundation theory should relate in Fig. 3.2(b) to a case where the ends of the beam are constrained against rotation. If the ends of the beam are free to rotate, as in the current problem, the length of contact will be reduced. New, more realistic estimates of the length of contact were introduced into the design method using the results shown in Table 3.1. These were given by:-

(a) for use in estimating the bending of the beam $\quad \alpha = \dfrac{1.5L}{K} \quad . \ 3.17$

(b) for use in estimating the compressive brickwork stress

$$\alpha = \dfrac{0.75L}{K} \quad . \ 3.18$$

(c) for use in estimating the horizontal shear stress

$$\alpha = \dfrac{1.0L}{K} \quad . \ 3.19$$

	K	Estimated B value		
		From measured contact length	From measured peak stress	From failure load
Plaster model tests	11.2	1.02	0.90	0.78
	15.1	1.16	0.77	0.96
	24.2	1.21	1.28	1.02
	14.4	1.09	0.98	0.90
Brick wall on encased steel beam tests	5.9	1.26	--	1.23
	8.6	1.08	1.16	1.10
	7.4	1.05	1.15	1.09
Brick wall on reinforced concrete beam tests	10.5	1.16	--	--
	15.4	1.28	--	--

Table 3.1   Summarised results from wall on beam tests

These new estimates were taken so that conservative results would be obtained when using these equations. The length of contact given for the shear stress was taken to be greater than that for the compressive vertical stress, because of their differing stress distributions as indicated in Figs. 3.1(a) and 3.1(b).

In a series of ten full scale wall on beam tests undertaken by Burhouse[9], the greatest beam deflection recorded at failure was L/840. This value is considerably less than values estimated by the first design method. This is due to the fact that the sagging moment is considerably reduced by the reduced length of contact, while the hogging moment due to the shear force, which is unchanged, was not included in the calculation. Since a beam deflection of L/840 is well below any probable beam deflection limit and the accurate determination of the deflection was likely to be difficult, the deflection condition was dropped from this design method.

This then left three conditions to consider

(a) Peak wall stress.

(b) Bending stress in the steel beam.

(c) Shear stress on the wall-beam interface.

3.3.3 Limiting condition of peak wall stress

As before from Eq. 3.15

$$f_b \, \alpha \, t = W_w$$

Introducing the assumption that $\frac{\alpha}{L} = \frac{0.75}{K}$ gives

$$\frac{0.75 f_b L t}{K} = W_w \qquad \qquad \ldots \; 3.20$$

Now $\qquad K = \sqrt[4]{\dfrac{E_w \, t \, L^3}{EI}}$

i.e. $\qquad I = \dfrac{E_w}{E} \cdot \dfrac{t \, L^3}{K^4} \qquad \qquad \ldots \; 3.21$

Combining Eq. 3.20 and 3.21 gives

$$I = \frac{E_w}{E} \cdot t \, L^3 \cdot \frac{W_w^4}{0.75^4 f_b^4 \, L^4 t^4}$$

i.e.
$$I = \frac{E_w}{E} \cdot \frac{W_w^4}{0.75^4 f_b^4 \, L t^3} \qquad \qquad \ldots \; 3.22$$

If the maximum permissible brickwork stress is P_b then

$$I \not< \frac{E_w}{E} \cdot \frac{W_w^4}{0.75^4 P_b^3 \, L t} \qquad \qquad \ldots \; 3.23$$

The ratio $E_w:E$ is assumed to be 1:30. This is thought to be a typical value when comparing a masonry wall with a steel beam. Taking this value Eq. 3.23 becomes

$$I \not< \frac{W_w^4}{9.5 L t^3 P_b^4} \qquad \qquad \ldots \; 3.24$$

Using Eq. 3.24, it is possible to find the lightest beam section that ensures that the limiting wall stress P_b is not exceeded. It is, however, necessary to check that the permissible bending stress of this steel section is not exceeded.

Again neglecting the reverse moment, the peak beam moment is given by

$$M = \frac{W_w \, \alpha}{6} \qquad \qquad \ldots \; 3.25$$

It is assumed for bending that $\dfrac{\alpha}{L} = \dfrac{1.5}{K}$

Thus
$$M = \frac{W_w L}{4K} \qquad \qquad \ldots \; 3.26$$

From Eq. 3.20

$$K = \frac{0.75}{W_w} P_b \, Lt$$

Thus $M = \dfrac{W_w^2}{3\,P_b\,t}$ ... 3.27

If the maximum permissible steel stress is P_{st}, the required section modulus, Z, of the beam is given by

$$Z \nless \dfrac{W_w^2}{3\,P_{st}\,P_b\,t}$$ ... 3.28

3.3.4 <u>Limiting condition of bending stress in the steel beam</u>

If the section chosen from Eq. 3.24 does not satisfy Eq. 3.28, it is then necessary to select a new steel section to satisfy the bending stress limit. This section will then automatically satisfy the brick-work stress limit provided its I value is greater than that given by Eq. 3.24. It would not be correct to choose a new section using Eq. 3.28 because Eq. 3.28 is only applicable when the wall is stressed to its maximum value P_b.

Using Eq. 3.26

Required $Z \nless \dfrac{W_w L}{4K\,P_{st}}$ ... 3.29

From Eq. 3.2 and assuming $\dfrac{E_w}{E} = \dfrac{1}{30}$, as before

$$K = \sqrt[4]{\dfrac{t\,L^3}{30I}}$$ ... 3.30

Combining Eq. 3.29 and 3.30 gives

$$Z \nless \dfrac{W_w L}{4\,P_{st}} \sqrt[4]{\dfrac{30I}{tL^3}}$$ ... 3.31

Using Eq. 3.31, it is possible, by trial and error, for a given loading, span and wall thickness, to find the lightest beam section and corresponding K value that satisfies the steel stress limit P_{st}. Using a Hewlett Packard programmable calculator, results were calculated for various spans and loading with a 9 inch wall and a steel limit of 23,500 lbf/in^2 which corresponds to mild steel. The results are shown in Table 3.2. Table 3.2 also includes results calculated using Eq. 3.24 with a wall stress limit of 450 lbf/in^2 and results calculated using a $\frac{Wl}{8}$ type design. For four span-loading combinations, approximate calculations were undertaken that included the effects of reverse moment, tie force and beam encasement and these results are also included in Table 3.2. Only compressive stresses were allowed in the encasement material in these calculations as the material was assumed to have cracked in tension. These last results indicate that both the steel and wall stresses will be below the design method estimates and thus the design method is conservative in these respects. The concrete encasement compressive stresses are well below the likely strength of the materials, and thus no problems should be experienced in this respect.

The results in Table 3.2 indicate that K is approximately related to the intensity of the wall loading. A graph of K against the loading per ft. was constructed taking a conservative value of K at each load level and this is shown in Fig. 3.4. Using this graph and Eq. 3.29, the beam could be designed directly without any iterative process. The graph applies only to systems with a 9 in. thick wall and a maximum permissible steel stress of 10.5T/in^2, i.e. 23,500 lbf/in^2. To obtain K graphs for other wall thickness and steel strength combinations, further calculations of the type above were required.

SPAN ft.	WALL THICKNESS in	LOAD/FT lbf	TOTAL LOAD lbf	REQUIRED SECTION FROM $M = \frac{WL}{8}$	REQUIRED SECTION FOR BRICKWORK STRESS LIMIT OF 450 lbf/in²	DESIGN METHOD				VALUES RECALCULATED FOR REVERSE MOMENT, TIE STRESS AND CONTRIBUTION OF CONCRETE TO I			
						DESIGN FOR STEEL LIMIT OF 10.5T/in².							ACCOUNTING FOR REVERSE
						REQUIRED SECTION	PARAMETER K	BEAM STRESS f_{st}	BRICKWORK STRESS f_b	K	f_{st}	f_b	CONCRETE COMPRESSIVE STRESS f_c
40	9	10,000	400000	NONE AVAILABLE	N.A.	UB 24x9x84	10.88	22467	1344	10.80	20,950	1333	471
		8,000	320000	UB 36x16½x230	N.A.	21x8¼x68	12.24	22426	1209				
		4,000	160000	33x11½x130	UB 30x10½x116	16x5½x31	17.25	23535	852				
		2,000	80000	24x9x94	16x5½x31	12x4x16.5	23.69	23154	585				
		1,000	40000	21x8¼x62	RSJ 6x3½x11.5	RSJ 6x3½x11.5	35.36	19200	437	33.46	16,490	413	499
25	9	10,000	250000	UB 33x11½x152	N.A.	UB 18x7½x45	10.35	22952	1278				
		8,000	200000	30x10½x116	N.A.	16x7x36	11.61	22955	1146				
		4,000	100000	21x8¼x82	UB 21x8¼x62	12x4x19	15.80	22187	780				
		2,000	50000	18x7½x45	12x4x16.5	RSJ 6x3½x11.5	24.86	21339	613				
		1,000	25000	14x6¼x30	RSJ 4x2½x6.5	4x2½x6.5	35.26	20296	435				
15	9	10,000	150000	UB 24x9x68	UB 36x12x170	UB 12x5x25	10.05	23405	1241				
		8,000	120000	18x7¼x66	27x10x114	12x4x19	10.77	23432	1064				
		4,000	60000	15x6x40	16x5½x26	RSJ 6x3½x11.5	16.95	22537	837				
		2,000	30000	12x3x25	RSJ 6x3½x11.5	4x2½x6.5	24.01	21435	594				
		1,000	15000	10x4x17	3x2x4.5	3x2x4.5	30.58	16595	378				
8	9	10,000	80000	UB 14x6¾x30	UB 24x9x68	RSJ 7x4x14.5	9.23	19906	1140	8.83	15,800	1090	367
		8,000	64000	12x5x28	18x6x45	6x3½x11.5	10.58	20544	1044				
		4,000	32000	8x5¼x20	10x4x15	4x2½x6.5	15.00	19539	741				
		2,000	16000	RSJ 7x4x14.5	RSJ 4x2½x6.5	3x2x4.5	19.09	15127	471				
		1,000	8000		3x2x4.5	3x2x4.5	19.09	7564	236	16.56	4,817	204	141

TABLE 3.2   BEAM SIZES FOR DIFFERENT SPANS AND LOADING TO
SATISFY DIFFERENT LIMITS
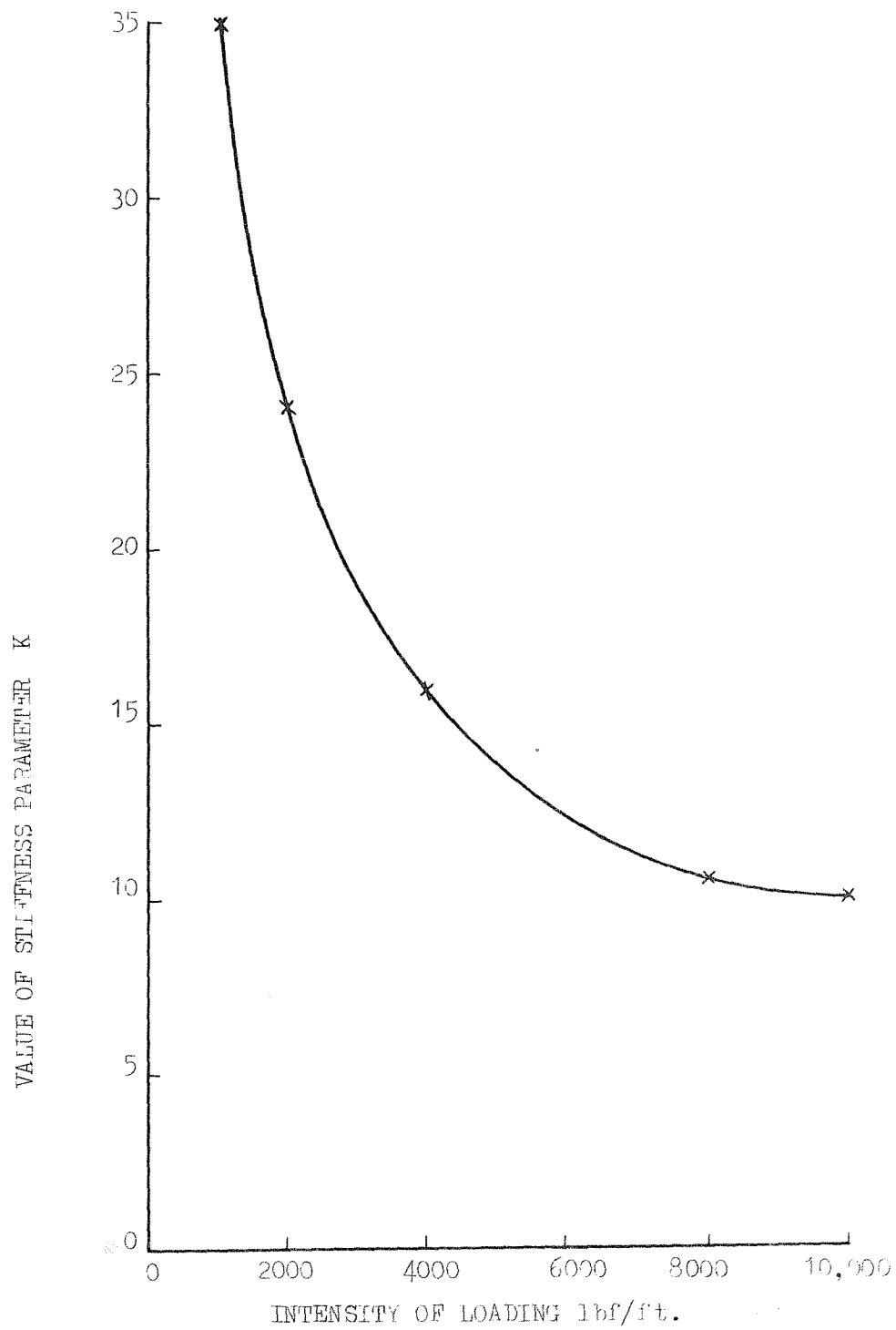
FIG. 3.4   VALUE OF STIFFNESS PARAMETER K

At this stage it was decided to convert the design method to limit state and metric form. The three main design equations 3.24, 3.28 and 3.29 required no alterations. The K graph did need changing to account for the higher design steel stress and the lower design loading.

Calculations were undertaken as before using Eq. 3.31 to determine by trial and error the lightest beam section that satisfied the steel stress limit for a range of spans and loading corresponding to those used previously in Table 3.2. Two steel strengths were taken corresponding to grades 43 and 50 steel and three wall thicknesses of 112.5 mm. ($4\frac{1}{2}$ in.), 225 mm. (9 in.) and 337.5 mm. ($13\frac{1}{2}$ in.) were also included. Taking the lowest K value for each loading level as before, six curves were constructed corresponding to the six steel strength/wall thickness combinations. So as to obtain more accurate points on the graph where the beam sections were small and the choice of sections limited, reverse calculations were undertaken. Starting with the beam section, the load carrying capacity of the structure was calculated using Eq. 3.31. The six design curves for K are shown in Fig. 3.5.

Using Eqs. 3.24, 3.28 and 3.29 and the K curves it was now possible to design the beam directly to account for the peak wall and beam stresses.

3.3.5 Shear force consideration

The tendency of the wall to arch across the ends of the supporting beam induces a horizontal shear force at each end. The shear strength of the wall-beam connection and the encasement of the beam must be adequate to transfer this shear force into the steel beam.

Since shear failure had not been detected in any tests where the wall height exceeded 0.6L, it was considered more convenient to include the shear force condition as a check rather than as a design criteria.
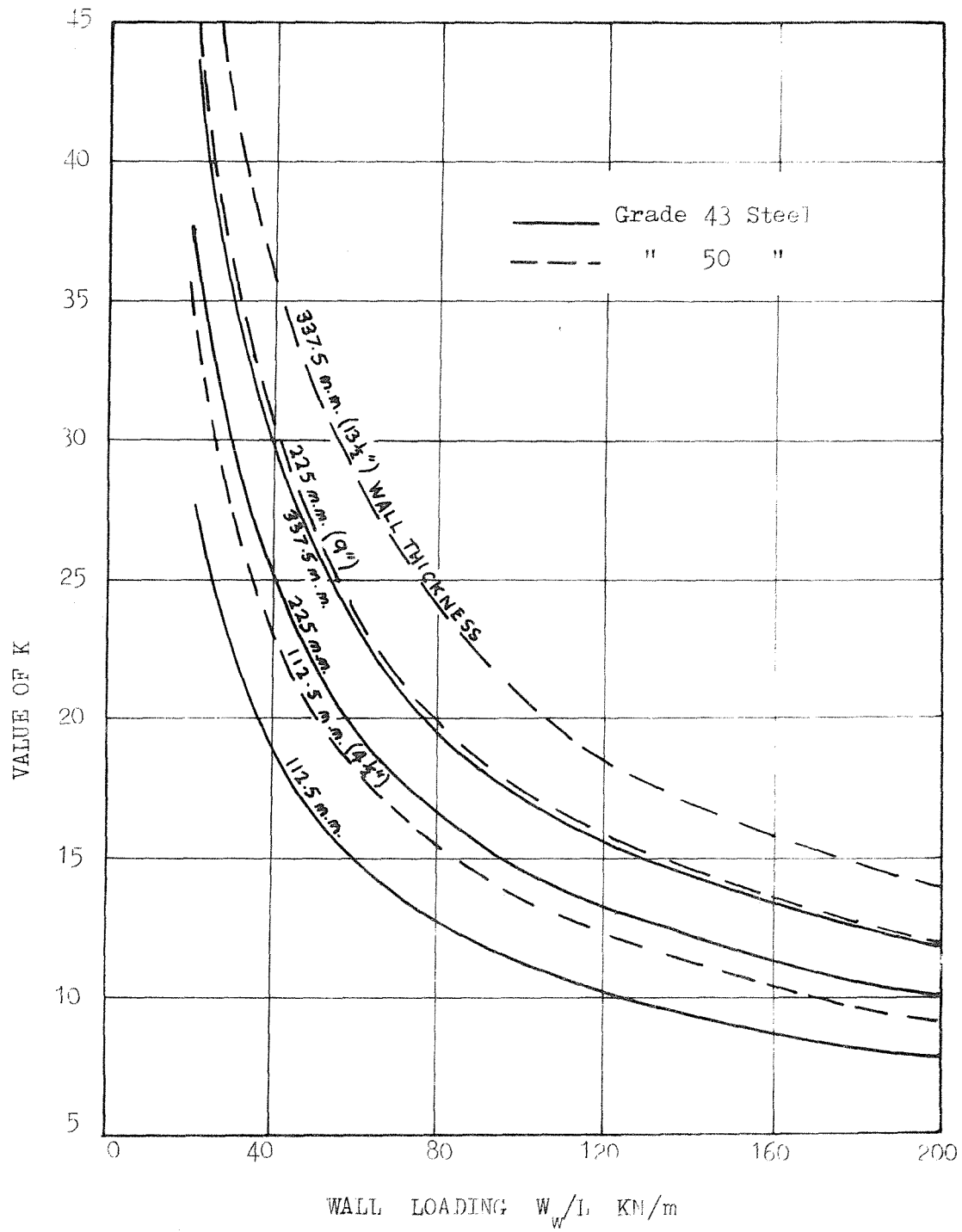
FIG. 3.5   VALUE OF STIFFNESS PARAMETER K AS A
FUNCTION OF LOADING INTENSITY

As before the value of the horizontal thrust is taken as $W_w/4.4$. This is distributed triangularly over a length of contact given in Eq. 3.19 as

$$\alpha = \frac{L}{K}$$

Thus the maximum horizontal force per unit length, H', is given by

$$H' = \frac{W_w K}{2.2L} \qquad \ldots \; 3.32$$

When the beam steel stress is limiting, the K value is already known from Fig. 3.5.

When the wall stress is limiting, the K value can be calculated using Eq. 3.20.. Combining Eqs. 3.20 and 3.32 gives

$$H' = 0.34 \, P_b \, t \qquad \ldots \; 3.33$$

3.3.6 <u>Required wall strength if $\frac{W_w L}{8}$ design beam used</u>

In certain design cases when a weak wall material is used, the beam section calculated when using the wall stress limit may be heavier than that taken when using a $\frac{W_w L}{8}$ type design. It was thought possible that some designers might prefer to use a lighter beam and then strengthen the wall. The minimum required wall design strength can be found by combining Eqs. 3.20 and 3.30

$$\text{i.e.} \qquad P_b \; \not< \; \frac{W_w}{0.75 \, Lt} \sqrt[4]{\frac{tL^3}{30I}}$$

$$\text{i.e.} \qquad P_b \; \not< \; 0.57 W_w \sqrt[4]{\frac{1}{Lt^3 I}} \qquad \ldots \; 3.34$$

3.3.7 <u>Summary of the design procedure for the second design method</u>

1. a) Select a beam to satisfy the wall stress condition using

$$I \not< \frac{W_w^4}{9.5Lt^3P_b^4} \qquad \dots \ 3.35$$

b) Check the selected section for the bending stress condition

using

$$Z \not< \frac{W_w^2}{3P_{st}\,P_b\,t} \qquad \dots \ 3.36$$

If the Z of the steel section chosen by Eq. 3.35 satisfies Eq.3.36, the beam is adequate in bending and Stages 3 and 4 remain to complete the design. If the section does not satisfy Eq. 3.36, proceed to Stage 2 .

2.   Using Fig. 3.5, find the value of K corresponding to the loading intensity W_w/L, the wall thickness and the appropriate grade of steel. Values of K for wall thicknesses between those given can be found by linear interpolation. Then select a section to satisfy

$$Z \not< \frac{W_w L}{4K\,P_{st}} \qquad \dots \ 3.37$$

Proceed to stage 4.

3.   If the steel section designed in Stage 1 is less economical then the section designed by

$$Z \not< \frac{W_w L}{8P_{st}} \qquad \dots \ 3.38$$

the latter may be used provided that the wall over the beam supports is increased to a minimum strength of

$$P_b = 0.57W_w \sqrt[4]{\frac{1}{Lt^3I}} \qquad \dots \ 3.39$$

The region of strengthened wall should extend horizontal and vertical distances of L/10 along the span and upwards, respectively from each support.

4.   A check on the adequacy of the mortar or encasement in resisting the tendency of the "arch" to spread can be made using one of the following formulae.

The maximum horizontal force per unit length, H', at the ends of the beam is given by:-

a)   when the wall stress is limiting or the beam is designed for $\dfrac{W_w L}{8}$

$$H' = 0.34\ P_b t \qquad \qquad \dots \ 3.40$$

b)   when the bending stress is limiting

$$H' = \dfrac{W_w K}{2.2L} \qquad \qquad \dots \ 3.41$$

3.4 Development of the third design method

3.4.1 Introduction

When developing the second design method, no consideration was given to beam self weight effects. In certain cases these effects can be important and so this third design method was developed to include allowances for these self weight effects. When beam level loading occurs, other than beam self weight, this can be accounted for in this third design method by using the WL/8 method.

This design method is based on the second design method and thus again considers the peak wall compressive and shear stresses and the beam bending stress as the main limiting factors.

3.4.2 Peak wall stress limit

The beam self weight will not affect the beam section required to satisfy the peak wall stress limit. Thus from Eq. 3.35

$$I \not< \frac{W_w^4}{9.5 \, Lt^3 P_b^4} \qquad\qquad 3.42$$

where W_w is the sum of the wall self weight and the superimposed loading on the wall.

Again it is necessary to check whether the section chosen from Eq. 3.42 satisfies the beam steel stress. Using Eq. 3.36 and adding the section modulus required for the beam self weight, Z_s, gives

$$Z \not< \frac{W_w^2}{3P_{st} P_b t} + Z_s \qquad\qquad 3.43$$

If the beam designed by Eq. 3.42 also satisfies Eq. 3.43, then both wall and beam stress are within their design values.

Again it should be noted that Eq. 3.43 must only be used to check beams designed by Eq. 3.42. It is not a general design equation because it is invalidated when the brickwork stress is not equal to P_b.

In certain cases of light loading with strong brickwork it is possible to design by this method a beam of such a small section that its self weight deflection is unacceptably large. An investigation of encased beam self weight deflections was undertaken using a Hewlett Packard programmable calculator. The steel sections were assumed to be encased with 5 cm. of cover and the encasement material was assumed to have cracked so that it could take no tensile stress. Spans between 2 m and 12 m were considered. As a result of this investigation a recommendation was introduced into the design method that the steel beam section depth D_B should not be less than $L/25$. This ensures that the total beam deflection due to wall loading and self weight should not exceed $L/300$.

This minimum beam depth restriction was found to have an important side effect. Repeated calculations showed that if the limit state design brickwork stress was less than 6000 KN/m^2, the wall thickness less than 340 mm., and the beam depth not less than $L/25$, then a beam design for wall stresses by Eq. 3.42 automatically satisfied the beam bending stress condition of Eq. 3.43. Therefore, the beam could be designed using only the brickwork limit and, if necessary, increasing the section depth to $L/25$ without any check on the beam stresses.

When the design brickwork stress is greater than 6000 KN/m^2, it is necessary to check the beam stress using Eq. 3.43. This check must be made before any increase of depth to $L/25$ as Eq. 3.43 assumes the wall stress is equal to its design value which would not be the case when the beam depth is increased.

3.4.3 Beam bending stress limit

If the beam design by Eq. 3.42 does not meet the requirement of Eq. 3.43, only the wall stresses are satisfied and it is necessary to redesign the beam to satisfy the steel stress condition.

The design should now be based on Eq. 3.37, but with the addition of the section modulus required for the beam self weight.

$$\text{i.e.} \qquad Z \not< \frac{W_w L}{4K' \, P_{st}} + Z_s \qquad \ldots \; 3.44$$

K' is defined by the same equation as K, i.e. Eq. 3.2. It is identified from K because when the beam is stiffened to account for self-weight, the resultant K' value is different from the value found from Fig. 3.5. Fig. 3.5 is thus not applicable to this third design method.

The design should now be based on Eq. 3.44. It should be noted that it would be incorrect to design the beam by first neglecting its self-weight, and then increasing the beam by Z_s to account for the self-weight. It would be incorrect because if the beam were stiffened to account for self weight, the K value would change, resulting in a spread of the wall/beam interaction forces towards the centre of the span. The overall effect would be to increase the beam moment to above the design value.

Eq. 3.44 can again only be solved iteratively, since Fig. 3.5 is not applicable. The problem was again studied using the programmable calculator for the same combination of four spans, three wall thicknesses and two steel strengths used in the second design method. Each calculation involved choosing a section and combining it with the span, wall and steel data. The value of K' and the corresponding Z_s value

were computed, together with the maximum wall loading, W_w, that the system could carry. The steel sections were assumed to be encased with 5 cm. of cover as before.

The results again revealed a relationship between K' and the intensity of loading W_w/L for each wall thickness and steel strength combination. The results for one combination are shown in Fig. 3.6. A set of curves was constructed for K' against W_w/L taking the most conservative points i.e. those with the least K' for a particular W_w/L value. These K' curves are shown in Fig. 3.7. As might be expected the greatest differences between the K' curves in Fig. 3.7 and the K curves in Fig. 3.5 occur for the lowest W_w/L values, when self weight effects become more important.

The results also indicated a reasonable relationship between Z_s/Z and W_w/L^2 as shown in Fig. 3.8. Thus relationship is virtually independent of wall thickness and steel strength. A conservative curve of $\log(1 - \dfrac{Z_s}{Z})$ against W_w/L^2 was constructed, as in Fig. 3.9. A log curve was chosen because it was more convenient to use for low W_w/L^2 values. The non-dimensional term $(1 - Z_s/Z)$, will be defined as a variable C.

From Eq. 3.44 $\qquad Z - Z_s \not< \dfrac{W_w L}{4K' P_{st}}$

therefore $\qquad Z \not< \dfrac{W_w L}{4K'(1 - \dfrac{Z_s}{Z})P_{st}}$

or $\qquad Z \not< \dfrac{W_w L}{4K' C P_{st}}$ $\qquad$ . . . 3.45

It is now possible to design a steel section directly for the steel stress condition using the curves in Fig. 3.7 and 3.9 and Eq. 3.45. For wall thicknesses between those given in Fig. 3.7, conservative
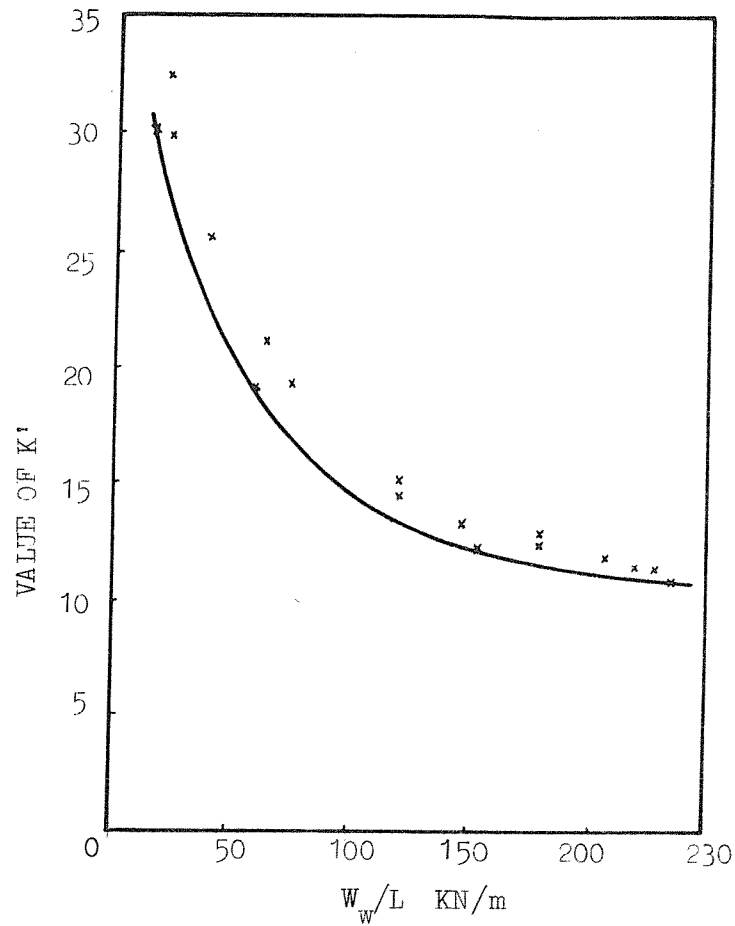
FIG. 3.6   RELATION BETWEEN K' AND W_w/L FOR GRADE 50
STEEL AND WALL THICKNESS OF 225 mm.
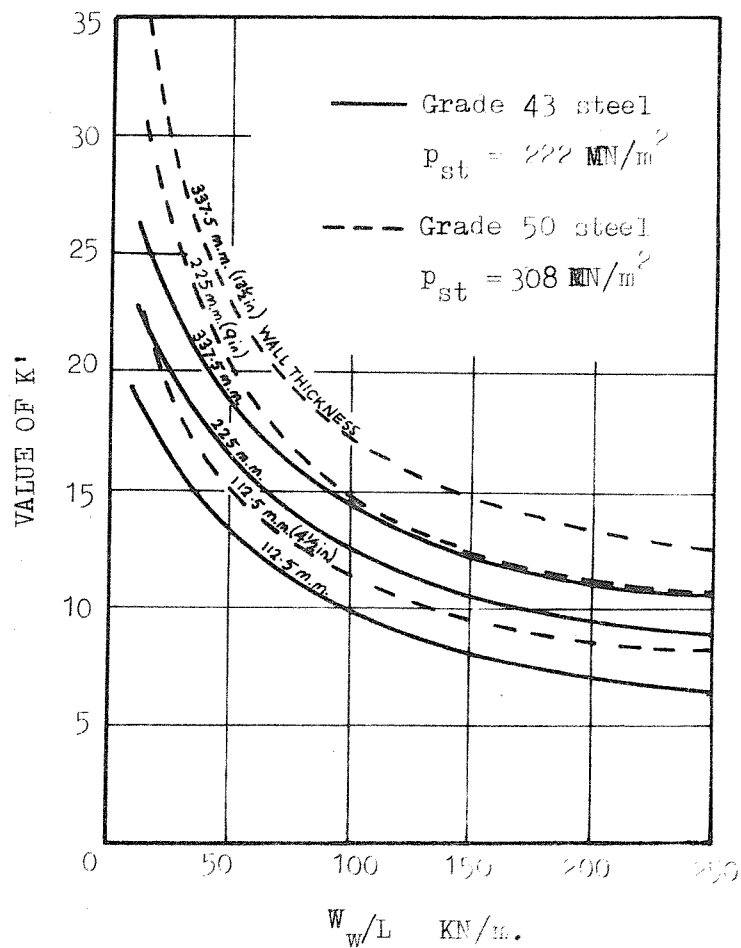
Fig. 3.7   VALUE OF STIFFNESS PARAMETER K' AS A FUNCTION
OF LOADING INTENSITY
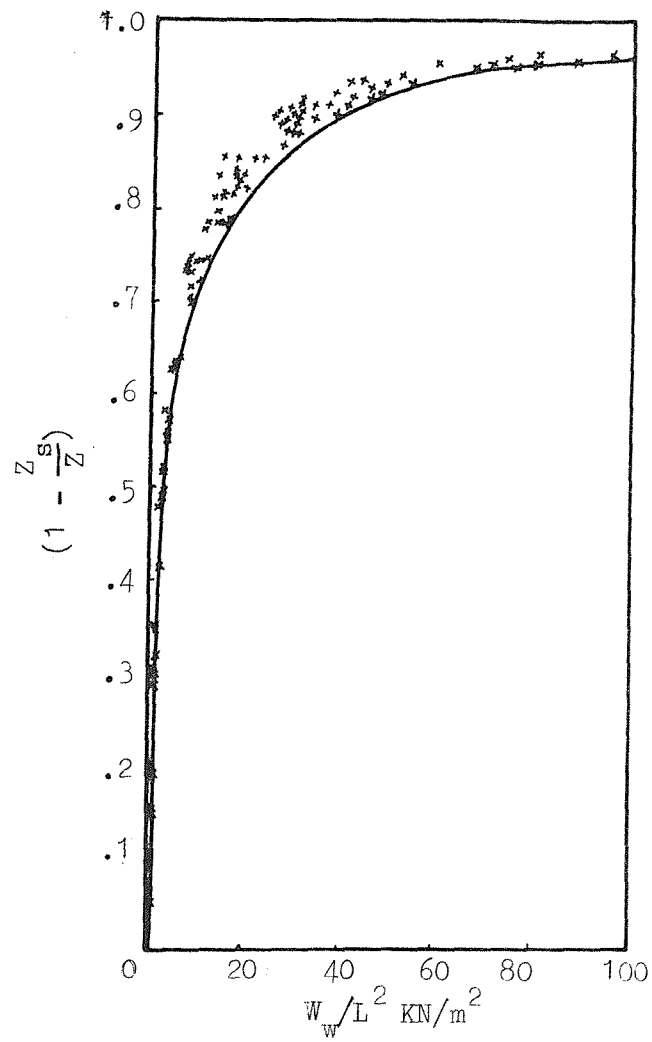
Fig. 3.8   RELATION BETWEEN $(1 - \frac{Z_s}{Z})$ AND W_w/L^2
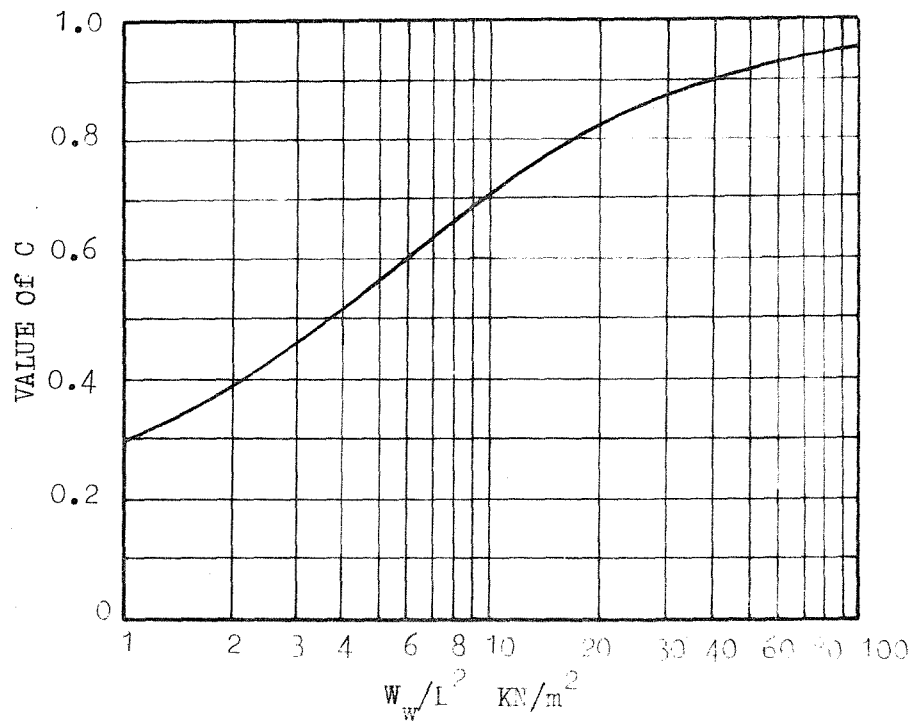
FIG. 3.9   VALUE OF C AS A FUNCTION OF W_w/L^2

values may be found by linear interpolation. If necessary the section depth should be increased as previously to L/25, as a safeguard against excessive self weight deflection.

3.4.4 Shear force consideration

The maximum horizontal force per unit length, H', on the wall-beam interface is given in Eq. 3.41 by

$$H' = \frac{W_w K'}{2.2 L} \qquad \qquad \ldots \ 3.46$$

Thus the peak shear stress, τ, on this boundary is given by

$$\tau = \frac{0.45 \ W_w K'}{Lt} \qquad \qquad \ldots \ 3.47$$

An estimate of the ultimate shear strength, f_s, is given by

$$f_s = f_{bs} + \mu \ \sigma_y \qquad \qquad \ldots \ 3.48$$

in which f_{bs} is the bond shear strength, μ the coefficient of internal friction and σ_y the compressive stress normal to the shearing plane.

A conservative estimate of μ between the brickwork and concrete encasement is 0.5 and, when unencased, between the brickwork and the steel beam is 0.3.[16]

Therefore, for an encased beam

$$f_s = f_{bs} + 0.5 \ \sigma_y \qquad \qquad \ldots \ 3.49$$

and for an unencased beam where bond between the brickwork and steel cannot be relied upon

$$f_s = 0.3 \ \sigma_y \qquad \qquad \ldots \ 3.50$$

The peak shear stress occurs close to the support at which point the value of σ_y is given by Eq. 3.20 as

$$\sigma_y = \frac{W_w K'}{0.75Lt} \qquad \qquad \cdots \ 3.51$$

Therefore the available strengths are:

for an encased beam

$$f_s = f_{bs} + 0.67 \frac{W_w K'}{Lt} \qquad \qquad \cdots \ 3.52$$

and for an unencased beam

$$f_s = 0.4 \frac{W_w K'}{Lt} \qquad \qquad \cdots \ 3.53$$

Considering Eqs. 3.47 and 3.52 for encased beams and the con-
servative assumptions taken for the shear stress distribution and for
μ, it seems reasonable to neglect shear failure as a limiting state.
No cases of shear failure are known to the author for tests on walls
of height greater than 0.6L.

However, considering Eqs. 3.47 and 3.52 for unencased sections,
the shear stress is likely to exceed the shear strength. Therefore
unencased beams are excluded from the design method unless special
means for lateral restraint of the wall are provided.

3.4.5 Design using WL/8 method.

This method can be used when beam loading due to adjacent slab
exists. The equations used in the second design method require no alter-
ation to account for beam loading, except that W_w in Eq. 3.37 should
be replaced by $(W_w + W_s)$, W_s is the self weight of the beam plus any
adjacent slab loading acting on the beam.

3.4.6 Summary of the design procedure for the third design method

Method I when the brickwork or blockwork design stress P_b does not
exceed 6000 KN/m^2

1. Select a steel section using

$$I \not< \frac{W_w^4}{9.5Lt^3P_b^4} \qquad \dots \ 3.54$$

2. If for the selected section, $D_B < L/25$ select an alternative section with $D_B \geq L/25$ and I not less than given by Eq. 3.54.

3. Check that the encased beam and its end connections have adequate shear strength.

Method II when the brickwork or blockwork design stress P_b exceeds 6000 KN/m^2.

1. Select a steel section using Eq. 3.54 of Method I.

2. Check that the section modulus of the chosen steel section satisfies

$$Z \not< \frac{W_w^2}{3P_{st} P_b t} + Z_s \qquad \dots \ 3.55$$

If Eq. 3.55 is satisfied, proceed to steps 2 and 3 in Method I. If not, proceed to step 3 below.

3. Use Figs. 3.7 and 3.9 to determine values of the dimensionless numbers K' and C, respectively, using interpolation if necessary. Then select an alternative section using

$$Z \not< \frac{W_w L}{4K'C P_{st}} \qquad \dots \ 3.56$$

Then proceed to steps 2 and 3 in Method I.

Method III when Methods I or II result in a heavier steel section than given by a design for distributed load moment WL/8 or if the beam supports any adjacent slabs in addition to the wall.

1. The beam should be designed for the distributed load condition to satisfy

$$Z \nless \frac{(W_w + W_s)L}{8 P_{st}} \qquad \ldots \ldots 3.57$$

in which W_s is the self weight of the encased beam plus the slab loading, if present.

2. The strength of the brickwork or blockwork within horizontal and vertical distances of $L/10$ from the supports, must be increased, if necessary to satisfy

$$P_b \nless 0.57 W_w \sqrt[4]{\frac{1}{Lt^3 I}} \qquad \ldots \quad 3.58$$

3.5 Development of the fourth design method

3.5.1 Introduction

The fourth design method is the method accepted by the British Standards Institute Committee. This method allows both beam self weight and other beam loading to be included in one simple design method. The main disadvantage of the third design method was that beam level loading, other than beam self weight, could only be included using the WL/8 method and this method tends to be inefficient because no account is taken of the reduced beam moment due to the wall arching. The WL/8 method was removed completely from this fourth design method because its other purpose of in some cases designing a lighter beam by strengthening the brickwork could also be achieved using the other method if the brickwork was strengthened.

The brickwork compressive stress and the beam bending stress are taken as the two limiting conditions. The wall shear stress is not considered because Section 3.4.4 showed it not to be limiting when the beam was encased.

3.5.2 Peak wall stress limit

The beam loading will not affect the size of beam required to satisfy the peak wall stress limit.

Thus from Eq. 3.54

$$I \not< \frac{W_w^4}{9.5Lt^3p_b^4} \qquad \ldots 3.59$$

Again it is necessary to check whether the section chosen from Eq. 3.59 satisfies the beam section. In the third design method it was found to be unnecessary to check the beam strength when the brick strength was greater than 6000 KN/m^2 and the beam depth was greater

than L/25. In this fourth design method, it will always be necessary
to check the beam stresses, because beam loading is allowed and this
increases the beam stresses.

Using Eq. 3.55, and adding the section modulus required for a uniformly
distributed beam load of W_s, which includes the beam self weight,
gives

$$Z \not< \frac{W_w^2}{3p_{st}p_b\,t} + \frac{W_s L}{8p_{st}} \qquad \ldots \; 3.60$$

If the beam designed by Eq. 3.59 also satisfies Eq. 3.60, then
both wall and beam stresses are within their design values.

Again it should be noted that Eq. 3.60 must only be used to check
beams designed by Eq. 3.59 because Eq. 3.59 is invalidated if the
brickwork stress is not equal to p_b.

If Eqs. 3.59 and 3.60 are both satisfied then the minimum depth
restriction of L/25 should again be applied.

3.5.3 Beam bending stress limit

If the beam designed by Eq. 3.59 does not meet the requirement
of Eq. 3.60, only the wall stresses are satisfied and it is necessary
to redesign the beam to meet the steel stress condition.

As explained in Section 3.4.3, it would be incorrect to design
the beam by first neglecting the beam loading, and then to increase
the beam by the section modulus required to sustain this beam loading.
It would be incorrect, because to stiffen the beam to account for the
beam loading, would reduce the K value, which would consequently
increase the beam moment due to the wall loading.

An investigation was undertaken to discover the magnitude of the
errors that developed when the beam was designed by considering the

wall and beam loading separately. The investigation was undertaken on a Wang mini-computer using a Basic language program. A whole range of beam spans, beam strengths, wall thicknesses, wall loading and beam loading were considered. First a beam span, beam strength, wall thickness and beam section were chosen. The K value for this configuration K_1, and the wall load, W_w, that this beam would take assuming that there was no beam loading were calculated using Eqs. 3.30 and 3.29. The beam loading, W_s, was then taken as a chosen proportion of the wall loading and the section modulus required to sustain this beam loading only was calculated. The sum of the section modulus of the original beam and the section modulus required for beam loading was calculated and a new beam section chosen from this value. The new K value, K_2, of the configuration using this section was calculated. The beam moment due to wall loading is inversely proportional to the K value. Thus the percentage increase in the beam moment due to wall loading, P_1, is given by:

$$P_1 = \frac{\dfrac{W_w L}{4K_2} - \dfrac{W_w L}{4K_1}}{\dfrac{W_w L}{4K_1}} \times 100\%$$

$$\text{or} \quad P_1 = K_1 \left(\frac{1}{K_2} - \frac{1}{K_1} \right) \times 100\% \qquad \qquad \dots \ 3.61$$

The percentage increase in the total beam moment, P_2, is given by

$$P_2 = \frac{\dfrac{W_w L}{4K_2} - \dfrac{W_w L}{4K_1}}{\dfrac{W_w L}{4K_1} + \dfrac{W_s L}{8}} \times 100\%$$

$$\text{or} \quad P_2 = \frac{W_w(\frac{1}{K_2} - \frac{1}{K_1})}{(\frac{W_w}{K_1} + \frac{W_s}{2})} \quad \text{x } 100\% \qquad \ldots \; 3.62$$

The P values relate to the errors that would develop in estimating the beam moment if the beam section was chosen by considering the wall loading and beam loading separately and then the results were summed.

The results of the investigation showed as might be expected, the errors in the proportion of the beam moment relating to the wall loading, P_1, increased as the beam loading increased.

The more important error term, P_2, relating to the total beam moment was found not to increase with increasing beam loading, but stayed fairly constant between 10 and 20 percent. This can be explained since although the P_1 error increases with increasing beam loading, the proportion of the total moment that P_1 relates to reduces at about the same rate as P_1 increases.

In formulating the second design method, very conservative assumptions had been made regarding the beam moment . These assumptions related to the cancelling effect of the reverse moment and the tie force. The computer analyses described in Chapter 4 confirmed this degree of conservation. It was thus thought that the beam moment could be calculated assuming that the wall and beam loading acted independently, without increasing the resulting moment by the factor of 20 percent.

The required section could thus be calculated from Eq. 3.37 of the second design method with the addition of the section modulus required for the beam loading.

$$\text{i.e.} \quad Z \; \not< \; \frac{W_w \, L}{4Kp_{st}} + \frac{W_s \, L}{8p_{st}} \qquad \ldots \; 3.63$$

The K curves of the second design method, shown in Fig. 3.5, will be applicable to Eq. 3.63 and thus no iteration procedure is required to select a beam section.

Since the beam moment had effectively been reduced by 17% in Eq. 3.63, it seemed reasonable to reduce the beam moment due to wall loading in Eq. 3.60 by a similar factor giving

$$ Z \not< \frac{W_w^2}{3.6p_{st}p_b} + \frac{W_s L}{8p_{st}} \qquad \ldots \ 3.64 $$

3.5.4 Other considerations

If a wall is built on an unpropped beam, the uncured wall will tend to distribute its weight uniformly along the beam length. Since such loading is not accounted for in the design, the beam must be propped during wall construction.

In order that composite action can develop, the wall is required to act as an arch. Any holes in the arching region of the wall would obviously affect its arching capacity. For this reason no holes are permitted in the wall in the arching region. The arching region taken for the purpose of the design method is shown in Fig. 3.10.

In developing the design method, the assumption was made that the wall loading W_w was reasonably uniformly spread across the span. For this reason, the provision is made that the line of action of the wall load is within the middle third of the span.

3.5.5 Summary of fourth design method

Provisions. The following provisions shall apply

(a) the beam shall be a uniform hot-rolled section symmetrical about
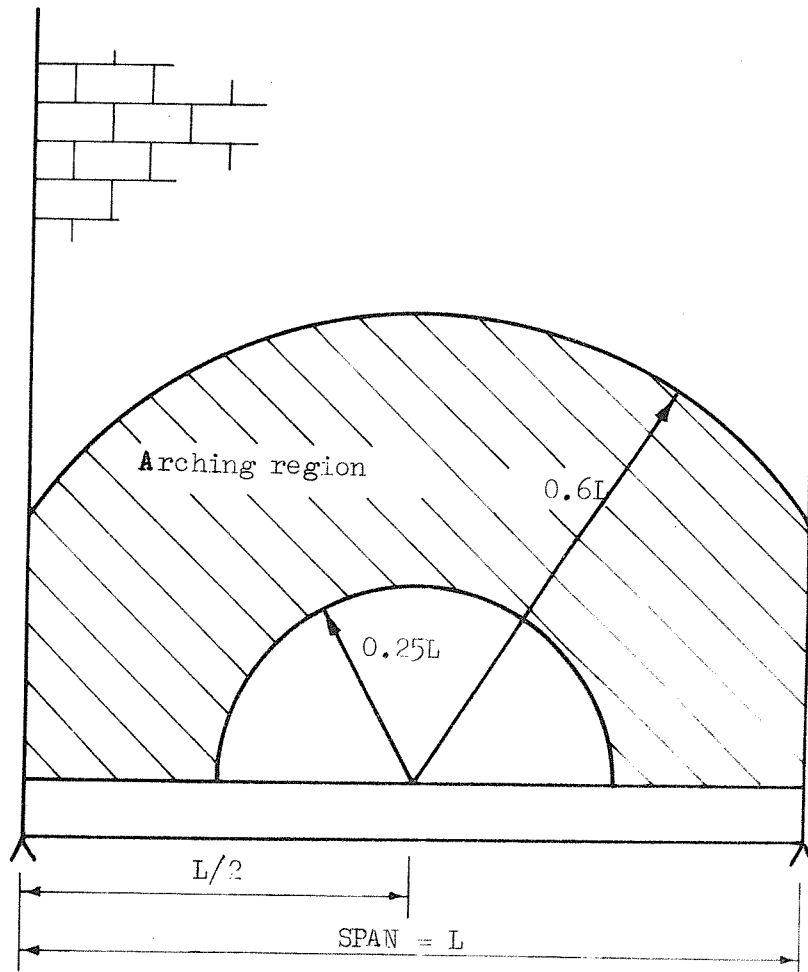
FIG. 3.10   ARCHING REGION — NO HOLES ALLOWED

its vertical axis and encased except when definite provision is made to transfer an outward thrust of $W_w/4$ from the ends of the wall to the beam.

(b) the beam shall be propped during construction and curing of the wall.

(c) the wall shall have a height/length ratio not less than 0.6 and shall be designed in accordance with CP 111.

(d) at the level of the base of the wall the resultant vertical line of action of the total wall load W_w must not lie outside the middle third of the span.

(e) the arching region shown in Fig. 3.10 must not be penetrated by holes. Holes are permitted in the wall above and below the arching region. However, in the case of holes above the arching region

 (1) the total width of openings at any horizontal cross-section must not exceed one-third of the span.

and (2) the portions of the wall left standing must individually satisfy the requirements of CP 111.

Notation

W_w — self weight of wall + superimposed load on wall, multiplied by appropriate collapse limit state load factors

W_s — self weight of beam + total slab load, multiplied by appropriate collapse limit state load factors.

p_{st} — steel characteristic strength $\div$ collapse limit state stress factor

p_b — (brickwork or blockwork characteristic strength $\div$ collapse limit state stress factor) multiplied by local allowable stress concentration factor, which is given in CP 111 as 1.5.

L   -   span of beam

t   -   thickness of wall.

Design procedure

Any consistent set of units may be used in Eqs. 3.65, 3.66 and
3.67. In Fig. 3.5, W_w/L is in KN/m.

The procedure is as follows:

(a)   Select a steel beam section to satisfy the permissible brickwork
(or blockwork) stress using

$$I \nless \frac{W_w^4}{9.5Lt^3p_b^4} \qquad \ldots \; 3.65$$

(b)   Check the adequacy of the selected section for bending stress
using

$$Z \nless \frac{W_w^2}{3.6p_{st}p_bt} + \frac{W_sL}{8p_{st}} \qquad \ldots \; 3.66$$

If Z is adequate, proceed to steps (d) and (e).

If Z is not adequate, proceed to step (c).

(c)   Use Fig. 3.5 to find the value of K appropriate to W_w/L, t and
p_{st}, interpolating if necessary.   Select a new section to satisfy
the bending stress using

$$Z \nless \frac{W_wL}{4Kp_{st}} + \frac{W_sL}{8p_{st}} \qquad \ldots \; 3.67$$

In this case the wall stress will be below the maximum permissible
value and need not be considered. Proceed to steps (d) and (e).

(d)   If necessary increase the depth of the steel section to give a
minimum depth/span ratio of 1/25 ensuring that the values of I
and Z are not reduced.

(e) Check the steel section for adequacy against vertical shear.

3.6 Conclusions

The main conclusions from this chapter can be summarized as follows:-

(1) The design of masonry walls on encased steel beams, subjected to vertical loading, can be simply achieved by using either the third or fourth design method.

(2) The fourth design method should be used when the supporting beam is subjected to floor loading in addition to the wall loading. When there is no floor loading, either the third or fourth design method can be used.

(3) These design methods should provide conservative designs, provided the provisions given in Section 3.5.5 are followed.

CHAPTER 4

WALLS ON BEAMS: COMPUTER ANALYSES

4.1 Introduction

This chapter is concerned with the numerical stress analysis of wall on beam structures. For the basic wall on beam problem, where the wall is of the same length as the beam and the beam is simply supported at its ends, separation cracking is known to occur between the wall and beam in the midspan region. In order to produce anything approaching an accurate elastic analysis of these structures, the analysis method must make allowance for this cracking.

The finite element programs developed in this chapter allow for the automatic generation of this separation crack. Using these programs, analyses were undertaken to study the behaviour of the basic wall on beam structure and thus check the validity of the design method developed in Chapter 3. Finally a brief investigation was made of the behaviour of more complicated wall on beam structures.

4.2 Development of finite element computer programs to analyse wall on beam problems

4.2.1 Introduction

Two separate computer programs were developed to analyse wall on beam structures. The main difference between the programs was the procedure used to represent separation cracking on the wall-beam interface. The first program was in the Algol computer language and in this program, cracking was represented by reducing the modulus of elasticity of wall-beam interface elements to zero. The second program was in Fortran language and in this program, cracking was represented by separating nodes on the wall-beam interface. Both programs were developed specifically to analyse wall-on-beam structures where both the loading and structure were symmetric about the vertical through the centre of span. To reduce computer store requirements, only the left hand half of the structures were analysed. Throughout the research period, the programs were being both modified and improved.

4.2.2 Algol program

This program was based on a program originally written by Choudhury[17]. It used the basic four node rectangular element with two degrees of freedom per node and linearly varying displacement functions along the boundaries of the form

$$u = A_1 + A_2 x + A_3 y + A_4 xy \qquad \ldots \quad 4.1$$
$$v = A_5 + A_6 x + A_7 y + A_8 xy \qquad \ldots \quad 4.2$$

The program supplied the solution in the form of the u and v displacements for each node, together with the centroid stresses. The stresses calculated were the horizontal, vertical and shear stresses

as well as the direction and magnitude of the principal stresses.

The program was of a form that enabled it to analyse brickwork, i.e. elements of two different elastic properties, representing brick and mortar, could be combined together.

The first alteration made to the program was to allow it to read in two more values of elastic modulus. The first was to represent the beam material and the second to represent the separation crack above the beam. The separation crack was represented by elements of extremely low modulus of elasticity.

The procedure consisted of analysing the structure initially with no separation crack elements. The vertical stress results for the elements immediately above the beam were then checked for tension. Separation crack element properties were introduced into the elements where tension occurred and the structure was reanalysed. The process was repeated until no more tension elements developed.

At this stage a few analyses were undertaken, but the inconvenience of the manually performed iteration procedure led to the next development of introducing an automatic iteration process. Also at this time a new type of finite element was introduced into the program. This new element, developed by Lau[18], was expected to give improved accuracy with the same number of degrees of freedom. It was a hybrid type four node rectangular element, based on the generalised energy principal, with as before, two degrees of freedom per node. Again linear displacement functions are assumed on the boundary, but internally independent linear direct stress functions are taken. The shear stress is taken as being constant over the element.

Several analyses were undertaken to test the new element against the previous element. These analyses seemed to indicate that the new

element did give slightly improved results, which was shown by
increases in beam deflection and stress concentration in the wall
above the supports.

Using the program in this form, with the new element and the
automatic generation of the separation crack, several further analyses
were undertaken. These mainly represented the plaster model tests
described in Section 5.2. The aim of these analyses was to obtain a
comparison between the experimental and theoretical results.

At this stage, it was decided to try a different method of
representing the separation crack. If the nodes could be separated
where the tension occurred, then possibly a more accurate result would
emerge, than that obtained at present by effectively removing the
elements above the beam. It was also considered desirable to switch
to Fortran because the majority of the other work in the department
was being conducted in Fortran.

For the above two reasons, a completely different Fortran program
was developed.

4.2.3 Fortran program

This program was based on a finite element program developed
initially by Lau[18]. In its original form, rectangular elements of the
new type were used. The program allowed for only one size of elements
with one material property. The solution was given for the x and y
displacements for each node together with the averaged stresses at the
nodes which included the principal stresses with their directions.

Several major modifications were required. The first was to
adapt the program to allow for different sized elements with different
material properties to represent brick, mortar and beam elements. The

next stage was to introduce a routine to create the separation crack by separation of nodes. It was desirable to achieve the separation of nodes without a complete renumbering. If two sets of nodes were introduced along the wall-beam interface and one set not used until separation, the result would be a greatly increased bandwidth in the stiffness matrix which was very undesirable. This is illustrated in Fig. 4.1. The method chosen to overcome these problems is now described. The structure was initially separated along the wall-beam interface with a different set of nodes for each side. A linking matrix was then introduced directly into the stiffness matrix for each pair of nodes to be joined. The linking matrix effectively represented a short, very stiff member that connected the two nodes. This forced the two nodes to have equal displacements. The positioning of the linking matrix in the stiffness matrix is shown in Fig. 4.2. To separate the nodes, the linking matrix was removed from the nodes concerned.

At this stage, problems developed regarding the use of nodal stresses. When nodal stresses were printed out before they were averaged, in a test problem, large differences were noticed in the stresses for the nodes on the wall-beam boundary. After averaging, a wave effect was noticed for the stress perpendicular to the wall-beam boundary as shown in Fig. 4.3. This was known to be incorrect. At the time this was thought to be due to the fact that the nodes were connected to elements of different material properties. On the boundary where two elements of different properties are joined, the stress should be continuous across the boundary, while the strain should be continuous parallel to the boundary. Later findings indicated that the type of element was probably at fault, but this was not suspected at the time.
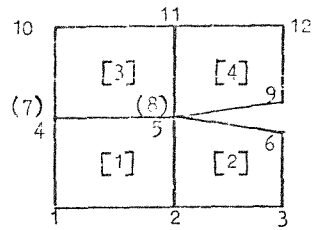
Element	(1)	(2)	(3)	(4)
[1]	1	2	5	4
[2]	2	3	6	5
[3]	4	5	11	10
[4]	5	9	12	11

Fig. 4.1   Effect on stiffness matrix band width of using dummy nodes

Connectivity Table

Element	(1)	(2)	(3)	(4)
[1]	1	2	5	4
[2]	2	3	6	5
[3]	7	8	11	10
[4]	8	9	12	11

	1	2	3	4	5	6	7	8	9	10	11	12
1	$K_{1,11}$	$K_{1,12}$	0	$K_{1,14}$	$K_{1,13}$	0	0	0	0	0	0	0
2		$K_{1,22}$ $K_{2,11}$	$K_{2,12}$	$K_{1,24}$	$K_{1,23}$ $K_{2,14}$	$K_{2,13}$	0	0	0	0	0	0
3			$K_{2,22}$	0	$K_{2,24}$	$K_{2,23}$	0	0	0	0	0	0
4				$K_{1,44}$ $+C_1$	$K_{1,43}$	0	$-C_1$	0	0	0	0	0
5					$K_{1,33}$ $K_{2,44}$ $+C_2$	$K_{2,43}$	0	$-C_2$	0	0	0	0
6						$K_{2,33}$	0	0	0	0	0	0
7							$K_{3,11}$ $+C_1$	$K_{3,12}$	0	$K_{3,14}$	$K_{3,13}$	0
8								$K_{3,22}$ $K_{4,11}$ $+C_2$	$K_{4,12}$	$K_{3,24}$	$K_{3,23}$ $K_{4,14}$	$K_{4,13}$
9									$K_{4,22}$	0	$K_{4,24}$	$K_{4,23}$
10										$K_{3,44}$	$K_{3,43}$	0
11											$K_{3,33}$ $K_{4,44}$	$K_{4,43}$
12												$K_{4,33}$
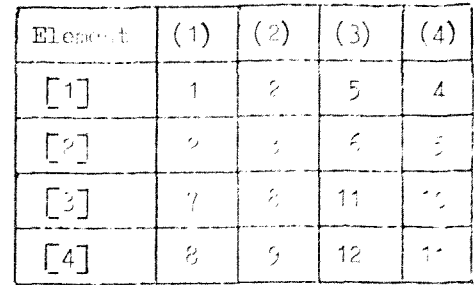
Fig. 4.2 Positioning of elements of linking matrices in stiffness matrix.

Beam span = 10 m.
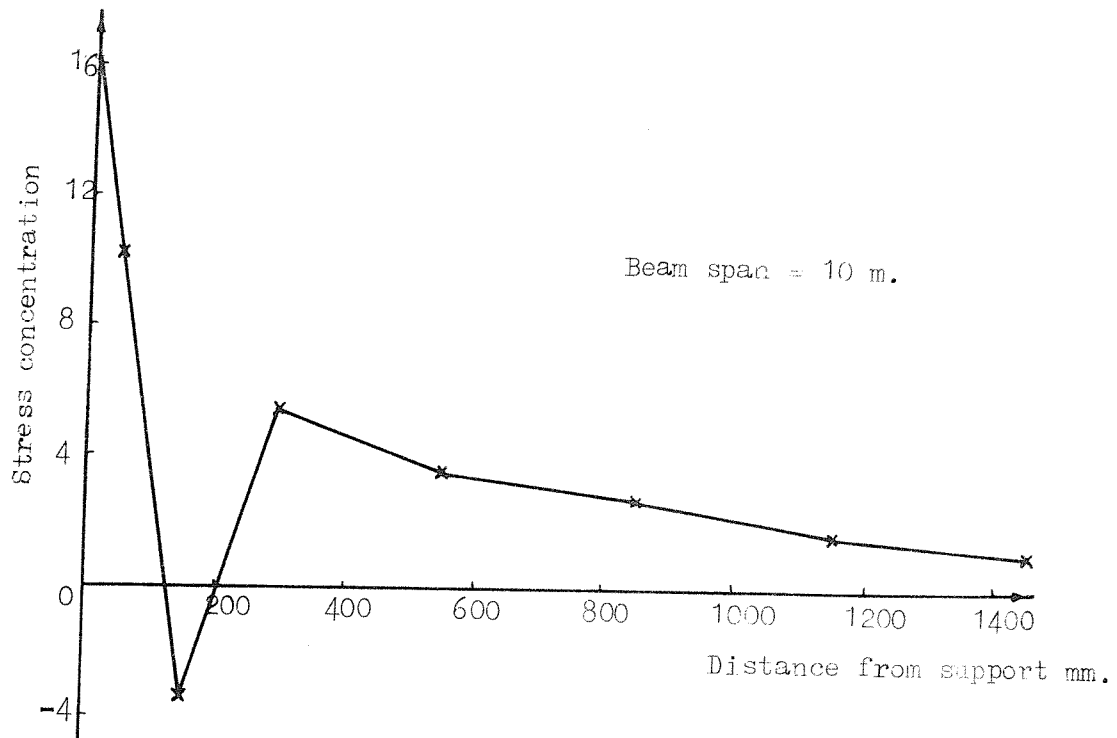
Fig. 4.3   VERTICAL STRESS ON WALL BEAM INTERFACE FOUND
            WHEN USING LAU TYPE FINITE ELEMENT

Wall height = 10 m.
Beam span   = 10 m.

Horizontal distance
from support mm.
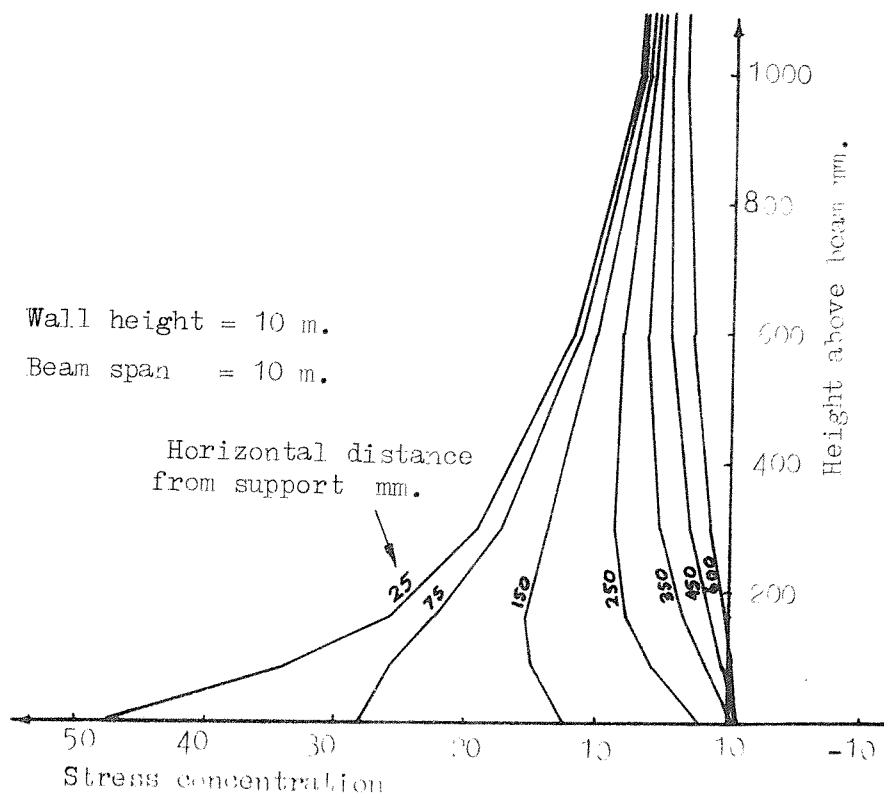
FIG. 4.4   VERTICAL STRESS DISTRIBUTION UP VERTICAL LINES

When the centroid stresses of the elements immediately above the wall-beam interface were calculated, the wave effect was not apparent. The centroid stresses were thus thought to be a suitable reference for the stresses on which the separation cracking could be based.

The separation crack was formed automatically by first analysing the structure with all nodes connected, and then starting from the centre of the beam, the elements above the beam were checked for vertical tensile stress. If a tension element was found, the node pair towards the centre of the beam were disconnected. This was continued until a compression element was found. The analysis and separation was repeated until no further elements became tensile. It was found to be necessary to check only the elements still connected, because the elements where separation had already occurred often changed to slight compression.

Using the program in this form, about thirty analyses were undertaken in which the parameters affecting the basic wall on beam problem were studied. Also several analyses were completed which reproduced the tests conducted at the Building Research Establishment and at the University of Southampton. These tests are described in Chapter 5.

It was found that the results from some of these analyses were dependent on the element grid adopted. This was due to the fact that the stresses change very rapidly close to the wall-beam interface as shown in Fig. 4.4. The length of separation in the analyses could be affected by both the vertical and horizontal distance of the element centroids from the wall-beam interface nodes. Also, because wall stresses vary very rapidly near the support, the centroid stress of the wall element closest to the support did not give a good indication of the peak wall stress.

Several different quadratic and cubic interpolation and extra-

polation functions were introduced into the program to try to solve the problem. The method which gave the most consistent results for different grids was based on a cubic function. The cubic function was first used to extrapolate the vertical stresses from the first four elements above the beam down to the wall-beam interface. This gave the vertical stress values on the wall-beam interface, centrally between the nodes. A cubic interpolation function was then used on these values to estimate the vertical stresses at the nodes. Separation of a node was undertaken when either the estimated nodal vertical stress or the central vertical stress on the support side of the node was in tension.

Although this method of separation may appear rather approximate, the results obtained were very consistent with different element grids. So as to obtain a peak wall stress estimate, the cubic extrapolation function was used to calculate the stress at the wall-beam interface node immediately above the support. Another estimate of the peak wall stress was obtained by using quadratic functions in a similar manner to the cubic functions.

At this stage a further ten parameter study analyses were conducted. Some of these analyses were on structures with beams of high flexural stiffness. The results from these analyses again indicated a wave effect on the vertical stress distribution of the type shown in Fig. 4.3. The deflection curves of the beams also appeared to be improbable as shown in Fig. 4.5. The reason for these results was traced to the type of finite element being used. One disadvantage of Lau's rectangular finite element is that the shear stress is constant over the whole element. In the basic rectangular element, the shear stress varies linearly over the element. In most problems, the constant shear stress characteristic caused no obvious errors, but unfortunately in the analyses where the beams had high flexural stiffness, the constant

Distance from support m.
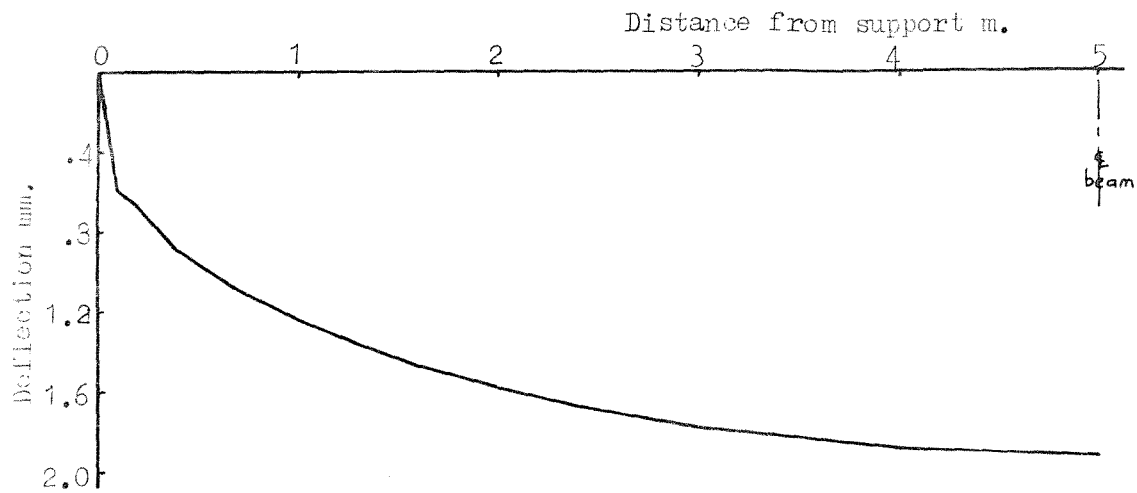
FIG. 4.5 BEAM DEFLECTION CURVE FOUND WHEN USING LAU TYPE FINITE
ELEMENT
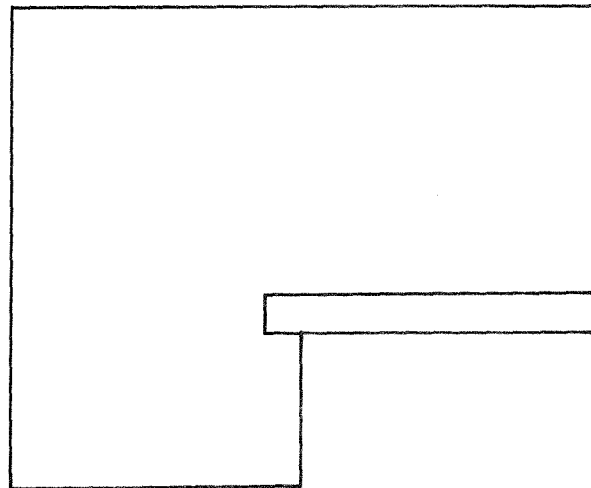
FIG. 4.6 FORM OF STRUCTURE THAT COULD BE ANALYSED BY THE WALL
ON BEAM COMPUTER PROGRAM
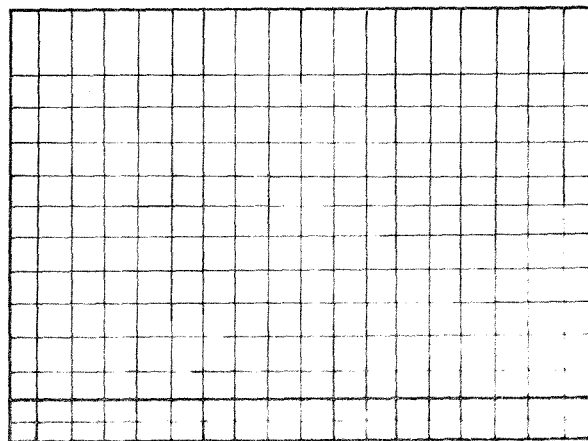
FIG. 4.7 FINITE ELEMENT MESH USED IN COMPARISON
PROBLEM ANALYSIS

shear stress failed to represent accurately the stresses close to the support. On further consideration, it was realised that the vertical stress wave effect, noticed when using nodal stresses, was also likely to have been caused by the shear stress characteristic of the finite element.

Due to the above problems, it was decided to revert back to the basic rectangular finite element . This was relatively simple, requiring only changes in the element stiffness and stress matrices. It was decided to continue using centroid stresses, because there was still doubt about the accuracy of averaging nodal stresses on the wall-beam boundary. Also the cubic functions appeared to give a good estimate of the peak wall stress. This estimate was likely to be better than that obtained using nodal stress, because the stress along the boundary of the element was represented by a linear function.

With the program in this form, approximately twenty parameter study problems were analysed. These analyses were mainly repeats of analyses undertaken using the other finite element. Less analyses were required because information was already available on which problems to study and which element grids to use.

Two final modifications were made to the program. In the first, the program was altered so that it could analyse structures of the type shown in Fig. 4.6, and in the second, the program was modified so that the moments and tie forces along the length of the beam could be automatically calculated and printed out.

4.3 Comparison of present analysis method with earlier analyses.

4.3.1 Earlier methods of analysis

Rosenhaupt[4-6], Coull[7], Colbourne[8] and Green[12,13] all attempted to analyse wall on beam structures using methods described in Chapter 2. Rosenhaupt used the Airy stress function and solved the resulting differential equations by the method of finite differences. He simplified the problem by assuming that the bending stiffness of the beam was negligible compared with that of the wall. Unfortunately this has the effect of eliminating the normal stress between the wall and beam, which results in the entire load being transferred through the bottom corners of the wall. Rosenhaupt's finite difference solution for the stress at the wall corners was thus dependent on the mesh size, since an exact solution would produce singularities at these corner points. For this reason, no comparison is given here between Rosenhaupt's method of analysis and the present method.

Coull used the method of Kanotorvich to minimise the energy of the system and thus obtain a solution to the problem. The stresses in the wall were expressed as a power series in the horizontal direction with the coefficients being functions of the height only. Colbourne used finite differences and Green used finite elements to obtain their solutions. In all of these solutions no separation was allowed on the wall-beam interface.

4.3.2 Comparison of results

The same problem had been analysed by Coull, Colbourne and Green. It was thus convenient to analyse this problem using the present computer program in order to get a comparison between the various solutions. The final version of the program was used in this comparison analysis

i.e. the Fortran program with the normal rectangular finite element.

The dimensions of the structure analysed were: wall height 72 in.; wall breadth 108 in.; wall thickness 4.5 in.; beam depth 8.592 in.; beam width 4.5 in. The ratio of the modulus of elasticity of the beam to that of the wall was taken as 30. A vertical compressive stress of 1 lb/in^2. was applied at the top of the wall. In the previous analyses the wall was split into 6 in. square elements. The same mesh was adopted for the present analysis except that the top row of elements was made 12 in. high so that the computer store requirement was reduced. Two rows of elements were taken in the beam. The mesh is shown in Fig. 4.7.

A comparison between the various solutions is shown in Figs. 4.8, 4.9 and 4.10. The results from Coull's, Colbourne's and Green's analyses were originally plotted by Green. The results from the present analyses were plotted from the no separation analysis since these results were comparable with the earlier analyses. For the stress distribution on the wall-beam interface, the extrapolated stress results were used.

Coull's results differ considerably from all the other results in the region close to the wall-beam interface. In deriving his solution, Coull only took the first two terms of the power series assumed for the vertical stress distribution, and as a result restricted the stress distribution curve to that of a parabola. Unfortunately, as can be seen in Fig. 4.8, the true stress distribution is not paraboloidal and this accounts for the differences.

Figs. 4.8, 4.9 and 4.10 indicate excellent agreement between the present analysis and Colbourne's and Green's analyses. As well as to some extent verifying the present finite element program, the results also indicate that the cubic extrapolation functions operate reasonably accurately. This is important because the separation crack is formed using these results.
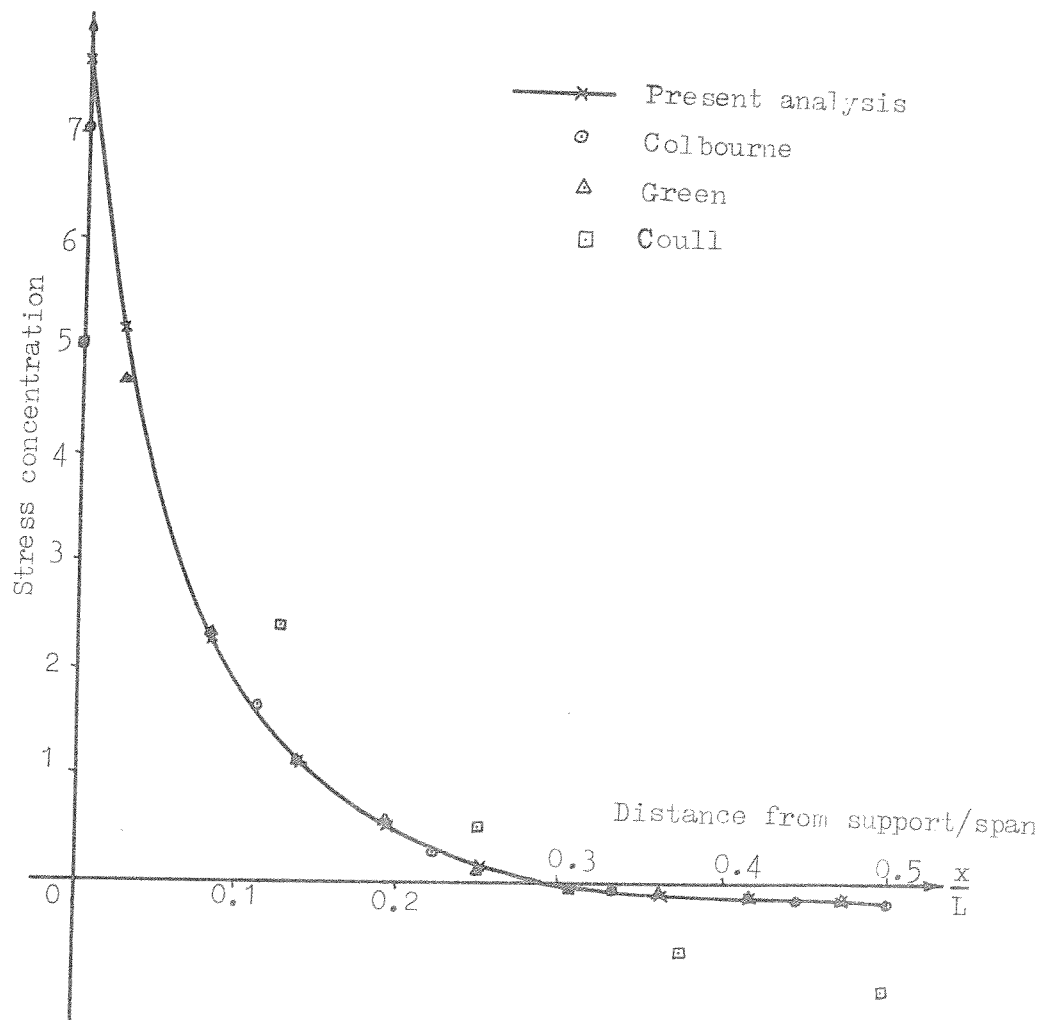
FIG. 4.8 VERTICAL STRESS DISTRIBUTION AT WALL-BEAM INTERFACE
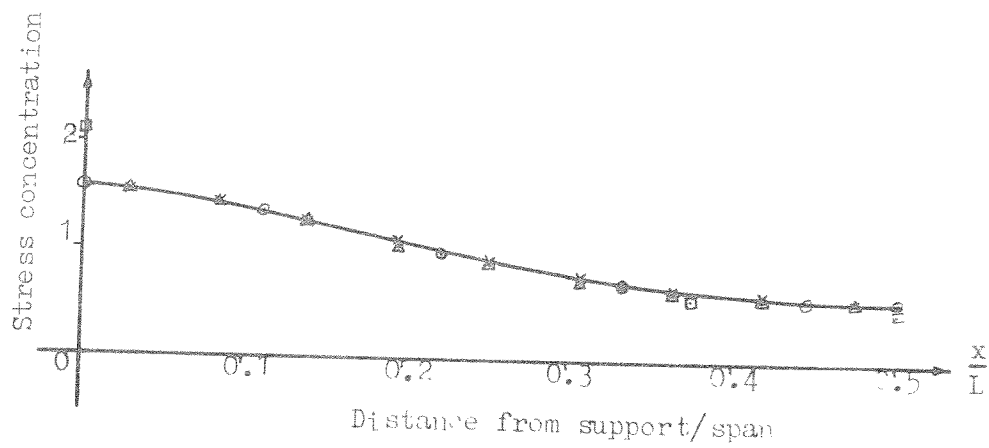
FIG. 4.9 VERTICAL STRESS DISTRIBUTION AT HALF WALL HEIGHT
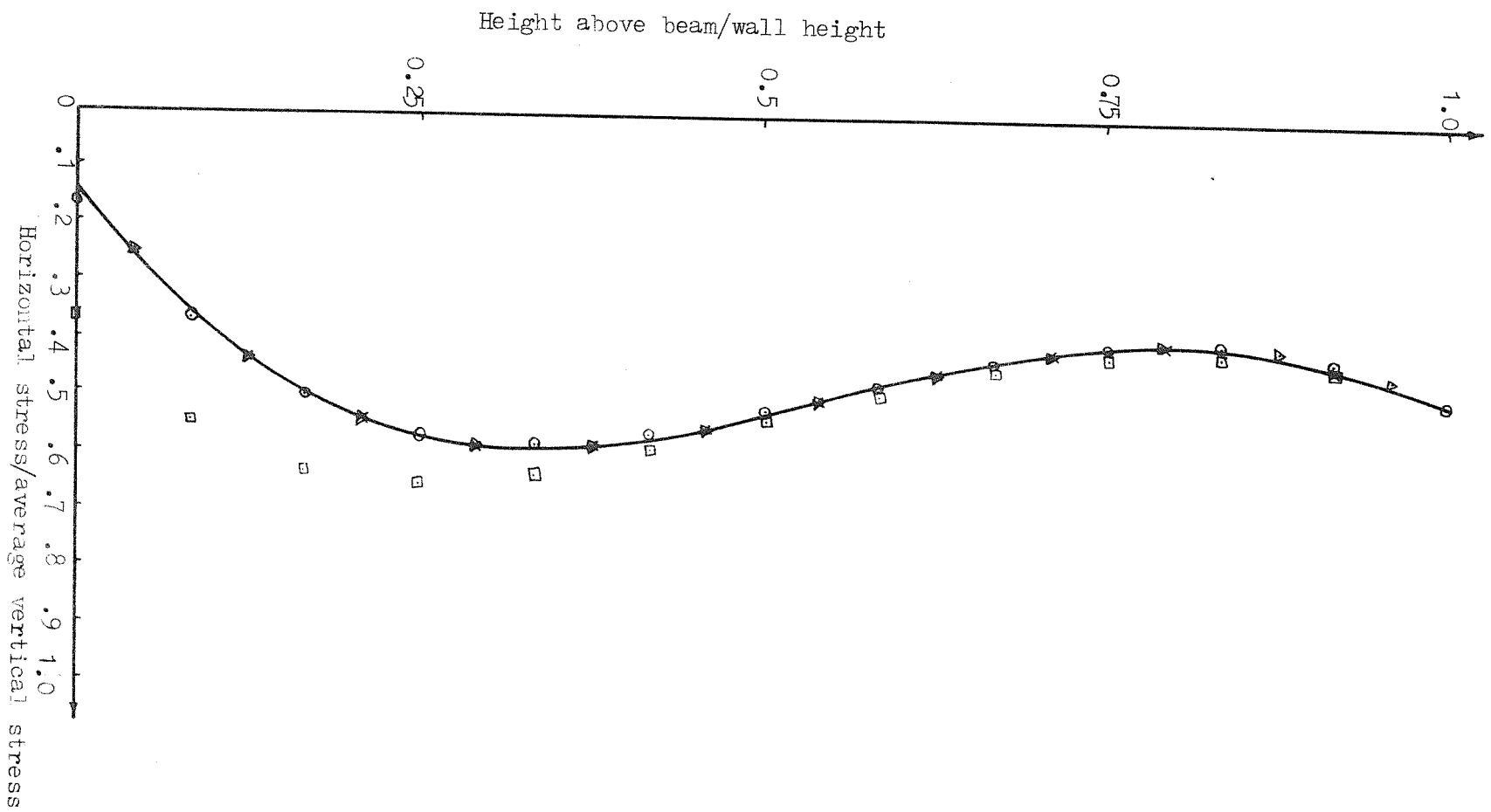
FIG. 4.10 HORIZONTAL MID-SPAN STRESS DISTRIBUTION

Height above beam/wall height

Horizontal stress/average vertical stress

68

4.4 Parameter study of the basic wall on beam structure

4.4.1 Introduction

A series of finite element analyses were undertaken to investigate the parameters controlling the behaviour of the basic wall on beam structure. The basic structure was taken as that of the wall being of the same length as the span of the beam with the beam being supported vertically without rotational restraint at each end. The loading was taken as vertical uniformly distributed loading at the top of the wall. This was the structure and loading assumed when developing the approximate design method described in Chapter 3. Although this representation of wall on beam structures may seem extremely simplified, the results for the peak wall stress, the peak beam sagging moment, tie force and deflection are conservative when compared with results obtained when the beam is built in, or the wall extends past the end of the span. The results of analyses of such structures are shown in Section 4.5 and indicate that the number of parameters controlling their behaviour becomes so great that no precise design recommendations can be given.

In this section, four parameters are considered to be possibly affecting the behaviour of the basic wall on beam structure. These are: the relative stiffness parameter K, the ratio of the elastic modulus of the beam to the wall, the relative height of the wall and the Poisson's ratios of the wall and beam.

4.4.2 Information gained from analyses using the Lau type finite element

As stated in Section 4.2.3, a considerably number of analyses of the basic wall on beam problem were undertaken using the version of the Fortran computer program that included the finite element developed by Lau. Although these results were not considered reliable enough to be

used quantitatively, they could be used to indicate the main parameters affecting the behaviour.

All the analyses had a beam span of 10 m, a wall and beam thickness of 100 m.m. and the wall was taken to be homogeneous with a modulus of elasticity of 10 KN/mm^2. A uniformly distributed load of 1000 KN was applied at the top of the wall. In the analyses the ratio between the beam and the wall modulus of elasticity was varied between 1 and 20. The beam depth was varied to give a range of K values between 5 and 30.

Four analyses were undertaken to establish the importance of the values taken for the Poisson's ratios of the wall and beam. Varying the Poisson's ratio between 0 and 0.25 was found to have little effect on the wall and beam stresses as can be seen in Table 4.1. Since the value of the Poisson's ratio was of little importance, a value of 0.15 was taken for both the wall and beam in all the future analyses. A Poisson's ratio value of 0.15, represents a typical value for brickwork and concrete.

In developing the approximate design method described in Chapter 3, the assumption was made that for wall heights greater than 0.6 x beam span, the structural behaviour was independent of wall height. Three analyses were undertaken with wall heights of 7 m, 10 m and 15 m and the results are also shown in Table 4.1. Again only small differences between the wall and beam stresses were revealed in the three analyses. The structural behaviour was thus considered to be independent of the wall height when this was greater than 0.6 x beam span. A wall height of 10 m was taken in all the later analyses.

Various finite element grids were tried before suitable grids were found. The grids had to give sufficiently accurate results, whilst being reasonably economical on computer time and store requirement. It

K	$\dfrac{E}{E_w}$	Notes	Estimated peak wall stress $\times 10^{-3} \mathrm{KN/mm}^2$	Beam stresses at centre of span	
				Bottom of beam $\times 10^{-3} \mathrm{KN/mm}^2$	Top of beam $\times\ 10^{-3} \mathrm{KN/mm}^2$
15	4	$\nu_{wall} = 0.15$ $\nu_{beam} = 0.15$	-19.6	8.62	2.94
15	4	$\nu_{wall} = 0.10$ $\nu_{beam} = 0.25$	-19.7	8.59	2.96
30	4	$\nu_{wall} = 0.15$ $\nu_{beam} = 0.15$	-38.9	9.76	7.76
30	4	$\nu_{wall} = 0.0$ $\nu_{beam} = 0.0$	-39.4	9.76	7.75
15	4	Wall height = 7 m	-19.6	8.68	3.03
15	4	Wall height = 10 m	-19.6	8.62	2.94
15	4	Wall height = 15 m	-19.6	8.62	2.94
5	4	2 rows of elements in beam	- 6.90	4.12	-1.04
5	4	4 rows of elements in beam	- 7.00	4.10	-1.06
5	1	2 rows of elements in beam	- 3.70	2.06	-0.35
5	1	4 rows of elements in beam	- 3.82	2.07	-0.38

Table 4.1   Finite element results for the basic wall on beam structure with the Lau type element.

was found to be perfectly adequate to have two rows of elements in the beams. Analyses undertaken with four rows of elements in the beam but with otherwise the same grid showed only marginal changes in wall and beam stress as shown in Table 4.1. In order to get accurate wall-beam interface stresses, the centroids of the elements above the interface had to be close to the interface. Also in order to estimate the end of the separation crack and the peak wall stresses accurately, the horizontal nodal spacing needed to be short in the support region. The grids finally adopted for most of the analyses had 156 elements with 12 elements across the half span. One of the grids finally adopted is shown in Fig. 4.11. It can be observed that some of the elements in the grid shown in Fig. 4.11 are far from square, which is not normally recommended when using rectangular finite elements. No obvious errors due to element shape were shown up when analyses with finer grids and squarer elements were undertaken for comparison purposes. The lack of significant errors is probably due to the fact that the elements with the highest length to breadth ratios were generally in areas of low stress gradient with the major principal stress running approximately parallel to the longest side.

4.4.3 Analyses of basic wall on beam structures using the final version of the computer program

Using the final version of the computer program, which included the normal four node rectangular element, a series of analyses were undertaken to study the behaviour of the basic wall on beam problem in relation to the two main controlling parameters, K and E/E_w. The earlier analyses had indicated that although the main controlling parameter was the K value of the system, which represented the relative
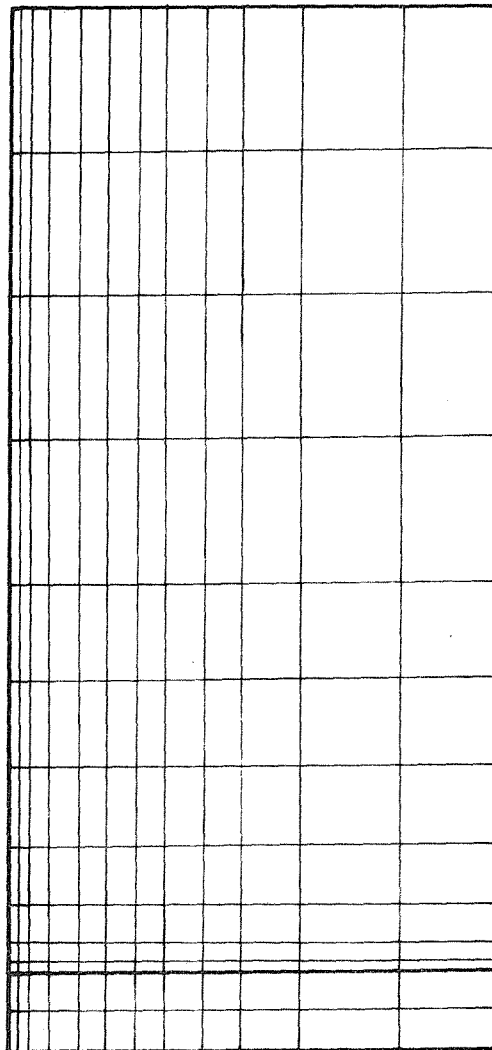
FIG. 4.11 TYPICAL FINITE ELEMENT GRID USED IN
WALL ON BEAM ANALYSES

stiffness of the wall to the beam, the ratio of the modulus of elasticity of the wall to the beam was also important. This modulus of elasticity ratio was important because for the same K value, the axial stiffness of the beam was varied by the modulus of elasticity ratio, which in turn affected the tie action of the beam.

The dimensions of the structures considered were: wall height and span 10 m, and wall and beam thickness 0.1 m. The wall had a modulus of elasticity of 10 KN/mm^3 and both wall and beam had Poisson's ratios of 0.15. The depth of the beam and its modulus of elasticity were varied to give the desired values of K and E/E_w. A uniformly distributed load of 1000 KN was applied at the top of the wall.

In the design method, described in Chapter 3, the bare steel beam depth was restricted to L/25. Trial calculations on various spans indicated that this restriction limited the K value to below 15. The K value for reinforced concrete beam systems would also be unlikely to exceed 15 because here again some minimum beam size restriction would be required to prevent excessive self weight deflection. The analyses were thus conducted for a range of K values between 2.5 and 15 in steps of 2.5. The K value of 2.5 represented extremely stiff beams and it was considered unlikely that anything stiffer would ever be used.

Two modulus of elasticity ratios were considered, of 4 and 30 for the whole range of the six K values. For three of the K values, additional analyses were conducted with modulus of elasticity ratios of 1 and 20.

From the analysis for K = 5 and E/E_w = 4, the compressive principal stress results, after separation, were plotted over the area of the wall as a proportion of the applied vertical stress as shown in Fig. 4.12.

5 4 3 2   1   0·5
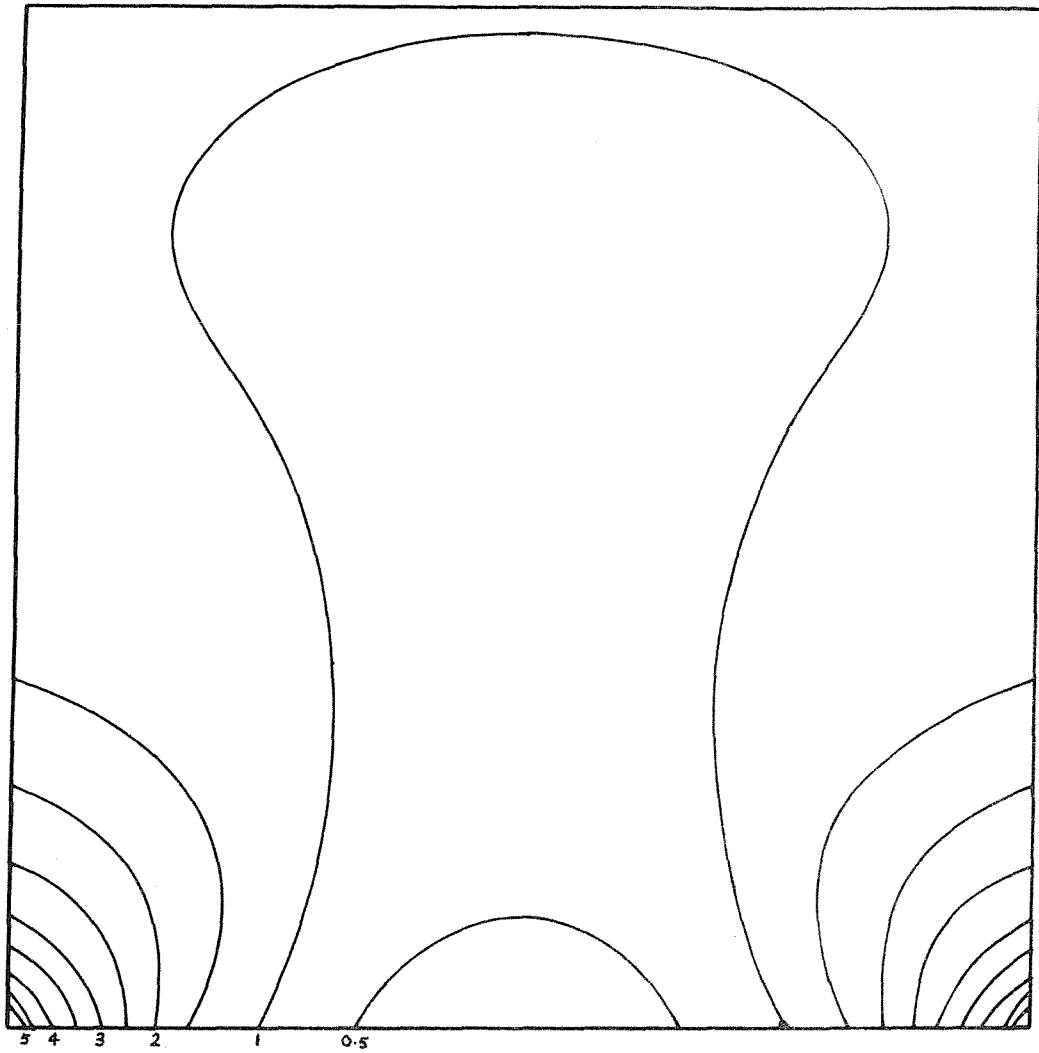
FIG. 4.12 PRINCIPAL COMPRESSIVE STRESS CONTOURS IN THE WALL OF A
          WALL ON BEAM STRUCTURE

The stress pattern clearly indicates the basic wall on beam behaviour with the wall arching between the supports and stress concentrations forming in the wall corners.

The work on the design method described in Chapter 3 had indicated that the main information required from the analyses was the peak compressive wall stress, the peak beam moment and tie force, and the central beam deflection. The peak tie force and moment were calculated in non dimensional form. For the tie force, the value k_1 was calculated where the tie force $T = W_w/k_1$, and for the moment, the value k_2 was calculated, where the moment $M = W_w L/k_2$. The peak wall stress was calculated in terms of stress concentration compared with the average applied stress at the top of the wall.

The results from the analyses before and after separation are shown in Tables 4.2 and 4.3. It will be seen that the effects of separation become more noticeable as the K value increases as might be expected. The separation effects also increase as the E/E_w ratio reduces for any K value. A reduction in the E/E_w ratio produces a reduction in the axial stiffness of the beam if the K value and thus the flexural stiffness is kept constant. The main effect of separation is to increase the peak wall stress and beam deflection. The maximum beam moment, which is generally located close to the supports, is reduced slightly by separation, while the centre span beam moment is considerably increased by separation. The maximum tie force, which is normally located close to the centre of span, is also usually reduced slightly by separation.

The main effect of increasing the K value is to increase the peak wall stress and deflection, whilst reducing the beam moments. The beam tie force tends to increase rapidly until full arching action occurs at

K	$\frac{E}{E_w}$	Peak wall stress concentration	k_1 (Tie force $= W_w/k_1$)	k_2 (Moment $= W_w L/k_2$)	Central beam deflection m.m.
2.5	4	2.56	7.47	15.5	0.75
2.5	30	3.74	7.42	14.6	0.37
5	1	3.68	4.24	36.8	3.12
5	4	6.92	3.75	50.4	1.54
5	20	9.48	3.57	49.1	1.20
5	30	9.79	3.59	47.7	1.18
7.5	4	11.00	3.92	91.4	2.01
7.5	30	15.32	3.42	92.0	1.58
10	1	9.16	5.30	92.0	4.06
10	4	15.43	4.26	123.2	2.31
10	20	20.29	3.59	108.7	1.83
10	30	20.78	3.50	103.1	1.79
12.5	4	20.22	4.57	171.0	2.57
12.5	30	27.30	3.63	148.7	2.01
15	1	15.46	5.21	164.3	4.58
15	4	25.43	4.33	227.2	2.80
15	20	33.01	3.94	223.4	2.27
15	30	33.73	3.76	217.5	2.21

Table 4.2   Wall on beam results before separation

K	$\frac{E}{E_w}$	Peak wall stress concentration	k_1 (Tie force $=W_w/k_1$)	k_2 (Moment $= W_w L/k_2$)	Central deflection m.m.
2.5	4	2.56	7.47	15.5	0.75
2.5	30	3.74	7.42	14.6	0.37
5	1	3.70	4.39	37.0	3.14
5	4	6.90	3.85	50.5	1.56
5	20	9.55	3.82	50.0	1.23
5	30	9.86	3.85	48.4	1.20
7.5	4	11.52	3.99	98.4	2.41
7.5	30	16.31	3.83	108.6	1.91
10	1	10.98	5.16	103.9	5.98
10	4	16.89	4.31	142.4	3.44
10	20	21.41	3.83	127.3	2.58
10	30	21.86	3.84	118.6	2.45
12.5	4	22.07	4.44	195.7	4.32
12.5	30	28.18	3.89	170.0	2.77
15	1	20.90	5.80	193.7	9.54
15	4	28.52	4.65	264.5	5.12
15	20	34.46	3.96	250.8	3.34
15	30	34.92	3.91	238.9	3.05

Table 4.3   Wall on beam results after separation

about K = 5. For higher K values the tie force reduces slightly as
the axial stiffness of the beam reduces and allows the arch to spread
further.

The effect of increasing the E/E_w ratio, and thus the beam axial
stiffness, for a constant K value, is to reduce the spread of the wall
arch. This is shown by increases in the peak wall stress and beam tie
force and reductions in the beam moments and deflection.

In Fig. 4.13 the moment values are plotted against K as a fraction
of a uniformly distributed load moment $W_w L/8$ and the tie force values
are plotted as a fraction of the applied load W_w. In Fig. 4.14 the
wall stress concentration factor values are plotted on a log graph
against a relative stiffness factor $E_w t L^3/EI$ or K^4. In Fig. 4.15, the
beam moment factor k_2 values are plotted on a log graph against K^4.

Since separation may not always fully occur in practice, due to
possible joint tensile strength, the most conservative values were
taken from the before and after separation values when constructing
Figs. 4.13 to 4.15. For the peak wall stress, the after separation
values were more conservative and for the beam tie force and moment,
the before separation values were usually more conservative.

The tie force results shown in Fig. 4.13 indicate that once the
composite action has become fully active at about K = 5, the tie force
remains reasonably steady for higher K values. Slightly higher tie
forces resulted from the analyses with the higher E_B/E_w ratio, as
might have been expected since the beams in these analyses had a higher
axial stiffness.

The tie force assumed in the design method of $W_w/4.4$ is apprec-
iably less than the analyses peak value of $W_w/3.4$. In Section 3.4.4 of
the third version of the design method, it was found that boundary
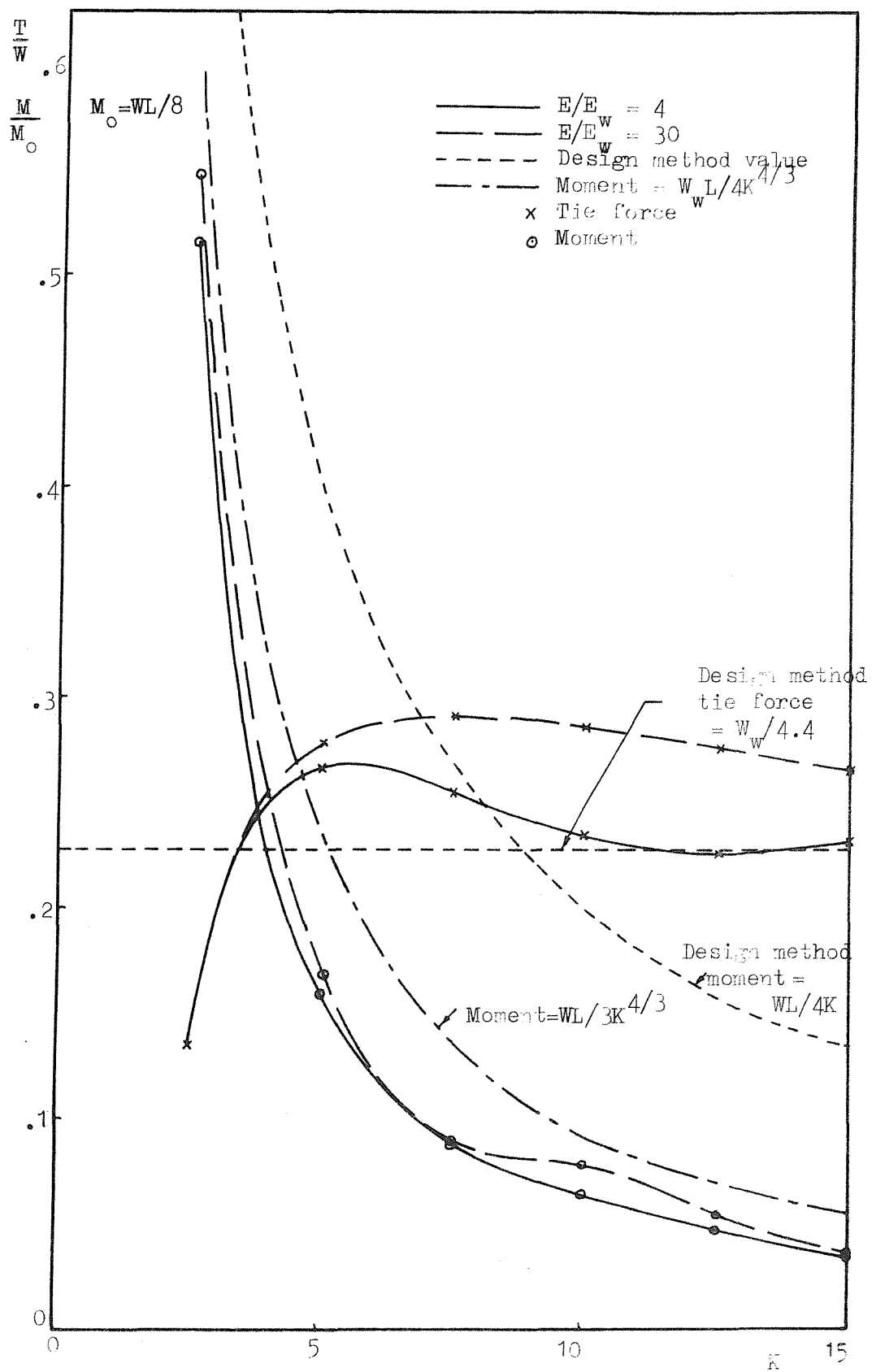
FIG. 4.13 WALL ON BEAM BASIC STRUCTURE RESULTS PLOTTED AGAINST K

FIG. 4.14   PEAK WALL STRESS RESULTS PLOTTED AGAINST LOG K^4

FIG. 4.15 PEAK BEAM MOMENT RESULTS PLOTTED AGAINST LOG K^4
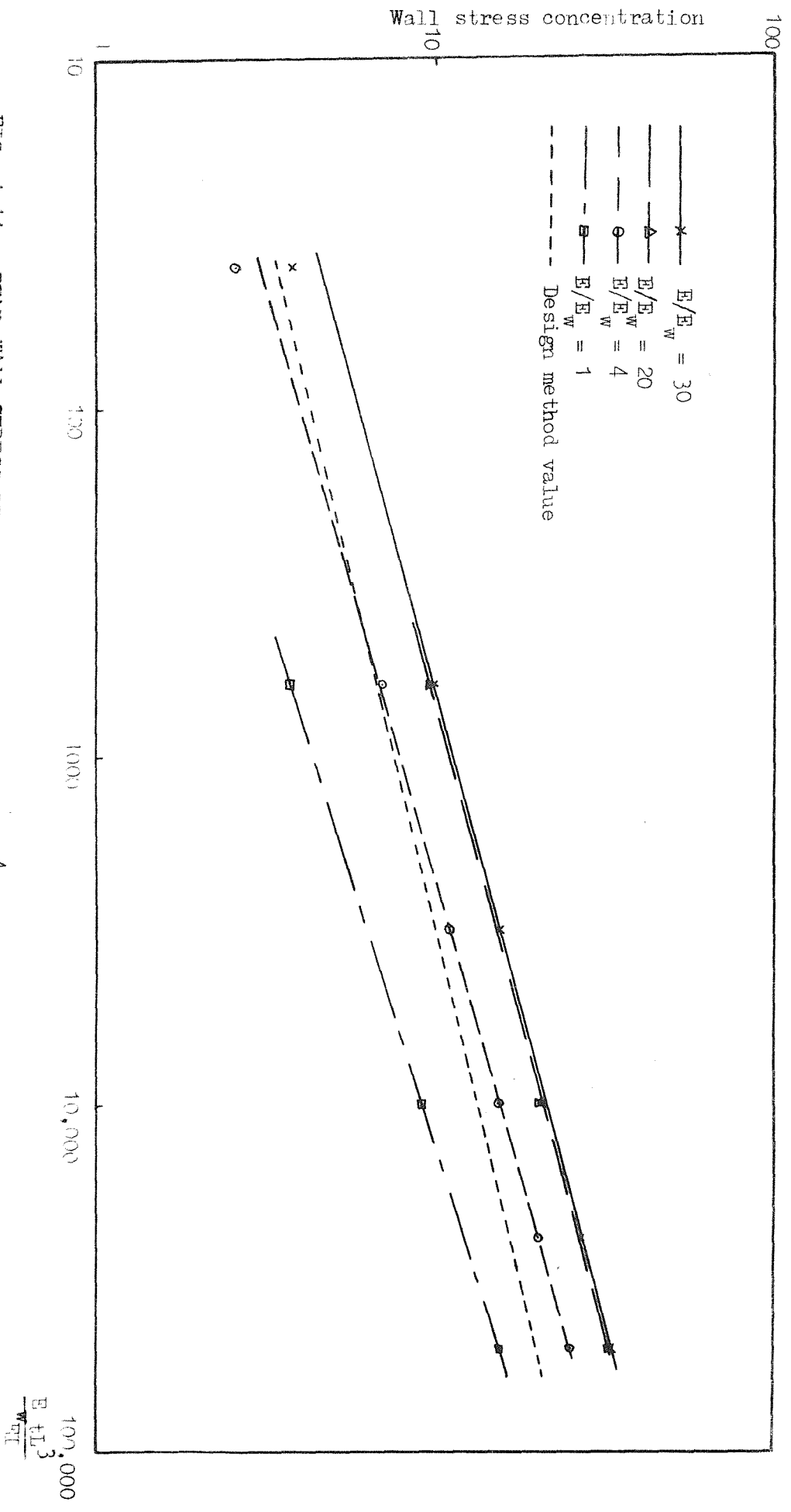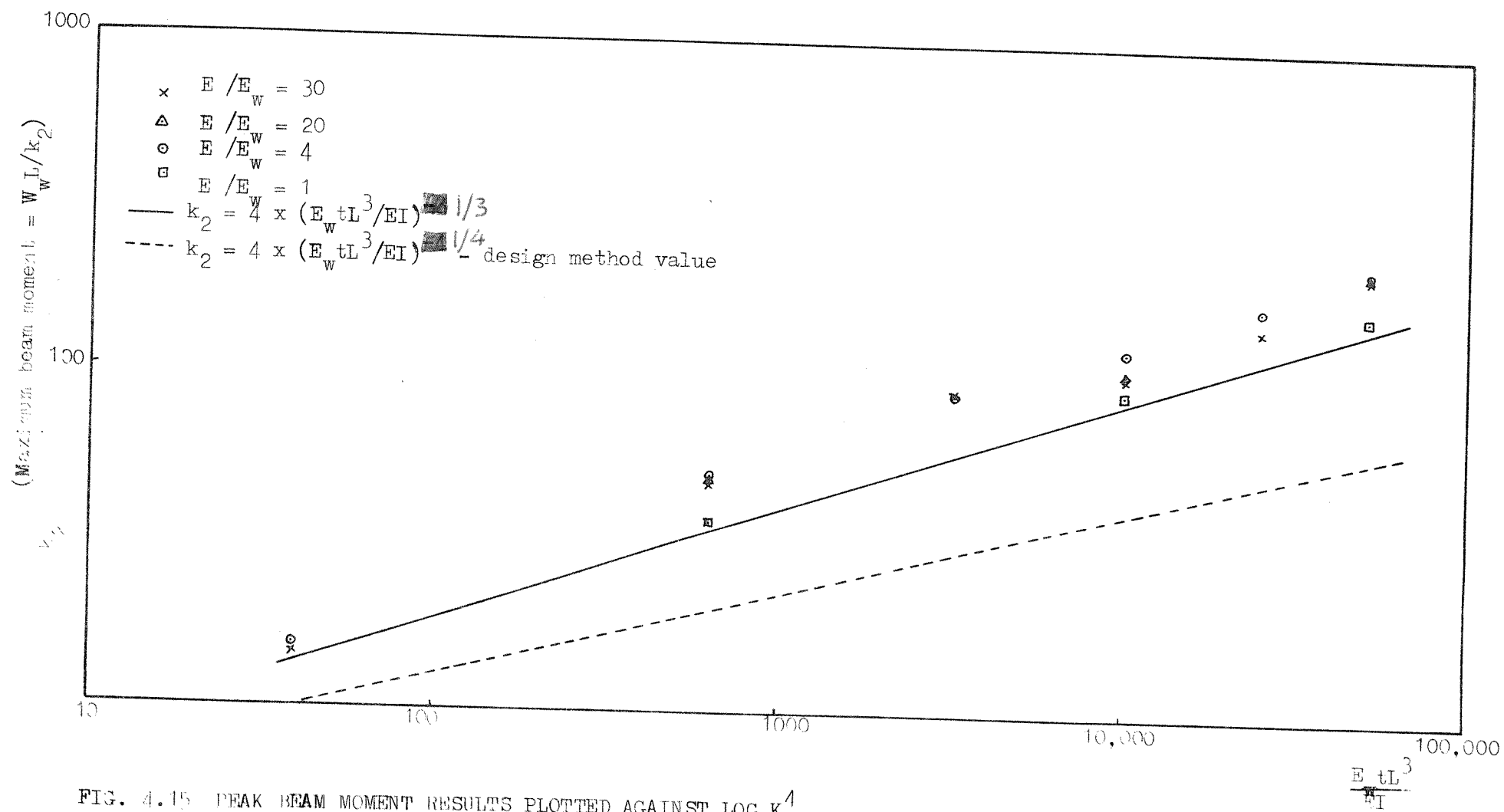
shear could be ignored if the beam was encased. This is still true with a tie force of $W_w/3.4$ because the available shear strength is still, from Eq. 3.52

$$f_s = f_{bs} + 0.67 \frac{W_w K'}{Lt} \qquad \ldots 4.3$$

while the new peak shear stress is given by

$$\tau = 0.59 \frac{W_w K'}{Lt} \qquad \ldots 4.4$$

Thus the analyses results do not affect the design method as regard to shear stress considerations. In any further work it would be conservative to assume a tie force value of $W_w/3.4$.

It can be seen from Figs. 4.13 and 4.15 that the design method estimate of beam moment is very conservative compared with the analyses moments. In the design method, however, no allowance is made for the tie force in the beam and the increase in stress due to this force has to be covered by the design moment stress. For a range of typical steel beam sections, calculations were undertaken to determine the percentage increase in stress that occurs in the beam, when the tie force is added to the analyses moments. It was found that this percentage value increased with K, so that for a K value of 15, the increase was in the order of 50%. The summed stresses were, however, still very conservative compared with the design moment stresses over the whole range of K values considered. Although it would have been possible to reduce the moment used in the design method, this was not considered worthwhile for the following reasons

(1) The $W_w L/4K$ design moment was already very economical compared with a uniformly distributed load moment, e.g. for $K = 10$, the design method moment is only 20% of the uniformly distributed load moment.

(2) When including beam level loading in the final version, of the design method, it was assumed that the the design method moment, due to wall loading, was conservative enough to absorb the increase in moment that resulted when the beam was stiffened to account for beam level loading. If the design moment was reduced, so that the design stresses matched the analyses stresses, the above assumption would be unsafe and some method of including the increase in moment would be needed.

(3) In many cases, the wall stress or the minimum beam depth restriction is the limiting factor in the design method, and in these cases, a reduction in the design moment due to wall loading would produce no economy.

If the peak beam moment alone is required, it can be seen from Figs. 4.13 and 4.15 that a conservative estimate of this is given by

$$W_w L/4 \ (E_w t L^3 / EI)^{1/3} \text{ or } W_w L / 4K^{4/3}$$

The wall stress concentration results are shown in Fig. 4.14. It will be seen that the analyses results are usually higher than the assumed design method values. The highest wall stresses were given by the analyses with $E/E_w = 30$. The equation best representing these results is:

$$\text{Stress concentration} = 1.63(E_w t L^3 / EI)^{1/3.6} \quad \ldots \quad 4.5$$

while the design method values are given by:

$$\text{Stress concentration} = 1.33(E_w t L^3 / EI)^{1/4} \quad \ldots \quad 4.6$$

Although the design could fairly easily have been altered to account for higher stress concentrations, this was not undertaken for the two following reasons:

(1) The design method values for stress concentration were taken from results of full size and model tests and were considered already con-

servative. The difference between the test and analytical results was thought to be due to the fact that compressive failure only occurred in the tests when the stress reached the compressive strength over a finite area, while in the analytical results, the stress is calculated at one extremely localised point.

(2) In practice, the wall is often continuous over the support and the beam usually has some rotational restraint, and both of these factors tend to reduce the peak wall stresses.

4.4.4 Conclusions

The main conclusion from this section can be summarized as follows:-

(1) Although the analyses results differed to some extent from the assumed design method values, none of the differences require any change in the design method.

(2) From the analyses results of the basic problem, the following factors can be estimated conservatively as

$$\text{Tie force} = W_w/3.4 \qquad \ldots \quad 4.7$$

$$\text{Beam moment} = W_w L/4(E_w tL^3/EI)^{1/3} \qquad \ldots \quad 4.8$$

$$\text{Wall stress concentration} = 1.63(E_w tL^3/EI)^{1/3.6} \qquad \ldots \quad 4.9$$

4.5 Analysis of other wall on beam problems

4.5.1 Introduction

The parameter study of Section 4.4 was concerned with the most basic wall on beam structure. This structure being a wall supported by a beam of the same length as the wall, with the beam being simply supported at its ends. In practice this situation will not often exist. The beam will usually have some rotational restraint at its supports due to either inbuilding into a wall or being connected with full or partial rigidity to supporting columns. In some cases the wall will be continuous over the support. The number of parameters controlling the behaviour of the structure under these conditions is high. The parameters which control the rotational restraint of the beam are: if the beam is inbuilt, the length of inbuilding and the height, properties and horizontal restraint of the wall below the support; if the beam is connected to columns, the rigidity of fixing and the properties and length of the columns. Other parameters affecting the structural behaviour include the length of the wall beyond the support and the height of the wall.

A comprehensive study of all of these parameters was outside the scope of this work. Instead, selected analyses were undertaken, varying some of the parameters, so that a qualitative, rather than quantitative understanding of the behaviour of these structures in relation to these parameters could be obtained.

4.5.2 Analyses and results

Fifteen analyses were undertaken in this part of the study. The results from the analyses are shown in Table 4.4. The notation for dimensions used in the analyses is shown in Fig. 4.16. In all of the

Analysis	Forms and Restraints	s m.	h mm.	Q m.	z' m.	Stress concentration	Central beam deflection mm.	k_1 ($T = W/k_1$)	Position *	k_2 (Sagging $M=WL/k_2$)	Position *	k_3 (Hogging $M=WL/k_3$)	Position *
Before 1 Separation		0	10	0	0	25.43	2.80	4.33	0.1	227	0.025	-	-
After 1 Separation		0	10	0	0	28.52	5.12	4.65	0.035	239	0.025	-	-
Before 2 Separation		0	5	0	0	25.80	3.07	4.39	0.5	227	0.063	-	-
After 2 Separation		0	5	0	0	28.36	4.95	4.31	0.5	260	0.083	-	-
3		.25	5	.25	0	11.18	2.23	4.42	0.5	769	0.083	-353	-0.006
4		.50	5	.50	0	6.43	2.00	4.46	0.5	1078	0.075	-335	0.006
5		.75	5	.75	0	5.84	1.89	4.45	0.5	1268	0.125	-328	0.013
6		.25	5	10	0	5.36	1.59	5.73	0.5	2044	-0.125	-394	0.013
7		.50	5	7	0	5.02	1.57	5.81	0.5	2144	0.125	-572	-0.013
8		.75	5	10	0	4.63	1.55	5.88	0.5	2167	0.125	-467	-0.013
9		.50	5	0	0	5.12	1.60	5.63	0.5	2023	0.125	-458	-0.013
10		.50	5	5	0	5.31	1.67	5.29	0.5	1943	0.125	-439	-0.013
11		.50	5	5	0	5.45	1.77	4.70	0.5	1870	0.125	-419	-0.013
12		.50	5	5	0	4.39	1.37	13.71	0.5	2420	0.125	-369	0.013
13		.50	5	5	5	2.99	2.73	7.68	0.5	3011	0.125	-1108	-0.013
14		.50	10	5	5	2.51	2.07	15.72	0.5	3721	0.1	-1572	-0.013
15		.50	10	5	5	2.43	2.42	6.16	0.5	3972	0.033	-2252	-0.013

* The position is given as the distance of the peak value away from the edge of the span as a proportion of the total span.

Table 4.4   Wall on beam analyses results
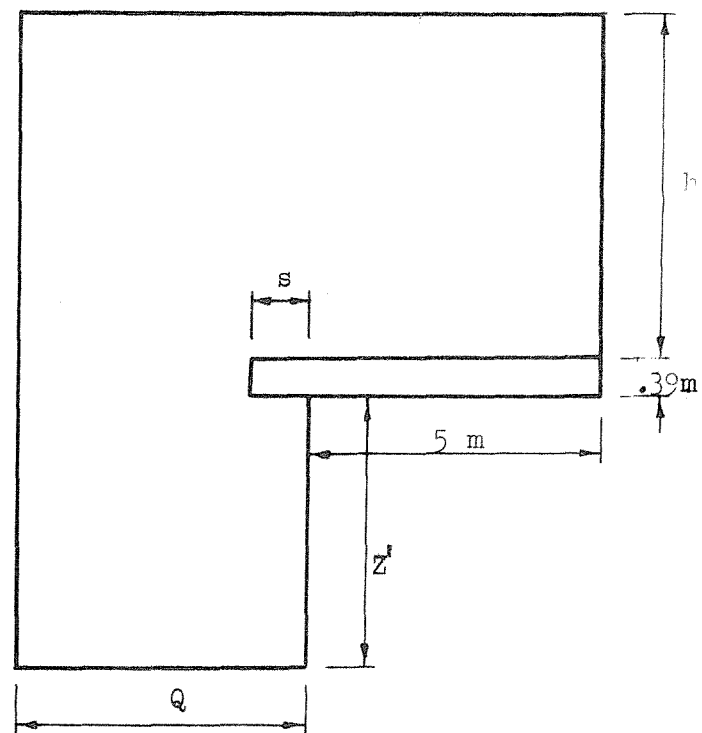
FIG. 4.16 NOTATION FOR TABLE 4.4

analyses the structures had a K value of 15 and an E/E_w ratio of 4. Analyses 1 and 2 were of the basic wall on beam structure with the two wall heights used in the other analyses. Analyses 3,4, and 5 were of a similar structure to the analysis 2 structure, except that differing lengths of vertical restraint were applied at the beam support. Analyses 6 to 11 were of structures with the wall extending past the support for differing lengths and with differing lengths of vertical restraint applied at the beam support. Finally analyses 13, 14 and 15 were of the most complicated structure with the wall extending both past the supports and down below the support.

In none of the analyses did any separation occur between the wall and beam, except in the two basic wall on beam structures (analyses 1 and 2). Comparing the analyses 3 to 15 results with the basic wall on beam analyses 1 and 2, some general trends are indicated. In all the analyses there is a reduction in peak wall stress concentrations and central beam deflections. There is also a reduction in the peak tie force with it always occurring at the centre of the span. In all of these analyses a hogging moment develops in the beam. The peak hogging moment exceeds the peak sagging moment, but this hogging moment is less than the sagging moment developed in the basic wall on beam structure. These peak moments develop in the beams at positions close to the support. These results indicate that a basic wall on beam analysis will give conservative results for these other structures, provided that an allowance is made for the hogging moment that is likely to develop close to the supports.

Fig. 4.17 shows the vertical stress in the wall above the beam for analyses 3, 4 and 5. In these analyses, the wall and beam were of the same length and the length of the support vertical restraint was
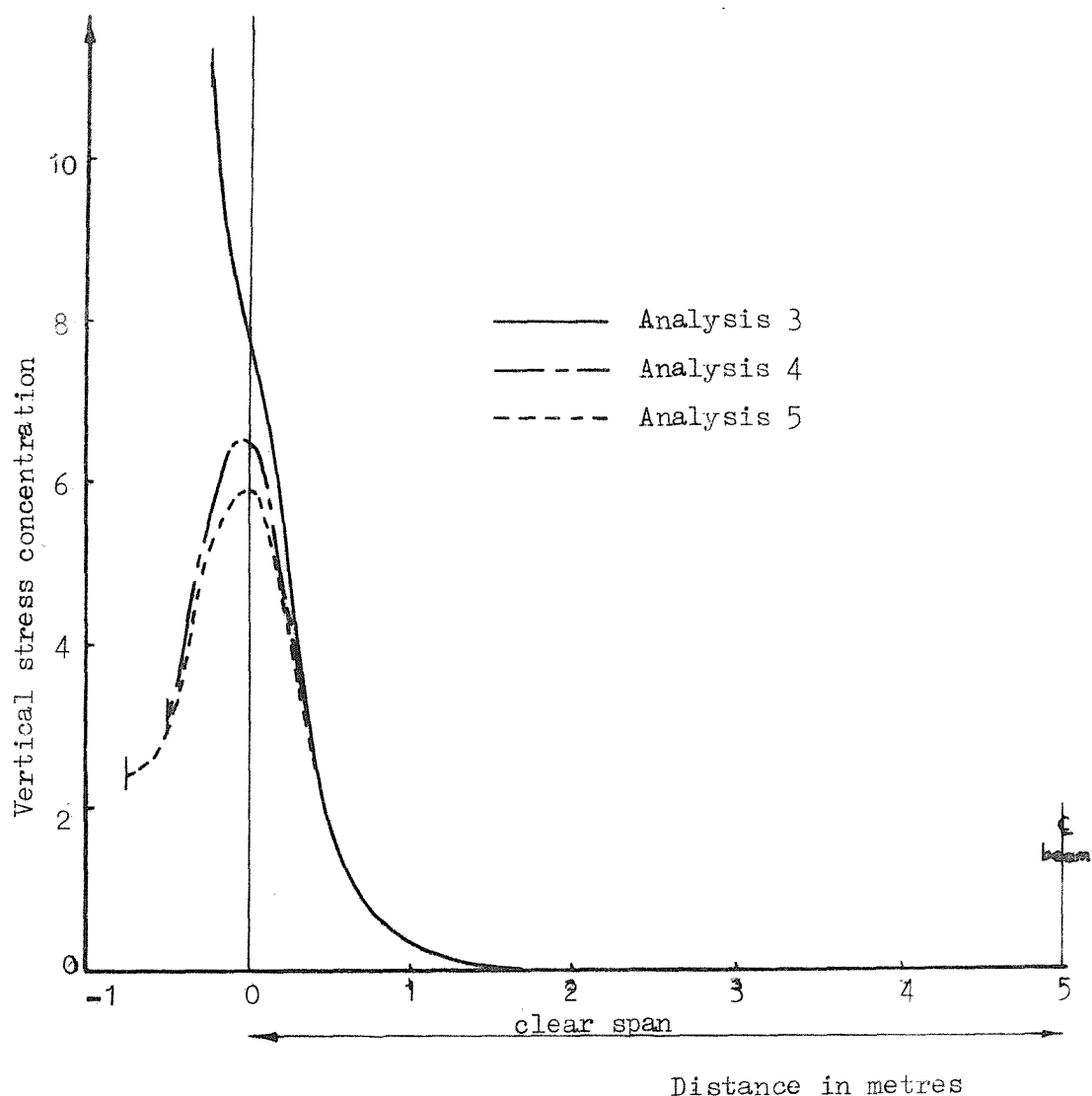
Fig. 4.17 VERTICAL STRESS DISTRIBUTION ON WALL BEAM INTERFACE
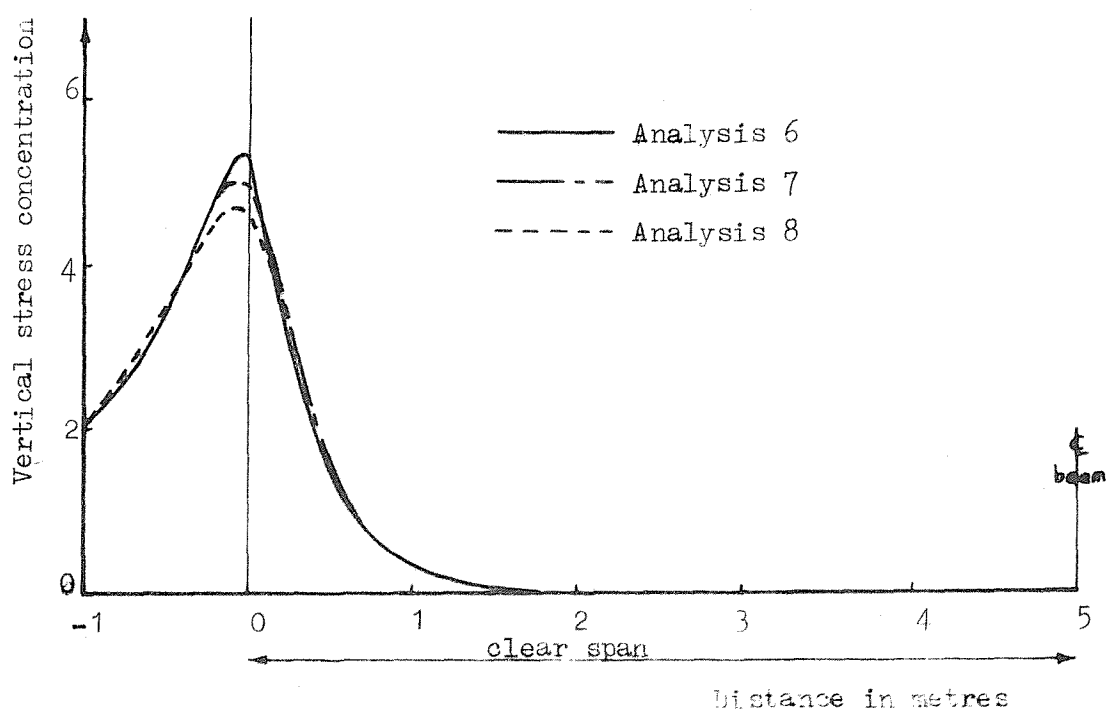
Fig. 4.18 VERTICAL STRESS DISTRIBUTION ON WALL BEAM INTERFACE

varied. The stress distribution, away from the supports is seen to be virtually unaltered by the restraint length changes, whilst in the support region considerable changes occur. The changes between the 0.25 and 0.5 m restraint analyses being greater than those between the 0.5 and 0.75 m restraint length analyses. The peak wall stress reduces with increasing beam rotational restraint, but the rate of reduction is less for the higher restraint lengths. Other behaviour trends are indicated by the results given in Table 4.4. The central beam deflection is reduced with increasing restraint length. The deflection for the smallest restraint length being less than half that of the basic wall on beam structure. The reduction in deflection for higher restraint lengths is relatively small and is seen to reduce further as the restraint length increases. The peak tie forces are virtually unchanged with increasing restraint length, although they are slightly less than the tie force in the basic wall on beam structure. The hogging moments in the beams increase slightly with increasing support restraint length, whilst the sagging moments reduce. The greatest hogging moment is however well below the peak sagging moment in the basic wall on beam structure.

Fig. 4.18 shows the vertical stresses in the walls at the wall-beam interface for analyses 6, 7 and 8. In these analyses the wall was extended 10 m. past the end of the span and the length of the vertical restraint at the beam support was again varied. The stress distributions for these analyses are very similar with the peak vertical stress at the edge of the span reducing only slightly with increasing restraint length. The peak stresses for these analyses are less than those for the corresponding analyses 3, 4 and 5 which were without the wall extension. Other behaviour trends are indicated by the results in Table 4.4. The central beam deflection, the peak beam tie force and

the peak sagging moment all reduce very slightly with increasing restraint length and are all less than the values given by analyses 3,4 and 5. The peak hogging moment also reduces with increasing restraint length which is opposite to the trend of the results from analyses 3, 4 and 5. The peak hogging moments are less than the analyses 3, 4 and 5 values.

In analyses 7, 9, 10 and 11 the wall extension length was varied whilst the length of vertical restraint at the beam support was kept constant. Again the results in Table 4.4 indicate some definite trends. For reducing wall extension length, the wall peak stress and the beam central deflection, peak tie force, peak sagging moment and peak hogging moment all increase. Analysis 12 was a repeat of analysis 10 with horizontal restraints applied at the beam support and along the length of the wall extension. All of the above factors were reduced, except for the peak hogging moment which was noticeably increased. As expected the reduction in the beam tie force was considerable.

The final three analyses (13,14 and 15) were on structures which took the form shown in Fig. 4.16. Problems with restraint application were experienced. In analysis 15, where only vertical restraints were applied at the base of the wall, the wall below beam level tended to act in bending, and this was thought to be unrealistic. In analyses 13 and 14, additional horizontal restraints were applied to the base and side of the wall as shown in Table 4.4. This level of restraint must be considered rather higher than would normally exist in practice. However one trend is clearly indicated by the results from analyses 13 and 14, and this is a reduction in all the previously mentioned factors with an increase in wall height.

4.5.3 Conclusions

The main conclusions from this section can be summarized as follows:-

(1) A wall on beam structure with beam rotational restraint and with the wall continuous over the supports can be designed conservatively using the results from the basic wall on beam structure analyses, provided an allowance is made for hogging as well as sagging moments. The peak hogging moment, which occurs close to the supports, can be taken conservatively as equal to the peak sagging moment found in the basic structure analyses.

(2) The height of the wall becomes an important behaviour parameter when the wall is continuous past the support. The percentage of load arching directly into the wall extensions is related to the wall height and the wall horizontal extension length as well as other parameters.

4.6 Conclusions

The main conclusions from this chapter may be summarized as follows:-

(1) The computer programs developed will give a reasonable indication of the elastic behaviour of walls on beams, even after any wall-beam separation cracking.

(2) Although the basic wall on beam analyses results differed to some extent from the assumed design method values, none of these differences require any change in the design method.

(3) The design method will give conservative results for wall on beam structures where there is some beam rotational restraint and the wall is continuous past the supports.

(4) A far more extensive study of the behaviour of wall on beam structures with beam rotational restraint and wall extensions past and below the supports would be required before more accurate design recommendations could be given.

CHAPTER 5

WALLS ON BEAMS: EXPERIMENTAL TESTING

5.1 Introduction

Four separate sets of tests are described in this chapter.
The first set of tests were model tests of plaster walls on steel
beams. The results from these first tests provided data for the
development of the approximate design method described in Chapter 3.

The second set of tests were again on models. These consisted
of araldite walls on steel beams. The results of these tests were
compared with results obtained from the finite element computer program,
so that the accuracy of the computer analyses results could be estab-
lished.

Two further sets of tests are described briefly. The first of
these were conducted at the Building Research Establishment on full
scale masonry walls supported by encased steel beams. The final tests
were conducted at the University of Southampton on small masonry walls
supported by reinforced concrete beams.

5.2 Plaster wall on steel beam model tests

5.2.1 Model and apparatus description

The walls in the models were of height 300 mm, width 450 mm. and were cast from dental plaster. This material was chosen because it could be cast easily and its material properties became stable within one week of casting. It was also known to be reasonably linear elastic at low strains.

The beams in the models were rectangular mild steel bars machined to the correct dimensions. The wall and beam widths were both 25 mm. Three beam depths of 18 mm, 12 mm. and 6 mm. were taken. These were calculated to give K values as defined in Eq. 3.2 of approximately 10, 15 and 25.

The walls were cast directly onto the beams so that initial fit problems would be avoided. At first they were cast vertically between glass sheets. Unfortunately, however, the plaster tended to expand on setting and this broke some of the glass sheets. In the final tests the walls were cast horizontally on a single glass sheet. For each casting, cylinder samples were also produced. These had a cross-sectional area of 2 square inches and a height of 3 inches. They were used to establish the modulus of elasticity and crushing strength of the plaster.

It was expected that a separation crack would develop on the wall-beam interface when the models were tested. It was important to measure the length of this crack as accurately as possible so that the length of contact could be found. The first method used to indicate the length of the crack was to paint a layer of a brittle varnish over the joint. This proved to be too strong and failed to crack along the full length

of the separation crack. The method finally adopted was to paint a layer of very weak plaster along the interface. This gave a clearly discernible crack when observed through a magnifying glass.

The models were tested in a reaction frame. Because of the span of the model, it was necessary to test it out of the plane of the reaction frame. A strong solid steel beam was placed across the reaction frame at the bottom and the model was supported on rollers on this beam. A diagrammatic representation of the testing arrangement is shown in Fig. 5.1. The loading was applied by means of a 10,000 lb mechanical jack through a load cell to a hydraulic load spreader. The load cell was connected to a pen recorder so that a continuous record of the applied load was obtained. Originally it had been the intention to use strain gauges in the wall corners to measure the stress concentration. In the event it proved to be impossible to attach them securely to the slightly damp and powdery surface of the plaster walls. For this reason, four Huggenburger tensometers were used to measure the vertical strain in the wall corners above the supports. They were set with a gauge length of half an inch.

5.2.2 Test procedure

After two trial tests, four final tests were conducted. One with a beam depth of 18 mm., two with a beam depth of 12 mm. and one with a beam depth of 6 mm.

Each model was subjected to two loadings before finally being loaded to failure. Loading increments of 1 KN were taken. The first loading was taken to 10 KN, while the second was taken to a higher value, depending on the beam depth.

As well as the four tensometer readings, the central beam deflection was also recorded by means of a dial gauge for each load increment.
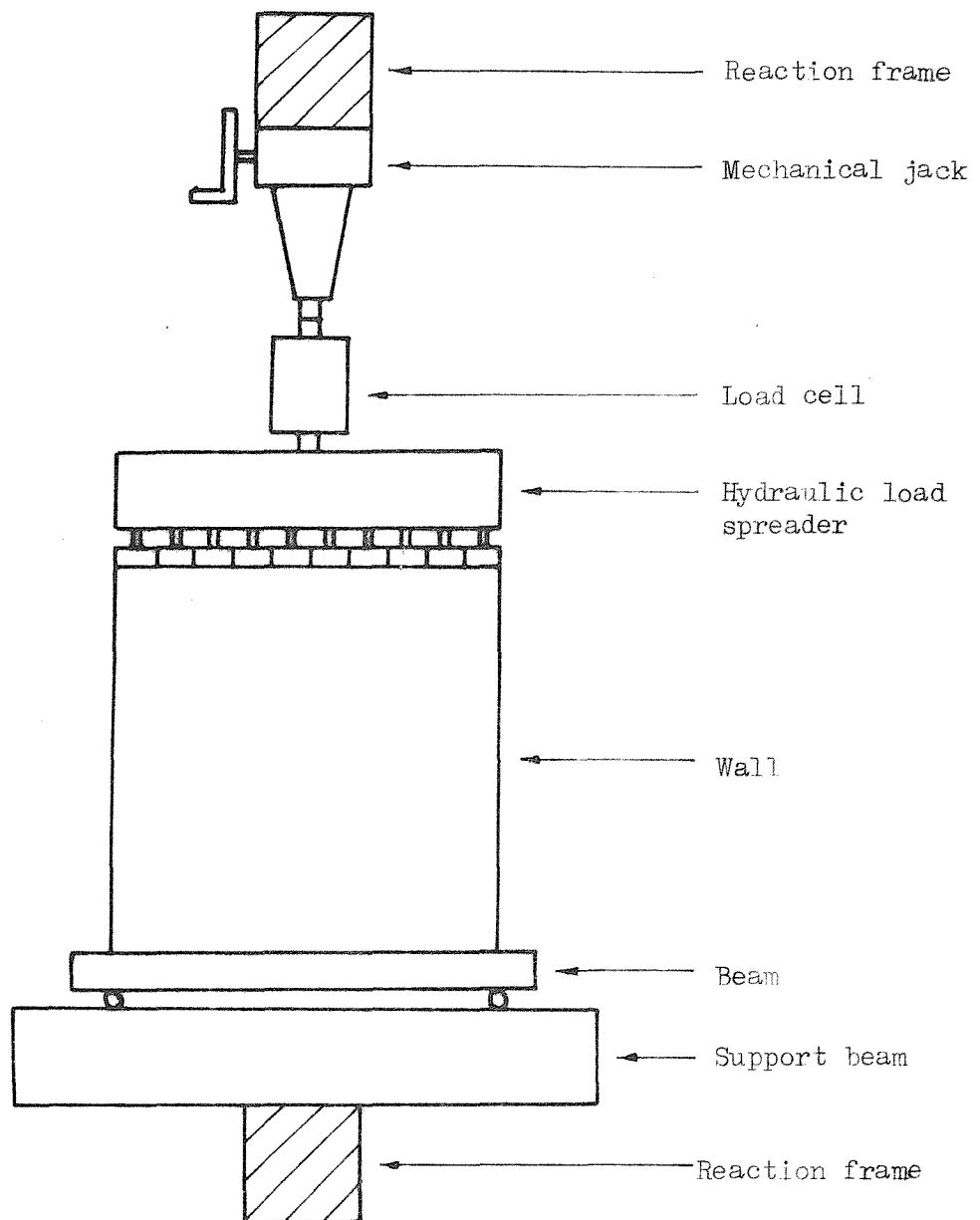
Fig. 5.1 TESTING ARRANGEMENT FOR PLASTER MODEL TESTS

Unfortunately these deflection figures had to be disregarded because it was later discovered that the main support beam was deflecting considerably more than the model beam and this deflection was included in the dial gauge readings. Averaged tensometer readings for the final test are shown in Fig. 5.2. Using the plaster modulus of elasticity, the vertical stress can be calculated directly since virtually no horizontal stress occurs in the corner regions.

When loaded to failure, the failure mechanism was always that of crushing in one of the wall corners above the support. As soon as crushing occurred, no higher load could be carried by the model. This was expected because when the corner fails the load is transferred towards the centre of the span. This results in increased beam bending and a corresponding shortening of the length of contact which in turn leads to further wall failure. Two failed walls are shown in Plate 5.1 together with their failed plaster cylinder samples.

On the same day as each model was tested, the corresponding plaster cylinders were also tested in a Dennison testing machine. With two tensometers attached to measure vertical strain, each cylinder was subjected to two loadings up to 15 KN in 1 KN increments. The averaged tensometer results for the cylinders corresponding to the final test are shown in Fig. 5.3. The linear elastic nature of the material is clearly demonstrated. From the results, the E value of the plaster could easily be calculated. After removal of the tensometers the cylinders were loaded to failure and the failure stress thus calculated.

5.2.3 Results calculations

It was thought that the length of contact α was related to the parameter K, defined in Eq. 3.2, by a relationship of the type
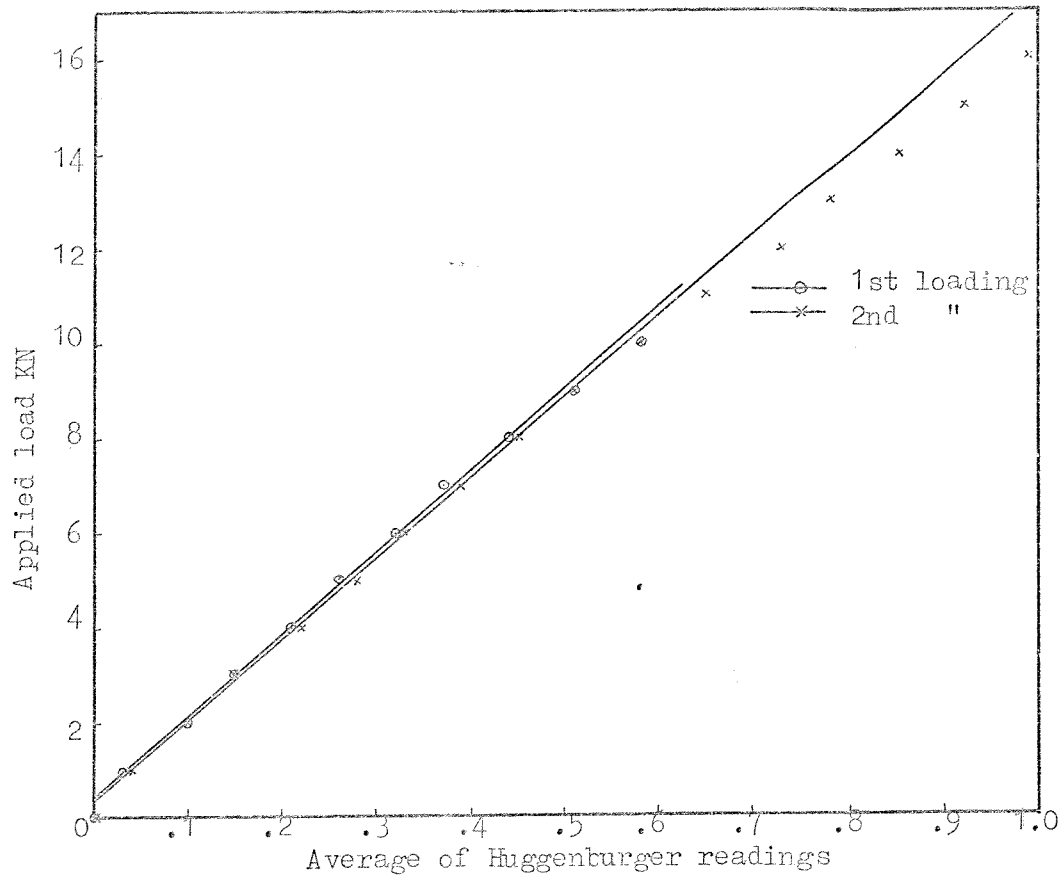
FIG. 5.2 AVERAGED TENSOMETER READINGS FOR FINAL PLASTER MODEL TEST
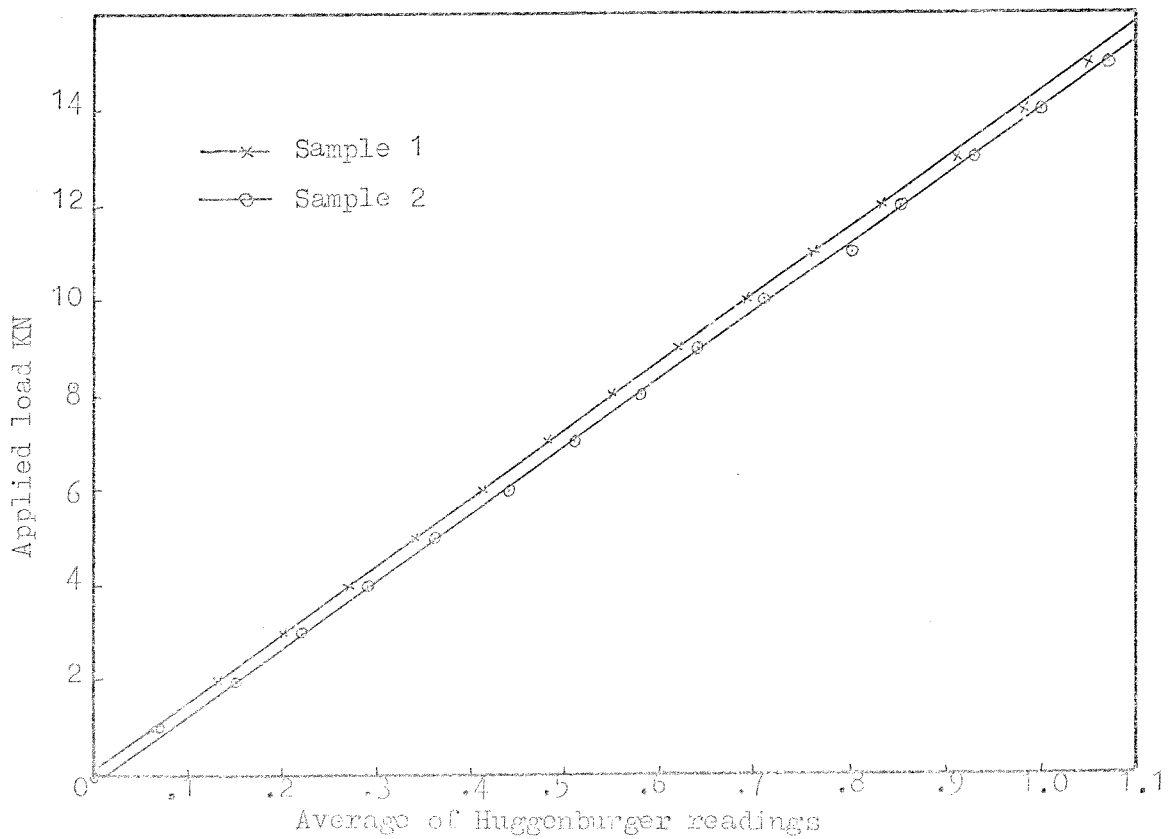
FIG. 5.3 AVERAGED TENSOMETER READINGS FOR PLASTER CYLINDERS
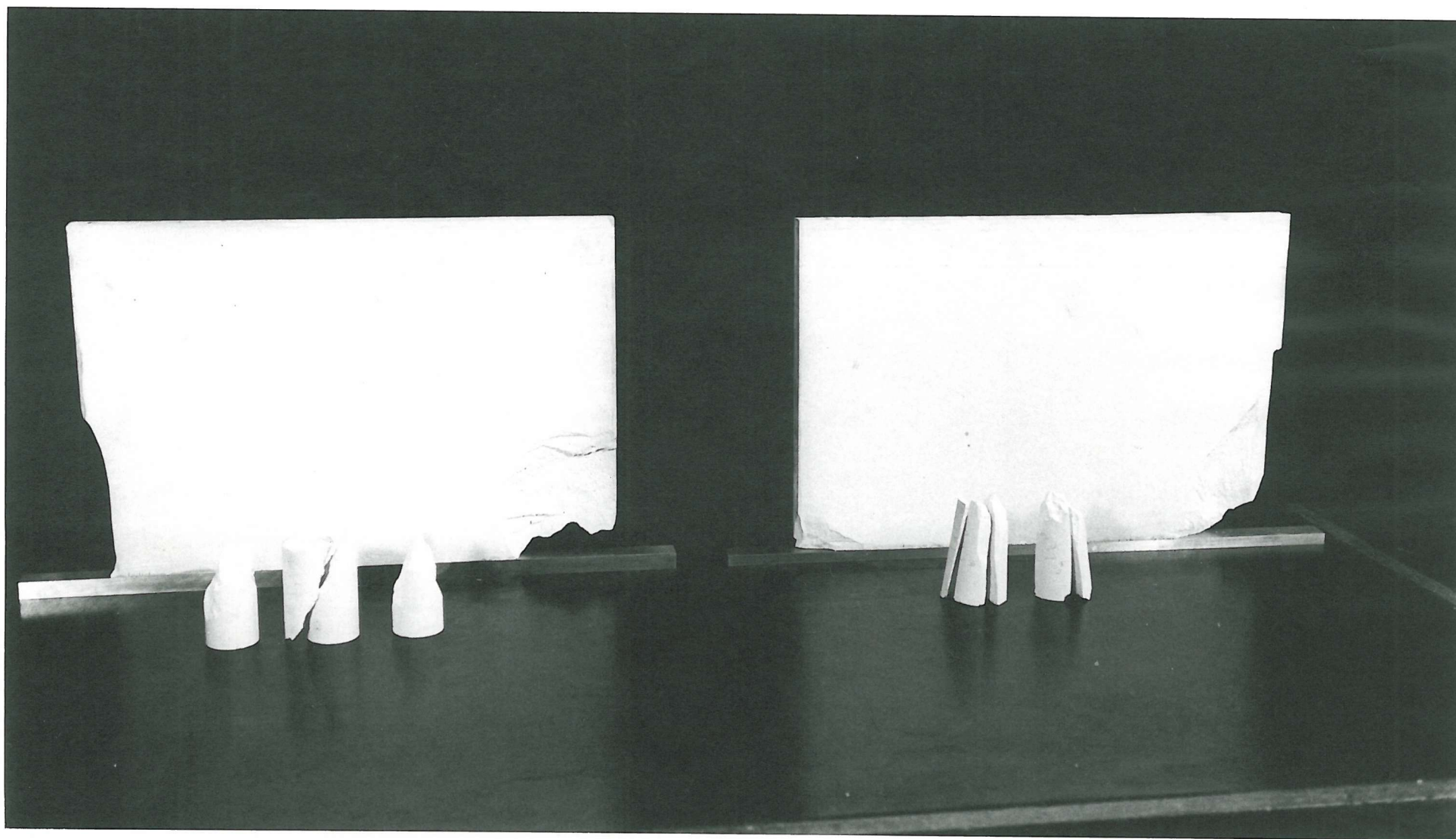
Plate 5.1 Failed plaster model walls and corresponding cylinder samples

$$\frac{\alpha}{L} = \frac{B}{K} \qquad \qquad \text{. . . } 5.1$$

where B is a constant to be determined.

The value of B was assumed initially in developing the approximate design method to be equal to 2.22. This value was obtained by considering the structure as a beam on an elastic foundation.

Using the plaster model test results it was possible to obtain three estimates for B from each test.

a) from the observed length of contact, using

$$B = \frac{\alpha K}{L} \qquad \qquad \text{. . . } 5.2$$

b) from the calculated peak wall stress f_b, using

$$B = \frac{W_w K}{f_b t L} \qquad \qquad \text{. . . } 5.3$$

where W_w is the applied vertical load.

c) from the wall crushing load W_{wf}, assuming that failure occurred when the triangularly distributed compressive stress distribution reached the compressive strength of the plaster f_{bu}.

$$B = \frac{W_{wf} K}{f_{bu} t L} \qquad \qquad \text{. . . } 5.4$$

It is suspected that the calculations based on Eq. 5.2 overestimate the true value of B because of the difficulty of observing the full length of the separation crack. Eqs. 5.3 and 5.4 are expected to underestimate B because the peak wall stress is higher than that given by a triangular stress distribution as shown in Fig. 3.1(b).

Table 5.1 shows the values of B as derived from these model test results by the above three methods. The disparity between these results and the assumed B value of 2.22 is considerable. The beam on elastic foundation theory assumed that the slope at the supports was zero. In the present tests, however, there is no rotational restraint at the supports and thus some beam rotation will occur. This has the effect of reducing the length of contact and thus the B value.

Unfortunately none of these test results could be used to give accurate verification of the finite element program. The test deflection results had had to be disregarded as explained previously. The separation crack was only approximately represented in the computer program and depended to some extent on the nodal spacing. The tensometer readings gave an average of the strain over a small length in the very rapidly changing stress field of the wall corners. The computer program calculated stresses at precise points in the wall. It was not possible to make an accurate estimate of the errors between the two.

In fact analyses were undertaken on four structures that represented the test structures as closely as possible. The results were encouraging with close agreement between the separation crack lengths and the wall stresses.

Test	Beam depth mm.	Plaster modulus of elasticity KN/mm^2	K	Estimated B value		
				From measured contact length	From measured peak stress	From failure load
1	18	16.3	11.2	1.02	0.90	0.78
2	12	16.1	15.1	1.16	0.77	0.96
3	6	13.5	24.2	1.21	1.28	1.02
4	12	13.5	14.4	1.09	0.98	0.90

Table 5.1   Derived B values from plaster model tests

5.3 Araldite wall on steel beam model tests

5.3.1 Model and loading apparatus

The object of these tests was to obtain results that could be compared with results calculated using the finite element program, so that the accuracy of the finite element program could be checked. To make this comparison, accurate measurements of wall and beam stresses as well as beam deflections were required.

The wall was formed from hot cured araldite CT200. This material was chosen because of its good linear elastic properties and long term stability. Silica flour was added to the mix to increase the modulus of elasticity of the wall, so that the E/E_w ratio would be reduced. The araldite mix proportions by weight were 100 parts araldite CT200, 30 parts hardener and 200 parts silica flour. A 25 mm. thick sheet of the araldite was cast vertically in a metal mould and the 450 mm. by 450 mm. wall was then cut and machined from this sheet. Three 25 mm. by 25 mm. by 100 mm. prism samples were also cut from the sheet. These were used to determine the modulus of elasticity and Poisson's ratio of the material. The remainder of the sheet was used for mounting dummy strain gauges. It was decided to test the one wall with three separate beams. It was considered that the coefficient of friction between the wall and beam materials would be sufficiently high so as to prevent any slippage on the wall-beam interface. The beams were machined from solid mild steel bar. They were 25 mm. thick and had depths of 40 mm, 15 mm. and 10 mm. which represented K values, as defined in Eq. 3.2, of approximately 5, 10 and 15.

A variable height reaction frame was designed and built to take these models. It is shown complete with the model and other equipment

in Plate 5.2. The base was designed to be very stiff so that the small beam deflections could be measured accurately. A 10,000 lb. mechanical jack was fitted at the top. Loading was measured by means of the proving ring attached below the jack and below the proving ring was fitted the hydraulic load spreader used in the plaster model tests. To provide lateral stability to the model, adjustable roller bearing were fitted and are shown in Plate 5.2. The beam supports shown in Fig. 5.4 and Plate 5.2 allowed two dimensional rotation so that no support eccentricity could develop.

5.3.2 Tests to determine the modulus of elasticity and Poisson's ratio of the araldite

Strain gauges of the same type as used on the model were attached to the araldite prism samples. On two opposite faces of each sample, 2 mm. foil strain gauges were attached vertically. On the two other faces 5 mm. foil strain rosettes were attached. Pressure sensitive strain gauge cement was used for all of the gauges. Two of these prism samples are on top of the data logger in Plate 5.2.

The specimens were loaded in a Dennison testing machine up to a load of 2000 lb. in 200 lb. increments. Strain readings were recorded using a Baldwin box for the vertical 2 mm. gauges. Two of the specimens were loaded again and readings were recorded for the horizontal and vertical 5 mm. gauges in the rosettes. The results are shown in Fig. 5.6. An average modulus of elasticity value of 11.77 KN/mm^2 and a Poisson's ratio value of 0.314 were calculated from these results. One sample was loaded finally up to 8,000 lb. to investigate the limit of the linear elastic behaviour. The results, shown in Fig. 5.5, indicate good elastic behaviour for strains well above those experienced in the model tests.
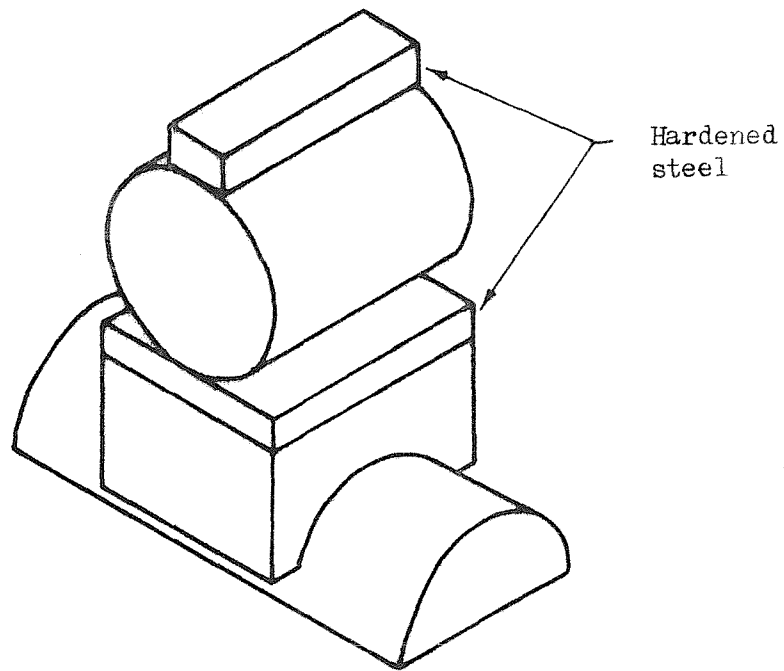
FIG. 5.4 FORM OF BEAM SUPPORTS
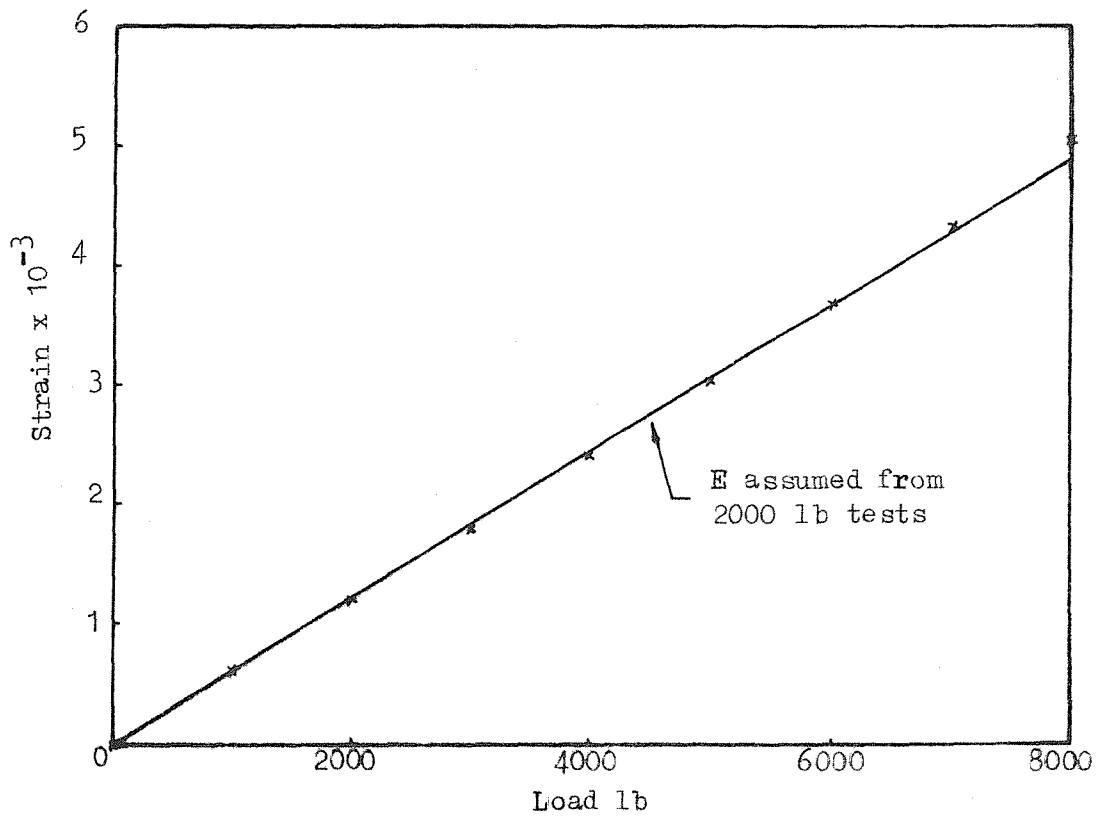
FIG. 5.5 RESULTS FROM ARALDITE PRISM WHEN RELOADED TO 8000 lb.
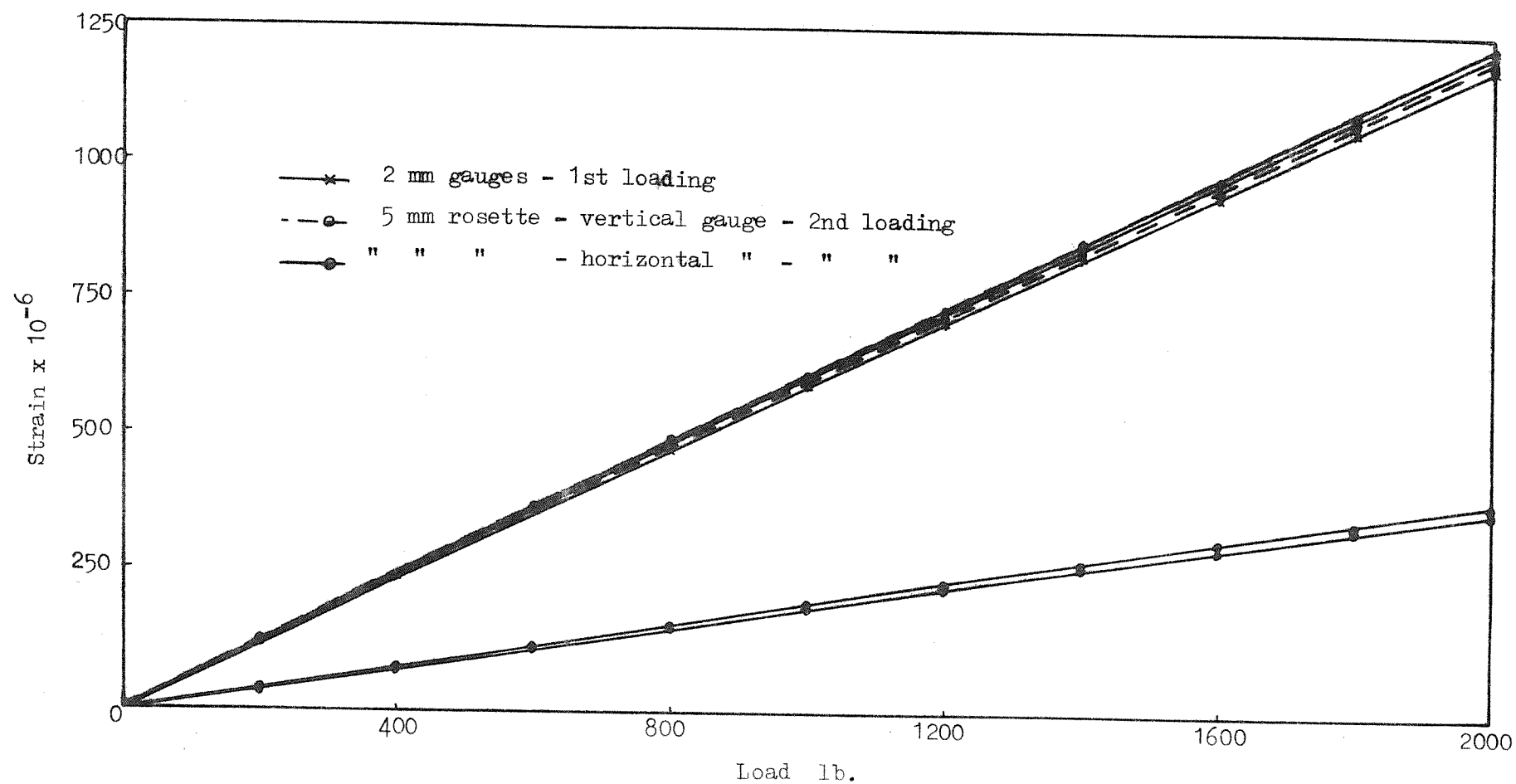
FIG. 5.6   RESULTS FOR ARALDITE PRISM TESTS
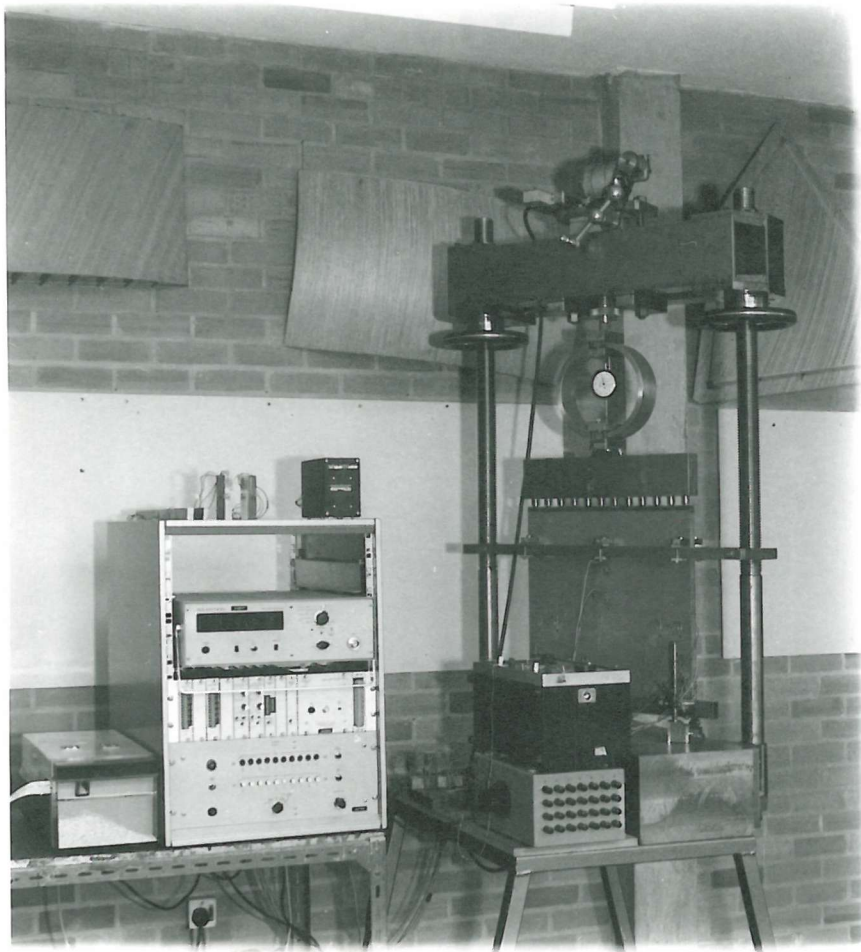
Plate 5.2 Araldite model testing apparatus
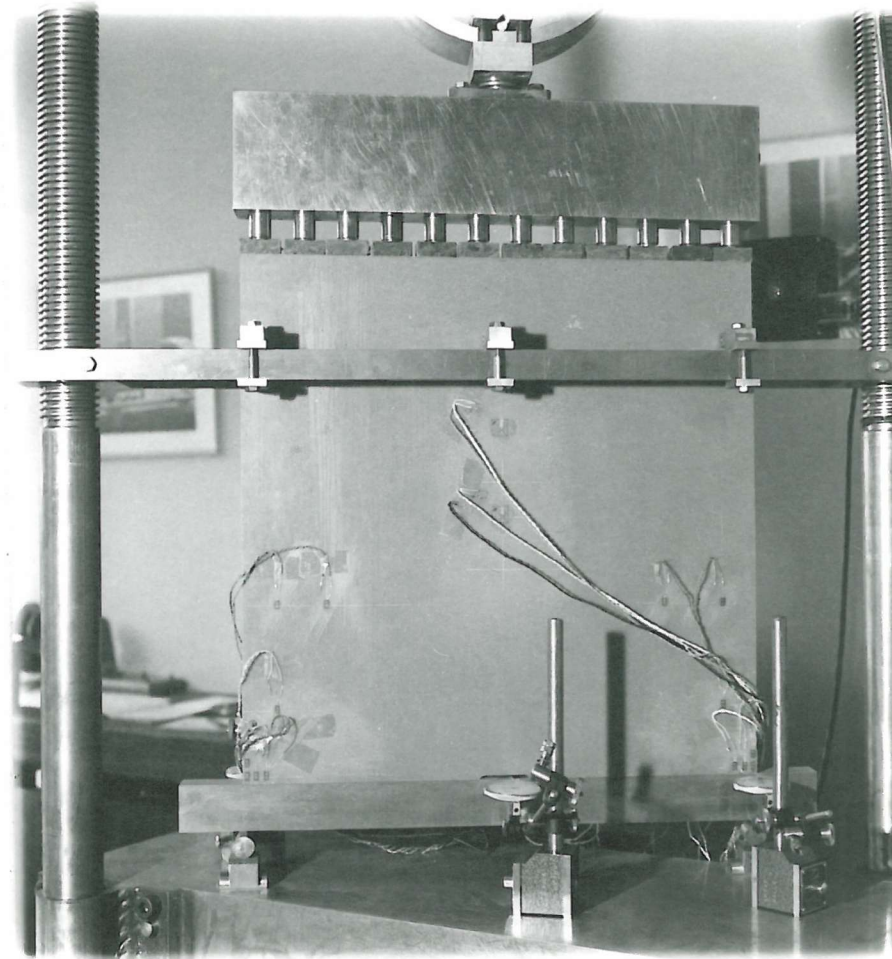
Plate 5.3 Araldite wall showing strain gauge positions

Towards the end of the testing period, nine months later, two specimens were retested to check the modulus of elasticity value. The resultant value was within 1% of the originally calculated value and indicates the high degree of stability of the material.

5.3.3 Tests to determine the modulus of elasticity of the steel beams

The 15 mm. beam was used to establish the modulus of elasticity of the mild steel. One 2 mm. strain gauge was attached to the top of the beam at mid-span and a second at the bottom of the beam. Both were positioned to measure the longitudinal strain in the beam. The beam was set on roller supports with a third point loading system. This created a constant beam moment over the middle third of the span. A dial gauge was positioned to measure the central beam deflections. The beam was loaded to 500 lb. in 100 lb. increments and deflection and strain readings were recorded. Again a Baldwin box was used to measure the strain changes.

The results from this test are shown in Fig. 5.7. Two separate modulus of elasticity estimates could be calculated from the results. Using the averaged strain readings, the first value was calculated to be 209 KN/mm^2. Using the deflection readings, the E value was calculated to be 204 KN/mm^2. An average value of 206.5 KN/mm^2 was taken for use in the analyses. The Poisson's ratio for the steel was not measured. The standard value for steel of 0.25 was assumed in the analyses.

5.3.4 Initial testing

Initially strain gauges were attached to both sides of the wall in the positions shown in Fig. 5.8. The corner positions represented centroid element positions in the grid chosen for the finite element
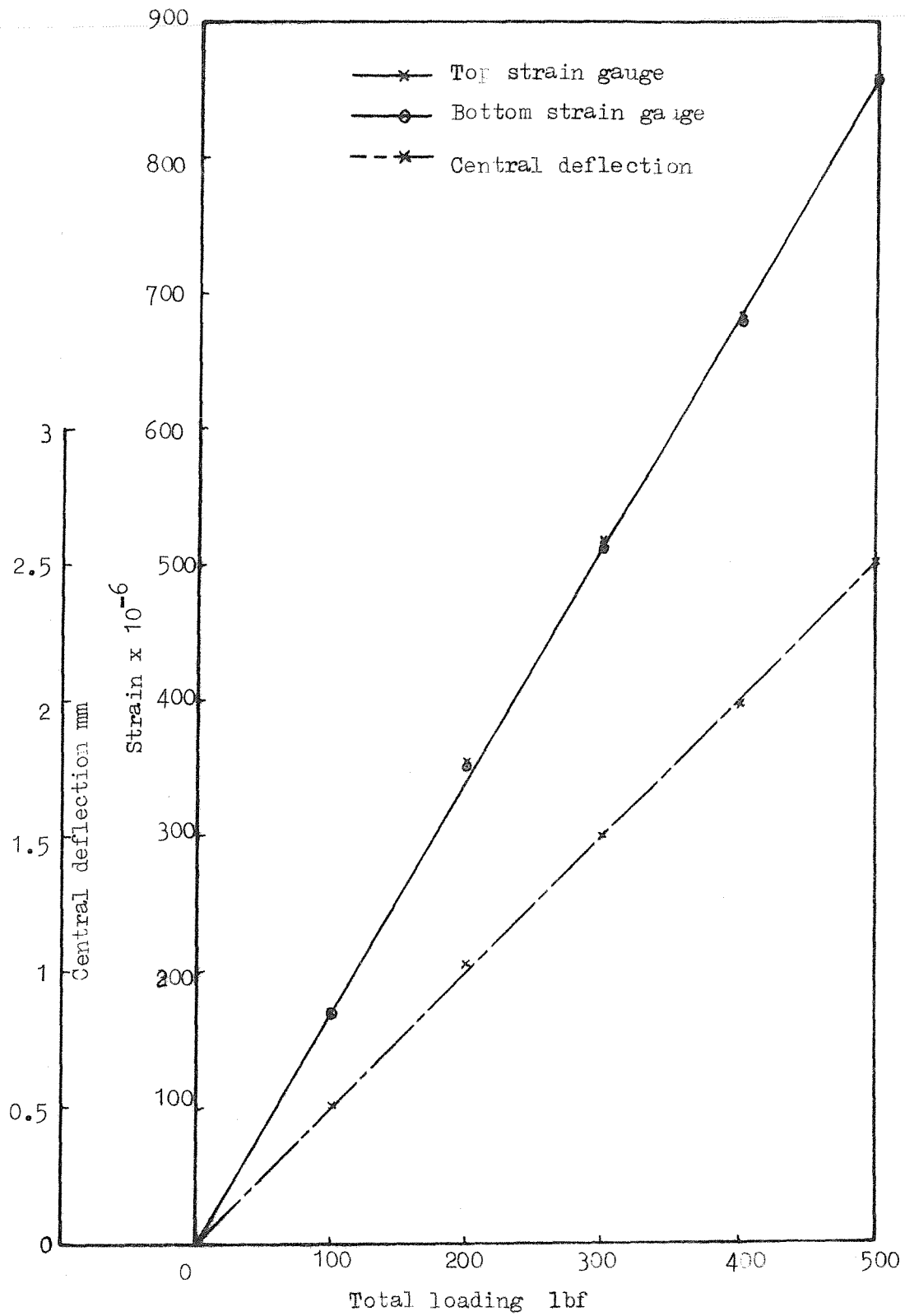
FIG. 5.7   RESULTS FROM THIRD POINT LOADING BEAM TEST
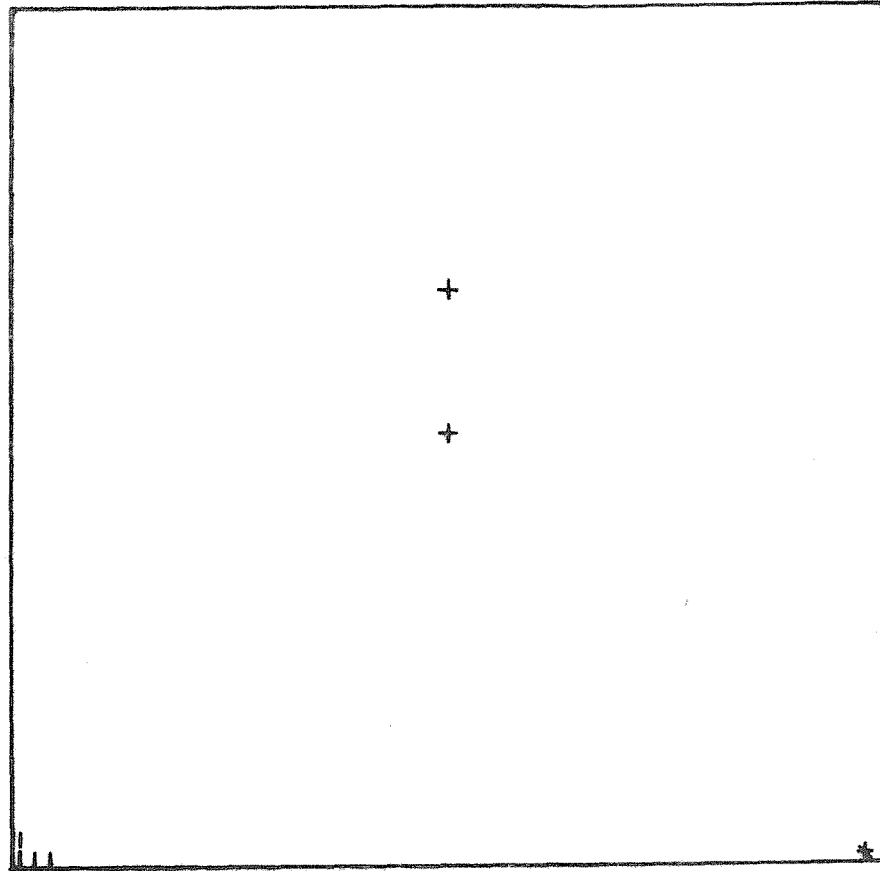
FIG. 5.8   INITIAL STRAIN GAUGE POSITIONS
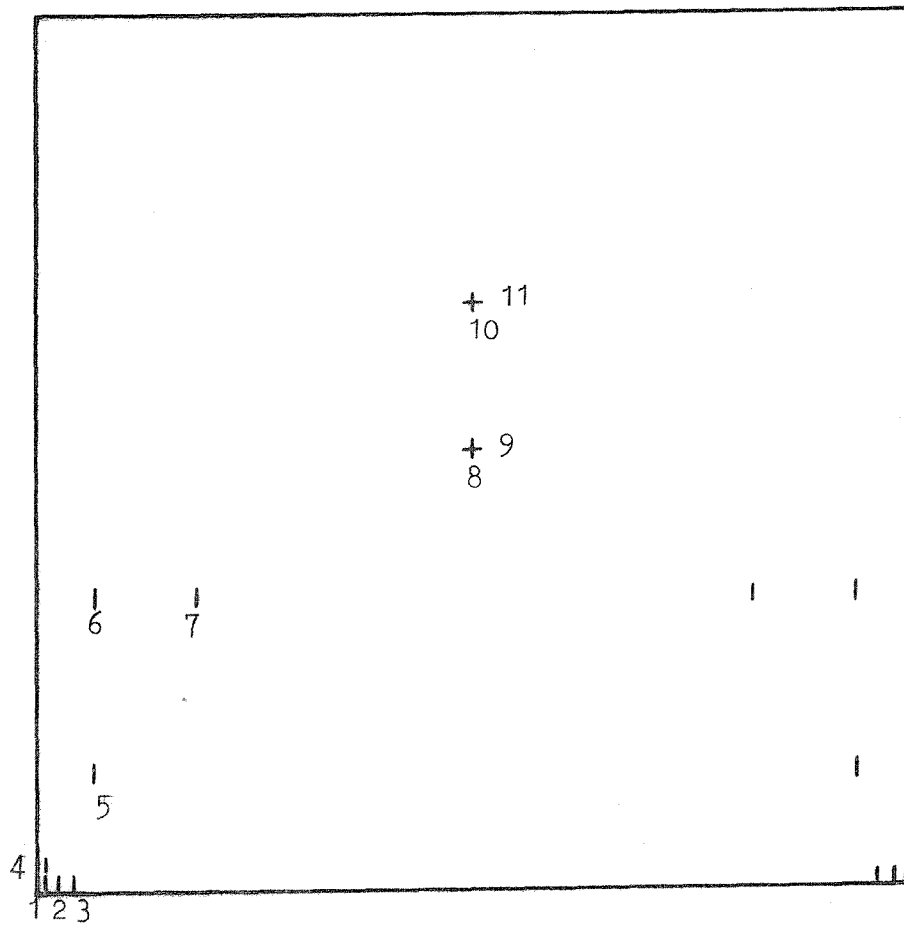
FIG. 5.9   FINAL STRAIN GAUGE POSITION

analyses. The single gauges had a gauge length of 2 mm. and the rosettes a gauge length of 5 mm. The 2 mm. gauge length was thought preferable because of the very rapid stress changes that occur in the wall corners.

The wall was tested with all three beams using this strain gauge arrangement. Initially all the gauges were read separately by hand using a Baldwin box with a separate dummy gauge for each active gauge. This was found to be very time consuming and when a Solatron datalogger became available, this was wired in to read the wall gauges. Only one dummy gauge was used with the datalogger and for this reason, the beam gauges, which required dummy gauges mounted on steel, were read separately by hand using the Baldwin box. The datalogger tape output could be fed into the departmental mini computer and thus the strain differences computed automatically. In addition to the strain measurements, dial gauges were used to measure the beam deflection at the supports and at the centre of span.

The results from these tests indicated that the rosettes in the wall corners were giving completely inaccurate readings. This could have been due to either the gauge length of 5 mm. being too large to accurately measure the rapidly changing stresses or possibly the fact that the three gauges overlay each other in the rosettes. It was decided to remove these corner rosettes and replace them with a similar arrangement of 2 mm. gauges as at the other corners. Because it was now far simpler to take the strain readings, twelve additional 2 mm. gauges were attached. The final positions of all the gauges is shown in Fig. 5.9 and Plate 5.3. Also at this time, a more modern datalogger became available and this was used to replace the older model.

Some considerable time was spent in getting the revised arrangement

to work reliably. When this was achieved, the final tests were
proceeded with.

5.3.5 Final tests and results

The wall was tested with each of the three beams for three
complete loading cycles. In addition the 10 mm. and 15 mm. beam
structures had one additional loading. In order that the wall would
suffer no damage the loading was limited to 8,000 lb. for the 40 mm.
beam, 5,000 lb. for the 15 mm. beam and 3,500 lb. for the 10 mm. beam.
For the 10 mm. and 15 mm. beams 500 lb. load increments were taken.
For the 40 mm. beam, 1000 lb. load increments were used.

The deflection and strain results indicated that it took two load
increments for all the tests before the model behaviour became linear.
This was probably due to some initial settling in of the wall onto the
beam and the taking up of the initial self weight beam deflection.
After the first two increments the behaviour generally was very linear,
although in the wall corners the strain readings did continue to decline
gradually. These strain gauges were within 5 mm. of the boundaries of
the wall, and considering the wall thickness of 25 mm., this non-
linearity was probably due to boundary effects. It was not due to
increasing contact length because all the wall-beam interface gauges
showed declining strain readings.

Excluding the first two load increments, the strain readings
were averaged to give the strain change for a 500 lb. load increment.
The beam's central deflection was obtained by averaging the support
deflections and subtracting this value from the measured central
deflection. Again the first two load increments were excluded.

The results are shown in Tables 5.2, 5.3 and 5.4. The structures
were analysed using the wall on beam computer program using the finite

Gauge position etc.	\multicolumn{11}{c}{Deflection values x 10^{-3} in. and Strain values x 10^{-6}}	Percentage Difference
	1st loading	2nd loading	2nd unloading	3rd loading	3rd unloading	4th loading	4th unloading	Loading average	Unloading average	Combined average	Computer results	
Beam Deflection	2.46	2.29	1.94	2.48	2.16	2.37	2.12	2.40	2.07	2.235	1.86	-16.8
Top beam gauge	2.0	2.2	-0.4	3.0	0.2	2.4	-1.0	2.4	-0.4	1.0	1.2	+20.0
Bottom beam gauge	-20.6	-21.2	-20.8	-21.6	-20.8	-21.2	-21.6	-21.2	-21.1	-21.15	-23.9	+13.0
1	321.0	316.8	285.4	307.1	278.3	304.5	278.4	312.3	280.7	296.5	299.4	+1.0
2	105.8	107.4	116.3	111.6	111.4	110.4	111.7	108.8	113.1	111.0	108.7	-2.1
3	-0.8	-1.8	- 4.7*	-2.5	-4.2	-2.9	-3.9	-2.0	-4.3	-3.2	15.4	-
4	235.2	233.0	218.5	225.8	214.2	224.0	213.9	227.0	215.5	221.3	206.6	-6.7
5	47.0	47.2	46.5	46.9	46.0	46.8	46.0	47.0	46.2	46.6	48.1	+3.2
6	30.7	30.6	30.0	30.2	29.4	29.9	29.7	30.3	29.7	30.0	29.8	-0.7
7	17.7	17.7	18.4	17.7	17.7	17.8	18.0	17.7	18.0	17.9	17.9	0
8	7.0*	8.5	9.1	8.7	8.7	8.4	8.5	8.1	8.6	8.4	9.5	+13.1
9	3.7*	3.2*	3.5*	1.9	2.4	1.5	2.3	2.6	2.7	2.7	3.2	+18.5
10	12.6	12.4	12.4	12.2	12.4	12.3	12.7	12.4	12.5	12.5	13.6	+8.8
11	0.7*	0.9*	0.5	-0.1	0.2	0	0.1	0.4	0.3	0.4	-0.7	-

* One or more gauges disregarded because of obvious errors.

Table 5.2   Experimental and analytical results for model with 10 mm. beam

Gauge Position etc.	Deflection values x 10^{-3} in. and Strain values x 10^{-6}											Percentage Difference
	1st loading	1st unloading	2nd loading	2nd unloading	3rd loading	3rd unloading	4th loading	Loading average	Unloading average	Combined average	Computer results	
Beam Deflection	1.48	1.46	1.51	1.41	1.47	1.39	1.55	1.50	1.42	1.46	1.28	-12.3
Top Beam Gauge	5.4	4.2	5.1	4.4	5.4	4.2	5.4	5.3	4.2	4.75	1.0	-63.2
Bottom Beam Gauge	-17.8	-18.0	-18.2	-17.5	-18.0	-17.7	-17.7	-17.9	-17.7	-17.8	-16.7	-6.2
1	254.0	228.0*	244.0	223.0	240.0	222.3	241.0	244.8	224.4	234.6	241.2	+2.8
2	119.4	132.0	133.5	129.7	133.0	127.2	132.8	129.7	129.6	129.7	127.7	-1.5
3	43.1	59.9	57.0	58.2	57.5	57.0	57.0	53.6	58.4	56.0	45.6	-18.6
4	199.0	184.8	193.0	182.6	191.8	182.2	191.0	193.7	183.2	188.4	177.1	-6.0
5	47.9	47.4	46.9	47.1	47.5	47.0	47.0	47.3	47.2	47.2	47.3	+0.2
6	30.4	30.0	29.6	28.8	29.9	29.5	29.6	29.9	29.4	29.6	28.9	-2.4
7	18.1*	18.6	17.4*	18.9	17.9	18.2	18.0	17.8	18.6	18.1	18.0	-0.6
8	9.8*	10.0*	9.3	9.5	9.5*	9.7*	9.5*	9.5	9.5	9.5	9.9	+4.2
9	3.8*	4.1*	3.3*	4.2*	3.6*	3.8*	3.9*	3.6	4.0	3.8	2.9	-23.7
10	12.7	12.9	12.1	13.0	12.6	12.7	12.8	12.6	12.6	12.6	13.8	+9.5
11	0.1	0.1	-0.9	0	-1.1	-0.4	-0.4	-0.6	-0.1	-0.35	-1.0	+186.0

* One or more gauges disregarded because of obvious errors.

Table 5.3   Experimental and analytical results for model with 15 mm. beam

Gauge Position etc.	Deflection values x 10^{-3} in. and Strain values x 10^{-6}										Percentage Difference
	1st loading	1st unloading	2nd loading	2nd unloading	3rd loading	3rd unloading	Loading average	Unloading average	Combined average	Computer results	
Beam Deflection	0.45	0.43	0.45	0.42	0.47	0.44	0.46	0.43	0.445	0.462	+3.8
Top Beam Gauge	7.5	6.6	7.4	6.3	7.0	6.4	7.3	6.4	6.85	5.5	-19.7
Bottom Beam Gauge	-11.5	-11.5	-11.3	-11.1	-10.9	-10.5	-11.3	-11.0	-11.15	-11.3	+1.3
1	120.5	112.8	118.0	112.8	117.0	112.2	118.5	112.6	115.6	117.0	+1.2
2	85.4	83.1	83.5	83.0	82.3	82.5	85.6	82.9	84.3	82.5	-2.1
3	52.2	58.2	54.3	58.0	54.7	58.0	53.7	58.1	55.9	60.8	+8.1
4	97.3	94.3	96.2	94.5	95.8	95.0	96.4	94.6	95.5	94.1	-1.5
5	42.2	40.1	41.8	40.0	42.0	40.4	42.0	40.2	41.1	40.8	-0.7
6	26.5	25.5	26.5	25.6	26.5	25.7	26.5	25.6	26.1	25.7	-1.5
7	18.9	18.6	19.0	18.9	19.1	18.6	19.0	18.7	18.9	18.6	-1.6
8	11.5*	11.1*	10.9	10.6	10.5	10.8	11.0	10.8	10.9	11.5	+5.5
9	1.2	1.4	1.1	1.3	1.0	1.6	1.1	1.4	1.3	1.4	+7.7
10	14.2	13.4	13.9	13.5	13.7	13.7	13.9	13.5	13.7	14.6	+6.6
11	-1.1*	-1.7	-1.5*	-1.5	-1.4	-1.3	-1.3	-1.5	-1.4	-2.0	+42.8

* One or more gauges disregarded because of obvious errors.

Table 5.4   Experimental and analytical results for model with 40 mm beam

117

element grid shown in Fig. 5.10. Strain values corresponding to the strain gauge positions and directions, were calculated from the analyses stress results and these are also included in Tables 5.2, 5.3 and 5.4. The percentage difference of the computer results from the test results was calculated and is also shown in the tables.

5.3.6 Comparison of test and analytical results

The results shown in Tables 5.2, 5.3 and 5.4 indicate a generally good level of agreement between the test and analytical results. As might be expected, the results from the stiffer beam analyses give better agreement than those from the more flexible beam analysis, because of greater length of contact between the wall and beam for stiffer beams. For example, in the 10 mm. beam analysis, only three nodes were left connected between the wall and beam at each support, while in the 40 mm. beam analyses, eight nodes were left connected.

These tests indicate that the finite element analysis will predict the beam deflections and stresses to within 20% for structures with a K value not greater than 15. The only error greater than this was for the top strain gauge on the 15 mm. beam, and even here, when the bending moment and tie force components were calculated for the beam, the error drops to around 20%. Generally, the analyses slightly under-estimated the beam moment and overestimated the tie force. If any slight slippage had occurred in the tests on the wall-beam interface, this would have led to an increase in the bending moment and a reduction in the tie force. Although no noticeable slip occurred in the tests, the possibility of some slippage cannot be entirely ruled out. Considering the fact that the central beam deflection for the 10 mm. beam structure more than doubles in the analysis as the crack is generated,
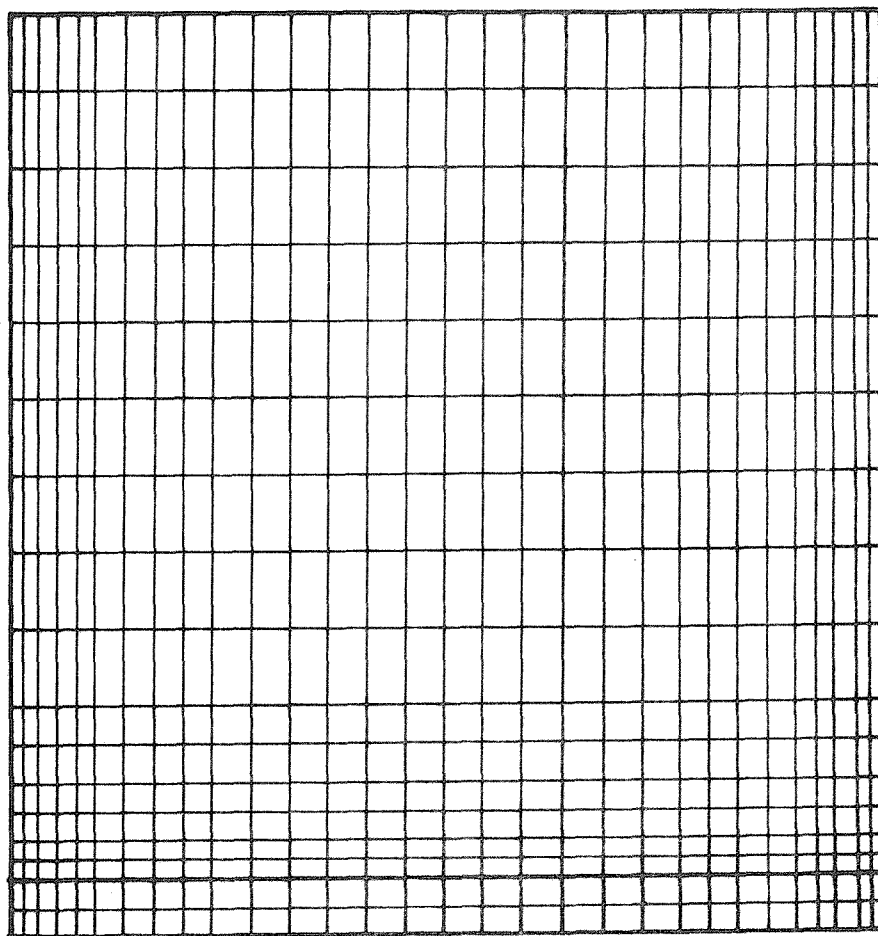
FIG. 5.10 FINITE ELEMENT GRID USED FOR ARALDITE MODEL ANALYSES

a final deflection error of 17% must be considered reasonable. Again though, any slippage might partly account for this difference.

The agreement between the test and analyses wall strain results was good except for the results from the rosettes and the position 3 gauges. The rosettes were of a similar type to those used earlier in the wall corners. Since the corner rosettes had also produced large errors, it was considered reasonable to disregard the errors indicated by the central wall rosettes. In the analyses, the length of the separation crack depends to some extent on the node positions. For the 10 mm. beam structure analysis, position 3 lies at the end of the length of contact and thus the strain estimate for this position is likely to be inaccurate. Similarly, for the 15 mm. beam analysis, position 3 is close to the end of the length of contact and thus the strain estimate for this position is also likely to be inaccurate. Excluding the position 3 and rosette results, the remaining test and analyses results differed by less than 10%.

5.3.7 Conclusions

For wall on beam structures with K values less than 15, the finite element analyses can predict wall stresses to within 10%, and beam stresses and deflections to within 20%.

5.4 Full scale tests at the Building Research Establishment

5.4.1 Introduction

Four full scale masonry wall on encased steel beam tests were conducted at the Building Research Establishment under the supervision of Mr. G. Weeks. These tests were undertaken to demonstrate testing techniques to students on teaching courses.

The author gratefully acknowledges the permission given by Mr. Weeks and the Building Research Establishment to observe these tests and report the results.

Since the tests were not personally conducted by the author, the tests will only be described briefly. The results were used by the author in formulating the design method described in Chapter 3. A comparison between the test results and a finite element analysis is also given.

5.4.2 Test description

The four tests were conducted in two sets of two with the two beams used in the first set being reused in the second set. For all of the tests the wall height was 6 feet, the span 10 feet and the wall thickness nominally $4\frac{1}{2}$ inches. Loading was approximately uniformly distributed and was achieved by means of underfloor hydraulic rams acting through steel cables to the top of the wall. The test arrangement is shown in Plate 5.4.

The two beams used in the tests were of different stiffness. The smaller beam had encased dimensions of 10 in. wide by 12 in. deep and contained a 8 in. by $5\frac{1}{4}$ in. by 17 lb. steel beam together with $\frac{1}{4}$ in. diameter binders. The other beam had encased dimensions of 10 in. wide
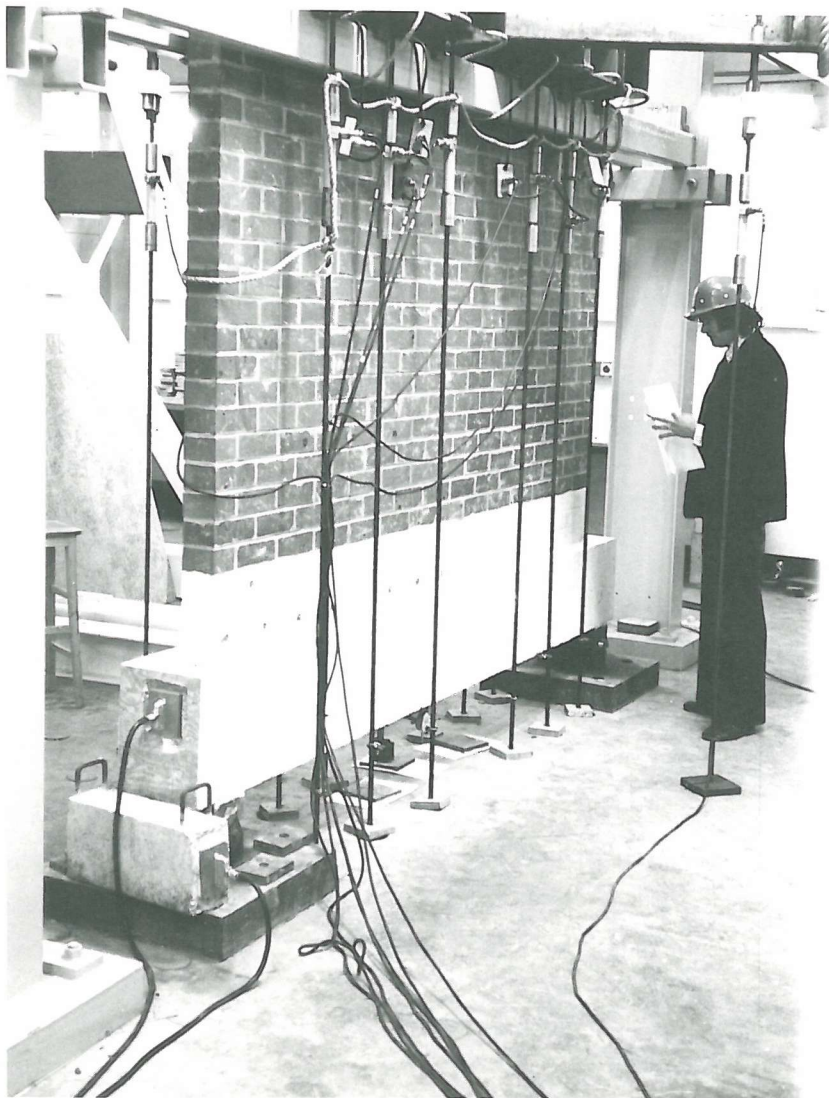
Plate 5.4   B.R.E. wall on beam test
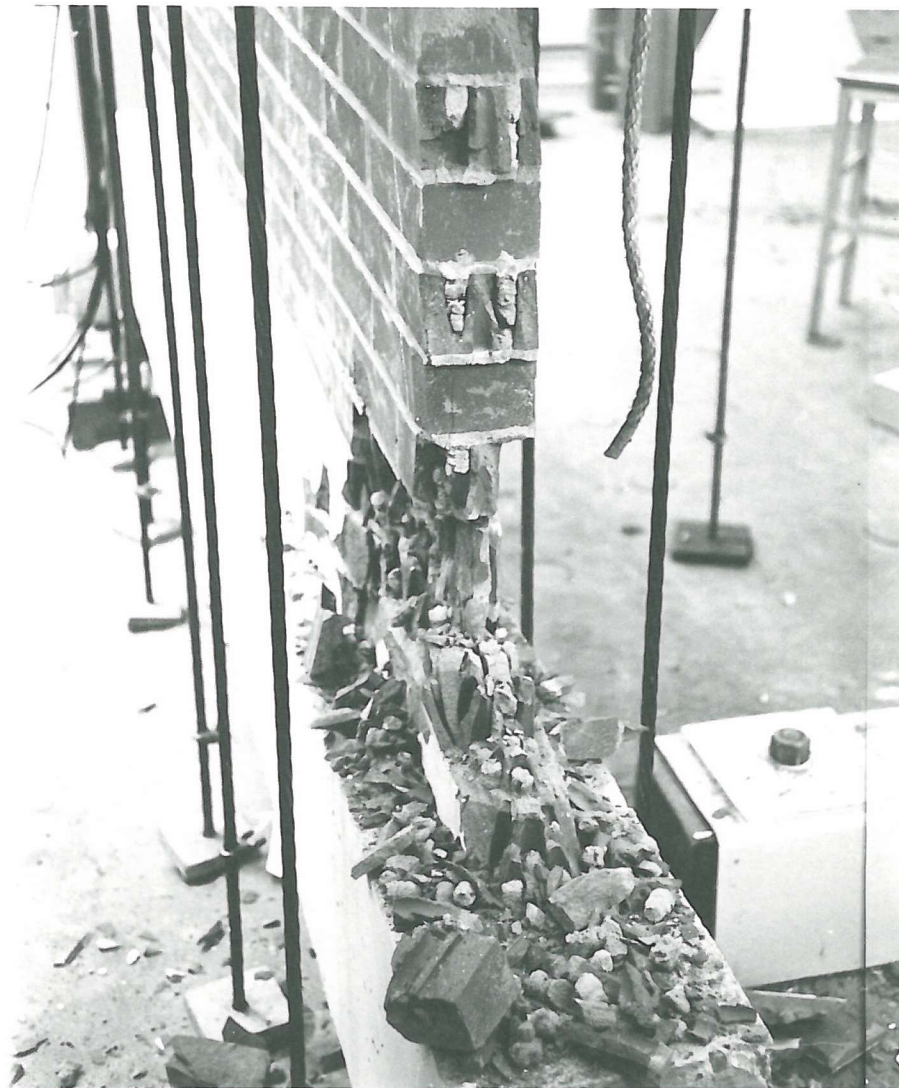
Plate 5.5   Wall after failure

by 14 in. deep and contained a 10 in. by $5\frac{3}{4}$ in. by 29 lb. steel beam
together with $\frac{1}{4}$ in. binders. The encasement concrete was designed
to have a strength of not less than 3000 lb/in^2 at 28 days. Before
encasement, strain gauges were attached to the top and bottom flanges
of the beam along half the span. Prior to constructing the walls,
the beams were subjected to quarter point loading in order to determine
their flexural stiffness from their deflections. The results are shown
in Table 5.5.

The two sets of two walls used in the tests were of different
strengths. The walls used in the first two tests were built with low
strength bricks and 1:1:6 mortar. The walls used in the final two tests
were built with high strength bricks and $1:\frac{1}{4}:3$ mortar. Brickwork pier
tests were undertaken to determine the modulus of elasticity and strength
of brickwork. The piers were nominally 9 in. by 9 in. by 12 courses
high. The averaged results are shown in Table 5.5.

The structures were taken through several load cycles before
being finally loaded to failure. Failure in all cases occurred due to
the walls crushing in one of the bottom corners. The form of failure
is shown in Plate 5.5.

Only the beam strains and deflections were recorded in the first
test. In the second test, the failure load and observed length of
contact were also recorded. In the final two tests, Demec readings
were taken on the wall above the wall-beam interface so that an
estimate of the wall strains could be obtained.

5.4.3 B value calculations

A maximum of three estimates of the B value could be obtained
from each test as explained in Section 5.2.3. These values are shown

in Table 5.5. Since only beam strains and deflections were measured
in Test 1, no B value estimates could be made for this test. The
peak wall stress B value could not be obtained from Test 2 either,
because no wall strain readings had been taken in this test. The peak
stress B values for Tests 3 and 4 were calculated by linearly extra-
polating the two vertical wall strain readings closest to the support,
up to the wall edge above the support. It can be seen from Table 5.5
that the estimated B values are very consistent with all the values
lying between 1.05 and 1.26.

| Test | Beam EI
lb in^2
x 10^9 | Wall E$_w$
lb/in^2
x 10^6 | Wall material
strength
lb/in^2 | K | Estimated B values | | |
					(1) Contact Length	(2) Peak Stress	(3) Failure
1	5.89	.57	880	5.10	-	-	-
2	3.26	.57	880	5.93	1.26	-	1.23
3	3.26	2.64	5600	8.63	1.08	1.16	1.10
4	5.89	2.64	5600	7.44	1.05	1.15	1.09

Table 5.5   Results from B.R.E. wall on beam tests.

5.4.4 Comparison with finite element analysis

A finite element analysis was undertaken to represent the wall on
beam structure of Test 1. The masonry wall was represented by a
homogeneous wall using the E$_w$ value obtained from the brickwork pier
tests. The beam was represented by a homogeneous beam with a beam
depth equal to the encased beam depth and using a calculated E value
that gave the flexural stiffness given by the quarter point loading
tests. This beam representation can only be considered approximate,

because the axial stiffness of the two beams could not be matched
and the flexural stiffness of the encased beam would tend to change
when subjected to axial forces such as the tie force. A uniformly
distributed load of 20 tons was applied at the top of the wall in the
analysis.

Comparisons between the test and computer analysis bending moment
and tie force diagrams are shown in Figs. 5.11 and 5.12 respectively.
The bending moment and tie force in the test beam were calculated from
the strain gauge results for a load of 20 tons. The calculated results
relate to the bending moment and tie force in the bare steel section
because it was not possible to estimate accurately the effects of the
encasement.

Considering the many approximations made in producing the comparisons
shown in Figs. 5.11 and 5.12, the level of agreement must be considered
reasonably good. The analysis and test central beam deflection also
gave good agreement with a test value of .030 in. and an analysis value
of .027 in. These results must therefore verify to some extent the
method of analysis.
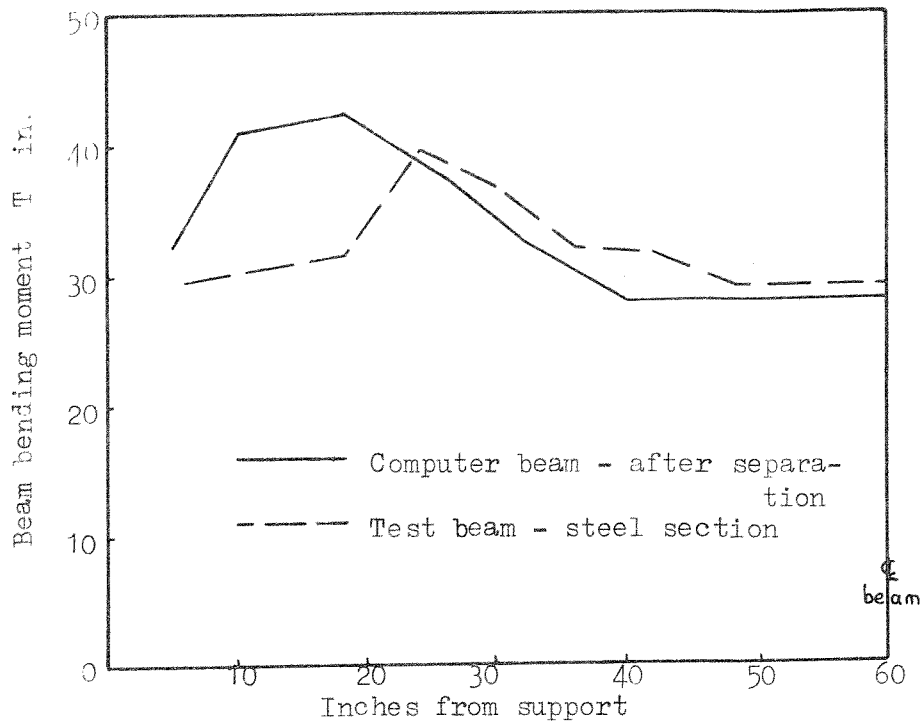
FIG. 5.11 COMPARISON BETWEEN TEST BEAM AND COMPUTER BENDING MOMENT
RESULTS
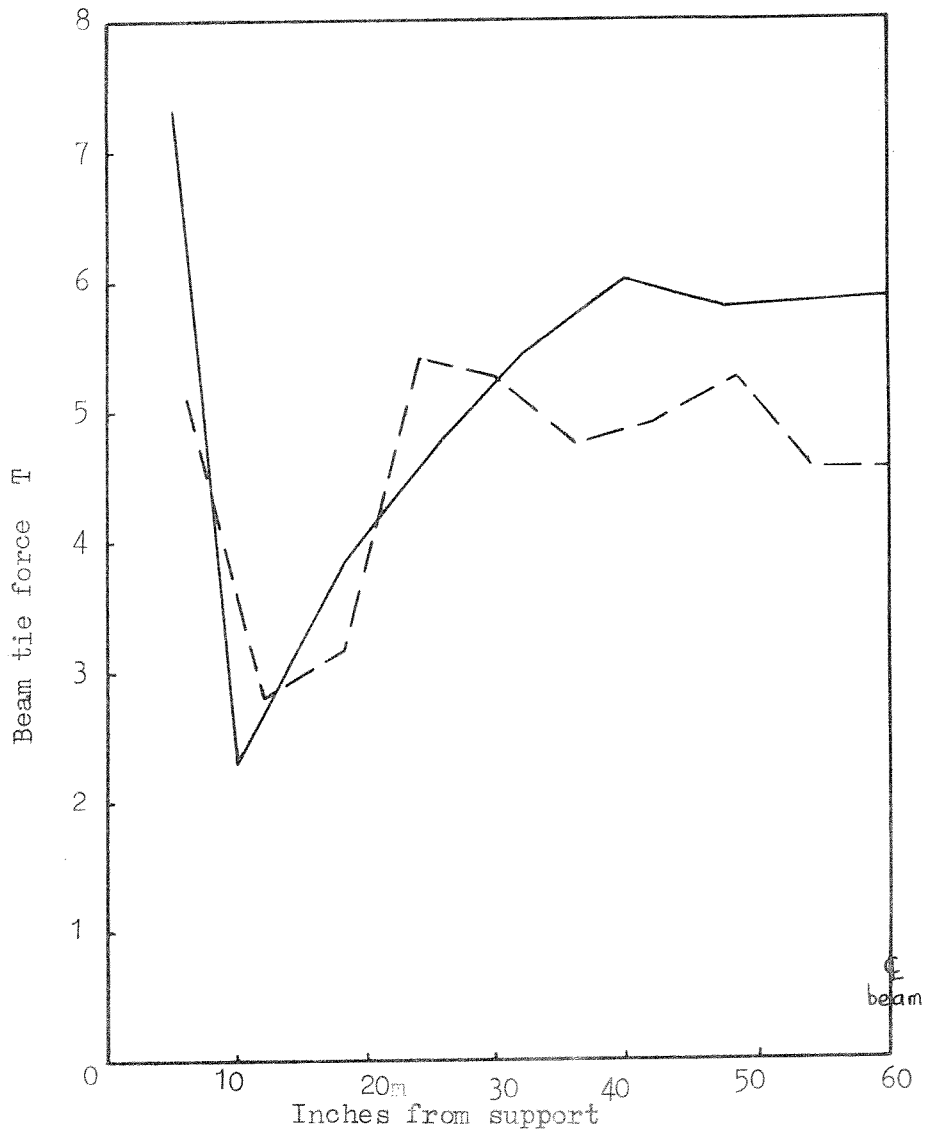
FIG. 5.12   COMPARISON BETWEEN TEST BEAM AND COMPUTER TIE FORCE RESULTS

5.5 Brickwork walls on reinforced concrete beams tests

5.5.1 Introduction

These tests were conducted as part of an undergraduate project[19]. They are briefly described here because some of their results were used in developing the approximate design method of Chapter 3.

5.5.2 Test description

Two tests were conducted with small brick walls on reinforced concrete beams. The single leaf walls were four bricks wide by ten bricks high and were both built with medium strength brickwork. The beams were $4\frac{1}{2}$ in. wide by 2 in. and 3 in. deep. They were both of balanced reinforcement design.

Prism tests were undertaken separately to establish the modulus of elasticity and Poisson's ratio values for the brick, the mortar and the beam concrete. The prism dimensions were 1 in. by 1 in. by 4 in. high and longitudinal and transverse strain measurements were made using strain gauges.

The wall on beam structures were loaded under approximately uniformly distributed loading. Strain measurements on the wall were obtained using strain gauges. The central beam deflection was also measured together with an estimate of the length of contact.

5.5.3 B value calculations

For the present work, the results of these tests were only used in calculating B value estimates. Of the three methods of obtaining B values, described in Section 5.2.3, only the measured contact length method could be used for these tests. The peak wall stress method could not be used because the strain gauge readings in the wall corners

had proved to be inconsistent and the failure load method could not be used because the brickwork strength was not known.

Table 5.6 shows the calculated B and K values for the structures. In calculating the K values, the modulus of elasticity of the wall was calculated from the brick and mortar values assuming the vertical proportions of the brick and mortar in the walls.

Beam depth in.	K value	B value
3	10.46	1.16
2	15.35	1.28

Table 5.6   Results from masonry wall on reinforced concrete beam tests

5.6 Conclusions

The main conclusions from this chapter can be summarized as follows:

(1) The plaster model tests clearly demonstrated the basic wall on beam behaviour assumed by the design method of Chapter 3, but indicated that the B values taken in the derivation of the first design method were inaccurate. Revised B values, based on the values found in these tests, were used in the later versions of the design method.

(2) The B value results obtained from the full scale tests conducted at the Building Research Establishment and the tests conducted at the University of Southampton were in good agreement with the B values calculated from the plaster model tests.

(3) The araldite model tests indicated that the results given by the finite element program developed in Chapter 4 should be accurate to within 10% for wall stresses and 20% for beam stresses and deflections.

CHAPTER 6

<u>INFILLED FRAMES: INTRODUCTION AND REVIEW</u>

<u>OF PREVIOUS WORK</u>

6.1 <u>Introduction</u>

When a structural frame is infilled with a masonry wall, the diaphragm action of the wall causes a substantial increase in the stiffness of the unit. The infill can be thought of as acting as a diagonal bracing strut. Although infilled frames can provide one of the most efficient means of resisting lateral wind loading, their structural properties have seldom been utilized in this country. This has mainly been due to the fact that no methods of design have ever been officially recognised in Britain. The design methods that have been developed by previous researchers have generally been complicated and difficult to apply.

A relatively simple design method is developed in this thesis for the design of infilled frames. This design method will probably be included in a new revised British Standard on structural steelwork design.

In addition to the development of the design method, a theoretical investigation was undertaken into the elastic behaviour of infilled frames. A finite element program was developed for this investigation which allowed for crack generation on the infill-frame boundaries as well as a friction or no friction connection on these boundaries.

6.2 Review of previous work

6.2.1 Introduction

In this section, a brief review of previous theoretical and experimental work on infilled frames is given. This previous research work can conveniently be split into three sections: (a) methods used to analyse infilled frames, (b) suggested methods of design or of simplified analysis of infilled frames and (c) experimental investigations.

6.2.2 Methods used to analyse infilled frames

Between 1952 and 1966, Polyakov[20-23] published several papers describing his work in Moscow. As part of this work, Polyakov undertook approximate analyses to determine the stresses in infills. Combinations of assumed infill boundary loading distributions were used with a theory of elasticity method.

In 1955, Whitney, Anderson and Cohen[24] published a paper in which a method of analysis was presented, based upon the assumption of integration between the frame and infill. The columns were assumed to be the flanges and the infill the web of a cantilever beam.

Between 1957 and 1960, Benjamin and Williams[25-28] published several papers describing their work at Stanford University. They undertook several analyses based on the lattice analogy approach, but concluded that a simple strength of materials approach would produce results of equal accuracy. Again a full integration between the infill and frame was assumed.

In 1960, Satchanski[29] published a paper in which a method of analysis was presented, based on the theory of elasticity method. The interaction forces between the frame and infill were replaced by thirty redundant reactions. A solution for these reactions was obtained using

the compatability of displacements of the frame and infill. Again the assumption of a continuous bond at the interface between the frame and infill was assumed.

Between 1962 and 1967, Stafford Smith[30-34] published several papers describing his work on infilled frames. As part of this work he used the finite difference method to analyse infills which were loaded under various assumed loading distributions. This work was later continued by Carter[35,36], who analysed infills by the finite element method. Carter used the same assumed loading distributions as Stafford Smith, but included the effects of a non linear elastic infill material. This was achieved by altering the modulus of elasticity of the elements in relation to their stress levels.

In 1967, Karamanski[37] published a paper in which, for the first time, the finite element method was used to analyse infilled frames. For these analyses the frame was taken to be rigidly connected to the infill and the frame members were assumed to carry axial forces only.

Later in 1967, Mallick and Severn[38] published a paper in which the finite element method was again used to analyse infilled frames. The techniques employed in these analyses were in several ways similar to those used in the present author's finite element analyses. Two sets of nodes were generated on the infill-frame boundaries and these were initially connected to give the same deflections perpendicular to the boundaries. After the first analysis, boundary node pairs were disconnected where tension across the boundary was detected. The analyses and disconnections were continued until no further separation occurred. The elements used for the frame did not, however, include the effects of axial forces and no allowance for boundary friction was included in the program.

In 1968, Mallick and Severn[39] published a paper in which the finite element method was used to study dynamic infill loading. In 1971, Mallick and Garg[40] published a paper in which the finite element method was used to study the effects of openings in infilled frames.

In 1968, Tomii[41] published a paper in which he analysed infilled frames elastically using stress functions. Tomii was concerned with reinforced concrete infills and thus made the assumption that the infill and boundary frame were bonded together.

In 1970, Liauw[42] published a paper in which he analysed infilled frames by means of the Airy stress function expressed in the form of a fourier series. In these analyses he also assumed the infill and boundary frame were bonded together.

Kadir[43], in his Ph.D. thesis of 1974, used the finite element method to analyse infilled frames. Again he defined two sets of nodes on the frame-infill interfaces. So as to prevent an iterative solution scheme, he initially only connected the frame to the infill over assumed lengths of contact. These nodes were again only connected for deflections across the boundaries which produced a no boundary friction type solution. In order to introduce friction, Kadir multiplied the boundary forces found in the no friction analysis by a coefficient of friction and applied these forces to the boundary nodes in a second analysis. This method of introducing boundary friction is, however, highly inaccurate because the friction forces considerably alter the forces perpendicular to the boundary.

6.2.3 Suggested methods of design or of simplified analysis of infilled frames

Polyakov[20-23] as a result of his experimental and theoretical work developed a design method in which the maximum theoretical shearing

stress in the infill is related to the infill material shear strength. Empirical formulae and design curves are used to take account of infill openings and variations in infill aspect ratio. Effects due to variations in frame stiffness are not considered.

Wood[44] in 1959, suggested an empirical interaction formula that related the infilled frame strength to the individual strengths of the infill and frame.

Benjamin and Williams[25-28] concluded from their experimental and theoretical work that the stiffness and strength of infilled frames was independent of frame stiffness, provided the frame was strong enough to produce infill failure. They went on to produce formulae for calculating the stiffness and strength of masonry infilled frames which were based on shear considerations.

Holmes[45], in his paper published in 1961, suggested a method of design for laterally loaded infilled frames based on the equivalent strut concept. Only the compressive mode of infill failure was considered in this method. The load carried by the infill at failure was calculated by multiplying the compressive strength of the infill material by the cross-sectional area of the equivalent strut. The width of the equivalent strut was taken as one third of the diagonal length of the infill and this resulted in the infill strength being independent of frame stiffness. The load carried by the frame at failure was calculated by assuming that the equivalent strut was shortened by an amount equal to its length multiplied by the failure strain of the infill material. In 1963, Holmes[46] published a second paper in which the method was extended to consider infilled frames subjected to combined vertical and lateral loading.

Tomii[47] in a series of papers, suggested methods for designing concrete infilled frames with and without openings. The failure load was calculated by relating the infill shearing deformation to the infill material failure shearing deformation.

Stafford Smith[30-34] also used the diagonal strut concept in developing his design method. From the results of his finite difference analyses he prepared design curves which related the effective width of the strut, the compressive failure load and the diagonal failure load to the frame stiffness and infill aspect ratio. This work was later extended by Carter[35,36] who included in his finite element analyses, the variation of infill modulus of elasticity with changing stress levels. Carter also produced curves for shear failure in masonry infills.

Liauw[48], in his 1972 paper, suggested an approximate method of analysis for infilled frames with and without openings, based on the concept of an equivalent frame. In developing this method, he assumed a constant connection on the frame-infill boundary. He conducted model tests, and as a result of these, concluded that his method was accurate for infills with large central openings.

Mainstone[49,50] has suggested formulae for calculating the stiffness, diagonal cracking load and the ultimate load of infilled frames. The formulae result from a series of model tests and again the diagonal strut concept was used. The formulae as presented, are not in a suitable form for design purposes.

Smolira[51] in his 1973 paper, suggested an approximate method of analysis based on the diagonal strut concept. He used the force-displacement method to solve rigidly jointed frames with diagonal infill struts. Although an indication is given in this paper of how to include the effects of lack of initial fit of the infill and contact pressure of

the infill on the frame members, the axial effects of the forces in the frame members were not included. For multistorey infilled frames, the suggested method of analysis requires a computer to produce the solution.

Kadir[43], in his thesis, suggested a method of design, again based on the diagonal strut concept. Using beam on elastic foundation theory, he first obtained expressions for the contact lengths between the infill and the columns and beams. The effective width of the diagonal strut was then assumed to be half the distance between the ends of the length of contact on the column and beam. The lateral stiffness of the infilled frame was calculated by assuming a rigidly jointed frame and a pin-ended diagonal strut. Also from this calculation the shear load carried by the infill was obtained. For the infill shear strength calculation, the shear load was averaged across the infill. For some unexplained reason, the vertical stress in the infill was taken as the vertical force component averaged across the infill multiplied by the ratio of the beam length of contact to the infill length. For the ultimate crushing strength calculation, the infill shear load was averaged over a column length related to the effective width.

6.2.4 Experimental investigations

A large number of model and full-sized tests have been carried out in the past twenty five years by different investigators. Only references to these tests are given here.[20-23,25-33,36,38-40,42,43,45,46,48,50,52-61] The most relevant of these tests to the present work are discussed in Section 7.3.

CHAPTER 7

INFILLED FRAMES: DEVELOPMENT OF A SIMPLE DESIGN METHOD

7.1 Introduction

This work was conducted at the instigation of the British

Standards Sub-Committee B/20/5, which required a design method for

the composite action of infilled frames, for its revision of BS449,

the structural steelwork code. Although the design method was

developed specifically for steel frames, with or without encasement,

it could also be applied to reinforced concrete frames if a lower

ratio of E/E_I is introduced.

Unlike the wall on beam design method described in Chapter 3,

this method was developed fairly directly to its final form, without

any major modifications. For this reason, the development of the

method can be presented in one section. The permissible stress

approach was used in developing the design method and only in its

final stages of development was it converted to a limit state approach.

For this reason the development of the method is shown in terms of

permissible stresses while the summary of the method is given in terms

of limit state design.

7.2 Development of the design method

7.2.1 Basic behaviour of infilled frames

Earlier research by Stafford Smith and Carter[30-36] has shown that when an infilled frame is loaded in shear, separation of the frame from the infill tends to occur in regions away from the compression corners, as shown in Fig. 7.1. The infill is then acting in effect as a diagonal compression strut. This earlier research also indicated that the contact length af and be is roughly equal to half the span, regardless of the frame stiffness, and that the lengths of contact ac and bh, defined here as α, are governed by the relative stiffness of the infill to the columns. It was found that α was related to the relative stiffness by an equation of the form

$$\frac{\alpha}{h} = \frac{\pi}{2\lambda h} \qquad \ldots \quad 7.1$$

in which λh is a non-dimensional parameter expressing the relative stiffness of the infill to the columns where

$$\lambda = \sqrt[4]{\frac{E_I\, t}{4EIh}} \qquad \ldots \quad 7.2$$

in which E_I, t and h are the Young's modulus, thickness, and height of the infill respectively; and E and I are the Young's modulus and second moment of area of the columns.

The similarity of λ to the characteristic parameter used in beam on elastic foundation theory is evident[15], as is the similarity of the problem, i.e. the in-plane interaction of flexural and plane stress components.

When the infill is of masonry, there are three possible modes of infill failure. The first mode is a horizontal shear failure in the
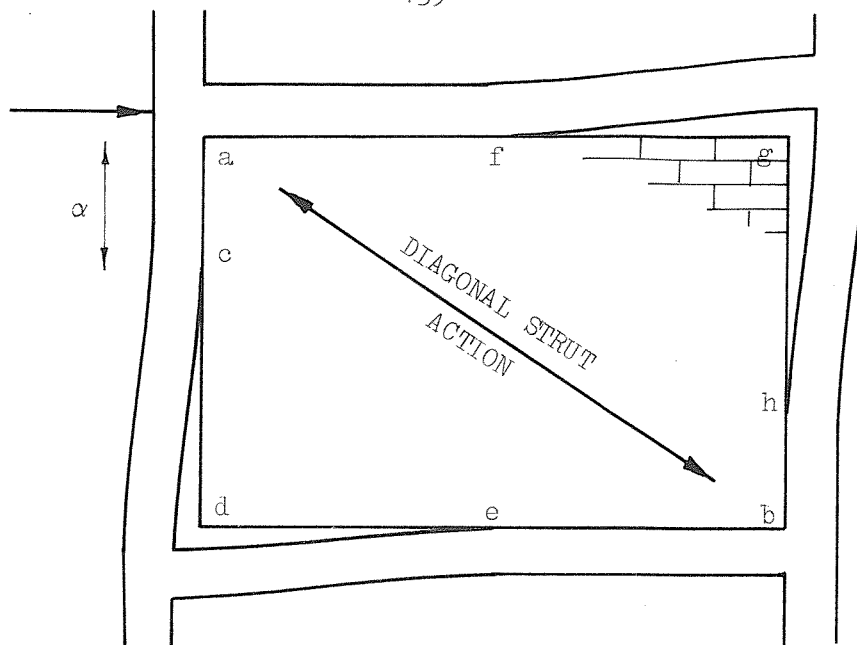
FIG. 7.1   BASIC BEHAVIOUR OF INFILLED FRAME
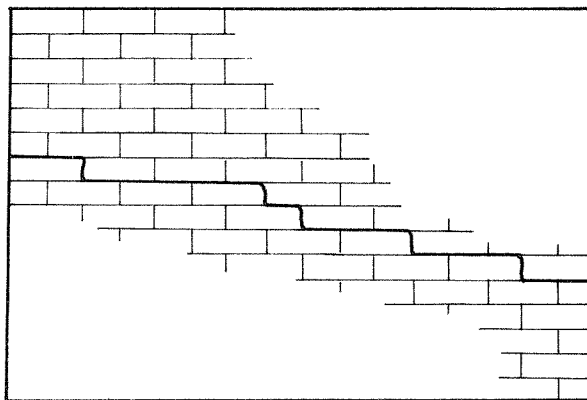
FIG. 7.2   SHEAR FAILURE IN INFILL
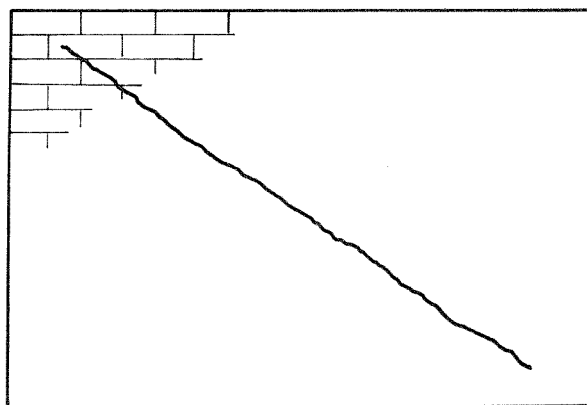
FIG. 7.3   DIAGONAL TENSILE FAILURE IN INFILL

mortar joints of the masonry, Fig. 7.2. The second is a diagonal tensile crack along the compression diagonal due to the combined effects of Poisson's ratio and the curvature of the stress trajectories, Fig. 7.3. The third failure mode is a compression failure in the loaded corners of the infill, Fig. 7.4.

In order to simplify the method, the horizontal shear force H is considered to be carried entirely by the infill. This assumption is conservative, but in most practical cases the difference is small because the stiffness contribution of the infill is normally much greater than that of the frame.

7.2.2 Stress analysis of infills

Stress analyses of infills with diagonal loading were undertaken previously by Stafford Smith[30-34]. The infills analysed had length to height proportions 1.0, 1.5, 2.0 and 2.5. In order to represent the various stiffnesses of the columns, the loading on the vertical face of the infill was applied over different lengths of contact. The loading was applied with half as direct stress and the other half as shear stress. The loading was taken to be distributed triangularly over a length of contact on the column sides equivalent to $\alpha/h = \frac{1}{8}, \frac{1}{4}, \frac{3}{8}$ and $\frac{1}{2}$. As shown in Fig. 7.5, the loading on the sides adjacent to the beams was distributed triangularly over half the span. The finite difference method was then used to solve the biharmonic equation at the nodes of a network over the infill.

The peak horizontal shear and principal tensile stresses were found to occur at the centre of the infill. The results for the range of cases analysed are shown in Table 7.1; these correspond to an infill of height 8 units, thickness 1 unit with a diagonal loading
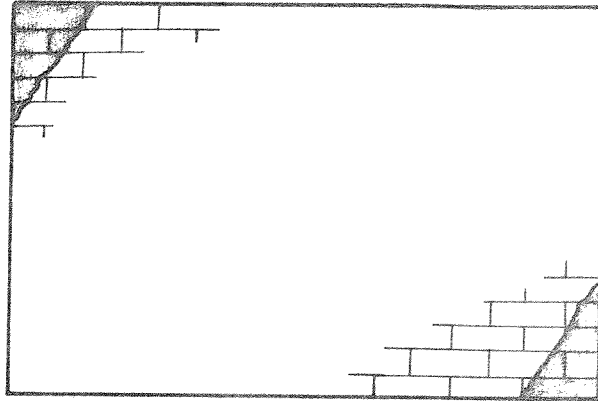
FIG. 7.4   COMPRESSIVE FAILURE IN CORNERS OF INFILL
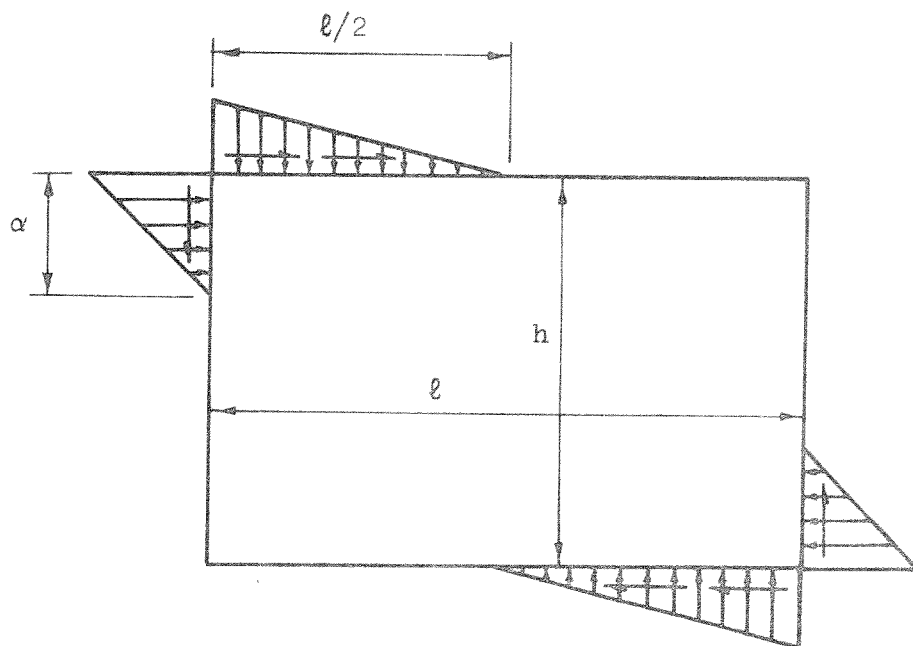
FIG. 7.5   ASSUMED LOADING INTERACTION DISTRIBUTION IN ANALYSES

$\frac{\ell}{h}$	$\frac{\alpha}{h}$	Peak Tensile Stress	Horizontal Shear Stress	Vertical Stress	Horizontal Stress
1	$\frac{1}{8}$	5.17	12.15	− 6.95	− 7.01
	$\frac{1}{4}$	4.94	11.97	− 6.99	− 7.08
	$\frac{3}{8}$	4.65	11.73	− 7.02	− 7.14
	$\frac{1}{2}$	−	−	−	−
1.5	$\frac{1}{8}$	3.92	9.67	− 3.14	− 9.32
	$\frac{1}{4}$	3.66	9.46	− 3.30	− 9.21
	$\frac{3}{8}$	3.43	9.30	− 3.44	− 9.15
	$\frac{1}{2}$	3.19	9.13	− 3.63	− 9.04
2	$\frac{1}{8}$	3.03	7.89	− 1.48	−10.76
	$\frac{1}{4}$	2.76	7.73	− 1.72	−10.58
	$\frac{3}{8}$	2.56	7.62	− 1.90	−10.46
	$\frac{1}{2}$	2.38	7.52	− 2.08	−10.31
2.5	$\frac{1}{8}$	2.47	6.61	− 0.66	−11.48
	$\frac{1}{4}$	2.20	6.51	− 0.93	−11.33
	$\frac{3}{8}$	2.04	6.42	− 1.08	−11.18
	$\frac{1}{2}$	1.89	6.37	− 1.24	−11.10

Table 7.1   Stress results at centre of infill

$\frac{h}{\ell}$	2.5	2.0	1.5	1.0	0.67	0.5	0.4
$\dfrac{\tau_{xy}\,\ell t}{H}$	1.43	1.41	1.39	1.37	1.39	1.41	1.43
$\dfrac{\sigma_y\,\ell t}{H}$	2.47	1.92	1.35	0.78	0.45	0.26	0.15
$\dfrac{\sigma_{dt}\,\ell t}{H}$	0.53	0.54	0.57	0.58	0.57	0.54	0.53

Table 7.2   Stress results converted into non-dimensional form

of 100 units.

The stresses at the centre are seen to be almost independent of the length of contact, i.e. the $\frac{\alpha}{h}$ ratio. This might have been expected from the St. Venant principle since the loading was relatively remote from the centre of the infill. To simplify the problem, the peak stresses were considered to be independent of the α/h ratio. The most conservative stress results, which corresponded to $\alpha/h = \frac{1}{8}$, were adopted in developing the design method.

In order to extend the range of results to values of $\ell/h < 1$, the assumption was made that the stress results for $h/\ell = 1.5, 2.0, 2.5$ could be taken as approximately equal to the results from $\ell/h = 1.5, 2.0, 2.5$, respectively. This followed from the assumption that the stress results were independent of the length of contact. For these values, the vertical and horizontal direct stress results from the analyses were reversed.

The stress results were converted to non-dimensional terms by dividing by the average shear stress $H/\ell t$, as shown in Table 7.2. It can be seen that the terms representing the shear stress and the diagonal tensile stress, $\tau_{xy}\ell t/H$ and $\sigma_{dt}\ell t/H$, are almost independent of the infill proportions. The most conservative values were again taken

i.e.
$$\frac{\tau_{xy}\ell t}{H} = 1.43 \qquad \ldots \; 7.3$$

and
$$\frac{\sigma_{dt}\ell t}{H} = 0.58 \qquad \ldots \; 7.4$$

When $\sigma_y \ell t/H$ was plotted against ℓ/h, as in Fig. 7.6, it could be seen that a close linear relationship existed between them.

The relationship took the form
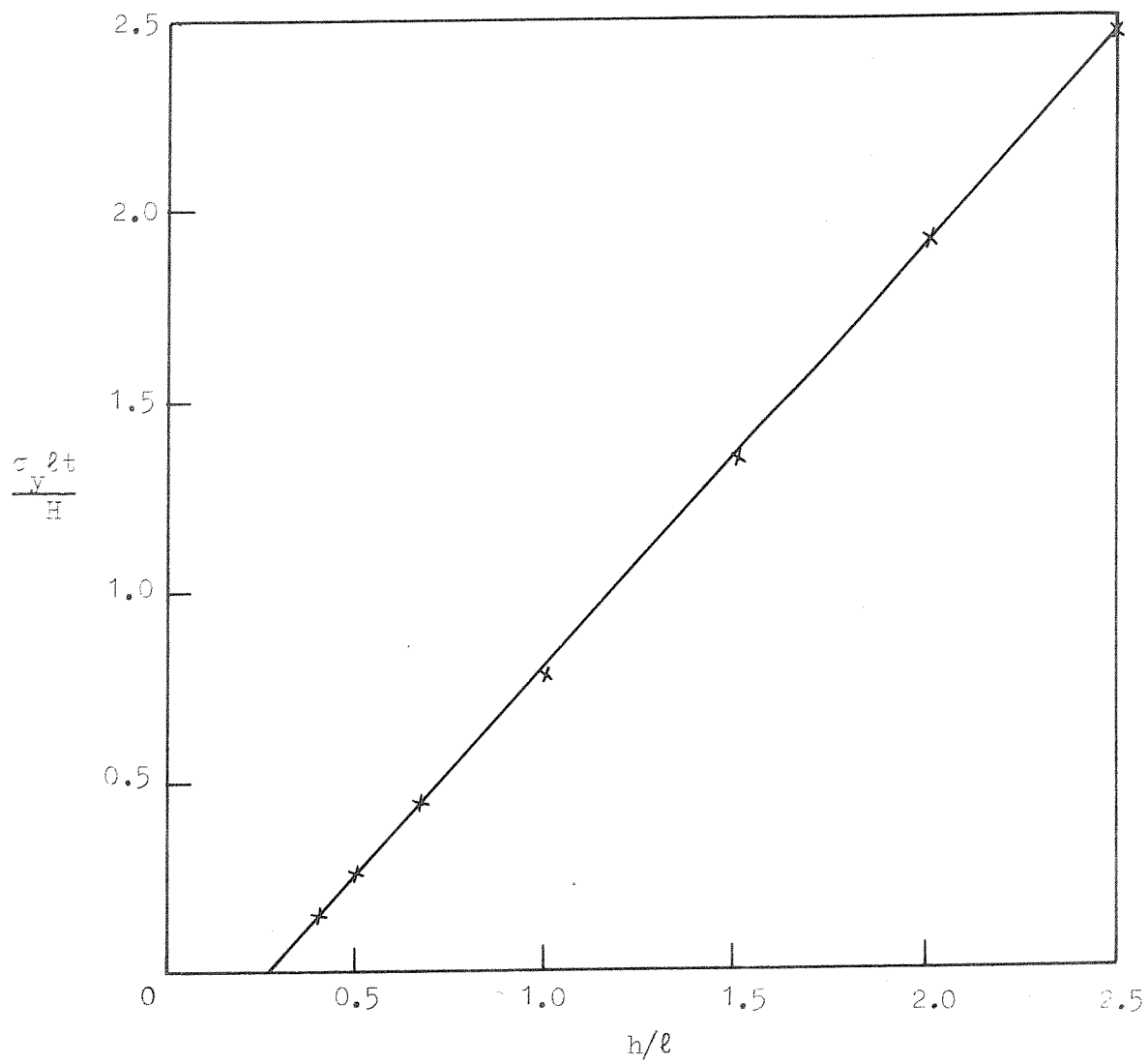
FIG. 7.6   RELATIONSHIP BETWEEN $\dfrac{\sigma_y \ell t}{H}$ AND $\dfrac{h}{\ell}$

$$\frac{\sigma_y \ell t}{H} = 1.1 \frac{h}{\ell} - 0.26 \qquad \qquad \ldots \; 7.5$$

Previous theoretical research[62,63] had indicated that the local stresses in mortar jointed masonry may exceed the stresses found from homogeneous analyses by up to 50% in some instances. The design method, however, was developed assuming that the homogeneous analyses results could be applied to masonry infills. This assumption could be justified because the predictions of strength from the design method, compared to the results from full scale tests, as described later, were still conservative.

It was now possible to consider the strength of the failure modes of the infill.

7.2.3 Failure modes of the infill

Shear failure

The permissible shear strength of brickwork is at present given in CP 111 as the lesser value of

$$f_s = 0.1 + 0.16\sigma_y \quad MN/m^2 \qquad \qquad \ldots \; 7.6$$

$$f_s = 0.5 \; MN/m^2 \qquad \qquad \ldots \; 7.7$$

At the strength limit $\tau_{xy} = f_s$ and combining Eqs. 7.3, 7.5 and 7.6 gives:

$$\frac{1.43H}{\ell t} = 0.1 + \frac{0.16H}{\ell t} \left(1.1 \frac{h}{\ell} - 0.26\right)$$

$$\text{i.e.} \quad H = \frac{\ell t}{14.7 - 1.76 \frac{h}{\ell}} \qquad \qquad \ldots \; 7.8$$

Combining Eqs. 7.3 and 7.7 gives:

$$\frac{1.43H}{\ell t} = 0.5$$

$$\text{i.e.} \quad H = 0.35\ell t \qquad \qquad \ldots \; 7.9$$

The maximum value of H to prevent shear failure will thus be given by the lesser result of Eqs. 7.8 and 7.9. Eqs. 7.8 and 7.9 are in units of MN and m.

<u>Diagonal tensile failure</u>

CP 111 at present gives the permissible tensile strength of brickwork in bending as $0.07 \; \text{MN/m}^2$. This is equivalent to approximately $\frac{1}{40}$ x the compressive failure strength of the weakest allowable mortar.

The diagonal tensile strength of brickwork can conservatively be taken as $\frac{1}{10}$ x the compressive strength of the mortar. Allowing for a typical factor of safety in brickwork of 4, the value of tensile strength in CP 111 of $0.07 \; \text{MN/m}^2$ seemed a reasonable value to adopt in the design method.

$$\text{i.e.} \quad f'_{dt} = 0.07 \; \text{MN/m}^2 \qquad \qquad \ldots \; 7.10$$

At the strength limit $\sigma_{dt} = f'_{dt}$ and combining Eqs. 7.4 and 7.10 gives:

$$\frac{0.58H}{\ell t} = 0.07$$

$$\text{i.e.} \quad H = 0.12\ell t \qquad \qquad \ldots \; 7.11$$

The maximum allowable value of H to avoid tensile failure will be given by Eq. 7.11. Eq. 7.11 is in units of MN and m.

It may be observed that Eq. 7.11 always gives a lower value of H than Eq. 7.9. Thus Eq. 7.9 could be dropped from the design method. Also Eq. 7.8 gives a lower H value than Eq. 7.11 when h/ℓ is less than 3.6. Since infilled frames with h/ℓ greater than 3.6 are extremely unlikely, Eq. 7.11 could also be dropped from the design method, providing a limit to h/ℓ was introduced. Thus diagonal tensile failure need not be considered if CP 111 shear and tensile strength values are used, although in practice, diagonal tensile failure may occur if the shear strength of masonry is above the CP 111 estimate.

Compressive failure in the corners of the infills

Stafford Smith[30-35] found from his model tests that the onset of this mode of failure was gradual and was accompanied by a rapidly increasing rate of deflection. It was thus assumed that a plastic mode of infill failure occurs. He also observed that the region in the corner of the infill where crushing takes place generally extends along the column over the length of contact α. Stafford Smith found that the expression

$$R = \alpha t \sec\theta \, f'_{cd} \qquad \qquad \ldots \; 7.12$$

(in which R is the diagonal load on the infill, θ the slope of the infill diagonal to the horizontal and f'_{cd} is the diagonal compressive strength of the infill) correlated reasonably well with his test results.

It has been assumed that

$$H = R \cos\theta \qquad \qquad \ldots \; 7.13$$

Thus from Eqs. 7.12 and 7.13

$$H = \alpha t \, f'_{cd} \qquad \qquad \ldots \; 7.14$$

Now from Eqs. 7.1 and 7.2

$$\alpha = \frac{\pi}{2} \sqrt[4]{\frac{4EIh}{E_I t}} \qquad \ldots \; 7.15$$

For a steel frame with a masonry infill, a reasonable estimate of E/E_I is 30. In fact α is not very sensitive to changes in E/E_I because of the fourth root relationship. Taking this value and combining Eqs. 7.14 and 7.15, the maximum value of H to avoid compressive failure is given by:

$$H = 5.2f'_{cd} \sqrt[4]{Iht^3} \qquad \ldots \; 7.16$$

Mainstone[49,50] conducted a large series of model tests on frames with both masonry and concrete infills. From the results of these tests, he concluded that the compressive strength of masonry infills was given by:

$$R = 1.12 \lambda h^{-0.88} f_k \, ht \cos \theta \qquad \ldots \; 7.17$$

in which f_k is the vertical compressive strength of the infill material.

Combining Eqs. 7.2, 7.13 and 7.17 and again taking $E/E_I = 30$ gives:

$$H = 1.12\left(\frac{th^3}{30I}\right)^{-0.22} f_k \, ht \cos^2 \theta \qquad \ldots \; 7.18$$

Eq. 7.17 can be approximated by the equation

$$H = 4f_k \cos^2 \theta \sqrt[4]{Iht^3} \qquad \ldots \; 7.19$$

The results from the diagonal compression testing, described in Chapter 9, indicated that the diagonal compressive strength of brickwork under infill type loading f'_{cd} was greater than the vertical

strength of the brickwork f_k. Thus the difference between Mainstone's and Stafford Smith's estimates of compression failure strength can not be accounted for by the difference between f'_{cd} and f_k.

It was decided to use in the design method Mainstone's equation for compression strength for the following reasons:

(1) Mainstone's equation gave more conservative results for H. In the majority of cases, taking the more conservative equation would have no effect on the design, because the shear equation is usually limiting.

(2) Stafford Smith's equation was independent of infill shape and this seemed illogical for infills with h/ℓ greater than 1. All of Stafford Smith's tests were conducted on infilled frames with h/ℓ less than or equal to 1.

(3) None of Stafford Smith's tests were conducted on frames with masonry infilling.

7.2.4 Forces and bending moments in the frame

The finite element computer analyses described in Chapter 8, indicated that the axial forces in the frame could be reasonably estimated by assuming the frame to be pin-jointed with each infill replaced by a single diagonal pin-jointed bracing strut.

The analyses also indicated that bending moments in infilled frames tend to be very small and that a maximum assumed moment of $Hh/20$ is conservative for both the columns and beams.

7.2.5 Lateral stiffness of infilled frames

The computer analyses described in Chapter 8, indicated that the lateral deflection of infilled frames was primarily dependent on the axial and not the flexural stiffness of the frame members. It was

thus thought reasonable to calculate the lateral deflection of infilled frames by considering the frame as being pin-jointed with the infills replaced by diagonal bracing struts. The analyses indicated that a conservative estimate of deflection would be obtained if the diagonal bracing strut was considered to have an effective width of 0.1 x its length.

7.2.6 Conversion of the design method to limit state form

Of the equations left in the design method, only Eq. 7.8 needed converting to limit state form, since this was the only dimensional equation.

Eq. 7.8 was formed by combining Eqs. 7.3, 7.5 and 7.6 and of these only Eq. 7.6 was dimensionsl as this was the CP 111 permissible shear strength equation. The shear strength equation can be rewritten in dimensionless form[64] as

$$f_s = f_{bs} + \mu\sigma_y \qquad \ldots \quad 7.20$$

in which f_{bs} is the bond shear strength of the brickwork or blockwork and μ is the coefficient of friction along the horizontal brickwork or blockwork mortar joints. In limit state terms, characteristic values of f_{bs} and μ are given implicitly in CP 111 as $f_{bs} = 0.4$ N/mm^2 and $\mu = 0.625$.

Combining Eqs. 7.3 , 7.5 and 7.17 gives the limit state equation for shear failure as

$$\frac{1.43\, \gamma_f\, H}{\ell t} = \frac{f_{bs}}{\gamma_{mv}} + \frac{\mu\, \gamma_f\, H}{\gamma_{mv}\, \ell t}\left(1.1\frac{h}{\ell} - 0.26\right)$$

i.e.
$$\gamma_f H = \frac{f_{bs}\, \ell t}{\gamma_{mv}\left(1.43 - \dfrac{\mu}{\gamma_{mv}}\left(1.1\dfrac{h}{\ell} - 0.26\right)\right)} \qquad \ldots \quad 7.21$$

in which γ_f and γ_{mv} are the partial safety factors for the load

and for the strength of brickwork or blockwork in shear respectively.

7.2.7 Modification of shear failure equation due to analyses information

The finite element analyses, described in Chapter 8, indicated that Eq. 7.5 overestimated the central infill vertical stresses by approximately 25%. Because this error could lead to unsafe designs, the equation for the vertical stress σ_y was modified to:

$$\sigma_y = \frac{H}{\ell t} \left(0.8 \frac{h}{\ell} - 0.2 \right) \qquad \ldots \; 7.22$$

This change resulted in the final shear failure equation being modified to:

$$\gamma_f H = \frac{f_{bs} \, \ell t}{\gamma_{mv} \left(1.43 - \frac{\mu}{\gamma_{mv}} \left(0.8 \frac{h}{\ell} - 0.2 \right) \right)} \qquad \ldots \; 7.23$$

7.2.8 Summary of design method

General. The disposition of infilled panels throughout a structure shall satisfy the following requirements to ensure general stability:

a) The designer shall take care to provide a sufficient number of panels in every storey of the building to allow alternative paths for horizontal loads in the event of an accidental or unwitting removal of a single panel.

b) The relative disposition of the infill braced bents and other calculated shear resistant elements in each storey height shall be such that in combination they will also resist torsional displacements of the entire building.

Provisions

a) The frame members may be of hot-rolled section, hot-formed rectangular tube or built-up section and they may be totally encased or unencased, or a combination of both, provided always that the steel section has an axis of symmetry parallel to the plane of the wall.

b) With unencased steel sections the appropriate axis of symmetry shall lie within the middle third of the thickness of the wall. With encased steel sections the appropriate axis of symmetry of the steel section shall lie within the thickness of the wall. The faces of the wall shall not protrude beyond the outside of adjacent columns or beams.

c) The wall shall be of brickwork or blockwork set in mortar not weaker than Grade (iii) as specified in CP 111 and shall have a height to length ratio within the range 0.3 to 3.

d) Excepting holes permitted by provision (f) care shall be taken during construction to avoid the presence of gaps between the wall and the frame on all sides.

e) The maximum slenderness ratio of the wall shall conform with Clause 4.1.1 of CP 111 assuming an effective height equal to the height of the infill.

f) Openings may only be located immediately adjacent to the surrounding frame and within the middle third of the sides of the infill. The maximum dimension of openings in the infill must not exceed one-tenth of the height or length of the infill, whichever is smaller.

g) In bents which are to be designed as braced by infills, it must be assumed that in any storey the infills carry the total horizontal load and that any horizontal strength contributed by the frame is neglected.

Notation

f_{bs} –   characteristic bond shear strength of brickwork or block-
work, given implicitly in CP 111 as equal to 0.4 N/mm^2.

f_k –   characteristic compressive strength of brickwork or block-
work as given in CP 111.

H   –   horizontal load.

h   –   height of infill.

I   –   second moment of area of column section about its axis
perpendicular to the plane of the frame.

ℓ –   length of infill.

t   –   thickness of infill

γ_f –   partial safety factor for load

γ_m –   partial safety factor for strength of brickwork or blockwork
in compression as given in CP 111.

γ_{mv} –   partial safety factor for strength of brickwork or blockwork
in shear as given in CP 111.

θ –   slope of the diagonal of the infill to the horizontal.

μ –   characteristic coefficient of friction along the horizontal
brickwork or blockwork mortar joints, given implicitly in
CP 111 as equal to 0.625.

Design of the infill

Two possible modes of failure must be considered. The first is
due to shear and exhibits cracking along the bedding joints of the
brickwork; this mode is defined as the serviceability limit state.
The second is due to compression and occurs by crushing and spalling
in the corners of the infill; this is defined as the collapse limit
state. Both states must be checked in all designs.

a) Serviceability limit state:

This is to be checked by the formula

$$\gamma_f H = \frac{f_{bs} \ell t}{\gamma_{mv} \left[1.43 - \frac{\mu}{\gamma_{mv}} \left(0.8 \frac{h}{\ell} - 0.2 \right) \right]} \qquad \dots \ 7.24$$

b) Collapse limit state:

This is to be checked by the formula

$$\gamma_f H = 4 \frac{f_k}{\gamma_m} \cos^2 \theta \sqrt[4]{I.h.t^3} \qquad \dots \ 7.25$$

To Check the Deflection of the Frame

A conservative estimate of the sway deflection of a frame braced by panels complying with this Section may be obtained by treating it as a pin-jointed frame, each bracing panel being replaced by a diagonal bracing member in compression of the following characteristics:

Cross sectional area = 0.1 x t x diagonal length of infill

Elastic Modulus for brickwork = 7×10^3 N/mm^2

$$= 1 \times 10^6 \ lb/in^2$$

To Check the Strength of the Frame

The members of the frame and their connections must be able to withstand forces resulting from the worst combination of dead, imposed and wind loads which may act on the infilled frame. The axial forces may be determined by simple static analysis of an equivalent frame with the columns pin-jointed at each storey level, the beams pin-jointed at their ends and the infills acting as diagonal pin-jointed bracing struts.

In addition to the axial forces described above:

a) the columns must be able to carry a bending moment equal to

γ_f Hh/20 applied in the plane of the frame in addition to the bending moments from other causes. However, the effects of the forces specified in (e) and (f) are to be excluded.

b) where the upper beam of the infilled panel is not restrained by an infill above, the beam must be able to withstand a mid-span hogging moment of γ_f Hh/20 in combination with the moment due to vertical dead loading.

c) where the lower beam of the infilled panel is not restrained by an infill below, the beam must be able to withstand a mid-span sagging moment of γ_f Hh/20 in addition to the moment due to vertical dead and live loading.

d) Each column adjacent to an infilled panel must be able to resist in shear an additional horizontal force γ_f H equal to that with-stood by the adjacent infill panel.

e) the beam above an infill within a length of $\ell/10$ from each end, and its connections, must be able to carry an additional upwards shear force of γ_f Hh/ℓ in combination with the shear force due to vertical dead loading.

f) the beam below an infill, within a length of $\ell/10$ from each end, and its connections, must be able to carry a downwards shear force of γ_f Hh/ℓ in addition to the shear force due to vertical dead and live loading.

7.3 Comparison of design method with test results

7.3.1 Full scale and model tests conducted by Benjamin and Williams[27]

Table 7.3 shows the results from a series of tests conducted by Benjamin and Williams on reinforced concrete frames with brickwork infilling. In using the design method to calculate the estimated cracking loads, Benjamin and Williams' values for f_{bs} and μ were used together with their workmanship factor.

The results indicate close agreement between the design method predicted loads and the actual cracking loads. Generally the predicted loads are slightly below the actual loads and are thus conservative.

7.3.2 Full scale tests conducted by Meli and Salgado[58,59]

Table 7.4 shows the results from a series of tests conducted by Meli and Salgado at the National University of Mexico on reinforced concrete frames with brickwork infilling. The specimens were approximately square with infill side lengths of the order of 2 m. The loading was applied horizontally to one upper corner of the frame. A uniformly distributed vertical pre-compression load was applied to the wall in some of the tests.

In using the design method to calculate design loads, CP 111 permissible values were used for f_{bs} and μ. Where pre-compression occurred, this was included in the calculations by assuming the stress to be uniformly distributed over the infill.

Considering that the design method load includes a safety factor of between 3.5 and 4, the design method is seen to give a reasonable value for the design cracking load. The ratio between the cracking load and the design load tended to increase when pre-compression was applied. This could be due to either the pre-compression stress not being uniformly distributed over the infill or the brickwork having

Infill dimensions h x ℓ (in.)	Infill thickness t (in.)	Cracking load (tons)	Design estimate (tons)	$\dfrac{\text{Cracking load}}{\text{Design load}}$
30.9 x 45.4	2.5	8.4	6.7	1.25
67.5 x 99	5.5	30.1	32.2	0.94
67.5 x 99	5.5	34.0	32.2	1.06
90 x 132	8.0	56.7	62.4	0.91
20 x 28	2.25	5.8	4.9	1.18
20 x 40	2.25	6.7	6.0	1.12
20 x 40	2.25	8.5	6.0	1.42
20 x 62	2.25	11.6	8.5	1.36
33.5 x 58	3.75	17.9	15.3	1.17
33.5 x 58	3.75	16.1	15.3	1.05
33.5 x 58	3.75	19.6	15.3	1.28
33.5 x 58	3.75	16.1	15.3	1.05

Notes   Design method estimates use Benjamin and Williams values

for μ and f_{bs} and include their workmanship factors.

Table 7.3   Benjamin and Williams' infilled frame test results.

Test	Pre-compression (kgf/cm^2)	Design load including safety factor (kgf)	Crack load (kgf)	Ultimate load (kgf)	$\dfrac{\text{Cracking load}}{\text{Design load}}$
801	0	1,470	4,400	5,830	3.0
802	3.6	2,300	11,600	13,450	5.0
803	0	1,470	6,430	11,000	4.4
901	0	1,830	5,080	5,080	2.8
902	6.2	3,630	13,220	14,020	3.6
Solid brick	0	1,840	5,200	8,800	2.8
	3	2,700	11,600	13,400	4.3
Perforated brick	0	1,840	6,900	9,300	3.7
	3	2,700	11,900	13,700	4.4
Hollow clay brick	0	1,840	6,600	7,300	3.6
	3	2,700	12,300	12,300	4.5
Sand lime brick	0	1,840	4,600	5,800	2.5
	3	2,700	11,800	13,100	4.4

Notes Design method loads calculated using CP 111 permissible values

for μ and f. The design method loads thus include a safety

factor of between 3.5 and 4.

Table 7.4 Meli and Salgado's infilled frame test results.

a higher value of μ than that assumed by CP 111 .

7.3.3 Full scale tests conducted by Mainstone and Weeks[60]

Table 7.5 shows the results from a series of tests conducted by Mainstone and Weeks at the Building Research Establishment on encased steel frames with brickwork infilling. The infilling had a ℓ/h ratio of approximately 1.2 with a height of 9 feet. The loading was applied diagonally. In using the design method to calculate the diagonal design loads, CP 111 permissible values were again used for f_{bs} and μ .

The design method is seen to give very conservative values for the design diagonal load, even after accounting for the safety factor of between 3.5 and 4. The most likely reason for this difference is that the shear strength of the brickwork used, could have been considerably higher than the strength assumed in CP 111. In Benjamin and Williams' tests, the brickwork used had a bond shear strength that was almost four times the CP 111 assumed strength. Another possible reason for the difference is the form of loading used in these tests. Diagonal loading does not truly correspond to normal infilled frame loading because all the frame members in this case are loaded in compression, whilst in a building, the windward columns tend towards tensile loading.

7.3.4 One-eighth scale tests conducted by Fiorato, Sozen and Gamble[61]
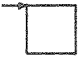
Table 7.6 shows the results from a series of tests conducted by Fiorato, Sozen and Gamble at the University of Illinois on reinforced concrete frames with model brickwork infilling. The infills had a ℓ/h ratio of 2 with a height of 15 inches. The loading scheme and form of the structures is shown in Table 7.6. In using the design method to

Wall thickness (mm.)	Design load including safety factor (KN)	Cracking load (KN)	Ultimate load (KN)	Cracking load / Design load
70	22.4	140	310	6.2
110	35.2	290	480	8.2
110	35.2	370	760	10.5
110	35.2	390	440	11.1
340	108.9	1340	1620	12.3

Notes   Loads given in terms of the diagonal load on the infilled frame. Design method loads calculated using CP 111 permissible values for μ and f_{bs}. The design method loads thus include a safety factor of between 3.5 and 4.

Table 7.5   Mainstone and Weeks' infilled frame test results

Test reference	Form of structure	Design load including safety factor (kips)	Cracking load (kips)	Ultimate load (kips)	Cracking load / Design load
S2H		0.272	3.2	3.2	11.8
S2I		0.272	3.7	3.7	13.6
F1C		0.272	2.5	2.5	9.2
F2B		0.272	2.9	2.9	10.7
F3B		0.272	3.7	4.5	13.6
F3C		0.272	3.8	5.6	13.9
M2B		0.272	3.2	5.3	11.8
M2C		0.272	1.7	2.0	6.2

Notes   Design method loads calculated using CP 111 permissible

values for μ and f_{bs}. The design method loads thus

include a safety factor of between 3.5 and 4.

Table 7.6   Fiorato, Sozen and Gamble's infilled frame test results.

calculate the design loads, CP 111 permissible values were again used for f_{bs} and μ.

After accounting for the safety factor of between 3.5 and 4, the design method is again seen to give very conservative values for the design load. This conservatism could also be due to the brickwork having a higher strength than that assumed in CP 111.

7.3.5 Small scale tests conducted by Kadir[43].

Table 7.7 shows the results from a series of tests conducted by Kadir at the University of Edinburgh on mild steel frames with model brickwork infilling. The infills had a vertical height of 15.75 inches. In using the design method to calculate the design loads, Kadir's assumed values for f_{bs}, μ and the compressive brickwork strength were used. Because the compressive brickwork strength was given for these tests, it was possible to calculate design crushing loads to compare with the test crushing loads.

The results indicate that the design method is conservative for both the shear cracking and crushing modes of failure. Although Kadir used a form of triplet testing to obtain a value for the bond shear stress of the brickwork, he did not use these tests to obtain a value for the coefficient of friction. Instead he used the value of coefficient of friction found by Hendry and Sinha[64]. The applicability of this value to Kadir's tests must be in doubt, particularly since Hendry and Sinha's tests were on full scale brickwork, while Kadir's tests were on approximately quarter scale brickwork. The scale of Kadir's tests is another reason to question their accuracy. The overall scale of the tests was approximately one eighth while the brickwork scale was approximately one quarter.

Infill shape ℓ/h	λh	Shear cracking (tons)	Design shear cracking (tons)	Cracking / Design cracking	Ultimate crushing	Design crushing	Crushing / Design cracking
1	7.07	0.845	0.547	1.54	3.66	2.21	1.65
1	5.26	0.908	0.547	1.66	3.94	3.00	1.31
1	4.27	1.219	0.547	2.23	6.70	3.73	1.80
1.6	7.07	0.994	0.716	1.39	3.51	3.13	1.10
1.6	5.26	1.276	0.716	1.78	5.28	4.32	1.22
1.6	4.27	1.268	0.716	1.77	7.70	5.36	1.44
2	7.07	1.152	0.840	1.37	3.60	3.54	1.02
2	5.26	1.188	0.840	1.41	6.23	4.80	1.30
2	4.27	1.299	0.840	1.55	8.57	5.96	1.44

Notes   Averaged test results. Results with frame joint failures excluded. Large variation in shear cracking values for normally identical samples. Greatest variation:highest value/ lowest value = 2.7. Design method loads calculated using Kadir's assumed values for μ and f_{bs}.

Table 7.7   Kadir's infilled frame test results.

7.4 <u>Conclusions</u>

The main conclusions from this chapter may be summarized as follows:-

(1) The design method presented gives a rational representation of the basic behaviour of infilled frames.

(2) The design method is simple and is thus very easy to apply.

(3) The design method allows for the safe design of infilled frames for which guidance was hitherto lacking.

CHAPTER 8

INFILLED FRAMES: COMPUTER ANALYSES

8.1 Introduction

This chapter is concerned with the numerical stress analysis of infilled frames. The main problem that has to be overcome before any accurate elastic analysis can be produced is that of the separation cracks that usually develop on the frame-infill boundaries. These cracks tend to form wherever there are tensile stresses across the frame-infill boundaries, because the tensile connection between the frame and infill is usually very weak.

The finite element program developed in this chapter allows for the automatic generation of these separation cracks. Using this program, analyses were undertaken to first check the validity of the design method developed in Chapter 7, and then to study the behaviour of infilled frames under combined vertical and horizontal loading.

6.2 <u>Development of the finite element programs to analyse infilled</u>

<u>frame problems</u>

Two finite element programs were developed specifically to

analyse infilled frame structures. The only difference between the

two Fortran language programs was the method employed to solve the

banded stiffness matrix.

The programs were developed with the following requirements in

mind:

(a)   that no symmetry of structure or loading need be assumed

(b)   that there should be no restriction, other than computer

capacity, on the complexity of the structure

(c)   that there should be automatic generation of separation

cracks on all the infill-frame interfaces

(d)   that there should be a choice of there being either a

friction or a sliding connection between the infills and

the surrounding frame

(e)   that there should be a choice between having the beams

either pin-jointed or fixed to the columns

(f)   that the frames need not all be infilled.

The programs were developed from the final wall on beam program.

The basic four node, two degrees of freedom per node, rectangular

finite element was retained. The rectangular element developed by

Lau[12] was not used because of the problems described in Section 4.2.3.

Initially the routines for the development of the separation crack

and the calculation of the beam moment and tie forces were removed

from the wall on beam program. The program was then altered so that

the physical properties of the new structure form could be read in

easily. The routine for the reading in of data relating to air spaces

was left unaltered.

Since it was assumed that cracking could occur on all the beam-infill and column-infill interfaces, the program was altered so that two rows of nodes were created on all the horizontal and vertical lines along these interfaces. The pairs of adjacent nodes on these lines could then be grouped into three types. The first group of node pairs were those that linked the various sections of the frame. The program was written so that these node pairs could be either linked permanently or left free. It was thus possible, for example, to represent a beam as being pinjointed to a column by linking only one pair of their adjacent nodes together. The second group of node pairs were those on the beam-infill interfaces. The program was written so that all these node pairs were initially linked. When a shear connection was required on these interfaces, the nodes were linked for both horizontal and vertical displacements, but if a no-friction connection was required, the nodes were linked only for vertical deflections. The third group of node pairs were those on the column-infill interfaces. These were linked in a manner similar to those of the second group except that when a no-friction connection was required, the nodes were only linked for horizontal deflections.

It was found to be more convenient to read in separately all the node pairs that were to be linked rather than to read in just the first and last nodes of a row or column of node pairs. Although the original data preparation using this method took longer, the continuation of an analysis which had stopped through lack of computer time was far easier. For the larger problems, the analyses often ran out of computer time before all the cracking iterations, usually five or six, were complete. Rather than repeat the whole analysis, it was

possible to restart the analysis with the node pairs that had already
separated as initially unlinked. This was easily achieved by removing
the linking data cards for the particular nodes concerned and
changing the two data cards that defined the number of node pairs to
be linked.

In the wall on beam programs described in Section 4.2, nodal
stresses were not used to determine the separation crack length on
the wall-beam interface. This was because the nodal stress on the
interface had indicated an oscillating wave form which was known to
be incorrect. At the time the wave effect was detected, the finite
element developed by Lau was being used in the wall on beam program.
It was later discovered that the wave effect was probably due to the
element type rather than the nodal stress calculations. It was thus
thought reasonable to attempt to use nodal stresses to calculate the
separation lengths in the infilled frame programs. The infilled frame
programs were thus developed with both nodal and centroid stresses
being calculated. On the beam-infill interfaces, separation of a node
pair was undertaken when the vertical stress indicated by the infill
node became tensile, and on the column-infill interfaces, when the
horizontal stress indicated by the infill node became tensile. This
method of calculating the separation lengths was far simpler than
the method used in the wall on beam program. To have used the cubic
extrapolation functions used in the wall on beam program, would have
been extremely tedious because of the number of interfaces where
separation could occur. In order that the crack lengths could easily
be detected at each iteration stage, the stress perpendicular to the
interface, for the infill node of each linked pair was printed out.

As previously mentioned, the difference between the two infilled frame programs was in the method chosen to solve the banded stiffness matrix. In the first program, the method used in the wall on beam program was retained, i.e. the whole of the half band stiffness matrix was stored in the core of the computer and this was then solved by the Gauss elimination method. In the second program, the half band stiffness matrix was stored on a magnetic disc or tape in the computer and this was then transferred in small blocks between the disc or tape and the computer core store where the actual solution was computed by the Gauss elimination method. The advantage of the second program, compared with the first program was that far larger problems could be solved because only a small part of the stiffness matrix was occupying the core store at any one time. The main disadvantage of the second program was that computing time was considerably increased by the many transfers between the disc or tape and the core store. For example, each of the thirty, three storey infilled frame analyses described in Sections 8.5 and 8.6 completely occupied the University's ICL 1907 computer for about one hour. For the above reasons, the first program was used for all the single frame analyses, while the second program was used for all the multiple frame analyses.

8.3 Analysis of wall on beam problems with the infilled frame program

The method of separation used in the infilled frame program was different from that used in the wall on beam program. Since the infilled frame program could be used to analyse wall on beam problems, it was thought desirable to analyse a couple of these problems in order that the results from the two programs could be compared.

Two wall on beam analyses were thus conducted using the infilled frame program. The lengths of separation found in the two analyses were identical to those found using the wall on beam program. This resulted in identical stress and deflection results except for those stress results obtained by interpolation in the wall on beam program.

These results indicated that the use of nodal stresses to calculate separation was reasonably accurate, even though the nodes were on a boundary between elements of different elastic properties. For the analyses of the basic wall on beam problem, the wall on beam program still had the advantage that the wall corner stress was calculated using a cubic function rather than the linear function assumed in the element stress matrix.

8.4 Single square infilled frames under diagonal loading

The results from Stafford Smith's finite difference analyses of infills under diagonal loading were used in deriving the approximate design method. It was thus considered desirable to compare his analyses results with results calculated using the infilled frame program where the frame is included in the analysis. In his earlier analyses, Stafford Smith assumed the same contact length on both the beams and columns of the frame and had no shear transfer on the infill boundaries. These analyses thus represented infilled frames under diagonal loading with a no friction infill boundary. Using the infilled frame computer program, an analysis was undertaken on a structure which represented as closely as possible one of Stafford Smith's analyses[32]. The infill was taken as 8 units high and wide and one unit thick. In Stafford Smith's analysis, the contact length was taken as 3 units. Thus for the present analysis, the frame strength was designed so as to give a α/h value of $\frac{3}{8}$ when using Eqs. 7.1 and 7.2. This represented a λh value of 4.2. A diagonal loading of 100 units was applied to the top left hand corner of the frame by means of 70.7 unit horizontal and vertical loads. The bottom right hand corner region of the frame was restrained both horizontally and vertically.

The results from this analysis (1.1) are shown in Table 8.1, and Figs. 8.1 and 8.2. It can be seen from Fig. 8.1 that before separation, considerable tensile stresses are formed which largely disappear when separation occurs, as shown in Fig. 8.2. It should be noted that the principal tensile stress contour divisions in Fig. 8.1 are five times greater than those in Figs. 8.2 to 8.6. Stafford Smith's results, Fig. 8.3, and the present results, Fig. 8.2, show close

Analysis Ref.	λh	Boundary Friction?	Central infill stresses			w/d
			τ_{xy}	σ_{dt}	σ_y	
1.1	4.2	No	12.5	+5.4	-6.5	.25
1.2	4.2	Yes	8.7	+5.3	-3.3	.60
1.3	6.3	Yes	9.6	+5.7	-3.9	.45
1.4	15	Yes	11.1	+5.7	-5.3	.30

Table 8.1   Single square infilled frames under diagonal loading

Compressive stress contours
Tensile stress contours

FIG. 8.1   PRINCIPAL STRESS CONTOURS FOR ANALYSIS 1.1 – BEFORE SEPARATION

FIG. 8.2   PRINCIPAL STRESS CONTOURS FOR ANALYSIS 1.1 – AFTER SEPARATION

FIG. 8.3   PRINCIPAL STRESS CONTOURS FOR STAFFORD SMITH'S ANALYSIS

agreement, particularly in the central infill region, which is the
critical area when considering tensile and shear infill failure modes.
Differences in the stress results in the corner regions result from
inaccuracies in Stafford Smith's assumptions on load application.
These differences do not, however, affect the design method because
the crushing failure equation was derived from model test results and
not analytical results.

Three analyses were undertaken with infill boundary friction
and diagonal loading. The first analysis (1.2) was with $\lambda h = 4.2$.
When no separation occurred, two further analyses (1.3) and (1.4)
were undertaken with lighter frames. These analyses also showed no
separation occurring. The results of these analyses are shown in
Figs. 8.4, 8.5 and 8.6 and in Table 8.1. The slight differences in
the stresses in the two loaded corners is due to the level of restraint
that was found to be necessary in the bottom right hand corner to
prevent any rotation of the structure.

The stress results indicate that as might be expected, as the
frame strength reduces and it carries less load, the central infill
stresses increase slightly. The reduction in frame strength is also
seen to result in increased peak corner stresses and reduced effective
strut width. The removal of boundary friction also results in in-
creased central and corner infill stresses and reduced effective strut
width. This increase in corner peak stress is due to the effect of
the infill sliding and being jammed in the two opposite corners of
the frame.

——————— Compressive stress contours

– – – – – Tensile stress contours
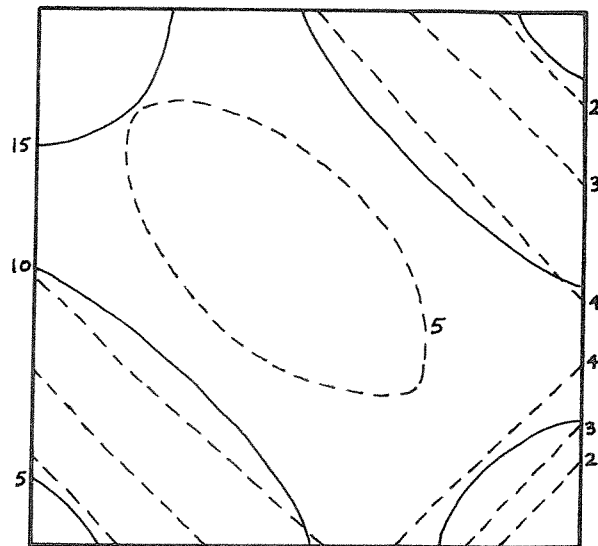
FIG. 8.4 PRINCIPAL STRESS CONTOURS FOR ANALYSIS 1.2
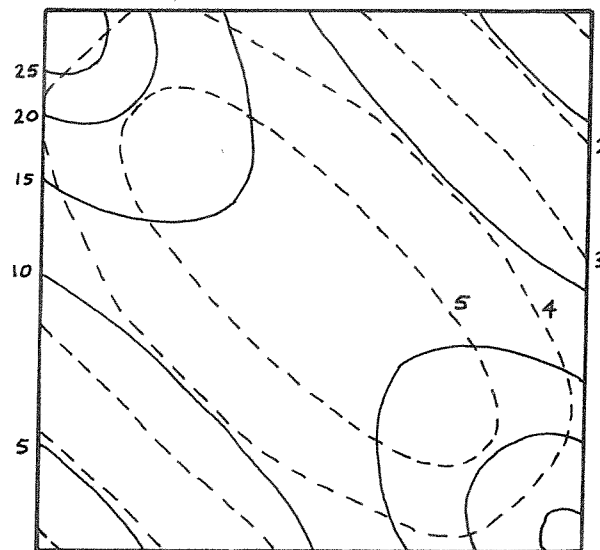
FIG. 8.5 PRINCIPAL STRESS CONTOURS FOR ANALYSIS 1.3
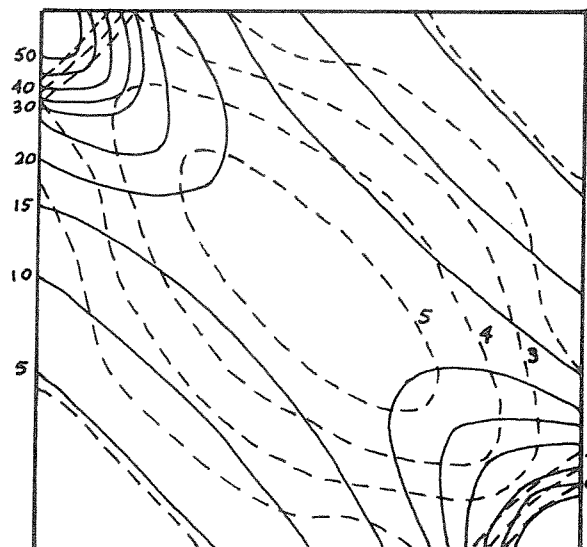
FIG. 8.6 PRINCIPAL STRESS CONTOURS FOR ANALYSIS 1.4

8.5 Infilled frames under lateral loading

8.5.1 Introduction

The most important parameters that determine the behaviour under lateral loading of infilled frames are: frame strength; level of boundary friction; infill aspect ratio; frame joint connections; modulus of elasticity ratio between frame and infill; and the inter-action between connected infills. Because of their large number, it was not possible to undertake a comprehensive parameter study. Instead, selective analyses were undertaken to determine the main effects of these parameters. In this manner the accuracy of the design method could be checked and a better understanding of the basic behaviour of infilled frames obtained.

8.5.2 Single square infilled frames

Ten analyses were undertaken on the basic square infilled frame under shear loading. The loading and restraint arrangement is shown in Fig. 8.7 together with the infill dimensions. The E ratio between the columns and infill was taken as 4 and column member depths adjusted to give the desired λh values using Eq. 7.2. The beam depths were made equal to the column depths. For the first six analyses the modulus of elasticity of the beams was made equal to that of the columns. In the final four analyses the modulus of elasticity of the beams was varied to give differing beam stiffnesses. The λh values considered, 3, 6.3 and 15, were chosen because $\lambda h = 3$ was thought to be representative of a very stiff frame, $\lambda h = 6.3$ of a medium stiffness frame and $\lambda h = 15$ of a very flexible frame. The level of shear connection on the frame-infill interfaces of an infilled frame varies according to the materials being used and the ratio between the shear-
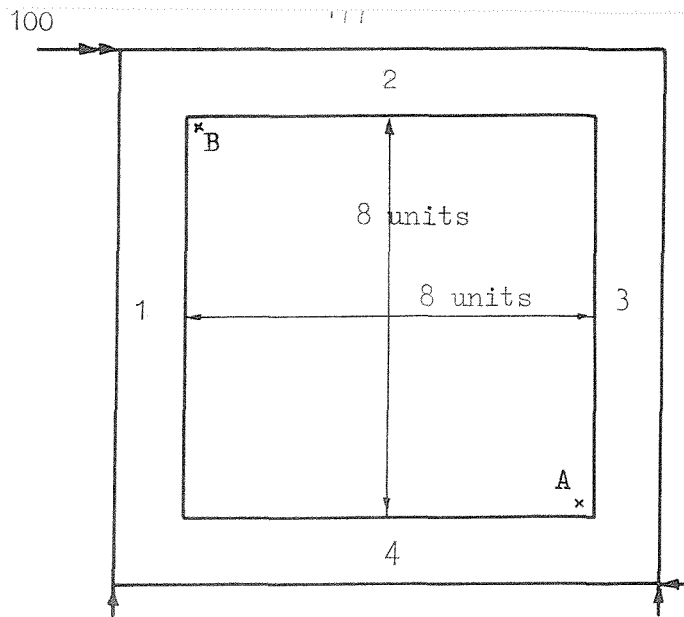
FIG. 8.7   LOADING AND RESTRAINT ARRANGEMENT FOR ANALYSES 2.1 to 2.10

———— Compressive stress contours

– – – – Tensile stress contours
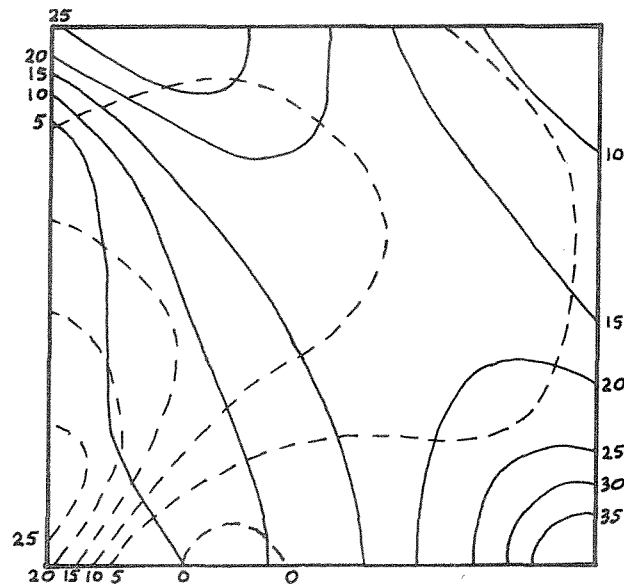
FIG. 8.8   PRINCIPAL STRESS CONTOURS FOR ANALYSIS 2.5 – BEFORE SEPARATION
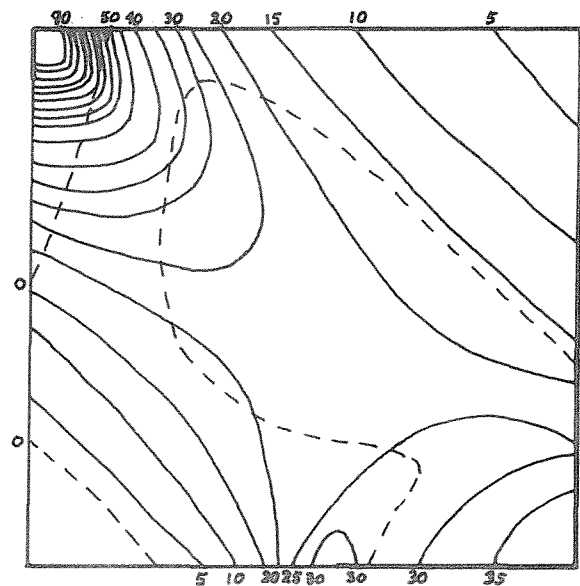
FIG. 8.9   PRINCIPAL STRESS CONTOURS FOR ANALYSIS 2.5 – AFTER SEPARATION

ing and the normal forces. Hence analyses were conducted for both the friction and no friction cases.

Figs 8.8 and 8.9 show the principal stress results in the infill, before and after separation for the analysis with $\lambda h = 6.3$ and boundary friction. Similarly Figs. 8.10 and 8.11 show results for $\lambda h = 15$ and boundary friction. It can be seen that before separation considerable tensile stresses develop, which largely dissipate when separation occurs. The after separation stress diagrams clearly demonstrate the basic diagonal strut action of the infills.

Fig. 8.12 shows the horizontal shear stress distribution for the $\lambda h = 6.3$, friction analysis after separation. Although the peak shear stress does not occur in the centre of the infill, it can be seen that this is likely to be the critical region, because in the regions of higher shear stress, the infill shear strength is likely to have increased by a proportionately greater amount due to increased vertical compressive stresses. For comparison purposes, Fig. 8.13 shows the horizontal shear stress distribution produced from an analysis with the same structure under a diagonal loading of $100\sqrt{2}$ units. Although no separation occurred in this analysis, the results are seen to be very similar to the Fig. 8.11 results in the region away from the two loaded corners.

Table 8.2 shows a summary of the results from this set of analyses together with the values that would have been calculated using the design method. For the first six analyses in which the beam and column stiffnesses were equal, it can be seen that considering the extreme simplicity of the design method, the analyses values and the estimated values are generally in good agreement. The deflection values were not expected to agree because the design method was made deliberately conservative to account for any non-linear behaviour of the infill

—————— Compressive stress contours
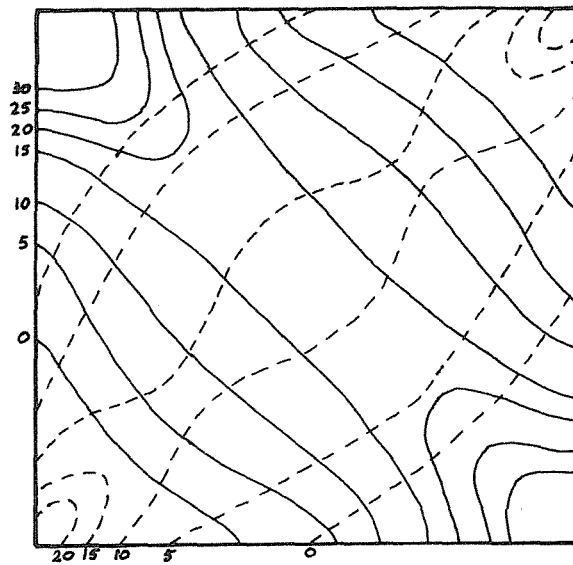
- - - - Tensile stress contours
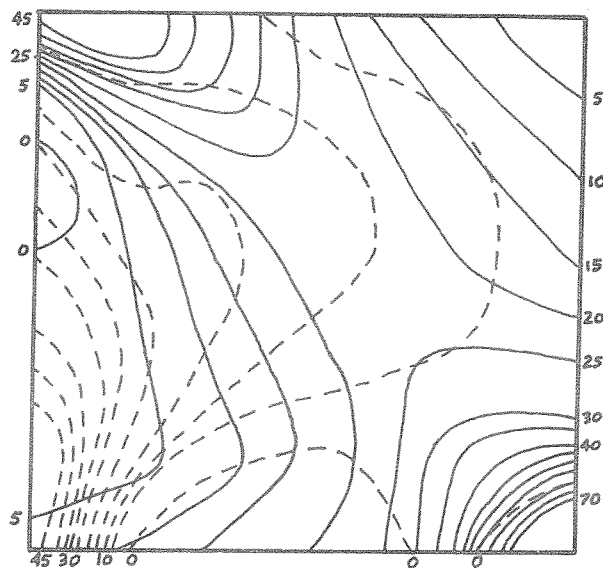
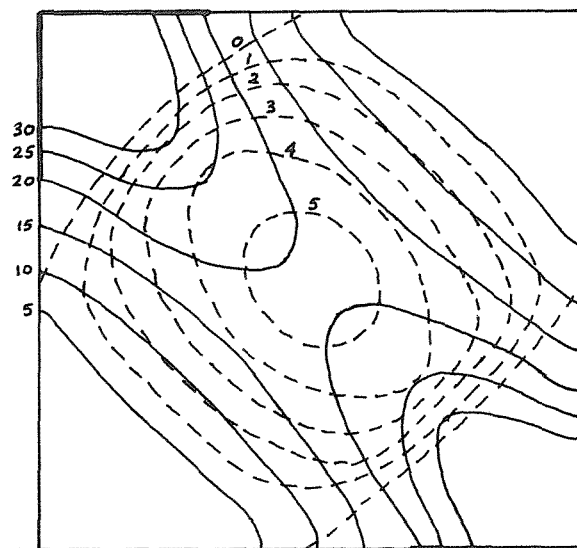FIG. 8.10 PRINCIPAL STRESS CONTOURS FOR ANALYSIS 2.6 – BEFORE SEPARATION

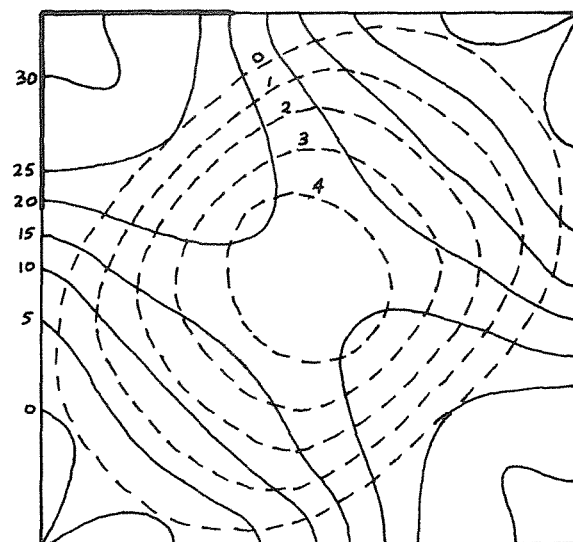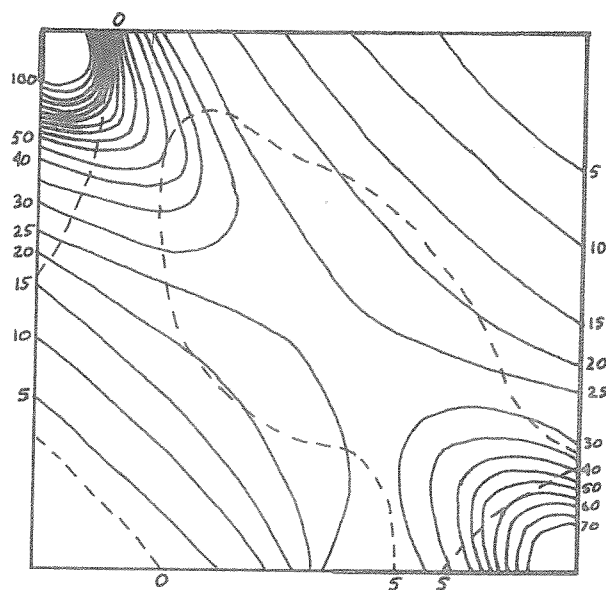FIG. 8.11 PRINCIPAL STRESS CONTOURS FOR ANALYSIS 2.6 – AFTER SEPARATION
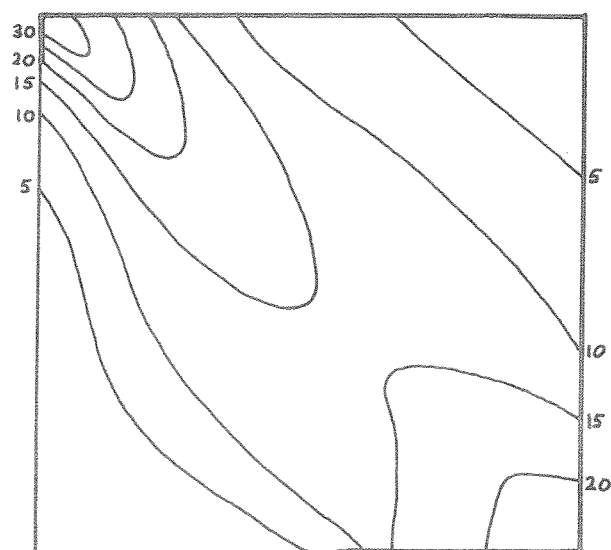
FIG. 8.12   HORIZONTAL SHEAR STRESS CONTOURS FOR ANALYSIS 2.5 -
AFTER SEPARATION
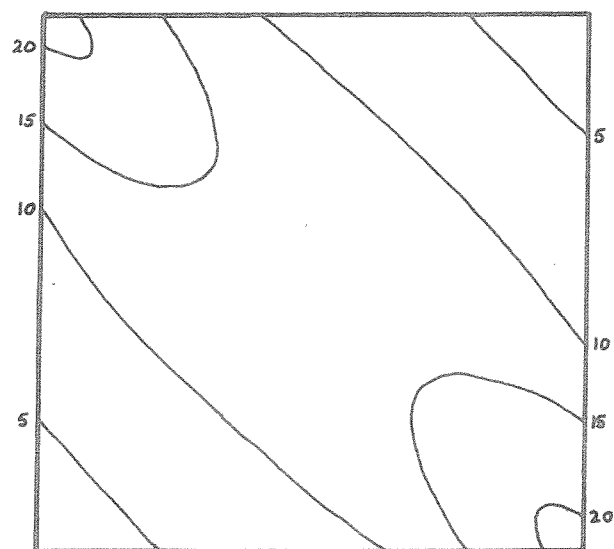
FIG. 8.13   HORIZONTAL SHEAR STRESS CONTOURS FOR ANALYSIS 2.5
STRUCTURE   LOADED DIAGONALLY - NO SEPARATION

Analysis reference	λh	Boundary friction?	Central infill stresses			Frame member axial forces				Lateral deflection	w/d	Infill corner stresses	
			τ_{xy}	σ_{dt}	σ_y	1	2	3	4			Position A	Position B
2.1	3	No	14.4	+5.2	-8.7	+100.0	-9.0	-11.4	-10.5	5.18	0.22	-103.3	-114.5
2.2	6.3	No	16.8	+6.3	-8.7	+102.8	-0.3	-0.5	-1.8	7.98	0.16	-175.3	-188.7
2.3	15	No	16.7	+6.3	-7.9	+100.7	+0.1	+0.1	-0.5	12.28	0.14	-247.8	-253.9
2.4	3	Yes	11.6	+5.0	-7.8	+95.3	-29.2	-27.2	-16.4	3.48	0.36	-20.6	-67.6
2.5	6.3	Yes	14.6	+6.2	-7.8	+100.0	-4.7	-16.3	-8.7	5.71	0.25	-46.3	-135.1
2.6	15	Yes	15.7	+6.2	-7.6	+100.3	-7.8	-7.7	-1.1	9.14	0.25	-106.3	-91.8
2.7*	6.3	No	16.9	+6.3	-8.7	+103.2	-0.4	-0.6	-1.5	7.70	0.16	-166.0	-176.9
2.8**	6.3	No	16.8	+6.3	-8.3	+102.0	-0.5	-0.6	-1.7	8.36	0.15	-188.9	-203.7
2.9*	6.3	Yes	15.3	+5.4	-9.0	+100.0	-1.4	-0.7	-3.7	6.04	0.23	-50.4	-125.3
2.10**	6.3	Yes	14.9	+6.2	-8.2	+100.3	-10.7	-15.2	-4.5	5.81	0.24	-57.1	-145.9
Design method values													
2.1 2.4	3	—	17.9	+7.3	-7.5	+100.0	0	0	0	10.72	0.10	—	—
2.2 2.8 2.5 2.9 2.7 2.10	6.3	—	17.9	+7.3	-7.5	+100.0	0	0	0	11.74	0.10	—	—
2.3 2.6	15	—	17.9	+7.3	-7.5	+100.0	0	0	0	15.12	0.10	—	—

Notes　　*　Double beam stiffness

　　　　**　Half beam stiffness

Table 8.2　Single square infilled frames under lateral loading

material. In the design method a plastic crushing failure form is anticipated. For this reason no design method estimate can be made to compare with the elastically calculated corner stresses shown. The corner stresses are included in Table 8.2 to indicate the relative magnitude of these stresses with varying λh values and boundary friction.

Considering the stresses at the centre of the infill for analyses 2.1 to 2.6, it can be seen that both the shear and tensile stresses increase slightly with a reduction in boundary friction and with an increase in λh. The shear and tensile stress values were, however, all within the estimated values given by the design method. The vertical compressive stress at the centre of the infill also increases slightly with a reduction in boundary friction, but it reduces with increasing λh. The vertical stress results are all greater than the design method estimate, which is thus conservative.

With regard to the frame forces for analyses 2.1 to 2.6, it can be seen that the design method estimates accurately the force in the tension column but fails to estimate the forces in the other frame members. This leads to considerable errors for the stiffer frames with boundary friction. In the three storey analyses described in Section 8.5.3, the beam forces were generally below the design method estimates. Since the three storey analyses are probably a more realistic representation of the behaviour of infilled frames in buildings, it seems reasonable to disregard the higher than design beam forces in these analyses.

The final four analyses were undertaken to investigate the importance of beam stiffness on frame behaviour. In analyses 2.7 and 2.9, the beam stiffness was doubled by doubling the modulus of

elasticity of the beams. In analyses 2.8 and 2.10, the beam stiffness was halved by halving the modulus of elasticity of the beams. The central infill stresses are seen to be little affected by the beam stiffness, with no clear trend of behaviour. Likewise, the tension column force is not significantly altered by beam stiffness changes. There are some changes in the other frame forces for the friction analyses, but these do not, however, exhibit any definite trend of behaviour. The deflection is seen to increase slightly with reducing beam stiffness for the no friction analyses, but for the friction analyses, again no clear trend is evident with very little difference in the three results. The corner stresses generally tend to increase with reducing beam stiffness. However, this stress change is only in the order of 15%. Since a fourfold reduction in beam stiffness was necessary to create this 15% stress change, the design method assumption that corner stresses are independent of beam stiffness must be considered reasonable.

8.5.3 Three storey square infilled frames - all infilled

Six analyses were undertaken on a basic three storey, rigid jointed, infilled frame structure under lateral loading. The loading and restraint arrangement is shown in Fig. 8.14. λh values of 3, 6.3 and 15 were again considered for both the friction and no friction cases. The E ratio between the frame and infill for these first six analyses was taken as 4 and the frame member depths were adjusted to give the desired λh values using Eq. 7.2.

Figs. 8.15 and 8.16 show the principal compressive stress diagrams, before and after separation respectively, for the bottom infill of the structure with $\lambda h = 6.3$ and a friction boundary. These diagrams
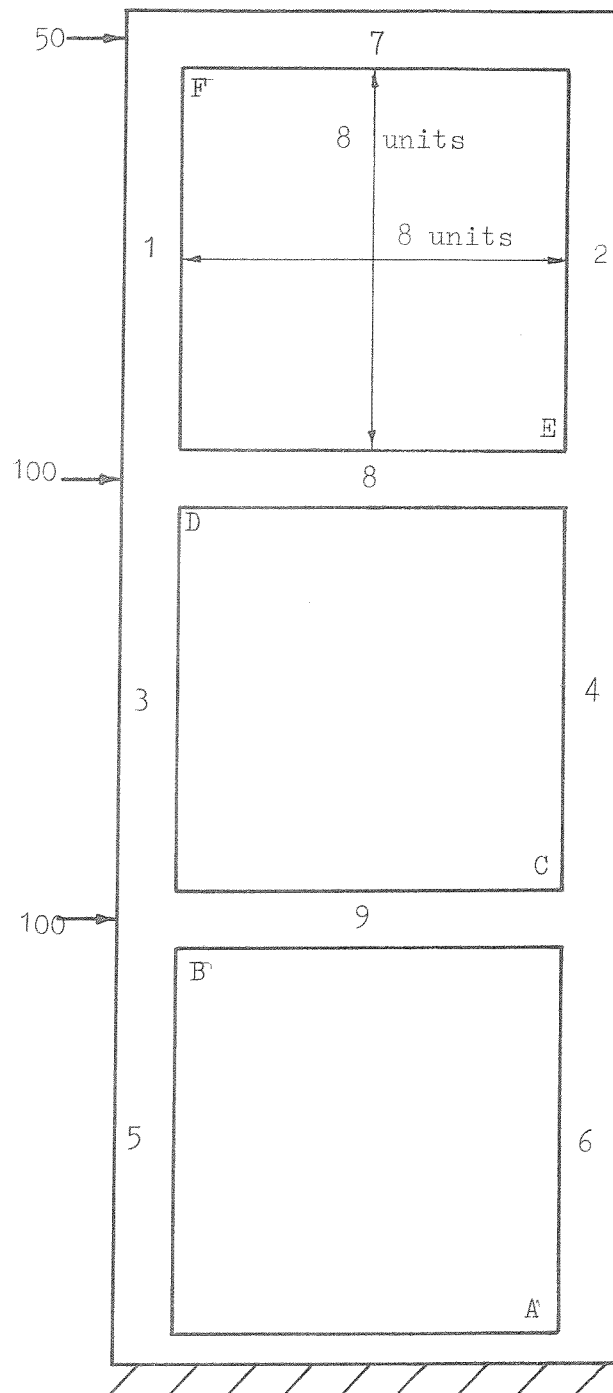
FIG. 8.14 LOADING AND RESTRAINT ARRANGEMENT FOR ANALYSES 3.1 to 3.9
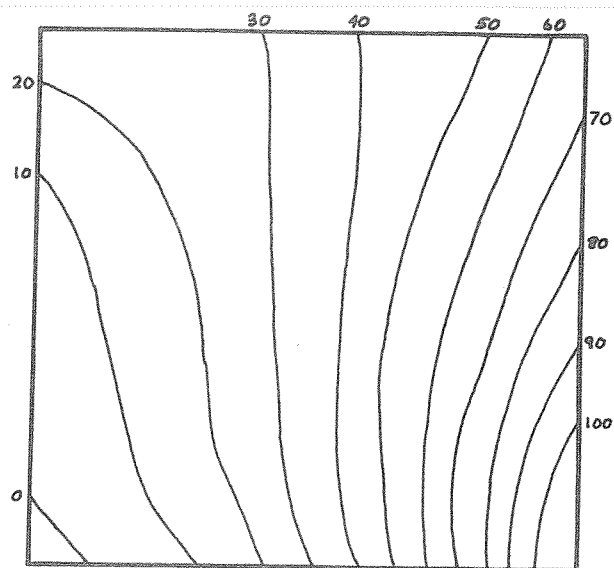
FIG. 8.15 PRINCIPAL COMPRESSIVE STRESS CONTOURS FOR THE BOTTOM INFILL
OF ANALYSIS 3.5 - BEFORE SEPARATION
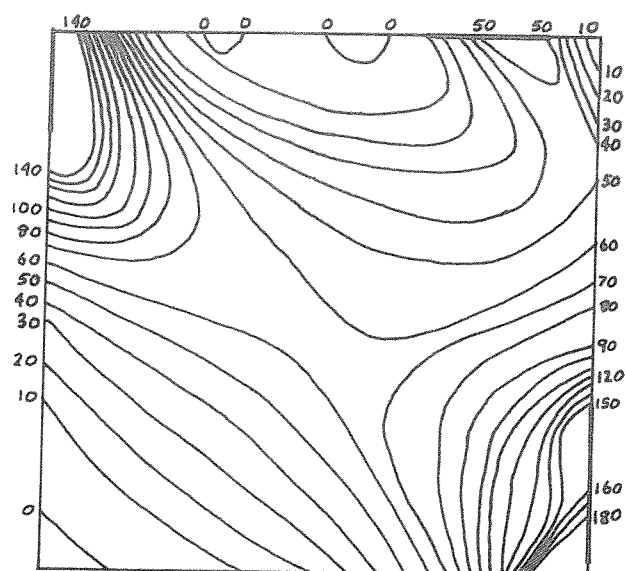
FIG. 8.16 PRINCIPAL COMPRESSIVE STRESS CONTOURS FOR THE BOTTOM INFILL
OF ANALYSIS 3.5 - AFTER SEPARATION
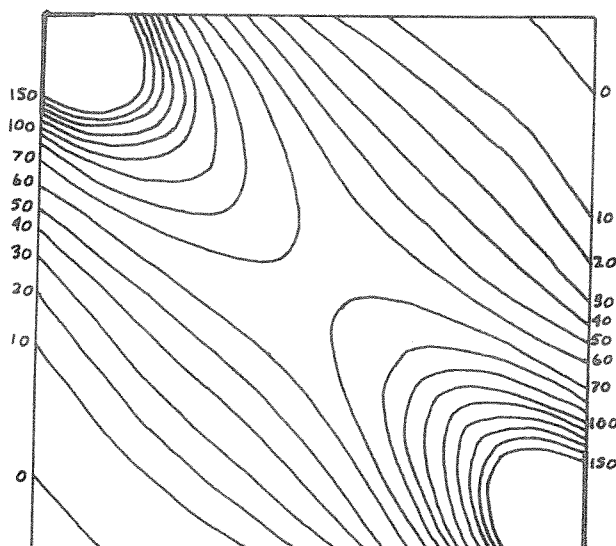
FIG. 8.17 PRINCIPAL COMPRESSIVE STRESS CONTOURS FOR THE BOTTOM INFILL
OF ANALYSIS 3.2 - AFTER SEPARATION

again clearly demonstrate the importance of separation. It can be
seen that in addition to the basic diagonal strut action of the infill,
some compressive stress is applied by the upper beam at the right hand
infill corner. On this contact length, considerable shear stresses
are transferred which greatly reduces the tie force in the beam (Fig.
8.22). Unless the friction bond between the infill and frame is
strong, shear failure is likely to occur on this joint which would
result in a stress pattern more closely resembling that given by the
no friction analyses (Fig. 8.17). Fig. 8.17 clearly demonstrates that
when there is no effective boundary friction, the infill behaves
purely as a diagonal strut.

Figs. 8.18 and 8.19 show the principal tensile stress diagrams,
before and after separation respectively for the analysis with $\lambda h = 6.3$
and friction. The tensile stress is seen to largely dissipate on
separation, except in the region where the upper beam is in contact
with the infill. If the shear strength on this joint is high enough
to maintain the contact, tensile cracking may occur in this region.
These high tensile stresses do not form when there is no boundary
friction as can be seen in Fig. 8.20. Fig. 8.21 shows that before
separation the infill acts under a fairly uniform shear stress dis-
tribution. The strut action is clearly seen after separation in
Figs. 8.22 and 8.23. The shear stress distribution for the friction
analysis, Fig. 8.22, shows the previously mentioned high shear stress
on the upper beam joint.

Fig. 8.24 shows the positions of joint contact for all the
analyses. It should be noted that the lengths of contact will only be
given approximately by the analyses because of the relatively coarse
spacing of the nodes (11 nodes per infill side). All the friction
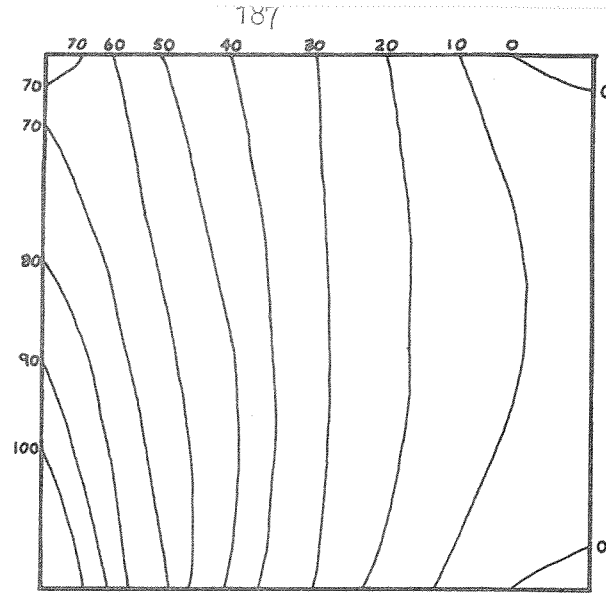
FIG. 8.18 PRINCIPAL TENSILE STRESS CONTOURS FOR THE BOTTOM INFILL OF
ANALYSIS 3.5 - BEFORE SEPARATION
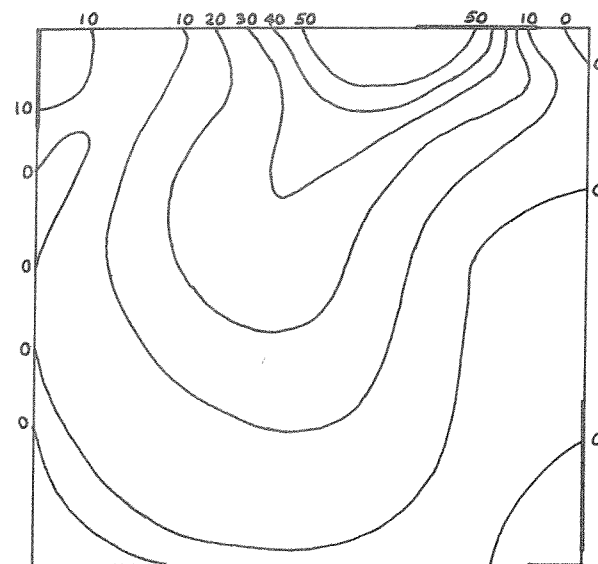
FIG. 8.19 PRINCIPAL TENSILE STRESS CONTOURS FOR THE BOTTOM INFILL OF
ANALYSIS 3.5 - AFTER SEPARATION
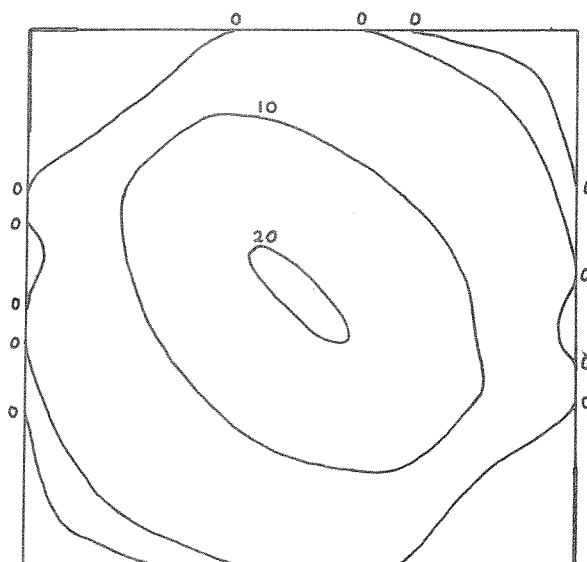
FIG. 8.20 PRINCIPAL TENSILE STRESS CONTOURS FOR THE BOTTOM INFILL OF
ANALYSIS 3.2 - AFTER SEPARATION
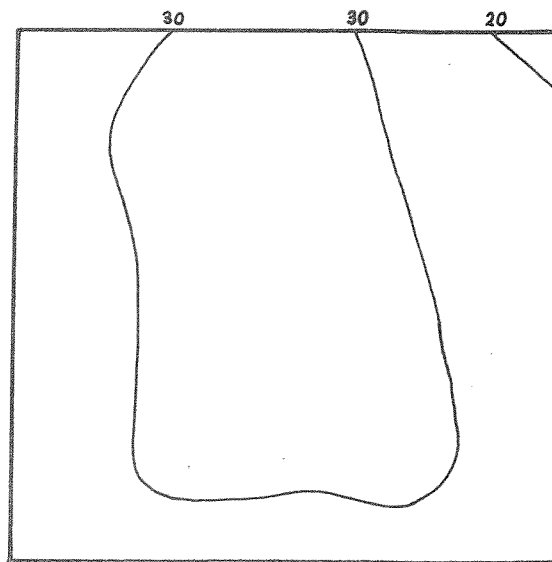
FIG. 8.21 HORIZONTAL SHEAR STRESS DISTRIBUTION FOR THE BOTTOM INFILL OF
ANALYSIS 3.5 - BEFORE SEPARATION
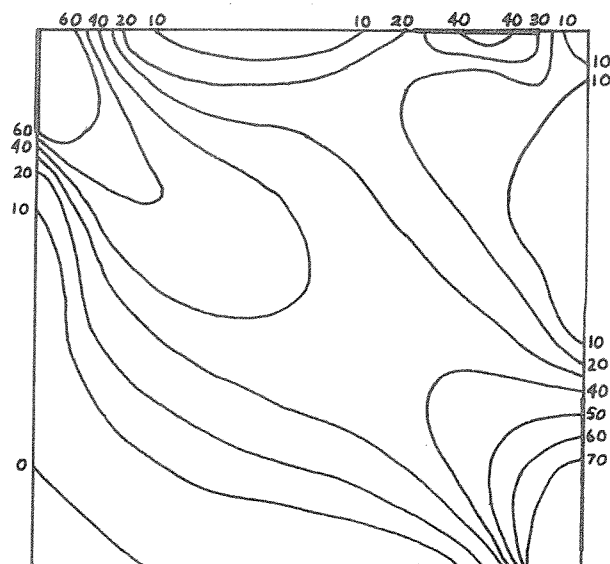
FIG. 8.22 HORIZONTAL SHEAR STRESS DISTRIBUTION FOR THE BOTTOM INFILL OF
ANALYSIS 3.5 - AFTER SEPARATION
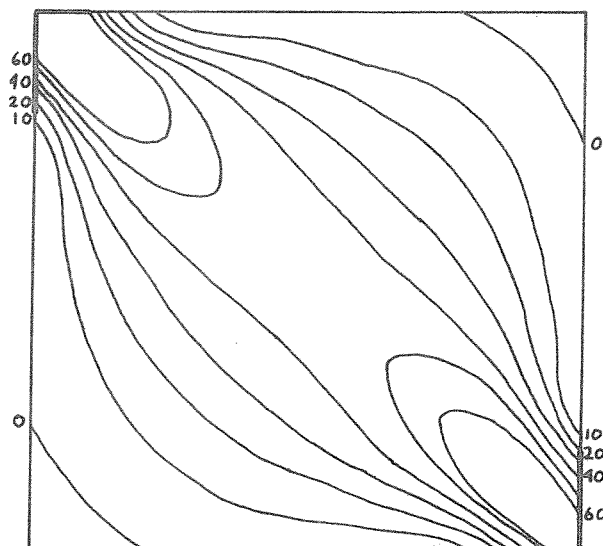
FIG. 8.23 HORIZONTAL SHEAR STRESS DISTRIBUTION FOR THE BOTTOM INFILL OF
ANALYSIS 3.2 - AFTER SEPARATION
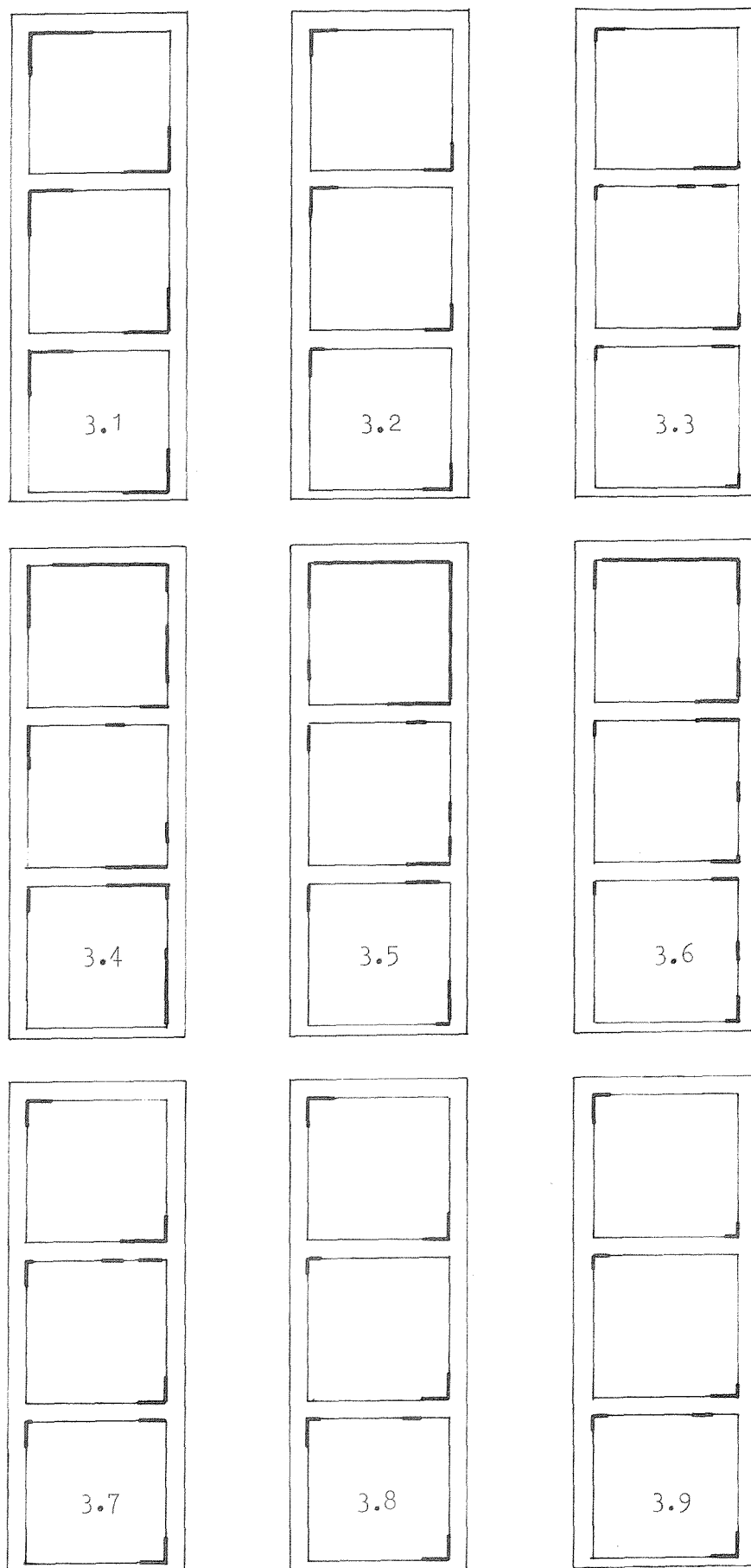
FIG. 8.24 LENGTHS OF CONTACT FOUND IN ANALYSES 3.1 to 3.9

analyses (3.4, 3.5 and 3.6) regardless of frame stiffness show the
characteristics of a transfer of shear load by the beams into the
infills at the right hand end of the beams. The effect of this is to
considerably reduce the tie force in the beams. The only no friction
analysis to indicate contact between the frame and infill in these
positions was analysis 3.3 in which the frame stiffness was extremely
low. Frames of this low relative stiffness ($\lambda h = 15$) are unlikely to
occur in practice. Fig. 8.24 indicates that generally the contact
lengths reduce with frame stiffness as was expected.

Table 8.3 shows the results of these analyses and includes for
comparison, values estimated using the approximate design method.
Considering the central infill stresses, the shear and diagonal tension
stress results are seen to compare well with the design method estimates.
The general tendency of these stresses is to reduce with an increase in
frame stiffness and boundary friction. The vertical compression stresses
are higher (conservative) than the design method values when there is no
friction, but generally lower than the design method values when there
is friction. This reduction in vertical stress is particularly notice-
able in the bottom infill.

The design method is seen to give a reasonable estimate of the
column forces for all the analyses. However, the correlation for the
no friction analyses is better than that for the friction analyses.
The beam forces also agree fairly closely for the no friction analyses.
The beam forces for the friction analyses are generally much lower
than the design method values due to the shear transfer from the beam
to the infill mentioned previously. In most practical cases, however,
this shear transfer could not be guaranteed, and so no beam force
reduction could be allowed in the beam design.

Table 8.3 — Three storey square infilled frames under lateral loading

Analysis	λh	Boundary friction	Central infill stresses — Bottom infill			Middle infill			Top infill			Frame member axial forces									Lateral Deflection	w/d values — bottom infill	bottom two infills	average all infills	Infill corner stresses					
			τ_{xy}	σ_{dt}	σ_y	τ_{xy}	σ_{dt}	σ_y	τ_{xy}	σ_{dt}	σ_y	1	2	3	4	5	6	7	8	9					A	B	C	D	E	F
3.1	3	No	36.4	+15.8	-19.2	24.5	+10.7	-14.0	8.6	+3.7	-5.0	+49.8	-2.2	+193.3	-57.6	+414.0	-217.0	-1.7	+37.3	+112.8	32.7	0.32	0.32	0.30	-239.9	-260.6	-168.5	-164.9	-57.6	-57.6
3.2	6.3	No	44.5	+19.9	-22.2	27.2	+12.2	-14.2	9.1	+4.1	-4.8	+50.5	0	+199.3	-49.6	+444.0	-199.8	0	+49.0	+147.4	65.1	0.19	0.20	0.20	-422.7	-448.9	-270.5	-266.4	-96.3	-96.2
3.3	15	No	44.8	+16.6	-22.6	27.2	+11.2	-15.2	9.3	+4.1	-5.3	+52.4	0	+203.0	-37.8	+450.4	-136.8	0	+50.3	+150.1	148.2	0.14	0.15	0.16	-679.3	-744.1	-362.0	-447.6	-135.3	-128.6
3.4	3	Yes	25.0	+13.5	-3.5	18.6	+8.2	-8.4	6.3	+2.9	-3.2	+43.5	-9.8	+199.3	-62.3	+395.0	-239.5	-13.2	-2.1	-4.8	25.1	0.61	0.63	0.61	-71.4	-42.5	-50.5	-35.0	-32.3	-18.7
3.5	6.3	Yes	39.3	+21.4	-7.2	23.5	+10.5	-10.4	7.0	+4.3	-5.4	+30.6	-6.1	+204.5	-38.9	+444.5	-179.0	-8.5	+16.0	+35.0	50.9	0.43	0.46	0.54	-181.4	-215.7	-71.9	-148.9	-12.5	-14.4
3.6	15	Yes	42.1	+20.3	-8.9	25.9	+12.3	-10.9	8.8	+3.8	-5.6	+54.8	-2.4	+208.0	-37.6	+444.6	-124.4	-2.6	-2.8	+37.8	125.4	0.50	0.60	0.79	-363.0	-281.2	-174.3	-207.9	-21.2	-37.4
3.7*	6.3	No	42.5	+16.6	-20.1	26.2	+10.7	-15.1	9.2	+4.1	-5.2	+51.6	+0.1	+200.0	-40.9	+439.0	-162.5	0.	+48.2	+143.5	162.8	0.16	0.18	0.79	-546.9	-664.4	-304.0	-339.5	-93.7	-90.5
3.8**	15	No	45.3	+19.9	-24.0	27.4	+12.3	-14.4	9.1	+4.1	-4.7	+50.3	+0.1	+201.5	-49.2	+450.0	-193.7	0.1	+50.1	+150.0	64.7	0.18	0.18	0.17	-511.8	-538.3	-321.6	-329.9	-107.5	-112.5
3.9***	6.3	No.	45.6	+20.3	-23.3	28.1	+12.5	-14.5	9.5	+4.3	-4.9	+52.0	+0.8	+203.5	-48.0	+447.0	-195.0	+0.7	+53.6	+154.0	73.3	0.15	0.15	0.15	-434.2	-615.6	-371.3	-368.9	-113.4	-125.4
Design Method Values																														
3.1 3.4 3.9	3	-	44.7	+18.1	-18.8	26.8	+10.9	-11.3	8.9	+3.6	-3.8	+50	0	+200.0	-50	+450	-200	0	+50	+150	62.7	0.10	0.10	0.10	-	-	-	-	-	-
3.2 3.5	6.3	-	"	"	"	"	"	"	"	"	"	"	"	"	"	"	"	"	"	"	87.6	"	"	"	-	-	-	-	-	-
3.3 3.6	15	-	"	"	"	"	"	"	"	"	"	"	"	"	"	"	"	"	"	"	170.7	"	"	"	-	-	-	-	-	-
3.7	6.3	-	"	"	"	"	"	"	"	"	"	"	"	"	"	"	"	"	"	"	184.1	"	"	"	-	-	-	-	-	-
3.8	15	-	"	"	"	"	"	"	"	"	"	"	"	"	"	"	"	"	"	"	85.1	"	"	"	-	-	-	-	-	-

Notes
* λh = 15 axial stiffness
** λh = 6.3 axial stiffness
*** Pin-jointed beams

Table 8.3   Three storey square infilled frames under lateral loading

For all the analyses the design method is conservative as regards to lateral deflection. Some conservation was intended so as to allow for plastic behaviour of the infill and any slight lack of initial fit. From the results it can be seen that the w/d ratio is generally increased by an increase in frame stiffness or an increase in boundary friction. The w/d ratio is also seen to be generally slightly smaller in the lower infills. This may be due to the column members for these infills being subjected to proportionally higher axial loads than the columns for the higher infills.

The principal compressive stresses in the infill corners have again been included in Table 8.3 in order that the main trends can be seen. As expected the corner stresses tend to increase with a reduction in boundary friction and frame stiffness.

In the design method, the assumption is made that the moments in the frame do not exceed Hh/20 at any point. This value was derived from the results of the three storey analyses. The maximum frame moment was calculated for all of the analyses and was found to always occur at the base of the compression column. The maximum moment was found to occur in analysis 3.9, where the beams were pin-jointed, λh = 6.3 and there was no boundary friction, and it had a value of Hh/20. Generally the moments in the frame are very small as shown in Fig. 8.25, where the column moments of analysis 3.5 are plotted as a percentage of the moments that would occur in an uninfilled frame. (i.e. Hh/2).

Three further analyses are included in Table 8.3. Analyses 3.7 and 3.8 were undertaken to determine whether the axial or the flexural stiffness of the frame was the predominant factor controlling its lateral deflection. In these analyses both the frame member depths
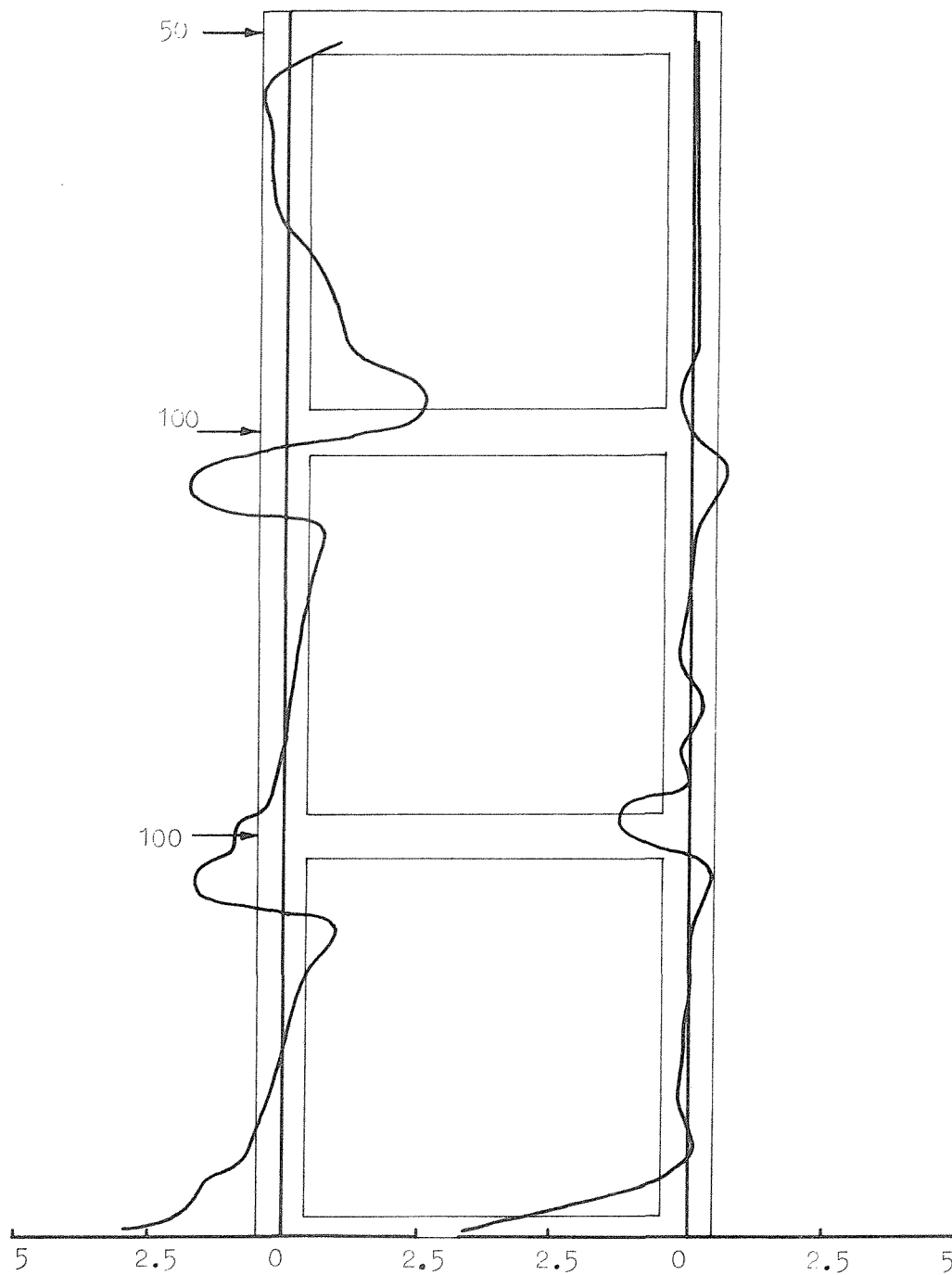
FIG. 8.25 COLUMN MOMENTS OF ANALYSIS 3.5 AS A PERCENTAGE OF THE
          UNFILLED FRAME MOMENT Hh/2

and the frame E values were adjusted to give the axial and flexural
stiffnesses shown in Table 8.3. The results indicate that as assumed
in the design method, the axial stiffness of the frame is the predom-
inant factor controlling its lateral deflection.

The final analysis (3.9) was a repeat of analysis 3.2 with the
beams pinned rather than rigidly connected to the columns. The results
indicate that the central infill stresses and the frame forces are
little affected by the rigidity of the joint connection. The lateral
deflection of the frame and the infill corner stresses do tend, however
to increase when the beams are pin-jointed to the columns rather than
rigidly connected. For analyses 3.2 and 3.9, the deflection increased
by 13% and the corner stresses increased by between 19% and 24%.

8.5.4 Three bay square infilled frames

Two finite element analyses were undertaken on three bay square
infilled frames. The arrangement is shown in Fig. 8.26 and the results
are shown in Table 8.4 together with the design method estimates.

The first analysis was with all the loading applied at one end
at position X. The results clearly demonstrate that in this case,
the loading is not distributed evenly between the three infills. The
infill loading drops off the further the infill is from the applied
load. The results from this analysis do not compare very well with
the design method estimates because of this uneven loading. (The
design method estimates assume an even spread of loading between the
infills). The applied loading was in fact rather unrealistic because
wind loading on buildings tends to be divided approximately equally
between the windward and leeward faces of a building. A negative
pressure is usually formed on the leeside of a building which is of the
same order of magnitude as the positive pressure on the windward side.
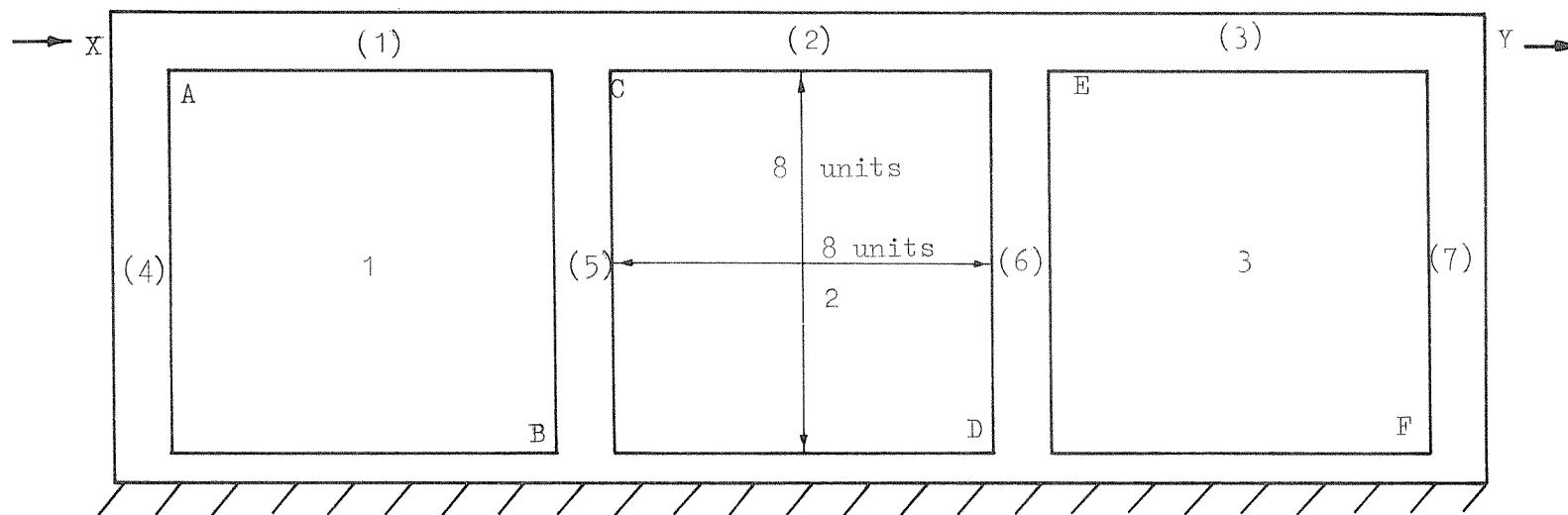
FIG. 8.26 LOADING AND RESTRAINT ARRANGEMENT FOR ANALYSES 4.1 and 4.2

Analysis Ref.	λh	Boundary friction?	Central infill stresses									Frame member axial forces							Lateral deflection		w/d values		Infill corner stresses					
			Infill 1			Infill 2			Infill 3			1	2	3	4	5	6	7	Point X	Point Y	Point X	Point Y	A	B	C	D	E	F
			τ_{xy}	σ_{dt}	σ_y	τ_{xy}	σ_{dt}	σ_y	τ_{xy}	σ_{dt}	σ_y																	
4.1*	6.3	No	22.3	+7.9	−10.8	18.6	+6.7	−5.6	13.3	+5.9	−5.9	−144.7	−59.8	+0.1	+125.4	+93.7	+70.9	+0.3	8.74	4.88	0.23	0.15	−260.4	−163.6	−162.8	−96.9	−117.3	−101.9
4.2**	6.3	No	18.2	+7.8	−8.5	17.8	+7.5	−7.5	17.7	+7.9	−8.9	−44.3	+48.8	+148.8	+99.6	+94.3	+97.3	−1.0	6.81	9.35	0.20	0.20	−188.7	−145.5	−169.2	−100.9	−182.3	−165.5
Design method values																												
4.1	6.3	−	17.9	+7.3	−7.9	17.9	+7.3	−7.9	17.9	+7.3	−7.9	−200	−100	0	+100	+100	+100	0	14.31	8.40	0.10	0.10	−	−	−	−	−	−
4.2	6.3	−	17.9	+7.3	−7.9	17.9	+7.3	−7.9	17.9	+7.3	−7.9	−50	+50	+150	+100	+100	+100	0	11.89	14.31	0.10	0.10	−	−	−	−	−	−

Notes   *   Horizontal loading − 300 units at X

0   units at Y

**   "   "   −   150 units at X

150 units at Y

Table 8.4   Three bay square infilled frames under lateral loading

A second analysis was therefore conducted with the applied load split evenly at points X and Y. The results from this analysis indicate that the load is split fairly evenly between the three infills. Slightly less load is taken by the central infill which indicates that in a long series of infills the infill loading might tend to fall off towards the centre of the group.

The behaviour of infilled frames connected together horizontally is thus largely dependent on the distribution of loading. Provided the loading is applied approximately equally at the two ends of a series of infills, or is distributed evenly by means of a floor etc., it should be reasonably accurate to calculate the overall strength of a series of infilled frames by summing their individual strengths, (provided they are of similar dimensions).

8.5.5 Single non-square infilled frames

Six analyses were undertaken on single non-square infilled frames. The medium stiffness frame with $\lambda h = 6.3$ was considered and the modulus of elasticity ratio was taken as 4. h/ℓ ratios of between 2 and .33 were considered for both the friction and no friction cases. The results from these analyses are shown in Table 8.5 together with the results from the two corresponding square analyses. Also included in Table 8.5 are the values estimated using the design method.

Considering the central infill stresses, close agreement is found between the design method estimates and the analyses results when h/ℓ is less than or equal to 1. For the analyses with $h/\ell = 2$, the design method is rather conservative for both the tensile and shear stresses.

The tension column forces are estimated fairly accurately by the design method. Only in the $h/\ell = 0.33$, no friction analysis does the

Analysis Ref.	h/ℓ	λh	Boundary friction?	Central infill stresses			Frame member axial forces				Lateral deflection	w/d	Infill corner stresses	
				τ_{xy}	σ_{dt}	σ_y	1	2	3	4			Position A	Position B
5.1	2	6.3	No	30.4	+9.2	−41.4	+184.0	−4.0	−5.2	−7.4	22.27	0.16	−400.6	−373.5
5.2	1	6.3	No	16.8	+6.3	−8.6	+102.8	−0.3	−0.5	−1.8	7.98	0.16	−175.3	−188.7
5.3	.5	6.3	No	9.0	+2.5	−0.4	+57.7	+1.1	+1.2	+0.4	6.24	0.11	−145.1	−155.2
5.4	.33	6.3	No	6.0	+2.0	+0.8	+42.7	+0.9	+12.3	+0.7	6.75	0.09	−126.5	−132.3
5.5	2	6.3	Yes	27.6	+10.5	−33.0	+174.3	−6.3	−28.2	−8.9	17.01	0.24	−75.2	−321.1
5.6	1	6.3	Yes	14.6	+6.2	−7.8	+100.0	−4.7	−16.3	−8.7	5.71	0.25	−46.3	−135.1
5.7	.5	6.3	Yes	7.4	+3.4	−0.5	+54.5	−19.6	−4.4	−19.6	2.20	0.35	−33.2	−34.1
5.8	.33	6.3	Yes	5.4	+2.8	+1.9	+38.0	−26.0	+1.3	−25.7	1.90	0.32	−30.9	−28.5
Design method values														
5.1 5.5	2	6.3	−	35.7	+14.5	−35.0	+176.5	0	0	0	31.45	0.10	−	−
5.2 5.6	1	6.3	−	17.9	+7.3	−7.5	+100	0	0	0	11.74	0.10	−	−
5.3 5.7	.5	6.3	−	8.9	+3.6	−1.2	+53.6	0	0	0	6.65	0.10	−	−
5.4 5.8	.33	6.3	−	6.0	+2.4	−0.3	+36.6	0	0	0	6.43	0.10	−	−

Table 8.5   Single non-square infilled frames under lateral loading

error exceed 10%. Although the design method calculates that no forces are taken by the other frame members, the analyses indicate that in some cases considerable forces do develop. The most significant of these forces are in the beams. In the three storey analyses described in Section 8.5.3, the beam forces were generally below the design method estimates. Since the three storey analyses are probably a more realistic representation of the behaviour of infilled frames in buildings, it seems reasonable to disregard the higher than design beam forces in these analyses.

In all but one of these analyses, the design method gave a conservative estimate of deflection. It is interesting to note that for the no friction analyses, the w/d ratio reduced with reducing h/ℓ , while for the friction analyses, the w/d ratio increased with reducing h/ℓ. These analyses thus emphasise the difficulty of trying to make accurate deflection predictions for infilled frames.

8.5.6 <u>Three storey square infilled frames - bottom infill omitted</u>

Four analyses were undertaken on three storey square infilled frames with the bottom infill omitted. The results are shown in Table 8.6. The frame numbering etc. and loading was as in Fig. 8.14.

Analysis 6.1 was with the basic frame and the restraints as analysed previously, with just the bottom infill removed. Fig. 8.27 shows the compression principal stress results for this analysis. The two infills are seen to be acting together rather as a single tall infill. The results in Table 8.6 show a very large lateral deflection and the behaviour of the frame is not in general as predicted by the design method.

It was considered to be unrealistic to have the bottom columns

Analysis Ref.	λh	Boundary friction?	Central infill stresses						Frame member axial forces									Lateral deflection	Infill corner stresses			
			Middle infill			Top infill			1	2	3	4	5	6	7	8	9		C	D	E	F
			τ_{xy}	σ_{dt}	σ_y	τ_{xy}	σ_{dt}	σ_y														
6.1	6.3	No	17.2	-7.2	-55.5	19.3	+9.8	-41.7	+151.0	0	+237.5	+161.0	+304.0	-304.0	+33.3	+48.7	+60.5	447.4	-471.4	-2.8	-211.5	-233.4
6.2*	6.3	No	30.3	+8.3	-21.7	10.1	+4.5	-7.4	+59.4	+0.7	+232.5	+3.6	+258.1	-258.1	+0.8	+57.9	+49.1	90.0	-406.1	-453.5	-78.8	-99.6
6.3**	6.3	No	27.2	+12.1	-13.7	9.2	+4.1	-4.9	+50.5	+0.1	+201.0	-49.7	+193.2	-193.2	+0.2	+48.9	-97.5	21.9	-271.9	-260.2	-87.1	-91.6
6.4***	6.3	No	30.8	+9.2	-21.1	10.2	+4.4	-8.4	+57.1	+1.1	+230.0	-1.3	+250.0	-250.0	+0.6	+61.7	+50.2	99.0	-512.5	-473.7	-79.7	-139.3
Design method values																						
6.1 6.2 6.3 6.4	6.3	-	26.8	+10.9	-11.3	8.9	+3.6	-3.8	+50	0	+200	-50	-	-	0	+50	-	-	-	-	-	-

Notes   *   Stiffened bottom columns

       **   "   "   " , horizontal 1st floor level restraint

       ***   "   "   " , pin-jointed beams

Table 8.6   Three storey square infilled frames with bottom infill omitted under lateral loading
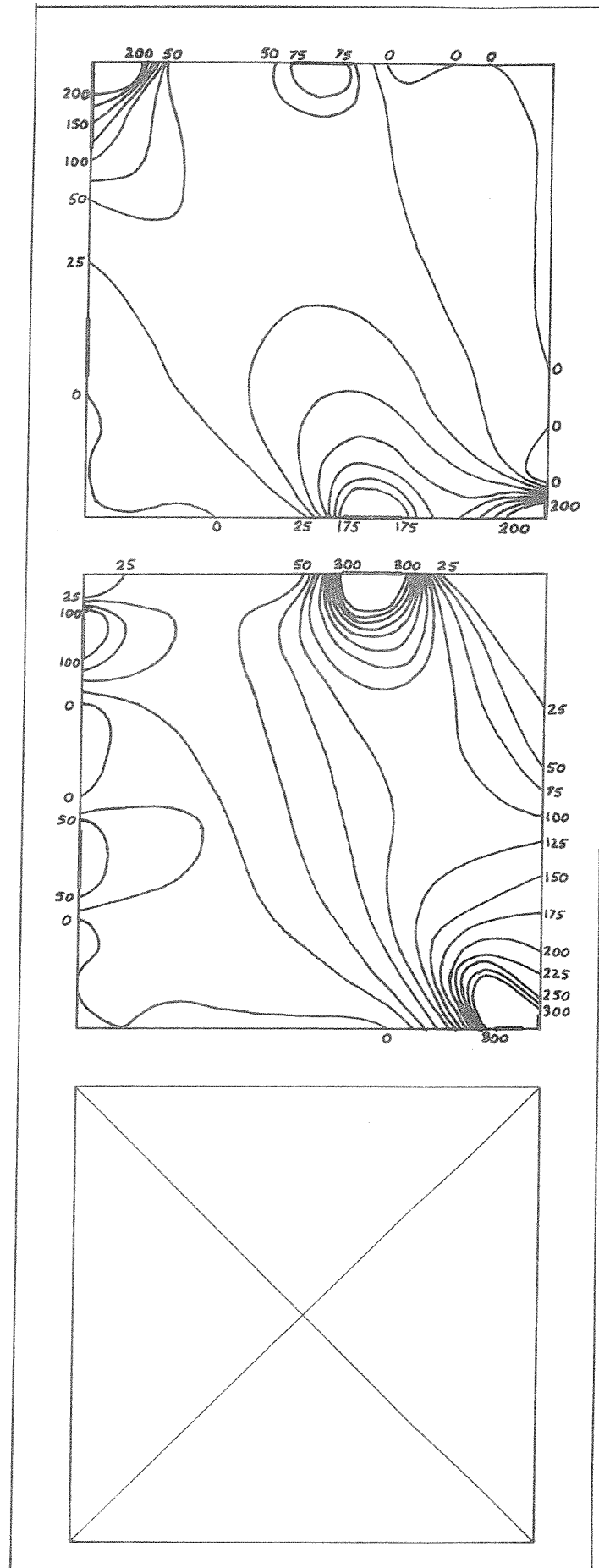
FIG. 8.27 PRINCIPAL COMPRESSIVE STRESS CONTOURS FOR ANALYSIS 6.1

of the same stiffness as the other columns when there was no bottom infill. In analysis 6.2, the bottom column stiffness was increased by a factor of ten. The results from this analysis show the behaviour of the structure returning towards that predicted by the design method. In analysis 6.3, a horizontal restraint was applied to the compression column at first floor level, in addition to having the columns stiffened as in the previous analysis. Fig. 8.28 shows the compression principal stress results for this analysis. The two infills are seen to be acting separately in this case, each with its own diagonal strut actions. The results in Table 8.6, show that the structure is now behaving entirely as predicted by the design method.

The final analysis, 6.4, was for a structure with pin-jointed beams and stiffened bottom columns, but no horizontal first floor restraint. The results were similar to those obtained previously with other pin-jointed beam analyses i.e. some increase in corner stresses and deflection, but little change in the frame forces and central infill stresses.

The main conclusion from this section is that the behaviour of the structure is largely dependent on the level of restraint to be found at the bottom of the first infilled panel. Unless the structure is restrained fairly rigidly at this level, the behaviour of the infilled panels above is likely to be unpredictable.
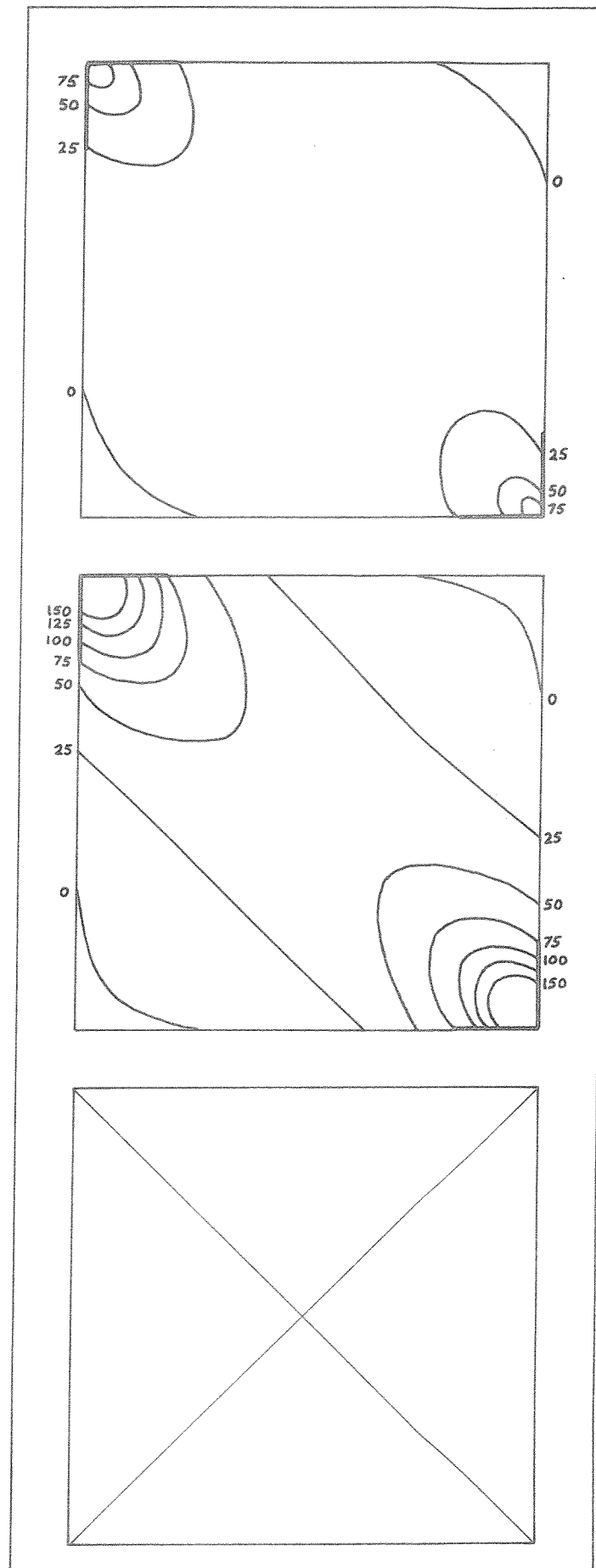
FIG. 8.28 PRINCIPAL COMPRESSIVE STRESS CONTOURS FOR ANALYSIS 6.3

8.6 Infilled frames under combined lateral and vertical loading

8.6.1 Introduction

Infilled frames are often subjected to vertical loading in addition to lateral loading. The vertical loading is due to floor loading being transmitted to the beams of the infilled frames. Unfortunately it is very difficult to analyse accurately the effects of vertical loading in infilled frames, because the division of load between the frame and infill is very dependent on the initial fit of the infill, the differing rates of creep of the frame and infill materials and the degree of shear connection between the frame and infill. The stage at which the infill is constructed will also affect the distribution of loading between the infills and columns and the moments in the beams. If the building frame and flooring is constructed before the infill is built, the infill will carry far less vertical load than if the infill is built as the building frame is constructed. To further complicate the problem, the behaviour of the structure is non-linear due to the boundary separation. The results from analyses for horizontal and vertical loading separately cannot be superimposed to provide the solution for combined loading.

Because of the above complications, the results from the following analyses could only be used to give a very conservative design estimate for combined loading behaviour. A considerable amount of further work would be required to give a more accurate method of combining the effects of vertical and horizontal loading.

8.6.2 Single square infilled frames

Five analyses were undertaken on square infilled frame structures loaded under differing combinations of vertical and lateral loading.

The arrangement of the restraints is shown in Fig. 8.7 and is similar to that used in Section 8.5.2. The modulus of elasticity ratio between the columns and infill was again taken as 4. The lateral loading was taken as in Fig. 8.7. The vertical loading was taken as 100 units and was uniformly distributed along the top beam.

The results from the analyses are shown in Table 8.7. These results should be compared with the results in Section 8.5.2 for which the structures were only loaded laterally. Figs. 8.29 and 8.30 show the principal compressive stress results for analyses 7.1 and 7.4 respectively. It can be seen that for the vertical loading only case, with no boundary friction, a wall on beam type situation exists, but that for the combined loading case, the diagonal strut action returns with increased lengths of contact. Figs. 8.31 and 8.32 show the principal compressive stress results for analyses 7.2 and 7.5 respectively. For the vertical loading case, analysis 7.5, where there is boundary friction, the load is transferred by shear into the columns over a considerable length and a wall on beam mode of behaviour does not occur. Again a diagonal strut action is seen to develop when lateral loading is applied.

Comparing the results for vertical and lateral loading (Table 8.7) with the results for lateral loading only (Table 8.2), the following general conclusions can be drawn. With regard to central infill stresses, the shear stress is little affected by vertical loading while the vertical stress is considerably increased and the diagonal tensile stress slightly reduced. The vertical load in these analyses has the effect of reducing the top corner infill stress while increasing the bottom corner infill stress. The vertical loading reduces the lateral deflection of the structures.

Analysis Ref.	λh	Boundary friction?	*Loading	Central infill stresses			Frame member axial forces				Lateral deflection	Infill corner stresses	
				τ_{xy}	σ_{dt}	σ_y	1	2	3	4		Position A	Position B
7.1	6.3	No	V,H	17.2	+5.3	−15.7	+55.6	−3.8	−27.2	+1.7	6.55	−207.1	−174.7
7.2	6.3	Yes	V,H	13.5	+5.1	−11.9	+50.3	−33.0	−45.2	−9.4	3.78	−54.3	−62.4
7.3	15	No	V,H	16.8	+4.4	−14.7	+51.1	−0.8	−13.8	+0.4	10.52	−309.8	+200.8
7.4	6.3	No	V	0	−1.4	−7.6	−16.1	−1.6	−16.1	+24.6	−0.61	−62.5	−0.2
7.5	6.3	Yes	V	0	−1.3	−6.2	−16.7	−5.9	−16.7	+16.0	−0.39	−12.2	−1.7

Notes   * V = 100 unit uniformly distributed vertical load

H = 100 unit horizontal load.

Table 8.7   Single square infilled frames under combined vertical and horizontal loading.
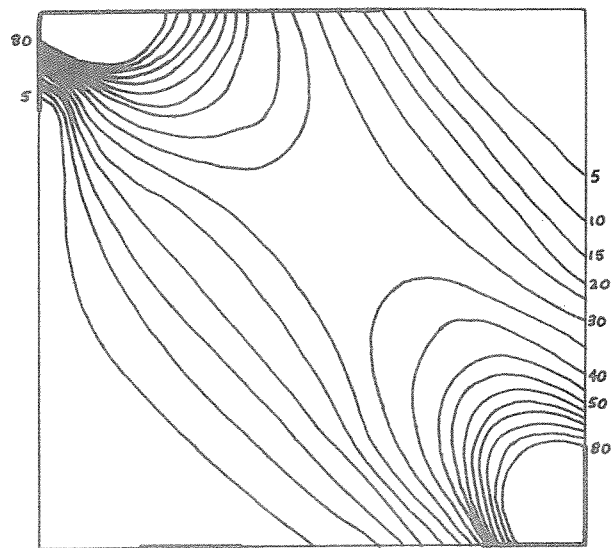
FIG. 8.29 PRINCIPAL COMPRESSIVE STRESS CONTOURS FOR ANALYSIS 7.1
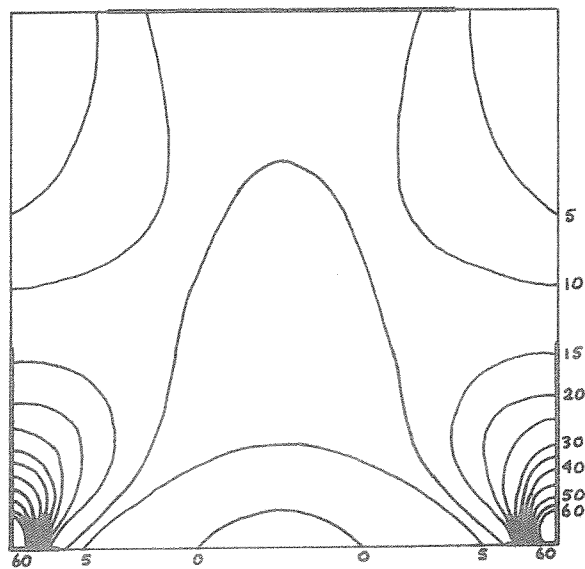
FIG. 8.30 PRINCIPAL COMPRESSIVE STRESS CONTOURS FOR ANALYSIS 7.4
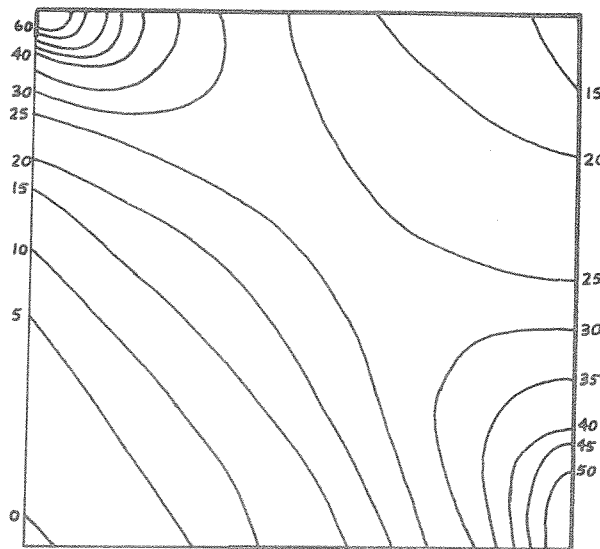
FIG. 8.31   PRINCIPAL COMPRESSIVE STRESS CONTOURS FOR ANALYSIS 7.2
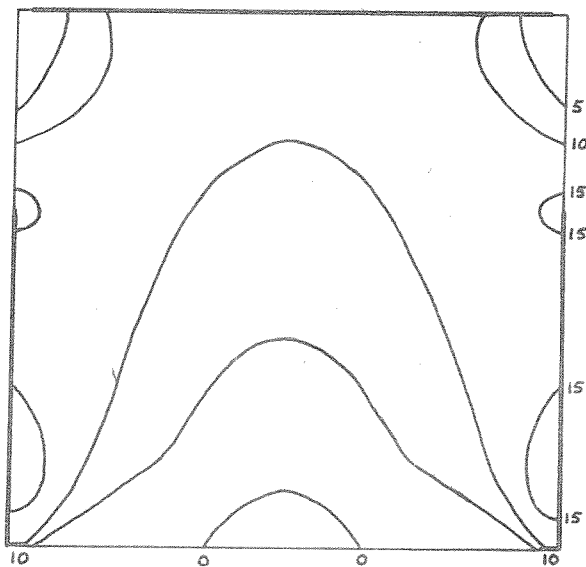
FIG. 8.32   PRINCIPAL COMPRESSIVE STRESS CONTOURS FOR ANALYSIS 7.5

For vertical loading only, the distribution of the load between the columns and infill depends on their relative axial stiffnesses. This does not however occur, when lateral loading is introduced. If the lateral loading is high enough, as in these analyses, to create a separation crack on the windward side of the bottom beam joint, then approximately half the vertical load is transferred directly into the windward column. This has the effect of reducing the tensile load in the column. The proportion of the vertical load carried by the leeward column is also increased by the application of lateral load. The amount of this increase is seen to be dependent on the level of boundary friction with more load being taken by the column for the friction analysis.

8.6.3 Three storey square infilled frames – all infilled

Seven analyses were undertaken on three storey square infilled frame structures, loaded under differing combinations of vertical and lateral loading. The restraint arrangement is shown in Fig. 8.14 and is similar to that used in Section 8.5.3. The modulus of elasticity ratio between the columns and infill was taken as 4 and the lateral loading was as in Fig. 8.14. Two vertical loading configurations were considered. The first had a load of 100 units uniformly distributed on each beam and the second had a load of 300 units on each beam. The second loading pattern was introduced because it was thought that the ratio of vertical to horizontal loading likely to occur in practice was in the order of 3.

The results from the analyses are shown in Table 8.8. These results should be compared with the results in Section 8.5.3 where the structures were only loaded laterally. Fig. 8.33 shows the positions of joint contact for all the analyses.

Analysis Ref.	λh	Boundary friction?	Loading*	Central infill stresses									Frame member axial forces									Lateral Deflection	Infill corner stresses					
				Bottom infill			Middle infill			Top infill			1	2	3	4	5	6	7	8	9		A	B	C	D	E	F
				τ_{xy}	σ_{dt}	σ_y	τ_{xy}	σ_{dt}	σ_y	τ_{xy}	σ_{dt}	σ_y																
8.1	6.3	No	V,H	45.4	+14.8	-36.9	28.3	+9.7	-27.5	9.7	+3.0	-14.4	+19.3	-16.9	+116.0	-97.8	+313.5	-264.0	-1.9	+50.6	+148.8	58.0	-437.1	-414.8	-279.5	-243.3	-112.3	-79.4
8.2	6.3	No	3V,H	48.6	+9.4	-90.8	29.2	+6.6	-59.9	10.3	+0.6	-32.1	-22.8	-44.0	-14.2	-170.5	+123.2	-356.0	-4.6	+59.7	+152.0	49.4	-449.3	-399.7	-311.6	-233.4	-169.8	-87.9
8.3	6.3	Yes	V,H	37.2	+10.3	-26.2	20.3	+4.6	-24.5	7.3	+2.2	-12.9	+9.3	-12.8	+131.9	-81.0	+296.5	-234.0	-13.1	+0.9	+30.1	43.0	-182.6	-196.2	-62.8	-41.5	-21.8	-13.5
8.4	6.3	Yes	3V,H	39.5	+5.6	-73.8	21.6	+4.0	-48.6	6.5	-1.9	-30.0	-18.0	-32.0	-21.4	-166.6	+109.8	-349.0	-29.5	-3.8	+3.6	32.2	-189.7	-41.2	-99.2	-36.2	-44.0	-7.7
8.5	15	No	3V,H	49.7	+2.3	-96.1	30.4	+4.9	-70.8	11.0	+0.8	-36.0	-9.7	-17.9	-8.8	-87.9	+118.9	-207.0	-0.6	+50.8	+151.4	83.8	-671.9	-53.3	-397.4	-322.3	-164.4	-112.2
8.6	6.3	No	V	0	+0.5	-26.3	0	0	-17.2	0	-0.2	-10.2	-11.0	-11.0	-33.8	-33.8	-49.4	-49.4	-0.9	+7.7	+5.9	-0.1	-27.2	-15.1	-30.2	-4.4	-30.7	-0.3
8.7	6.3	Yes	V	0	+0.2	-25.1	0	-0.5	-16.0	0	-0.7	-9.8	-9.1	-9.1	-33.8	-33.8	-52.2	-52.2	-4.2	+4.0	+4.8	-0.1	-24.1	-17.8	-16.5	-8.8	-9.6	-0.3

Notes   *   V = 100 unit uniformly distributed vertical load on each beam

         3V = 300   "   "   "   "   "   "   "

         H =   50 unit horizontal load applied at top beam level

           100   "   "   "   "   " middle beam level

           100   "   "   "   "   " bottom beam level

Table 8.8   Three storey square infilled frames under combined vertical and horizontal loading
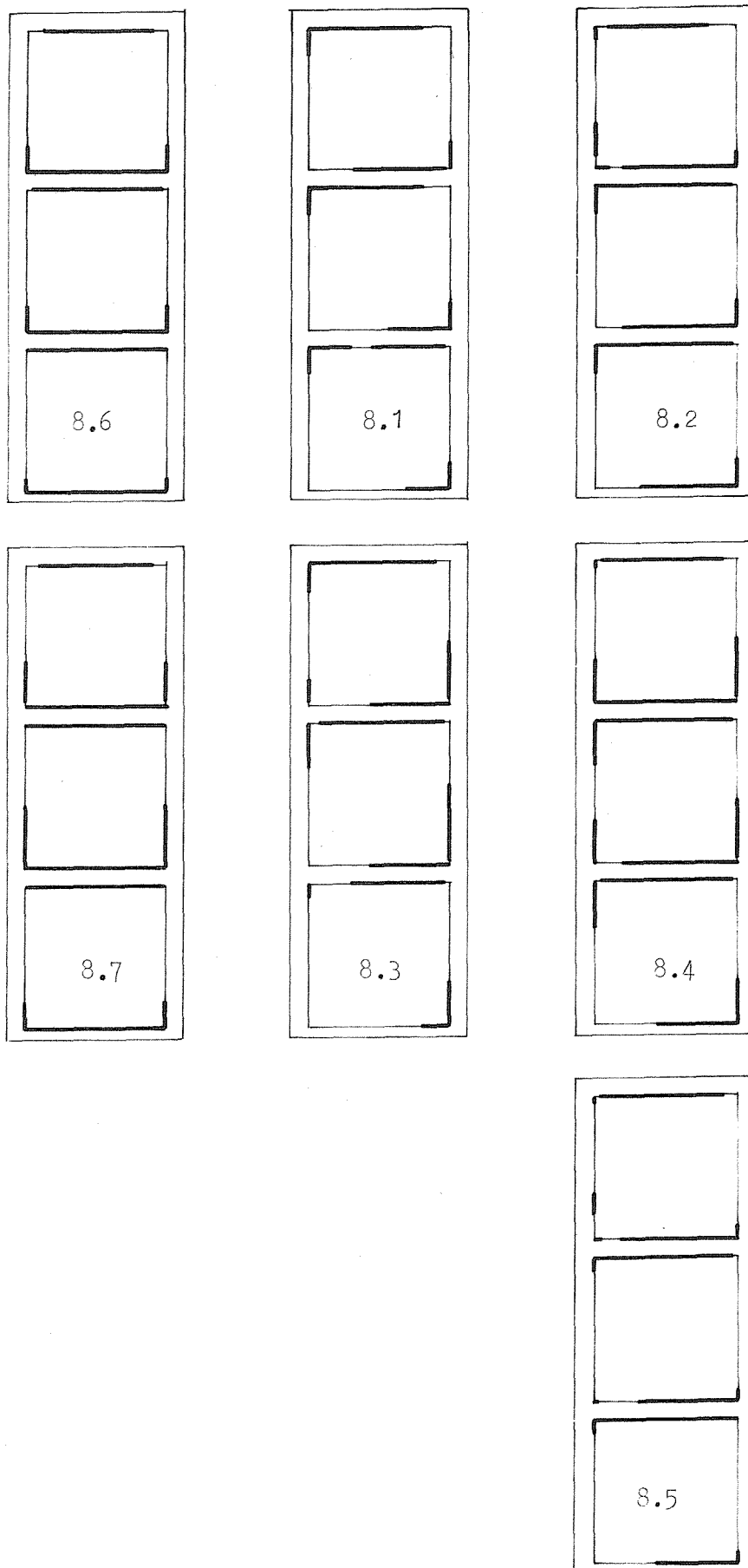
FIG. 8.33 LENGTHS OF CONTACT FOUND IN ANALYSES 8.1 to 8.7

Again it should be noted that the lengths of contact will only be given approximately by the analyses, because of the relatively coarse spacing of the nodes. Comparing the lengths of contact shown in Fig. 8.33 with the results for lateral loading only shown in Fig. 8.24, the contact lengths on the beam joints are seen to be increased by vertical loading, whilst those on the column joints show no definite trend of change. The strut action of the infills is seen to be more clearly defined in the lower infills than in the top infill. This is probably caused by the fact that the forces due to vertical loading increase linearly down the structure, whilst the forces in the columns due to lateral loading increase more rapidly.

Comparing the results for vertical and lateral loading (Table 8.8) with the results for lateral loading (Table 8.3), the following general conclusions can be drawn. With regard to the central infill stresses, the shear stresses for the no friction analyses are slightly increased by vertical loading, whilst for the friction analyses the shear stresses remain unchanged or are reduced slightly. The central infill vertical stress is increased by the vertical loading and this more than compensates for any increase in shear stress with regard to strength considerations. The diagonal tensile stress is reduced by the vertical loading. The corner infill stresses are also affected by the vertical loading with the bottom corner stresses being increased and the top corner stresses being reduced. The vertical loading reduces the lateral deflection of the structures.

The beams of the frames are not affected by vertical loading for the no friction analyses, but some compression force increase occurs in the beams for the friction analyses. In all the analyses, the vertical loading increases the compression force in all the columns. In the case of the windward columns, this has the effect of

reducing the tension force. The proportion of the vertical force carried by the columns is seen to vary with the level of boundary friction and the position and axial stiffness of the columns. For the no friction analyses, the proportion carried by the tension columns is not very dependent on their axial stiffness.

8.6.4 Three storey square infilled frames - bottom infill omitted

Eight analyses were undertaken on three storey square infilled frames with the bottom infill omitted and loaded under differing combinations of vertical and lateral loading. The structures were similar to those considered in Section 8.5.6. The loading configurations applied were those used in Section 8.6.3.

The results are shown in Table 8.9. The results indicate similar effects to those found in the lateral loading analyses of Section 8.5.6 in that the basic behaviour of the structures is mainly dependent on the degree of first floor level lateral restraint. Considering the vertical loading analyses and comparing the results with those in Table 8.8, it is seen that the removal of the bottom infill considerably increases the bottom corner stresses of the infills for the no friction analysis, but little change occurs for the friction analysis. The rigidity of the beam connections is seen to be relatively unimportant when there is only vertical loading in that the results from analysis 9.6 with pin-jointed beams are very similar to those from analysis 9.5 with rigidly connected beams. The only significant difference occurs in the first floor beam, where the tensile force is almost halved in the pin-jointed beam analysis.

Comparing the results from analysis 9.3 with combined vertical and lateral loading and first floor lateral restraint with those from

Analysis Ref.	λh	Boundary Friction?	Loading*	Central infill stresses						Frame member axial forces									Lateral Deflection	Infill corner stresses			
				Middle infill			Top infill			1	2	3	4	5	6	7	8	9		C	D	E	F
				τ_{xy}	σ_{dt}	σ_y	τ_{xy}	σ_{dt}	σ_y														
9.1	6.3	No	V,H	35.0	+5.1	-59.0	10.0	+4.0	-36.6	+100.5	+19.2	+154.9	+10.0	+158.0	-458.0	+6.0	+59.2	+123.3	379.7	-676.1	-150.3	-71.0	-132.8
9.2**	6.3	No	V,H	32.3	+8.3	-39.9	9.8	+3.7	-25.4	+55.5	-5.4	+130.0	-47.6	+108.6	-408.6	+0.3	+53.5	+52.3	94.3	-524.9	-604.7	-77.2	-334.9
9.3***	6.3	No	3V,H	27.0	0	-41.3	9.3	-2.2	-28.3	-25.6	-48.9	-47.6	-234.5	-249.0	-650.0	-5.8	+68.7	-39.0	18.5	-601.7	-209.7	-83.1	-88.0
9.4***	6.3	Yes	3V,H	19.4	-5.3	-33.4	6.9	-1.4	-30.9	-17.2	-31.3	-44.7	-212.8	-252.0	-648.0	-28.9	-13.2	-55.1	10.7	-343.0	-33.7	-43.4	-7.9
9.5	6.3	No	V	0	-4.6	-10.2	0	-1.5	-8.6	-14.5	-14.5	-59.2	-59.2	-150.0	-150.0	-1.4	+15.5	+49.1	-0.1	-102.2	-0.2	-54.3	-0.2
9.6****	6.3	No	V	0	-3.4	-8.1	0	-1.6	-7.3	-14.3	-14.3	-60.6	-60.6	-150.0	-150.0	-1.0	+13.3	+27.5	-0.1	-96.2	-0.2	-67.5	-0.2
9.7	6.3	Yes	V	0	-5.3	-9.6	0	-0.6	-10.0	-9.0	-9.0	-46.5	-46.5	-150.0	-150.0	-4.0	+1.0	+41.6	-0.1	-11.9	-11.0	-9.7	-0.3
9.8	15	No	V	0	-6.1	-12.0	0	-1.5	-9.7	-6.6	-6.6	-38.4	-38.4	-150.0	-150.0	-0.3	+9.1	+54.6	0	-143.7	-0.5	-60.1	-0.4

Notes   *   V = 100 unit uniformly distributed vertical load on each beam   **   Stiffened bottom columns

3V = 300   "   "   "   "   "   "   "   "   ***   "   "   " , 1st floor restraint

H = 50 unit horizontal load applied at top beam level

     100   "   "   "   "   " middle beam level   ****   Pin-jointed beams

     100   "   "   "   "   " bottom "   "

Table 8.9   Three storey square infilled frames with bottom infill omitted under combined vertical and horizontal loadi₁

214

the lateral loading only analysis 6.3 (Table 8.6), it can be seen that for the central infill stresses, the shear and diagonal tension stresses are reduced while the vertical compressive stresses are increased when vertical loading is applied. The lateral deflection of the structure is also reduced. The only corner infill stress significantly increased by the addition of vertical loading is that in the infill corner immediately above the omitted infill.

8.6.5 Inclusion of vertical loading into the design method

As previously mentioned, many parameters control the behaviour of infilled frames subjected to combined vertical and lateral loading. These parameters have not been comprehensibly investigated in the preceding sections and therefore only very approximate, but conservative recommendations can be given here for including vertical loading in the design method developed in Chapter 7. A much more detailed study would be required to improve upon these recommendations.

Considering the infill stresses, the application of vertical loading to the laterally loaded structures has had the effects of reducing the central infill shear and diagonal tensile stresses, whilst increasing the central infill vertical compressive stress and the bottom infill corner principal compressive stress. These stress changes will result in increased failure loads for the shear and tensile modes of failure and reduced failure loads for the compressive corner failure mode. The increase in the corner stresses varies greatly with the type of structure and the position of the infill in the structure. For example for the three storey structures analysed in Section 8.6.3, the increase in corner stress in the bottom infills was less than 7%. whilst the increase in the top infills was up to 100% for the no friction analyses. For the friction analyses, where

the corner stresses are much lower, the increase in the corner stress in the top infill was even higher.

As a result of these findings for infill stress changes, it is suggested that the following modifications are made to the approximate design method derived in Chapter 7, when vertical loading is to be considered. For the shear failure mode, the lateral failure load should be taken as given in Eq. 7.24. For the compression corner failure mode, the lateral failure load should be taken as one half of that given by Eq. 7.25, when the vertical loading is between one half and three times the lateral loading. The halving of the Eq. 7.25 load is not as restrictive as it might at first appear, because for the lateral loading only cases, Eq. 7.25 is not usually limiting. For vertical loading less than one half of the lateral loading, the lateral failure load should be taken as that given in Eq. 7.25. Vertical loading greater than three times the lateral loading is beyond the scope of the present work.

The lateral deflection of all the structures was reduced by the addition of vertical loading. Thus a conservative estimate of lateral deflection can be obtained by using the design method of Chapter 7 and ignoring the vertical loading.

Considering the frame forces, it is suggested that these can be estimated conservatively in the following manner. The forces should first be calculated by assuming only lateral loading and using the design method of Chapter 7. The design beam forces for combined loading can be taken as these values. The design force for the columns should be taken as the highest value of the following forces: (a) the force calculated above, (b) the force calculated assuming the vertical load to be carried entirely by the columns, and (c) the sum of (a) and (b).

8.7 Conclusions

The main conclusions from this section of work can be summarized as follows:-

(1) The computer programs developed appear to give a fair representation of the elastic behaviour of infilled frames even after boundary cracking, provided that a good initial fit of the infills is achieved.

(2) The lateral load analyses indicate that the design method of Chapter 7 gives a fair representation of the behaviour of infilled frames and conservative estimates for the forces, stresses and deflections in infilled frames.

(3) The recommendations for the inclusion of vertical loading into the design method of Chapter 7 contained in Section 8.6.5 are conservative and simple, but very approximate. A far more extensive and detailed study would be required to make more precise recommendations. Stricter building controls would also be essential, because infilled frame behaviour under vertical loading is far more sensitive to initial fit and frame prestressing than is its behaviour under lateral loading.

CHAPTER   9

INFILLED FRAMES: DIAGONAL COMPRESSION TESTS

9.1 Introduction

One mode of infilled frame failure indicated in the previous chapters was that of diagonal crushing in the corners of the infill. To the best of the author's knowledge, no tests have ever been conducted to investigate the compressive strength of masonry under diagonal loading, with the type of restraints found in infilled frames. The results from masonry infilled frame tests have normally been related to the vertical strength of the masonry.

The tests described below were undertaken to try to determine a relationship between the diagonal failure strength of masonry and its vertical strength as measured by a standard wall test. The equipment for these tests was designed and built at the University of Southampton. The testing was carried out at Redland Research and Development Ltd. under the supervision of Dr. H. Barker. The author wishes to record his appreciation for the help given by Redland Research and Development and Dr. Barker.

At the time of writing, the test programme had not been completed. A considerable number of additional tests are required to give adequately comprehensive information.

9.2 Design of apparatus

In designing the test equipment, the following points had to be considered.

(1) When corner failure occurs in an infill, the adjacent beam and column are in contact with the infill over a definite "length of contact". In the diagonal loading tests, this form of loading had to be represented as accurately as possible.

(2) For the small sample sizes that were to be considered in these tests, considerable restraint had to be applied in order to prevent any shear or diagonal tensile failure in the samples.

(3) Corner compressive failure as a primary mode of failure is only likely to occur for low strength masonry.

The testing apparatus designed on the basis of these considerations is shown in Plate 9.1 and Fig. 9.1. The diagonal loading was applied by the two corner bearings at the top and bottom of the sample. The length of side of the bearings was intended to represent the "length of contact" between the beam or column and the infill. The load was applied by a 50 Tonne hydraulic jack at the top. The surrounding reaction frame was designed to withstand this 50 Tonne maximum load. In order to prevent shear or diagonal tensile failure in the samples, the horizontal diagonally opposite corners of the sample were rigidly clamped together using the specially designed clamp shown in Plate 9.1, and Fig. 9.1. This clamp was designed to be very stiff so that little spread of the sample and thus no diagonal cracking would occur. The clamp was suspended from the top of the reaction frame so that no vertical load was applied to the test sample.
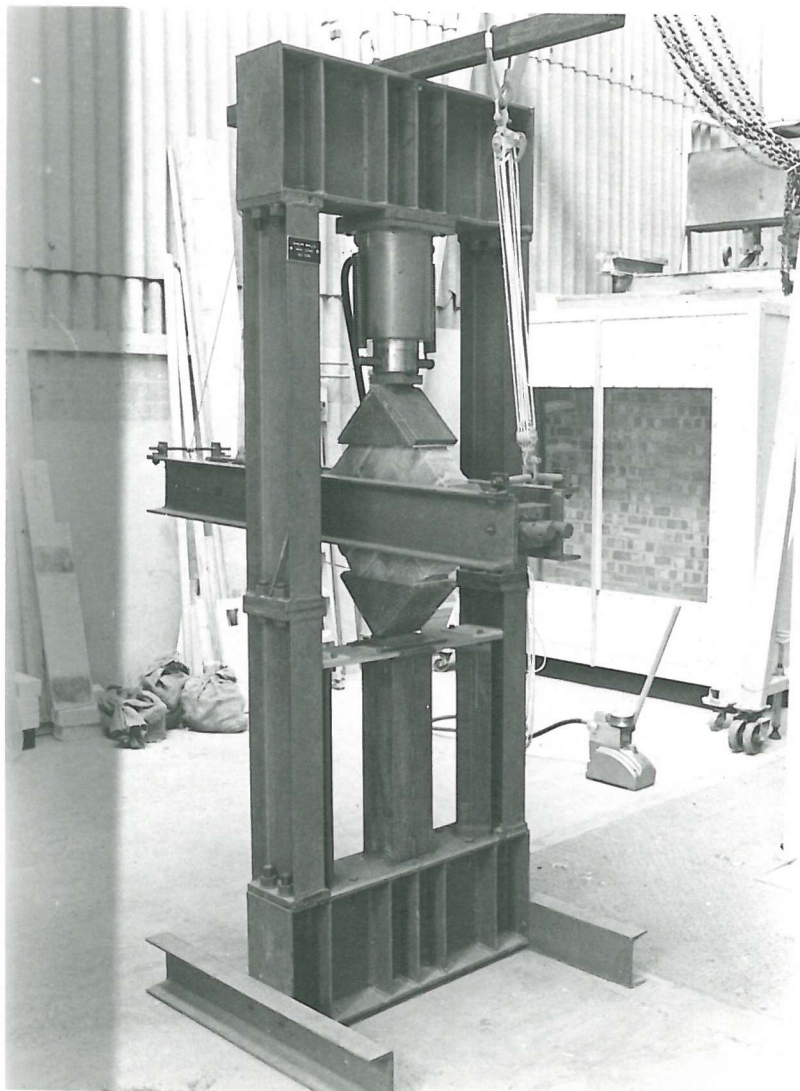
Plate 9:1   Diagonal compression test apparatus with
two brick square sample
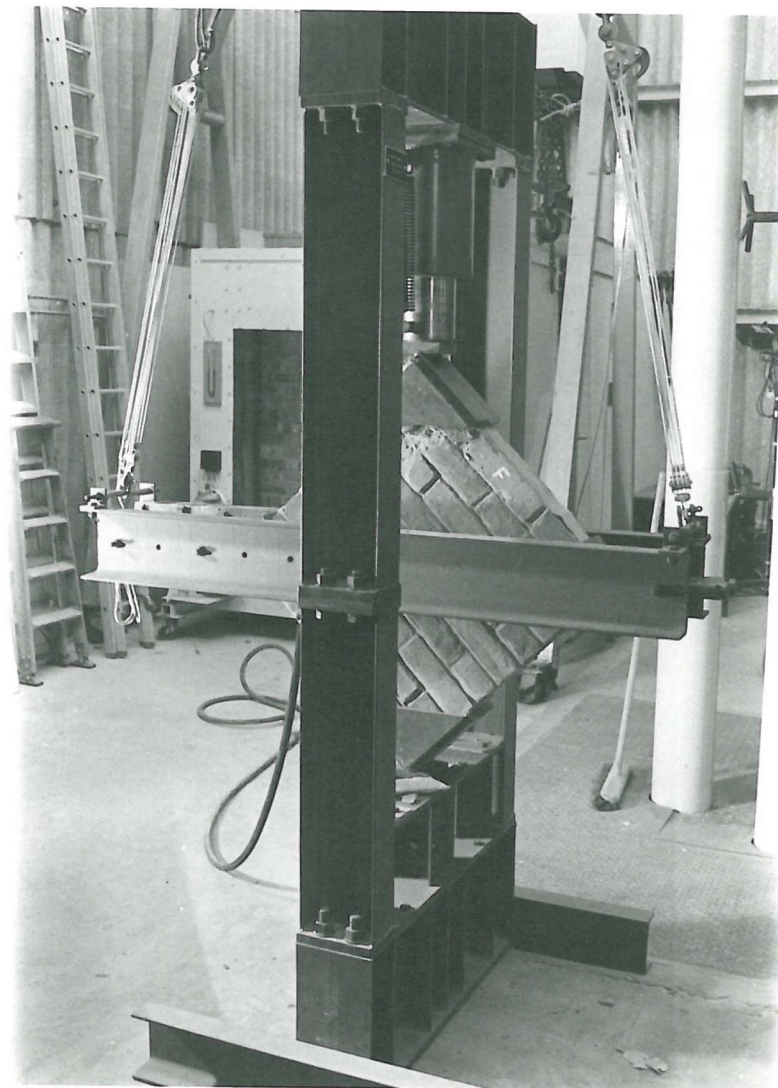
Plate 9.2   Diagonal compression test apparatus with
three brick square sample after failure
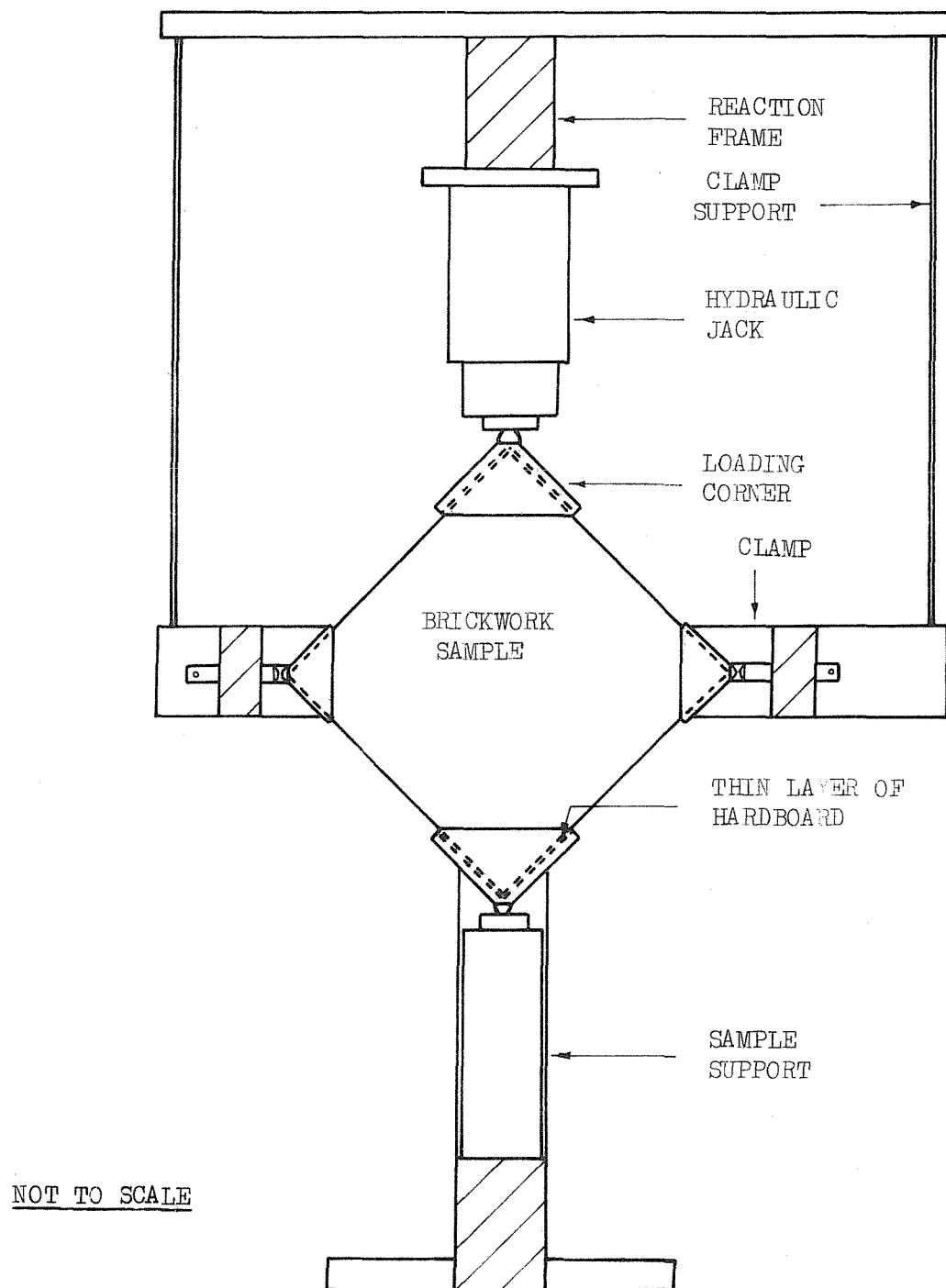
FIG. 9.1   TESTING APPARATUS FOR DIAGONAL COMPRESSION TESTS

9.3 Tests completed

Initially a total of twelve square samples were tested to check the effectiveness of the apparatus. These included three brick strengths and two sample sizes, which were 2 bricks wide by 6 bricks high and 3 bricks wide by 9 bricks high. The loading corners used in these tests had side lengths of 200 mm. These tests indicated that variations in the initial tightness of the clamp did not significantly affect the strength of the samples, provided the clamp was tight enough to prevent any shear or diagonal tensile failure.

In order to compare the vertical and diagonal strength of the masonry, it was necessary to obtain for each diagonal test a corresponding value of vertical strength. Appendix C of the "Draft British Standard Specification For the Structural Use of Masonry Part 1: Unreinforced Masonry"[65] gives details of a standard wall test that can be used to determine vertical masonry strength. For each test series conducted subsequent to the initial tests, single leaf walls 6 bricks wide by 27 high were constructed and loaded vertically to failure to determine the vertical strength of the masonry used in the diagonal tests. This wall size conforms with the recommendations given in the draft code.

Only one set of diagonal tests has been completed at the time of writing, these were conducted on masonry built with bricks of 10 MN/m^2 and 1:1:6 mortar. The set of tests consisted of 5 square samples 2 bricks wide, 6 courses high and 5 square samples 3 bricks wide, 9 courses high. In addition 3 of the larger walls were constructed and tested to obtain the vertical masonry strength. Loading corners with 200 mm. side lengths were used in these diagonal tests.

The results from the diagonal loading tests are shown in Table 9.1

Sample Size	Sample Number	Failure Load Tonnes	Diagonal Strength T/m^2	Diagonal Strength Av. Vertical Strength
2 bricks wide by 6 courses high	1	20.4	721	1.63
	2	21.4	756	1.71
	3	25.5	901	2.04
	4	19.4	686	1.55
	5	24.5	865	1.96
	Average	22.2	784	1.78
3 bricks wide by 9 courses high	1	19.4	686	1.55
	2	18.4	650	1.47
	3	19.4	686	1.55
	4	22.4	791	1.79
	5	27.5	972	2.20
	Average	21.4	756	1.71

Table 9.1   Results from diagonal loading tests

Sample Size	Sample Number	Failure Load Tonnes	Vertical Strength T/m^2
6 bricks wide by 27 bricks high	1	56	421
	2	58	436
	3	62	466
	Average	58.7	441

Table 9.2   Results from vertical loading tests

and those from the vertical wall tests are shown in Table 9.2. The results in Table 9.1 indicate that the smaller samples were on average slightly stronger than the larger samples. The difference however is very small compared with the deviation of results within each sample size. This is important because for the information obtained from these tests to be relevant to full size infills, the results must be independent of sample size. One difference between the two sample sizes was their failure modes. The larger samples tended to crush only in the loading corner region as shown in Plates 9.2 and 9.3 whilst the smaller samples tended to crush over virtually their whole area.

For vertical loading, the area of loading is well defined. Unfortunately for the form of loading used in the diagonal loading tests, no area of loading is clearly defined. For the purpose of these tests, the area of loading will be defined as the cross-sectional area of the infill between the ends of the two lengths of contact.

Thus the loading area $= 0.2 \times \sqrt{2} \times 0.1 = 0.0283 \ m^2$.

The average strength of the ten samples $= 21.8$ Tonnes.

Thus the diagonal failure stress $= 21.8/0.0283 = 770 \ Tonnes/m^2$.

Considering the vertically loaded walls

The area of loading $= 0.1 \times 1.33 = 0.133 \ m^2$

The average failure load $= 58.7$ Tonnes.

Thus the vertical failure stress $= 58.7/0.133 = 441 \ Tonnes/m^2$.

Comparing the diagonal and vertical strengths

$$\frac{\text{diagonal strength}}{\text{vertical strength}} = \frac{770}{441} = 1.75$$

These initial results indicate that the diagonal strength of masonry is considerably greater than its vertical strength when the loading is of the type experienced in infilled frames and the loading area is defined as above.
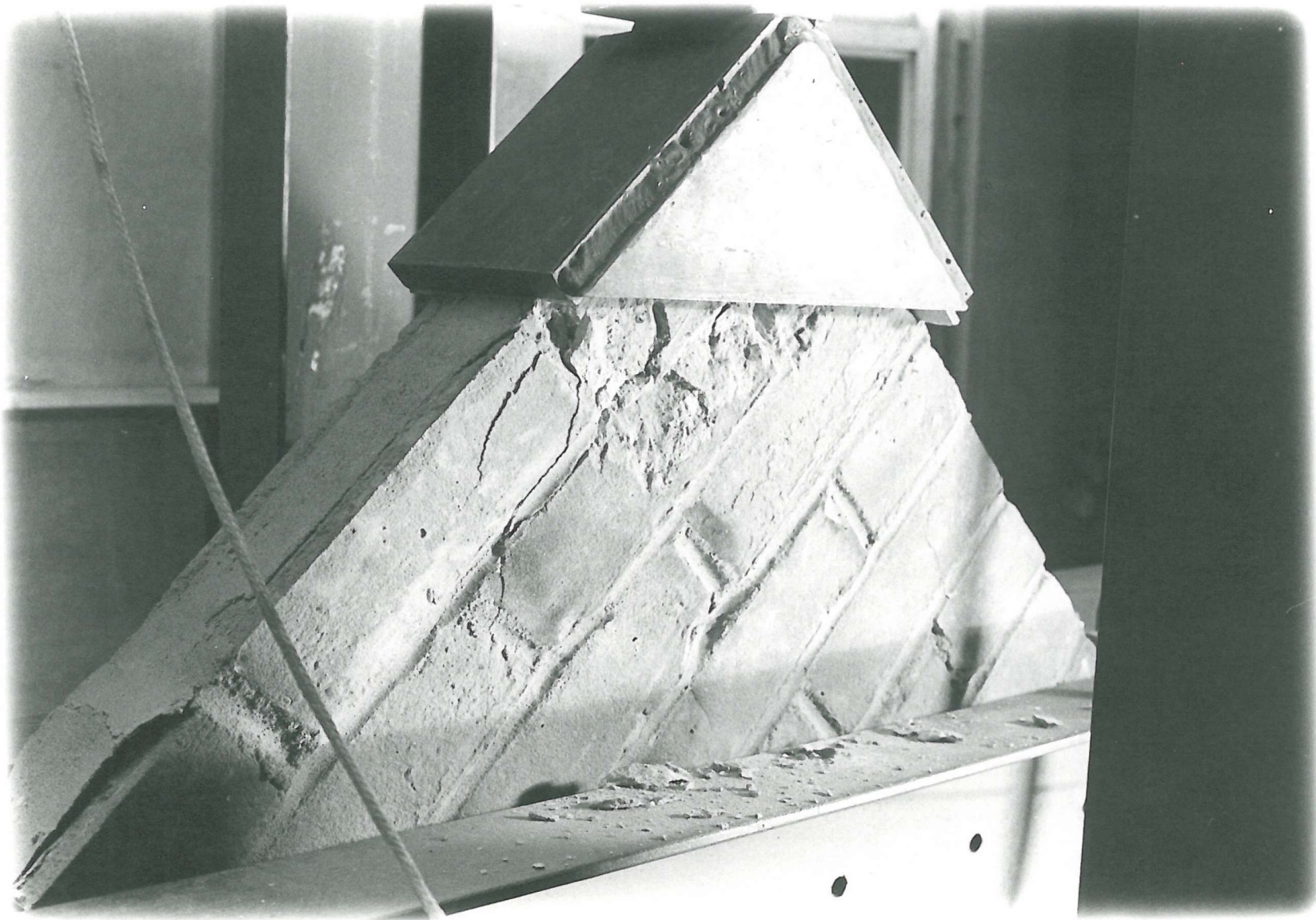
Plate 9.3 Three brick square sample after failure

9.4 Further testing

Several further sets of tests are planned in which different parameters will be varied. The strength of masonry and the type of brick, e.g. frogged, perforated, will be varied to see if a constant ratio between the diagonal and vertical strength exists. The size of the loading corners will also be varied to see if scale effects are important. Finally non-square samples will be tested to assess the effects of changes in the angle between the loading line and bedding plane.

9.5 Conclusions

The main conclusions from this section of work can be summarized as follows:

(1) The tests completed up to the time of writing indicate that the diagonal strength of masonry is greater than its vertical strength, when the diagonal loading is of the type experienced in infilled frames and the loading area is defined as the cross-sectional area between the ends of the two lengths of contact. For the tests completed, the diagonal strength was approximately 75% greater than the vertical strength.

(2) Further testing is required before final conclusions regarding diagonal compressive strength can be reached.

CHAPTER 10

GENERAL CONCLUSIONS

The main conclusions from the work contained in this thesis can be summarised as follows:

(1) The methods presented for the design of vertically loaded masonry walls supported on encased steel beams are simple to apply. They can, however, be very conservative, if the beam has a high level of support rotational restraint and the wall is continuous past the support.

(2) The method presented for the design of laterally loaded infilled frames is also very simple to apply. The recommendations for the inclusion of vertical loading into the design are very conservative. To improve upon these recommendations, a far more detailed and extensive study would be required. Stricter building controls would also be essential, because infilled frame behaviour under vertical loading is far more sensitive to initial infill fit and frame prestressing than is its behaviour under lateral loading.

(3) The finite element programs developed will give a good indication of the elastic behaviour of walls on beams and infilled frames, even after boundary cracking. The analyses completed indicate that boundary cracking significantly affects infilled frame behaviour, while for walls on beams, the only parameter that has been found to be greatly affected by boundary cracking is the beam deflection.

(4) The finite element analyses of the basic wall on beam structure have produced equations that relate the maximum stresses, forces and moments in the structure to the dominant controlling parameter. Although these equations differed to some extent from the equations

assumed in the design methods, these differences did not necessitate any alteration to the design methods. To obtain similar equations for wall on beam structures, where the beam is subjected to support rotational restraint and the wall is continuous past the support would require a very extensive series of analyses, because of the large number of controlling parameters.

(5) The finite element analyses of infilled frames under lateral loading have indicated that the equations assumed in the development of the design method were reasonably accurate. Only in the case of the central infill vertical stresses were the differences significant enough to necessitate changes to the design method.

(6) The initial diagonal compression tests have indicated that the compressive strength of masonry with infill type loading is in the order of 75% greater than its strength under standard vertical loading. Many more sets of tests are required, however, before final conclusions can be reached.

REFERENCES

1. Dischinger, F. "Beitrag zur theorie de halbscheibe und des wandartigen balkens". International Association for Bridge and Structural Engineering, 1932, I, pp.69-93.

2. Durant, N.J. and Garwood, F. "Stresses in a deep beam". Ministry of Works Technical Note No.78, Oct. 1947.

3. Wood, R.H. "Studies in composite construction, Part 1. The composite action of brick panel walls supported on reinforced concrete beams". National Building Studies, Research Paper No.13, 1952.

4. Rosenhaupt, S. "Composite walls". D.Sc. thesis, Israel Institute of Technology, Feb. 1960.

5. Rosenhaupt, S. "Experimental study of masonry walls on beams". Proc. A.S.C.E., Vol.88, ST3, pp.137-166, June 1962.

6. Rosenhaupt, S. "Stresses in point supported composite walls". Journal of the American Concrete Institute, Vol.61, No.7, pp.795-809, July 1964.

7. Coull, A. "Composite action of walls supported on beams". Building Science, Vol.1, pp.259-270, 1966.

8. Colbourne, J.R. "Studies in composite construction: an elastic analysis of wall-beam structures". Building Research Station, Current Paper 15/69, May 1969.

9. Burhouse, P. "Composite action between brick panel walls and their supporting beams". Proc. I.C.E., Vol.43, pp.175-194, June 1969.

10. Wood, R.H. and Simms, L.G. "A tentative design method for the composite action of heavily loaded brick panel walls supported on reinforced concrete beams". Building Research Station, Current Paper 26/69, July 1969.

11. Male, D.J. and Arbon, P.F. "A finite element study of composite action in walls". 2nd Australasian Conf. Mech. Structures and Mats., University of Adelaide, August 1969.

12. Green, D.R. "The stress analysis of shear walls". Ph.D. Thesis, University of Glasgow, August 1970.

13. Green, D.R. "The interaction of solid shear walls and their supporting structures". Building Science, Vol.7, pp.239-248, 1972.

14. Vettram, A.L. and Hirst, M.J.S. "An elastic analysis for the composite action of walls supported on simple beams". Building Science, Vol.6, pp.151-159, 1971.

15. Hetényi, M. "Beams on elastic foundations". University of Michigan Studies, Scientific Series Vol. XVI, 1946.

16. Private communication with Mr. A.L. Randall, Redpath Dorman Long Limited.

17. Choudhury, J.R. "Analysis of plane and spatial systems of interconnected shear walls". Ph.D. thesis, University of Southampton, 1968.

18. Lau, P.C.M. "The structural behaviour of panel type buildings". Ph.D. thesis, University of Southampton, 1972.

19. Riddington, J.R. "Composite action of masonry walls supported on reinforced concrete beams". B.Sc. Honours Project, University of Southampton, 1971.

20. Polyakov, S.V. "On the strength and deformation of stone masonry filling in framed walls under shearing load". Building Industry, No.3, 1952, Moscow (In Russian).

21. Polyakov, S.V. "Masonry in framed buildings". 1956, English translation by G.L. Cains (1963).

22. Polyakov, S.V. "On the interaction between masonry filler walls and enclosing frame when loaded in the plane of the wall". Earthquake Engineering Research Institute, San Francisco, 1960.

23. Polyakov, S.V. "Some investigations of the problem of the strength of elements of buildings subjected to horizontal loads". Symposium on tall buildings, Edited by A. Coull and B. Stafford Smith, Pergamon Press, 1967.

24. Whitney, C.S., Anderson, B.G. and Cohen, E. "Design of blast resistance construction for atomic explosions". Journal of the American Concrete Institute, Vol.51, pp.655-673, 1955.

25. Benjamin, J.C. and Williams, H.A. "The behaviour of one-storey reinforced concrete shear walls". Proc. A.S.C.E., Vol.83, ST3, 1957.

26. Benjamin, J.C. and Williams, H.A. "Behaviour of one-storey walls containing openings". Journal of the American Concrete Institute, Vol.55, pp.605-618, 1958.

27. Benjamin, J.C. and Williams, H.A. "The behaviour of one-storey brick shear walls". Proc. A.S.C.E. Vol.84, ST4, 1958.

28. Benjamin, J.C. and Williams, H.A. "Reinforced concrete shear wall assemblies". Proc. A.S.C.E., Vol.86, ST8, 1960.

29. Satchanski, S. "Analysis of the earthquake resistance of frame buildings taking into consideration the carrying capacity of the filling masonry: Proc. 2nd World Conference on Earthquake Engineering, Vol.3, pp. 2127-2141, Japan 1960.

30. Stafford Smith, B. "The stiffness and strength of infilled frames". Ph.D. thesis, Bristol University, 1963.

31. Stafford Smith, B. "Lateral stiffness of infilled frames". Proc. A.S.C.E., Vol.88, ST6, pp.183-199, 1962.

32. Stafford Smith, B. "Behaviour of square infilled frames". Proc. A.S.C.E., Vol.92, ST1, pp.381-403, 1966.

33. Stafford Smith, B. "Methods of predicting the lateral stiffness and strength of multi-storey infilled frames". Building Science, Vol.2, pp.247-57, 1967.

34. Stafford Smith, B. "The composite behaviour of infilled frames. "Symposium on tall buildings, Edited by A. Coull and B. Stafford Smith, Pergamon Press, 1967.

35. Stafford Smith, B. and Carter, C. "A method of analysis for infilled frames". Proc. I.C.E., Vol.44, pp.31-49, Sept. 1969.

36. Carter, C. "The behaviour of infilled frames when subjected to lateral loading". Ph.D. thesis, University of Southampton, 1970.

37. Karamanski, T. "Calculating infilled frames by the method of finite elements". Symposium on tall buildings, Edited by A. Coull and B. Stafford Smith, Pergamon Press, 1967.

38. Mallick, D.V. and Severn, R.T. "The behaviour of infilled frames under static loading". Proc. I.C.E., Vol.38, pp.639-656, Dec. 1967.

39. Mallick, D.V. and Severn, R.T. "Dynamic characteristics of infilled frames". Proc. I.C.E., Vol.39, pp.261-287, Feb. 1968.

40. Mallick, D.V. and Garg, R.P. "Effects of openings on the lateral stiffness of infilled frames". Proc. I.C.E., Vol.49, pp.193-203, June 1971.

41. Tomii, M. "General analysis of elasticity of shear walls by stress functions". Recent researches of structural mechanics, April 1968, Tokyo, Japan.

42. Liauw, T.C. "Elastic behaviour of infilled frames". Proc. I.C.E. Vol.46, pp.343-349, July 1970.

43. Kadir, M.R.A. "The structural behaviour of masonry infill panels in frame structures". Ph.D. thesis, Edinburgh University, 1974.

44. Wood, R.H. "Discussion on the stability of tall buildings". Proc. I.C.E., Vol.12, pp.502-522, 1959.

45. Holmes, M. "Steel frames with brickwork and concrete infilling". Proc. I.C.E., Vol.19, pp.473-478, Aug. 1961.

46. Holmes, M. "Combined loading on infilled frames". Proc. I.C.E. Vol.25, pp.31-38, May 1963.

47. Tomii, M. "Design procedures of concrete shear walls". Department of Architecture report, April 1966, Kyushu University, Japan.

48. Liauw, T.C. "An approximate method of analysis for infilled frames with or without openings". Building Science, Vol.7, pp.233-238, 1972.

49. Mainstone, R.J. "On the stiffnesses and strengths of infilled frames". Proc. I.C.E. Supplement (IV), 1971.

50. Mainstone, R.J. "Supplementary note on the stiffnesses and strengths of infilled frames". Current paper 13/74, Feb. 1974, Building Research Establishment.

51. Smolira, M. "Analysis of infilled frames". Proc. I.C.E., Part 2, Vol.55, pp.895-912, Dec. 1973.

52. Thomas, F.G. "The strength of brickwork". The Structural Engineer", pp.35-46, Feb. 1953.

53. Wood, R.H. "The stability of tall buildings". Proc. I.C.E. Vol.11, pp.69-102, Sept. 1958.

54. Esteva, L. "Behaviour under alternating loads of masonry diaphragms framed by reinforced concrete members". Symposium on the effects of repeated loading on materials and structural elements, RILEM, Mexico, 1966.

55. Simms, L.G. "The behaviour of no-fines concrete panels as the infill in reinforced concrete frames". Civil Engineering and Public Works Review, pp.1245-1250, Nov. 1967.

56. Stafford Smith, B. "Model test results of vertical and horizontal loading of infilled frames". Journal of the American Concrete Institute, pp.618-624, Aug. 1968.

57. Trigo, J. "Estruturas de paneis sob a accao de solicitacoes horizontais". (In Portuguese), National Laboratories of Civil Engineering, Portugal, 1968.

58. Meli, R. and Salgado, G. "Comportamiento de muros de mamposteria sujetos a cargo lateral" (In Spanish), National University of Mexico, Sept. 1969.

59. Meli, R. "Behaviour of masonry walls under lateral loading". National University of Mexico.

60. Mainstone, R.J. and Weeks, G.A. "The influence of a bounding frame on the racking stiffnesses and strengths of brick walls". Proc. of the 2nd International Brick Masonry Conference, Stoke-on-Trent, April 1970.

61. Fiorato, A.E., Sozen, M.A. and Gamble, W.L. "An investigation of the interaction of reinforced concrete frames with masonry filler walls". University of Illinois, Nov. 1970.

62. Stafford Smith, B. and Rahman, K.M.K. "The variations of stress in vertically loaded brickwork walls". Proc. I.C.E., Vol.51, pp.689-700, April 1972.

63. Stafford Smith, B., Carter, C. and Choudhury, J.R. "The diagonal tensile strength of brickwork". The Structural Engineer, Vol.48, pp.219-225, June 1970.

64. Hendry, A.W. and Sinha, B.P. "Shear tests on full-scale single-storey brickwork structures subjected to precompression". The British Ceramic Research Association. Technical Note 134.

65. "Draft British Standard specification for the structural use of masonry. Part 1: Unreinforced masonry". British Standards Institution. Document 74/10483 DC.

APPENDIX A : WALL ON BEAM COMPUTER PROGRAM

SCOPE:　　　　The computer program was used to analyse symmetric wall on beam problems. The left hand half of the structure is analysed.

FACILITIES:　　1. Concentrated loads can be applied at nodal points.

2. Non-zero displacements can be applied at nodes.

3. Generation of node and element connectivity is achieved automatically.

4. The wall can be continuous past the end of the beam and can continue below the beam level.

5. Separation cracking on the wall beam boundary is automatically generated.

OUTPUT:　　　Printing of input data.

Element connectivity.

Displacements at nodel points.

Stresses at element centroids.

Extrapolated stresses on wall-beam boundary.

Tie force and moments along length of beam (optional).

DATA INPUT INSTRUCTIONS:

A. Problem number card (I2)

Column	Variable name	Description
1-2	NO	Problem number

B. Problem description card (10 I3)

1-3	NEL	Number of elements
4-6	NN	Number of nodes
7-9	NRN	Number of restraints or applied displacements

10-12	NLOADC	Set to 1
13-15	NTYPE	" " "
16-18	LX	Number of elements in x-direction
19-21	LY	Number of elements in y-direction
22-24	INN	Set to 1
25-27	IEN	" " "
28-30	MDN	Number of nodes in x-direction

C. <u>Element dimensions in x-direction cards</u> (F8.2) (LX cards)

1-8	DLX(I)	Horizontal dimensions of elements in order from left

D. <u>Element dimensions in y-direction cards</u> (F 8.2) (LY cards)

1-8	DLY(I)	Vertical dimensions of elements in order from bottom

E. <u>Material properties card</u> (7F6.2, 2I3)

1-6	DZ	Thickness of elements
7-12	EB	Brick or wall modulus of elasticity E_b
13-18	VB	Brick or wall Poisson's ratio ν_b
19-24	ER	Ratio E_m/E_b, (E_m = mortar modulus of elasticity)(Set to 1 if homogeneous wall)
25-30	VR	Ratio ν_m/ν_b, (ν_m = mortar Poisson's ratio)(Set to 1 if homogeneous wall)
31-36	EC	Beam modulus of elasticity
37-42	VC	Beam Poisson's ratio

43-45	NC	Last beam element
46-48	NNS	Last beam node

F. <u>Number of mortar elements per row cards</u> (I3) (LY cards)

1-3	NER	Number of mortar elements in each horizontal row in order from bottom (Blank card if homogeneous wall) (Repeated with G cards if non homogeneous wall)

G. <u>Mortar element position cards</u> (I3) (NER cards, required only if $0 < NER < LX$)

1-3	NERP	Mortar element position, referenced to the lowest row of elements

H. <u>Number of rows of air space card</u> (I3)

1-3	K	Number of horizontal rows of air space elements

I. <u>Air space element position cards</u> (2I3) (K cards)

1-3	L	First element of air space of row considered
4-6	M	Last row of air space of row considered

J. <u>Number of rows of beam card</u> (I3)

1-3	K	Number of horizontal rows of beam elements

K. <u>Beam element position cards</u> (2 I3) (K cards)

1-3	L	First element of beam of row considered
4-6	M	Last element of beam of row considered

L. <u>Number of applied loads card</u> (I3)

1-3	NALOAD	Number of applied loads

M. <u>Load information cards</u> (2 I3, F 8.3) (NALOAD cards)

1-3	N1	Node number at which load is applied
4-6	N2	Direction of load, 1 = x-direction 2 = y-direction
7-14	E3	Magnitude of load

N. <u>Restraint or applied displacement cards</u> (2 I3, F 10.7)(NRN cards)

1-3	N1	Node number at which restraint or displacement is applied
4-6	N2	Direction of restraint or displacement, 1 = x-direction 2 = y-direction
7-16	DISP	Magnitude of displacement. If restraint, leave blank

O. <u>Information for calculation of beam moments and tie force card</u>
$$(I1, 2F\ 10.3,\ 2\ I3)$$

1	KT	Are moments and tie forces in beam required? 1 = Yes (Only permissible if 2 rows of elements in beam) Blank card = No
2-11	WT	Load to be considered on full span of beam
12-21	TL	Length of full span of beam
22-24	IT	First element of beam on bottom row
25-27	JT	Last element of beam on bottom row

```
   1          LIST LP
   2          PROGRAM (G2PN)
   3          EXTENDED DATA
   4          INPUT 5 =CR0
   5          OUTPUT 6 = LPO
   6      .   COMPRESS INTEGER AND LOGICAL
   7          END
   8
   9
  10
  11          MASTER  FEMSA
  12          COMMON /CDATA/NEL,NN,NRN,NLOADC,NTYPE,NEN,NND,NBW,MDN,NNS
  13         1,MDNA,MDNN,NREP,NC,LX,KT,WT,TL,IT,JT
  14          COMMON/CEL/ELX(255),ELY(255),ELZ(255),EEE(255),VVV(255)
  15          COMMON/CEST/NCON(255,4),NR(60),ALOAD(608,2),SKA(608,36),U(608)
  16        1 READ (5,2080) NO
  17     2080 FORMAT (I2)
  18          IF (NO.EQ.0) GO TO 2
  19          WRITE (6,2081)  NO
  20     2081 FORMAT (1H1,40X,'PROBLEM NO,=',I2//)
  21          CALL  SETUP
  22      299 CONTINUE
  23          CALL  ASSEMBLE
  24          CALL  STRESSES
  25          IF(NREP.EQ.1)GO TO 299
  26          GO TO  1
  27        2 STOP
  28          END
  29
  30
  31
  32          SUBROUTINE  SETUP
  33          COMMON /CDATA/NEL,NN,NRN,NLOADC,NTYPE,NEN,NND,NBW,MDN,NNS
  34         1,MDNA,MDNN,NREP,NC,LX,KT,WT,TL,IT,JT
  35          COMMON/CEL/ELX(255),ELY(255),ELZ(255),EEE(255),VVV(255)
  36          COMMON/CEST/NCON(255,4),NR(60),ALOAD(608,2),SKA(608,36),U(608)
  37          DIMENSION DLX(15),DLY(17)
  38          READ(5,2001)NEL,NN,NRN,NLOADC,NTYPE,LX,LY,INN,IEN,MDN
  39     2001 FORMAT( 10I5)
  40          DO 900 I=1,LX
  41          READ (5,9000) DLX(I)
  42     9000 FORMAT (F8,2)
  43      900 CONTINUE
  44          DO 901 I=1,LY
  45          READ (5,9001) DLY(I)
  46     9001 FORMAT (F8,2)
  47      901 CONTINUE
  48          READ (5,9002) DZ,E0,VB,ER,VR,EC,VC,NC,NNS
  49     9002 FORMAT (7F6,2,2I5)
  50          DO 903 I=1,LY
  51          DO 904 J=1,LX
  52          K=(I-1)*LX+J
  53          ELX(K)=DLX(J)
  54          ELZ(K)=DZ
  55          EEE(K)=E0
  56          VVV(K)=VB
  57      904 ELY(K)=DLY(I)
```

```
58            READ (5,9003) NER
59      9003  FORMAT (I3)
60            IF (NER.EQ.0) GO TO 903
61            IF (LX-NER) 906,909,905
62      905   DO 908 J=1,NER
63            READ (5,9004) NERP
64      9004  FORMAT (I3)
65            K=(I-1)*LX+NERP
66            EEE(K)=ER*EB
67            VVV(K)=VR*VB
68      908   CONTINUE
69            GO TO 903
70      906   DO 910 J=1,LX
71            K=(I-1)*LX+J
72            EEE(K)=ER*EB
73            VVV(K)=VR*VB
74      910   CONTINUE
75      903   CONTINUE
76            READ(5,9005)K
77      9005  FORMAT(I3)
78            IF (K.EQ.0) GO TO 916
79            DO 912 I=1,K
80            READ(5,9006)L,M
81      9006  FORMAT(2I3)
82            DO 913 J=L,M
83      913   EEE(J)=0.000001
84      912   CONTINUE
85      916   CONTINUE
86            READ(5,9005)K
87            DO 914 I=1,K
88            READ(5,9006)L,M
89            DO 915 J=L,M
90            EEE(J)=EC
91      915   VVV(J)=VC
92      914   CONTINUE
93            NEN=4
94            NND=2
95
96            DO 50 I= 1,NC
97            K=I+IEN-1
98      51    NCON(K,1)=(INN-1)+((LX+1)*I-1)/LX
99            NCON (K,2)=NCON(K,1)+1
100           NCON(K,3)= NCON(K,2)+MDN
101           NCON(K,4)=NCON(K,1)+MDN
102     50    CONTINUE
103           JJ=NC+1
104           J=LX*LY


105           DO 300 K=JJ,J
106           NCON(K,1)=(INN-1)+((LX+1)*K-1)/LX+MDN
107           NCON (K,2)=NCON(K,1)+1
108           NCON(K,3)= NCON(K,2)+MDN
109           NCON(K,4)=NCON(K,1)+MDN
110     300   CONTINUE
111           WRITE (6,2004)
112     2004  FORMAT(35X,'FINITE ELEMENT  2-D  ANALYSIS'//)
113           WRITE (6,2005) NEL,NN,NRN,NLOADC
114     2005  FORMAT(5X,'NO OF RECTANGULAR ELEMENTS              ',I3/
115          15X,'NO OF NODES                             ',I3/
116          2 5X,'NO OF RESTRAINTS                        ',I3/
```

```
117          55X,'NO OF APPLIED LOAD CASES                        ',I5//)
118          IF (NTYPE-1)54,54,55
119       54 WRITE (6,2006)
120          GO TO 56
121       55 WRITE (6,2007)
122       56 CONTINUE
123     2006 FORMAT (5X,' PLANE STRESS'//)
124     2007 FORMAT (5X,' PLANE STRAIN'//)
125          WRITE(6,2008)
126     2008 FORMAT(/10X,'CONNECTIVITY AND DIMENSIONS OF RECTANGULAR
127         1ELEMENTS'//5X,'EL. NO',4(5X,'NODE'),10X,'X',10X, 'Y',10X,
128         2'T',10X,'E',10X,
129         3'V'/ 10X,'1',8X,'2',8X,'3',8X,'4'/)
130          NNN=2*NN
131          DO 57 I=1,NEL
132          WRITE (6,2009) I,(NCON(I,J),J=1,4),ELX(I),ELY(I),ELZ(I),EEE(I),
133         2VVV(I)
134       57 CONTINUE
135     2009 FORMAT (I9    ,4(I9),7X,5(F11,6))
136          DO 60 I=1,NNN
137          DO 60 J=1,NLOADC
138          U(I)=0.0
139       60 ALOAD(I,J)=0
140          WRITE (6,2010)
141     2010 FORMAT (1H1,5X,'APPLIED LOAD'///)
142          DO 58 I=1,NLOADC
143          READ (5,2100) NALOAD
144     2100 FORMAT (I3)
145          WRITE (6,2200) I
146     2200 FORMAT(/' LOAD CASE ',I3//5X,'NODE NO.',5X,'SENSE',
147         15X, 'MAGNITUDE'/)
148          DO 58 J=1,NALOAD
149          READ(5,2011)N1,N2,E3
150     2011 FORMAT ( 2I5, F8 ,2 )
151          L=(N1-1)*2+N2
152          ALOAD(L,I)=E3
153       58 WRITE (6,2012) N1,N2,ALOAD(L,I)
154     2012 FORMAT(2I10,9X,F10.5)
155          WRITE (6,2013)
156     2013 FORMAT(1H1,5X,'RESTRAINED NODES'// 5X,'NODE NO.',5X,'SENSE'/)
157          K=0
158          DO 59 I=1,NRN
159          READ (5,2014) N1,N2,DISP
160          WRITE (6,2015)N1,N2,DISP
161          L=(N1-1)*2+N2
162          K=K+1
163          NR(K)=L

164          U(L)=DISP
165       59 CONTINUE
166     2014 FORMAT(2I3,F10.7)
167     2015 FORMAT(2I10,F20.7)
168          READ(5,2017)KT,WT,IL,IT,JT
169          WRITE(6,2018)WT
170     2017 FORMAT(I1,2F10.5,2I5)
171     2018 FORMAT(//' EQUIVALENT LOAD ON BEAM =',F10.5//)
172          WRITE(6,2019)TL
173     2019 FORMAT(//' SPAN OF BEAM =',F10.5//)
174          NEN1=NEN-1
175          NBW2= 0
```

```
176          DO 61 I=1,NEL
177          DO 61 J=1,NEN1
178          JJ=J+1
179          DO 61 K=JJ,NEN
180          NBW1=NCON(I,J)-NCON(I,K)
181          IF(NBW1)62,62,63
182       62 NBW1=-NBW1
183       63 IF(NBW1-NBW2) 61,61,64
184       64 NBW2=NBW1
185       61 CONTINUE
186          NBW=(NBW2+1)*NND*2-1
187          WRITE(6,2016)NBW
188     2016 FORMAT(//' BAND WIDTH = ', I2//)
189          NN2=2*NN
190          DO 69 I=1,NN2
191       69 ALOAD(I,2)=ALOAD(I,1)
192          MDNA=MDN
193          MDNN=MDN
194          RETURN
195          END
196
197
198
199          SUBROUTINE SOLVEHALF(A,B,NO,NW,NR,NL)
200          DIMENSION A(608,56),B(608,1)
201          M=(NW+1)/2
202          MM1=M-1
203          I=NO
204          DO 400 L1=1,NO
205          IF(NL)401,402,401
206      401 A(I,M)=1.0/A(I,M)
207          J=MM1
208          DO 403 L2=1,MM1
209          IF(I+J-M)402,402,404
210      404 A(I,J)=A(I,J)*A(I,M)
211          J=J-1
212      403 CONTINUE
213      402 DO 405 L=1,NR
214          B(I,L)=B(I,L)*A(I,M)
215      405 CONTINUE
216          IF(I-1)407,407,406
217      406 DO 408  K=1,MM1
218          I1=I-K
219          IF(I1)409,409,410
220      410 I2=M-K
221          IF(NL)411,412,411
222      411 J=MM1
```

```
223          MM2=MM1-K+1
224          DO 413 L2=1,MM2
225          IF(I+J-M-K+1)412,412,414
226      414 I3=J+1
227          A(I1,I3)=A(I1,I3)-A(I,(J-K+1))*A(I,I2)/A(I,M)
228          J=J-1
229      413 CONTINUE
230      412 DO 408 L=1,NR
231          B(I1,L)=B(I1,L)-B(I,L)*A(I,I2)/A(I,M)
232      408 CONTINUE
233      409 I=I-1
234      400 CONTINUE
```

```
235       407 DO 416 I=2,NO
236           J=MM1
237           DO 416 L1=1,MM1
238           I1=I+J-M
239           IF(I1)410,416,417
240       417 DO 418 L=1,NR
241           B(I,L)=B(I,L)-B(I1,L)*A(I,J)
242       418 CONTINUE
243           J=J-1
244       416 CONTINUE
245           RETURN
246           END
247
248
249
250           SUBROUTINE ASSEMBLE
251           COMMON /CDATA/NEL,NN,NRN,NLOADC,NTYPE,NEN,NND,NBW,MDN,NNS
252          1,MDNA,MDNN,NREP,NC,LX,KT,WT,TL,IT,JT
253           COMMON/CEL/ELX(255),ELY(255),ELZ(255),EEE(255),VVV(255)
254           COMMON/CEST/NCON(255,4),NR(60),ALOAD(608,2),SKA(608,36),U(608)
255           DIMENSION ST(8,8)
256           NN2=2*NN
257           DO 68 I=1,NN2
258        68 ALOAD(I,1)=ALOAD(I,2)
259           NHBW=(NBW-1)/2
260           MM=2*NN
261           MHBW=NHBW+1
262           DO 101 I= 1,MM
263           DO 101 J=1,MHBW
264       101 SKA(I,J)=0
265           DO 100 I=1,NEL
266           A=ELX(I)
267           B=ELY(I)
268           C=ELZ(I)
269           V=VVV(I)
270           E=EEE(I)
271           V1=V
272           EB=E
273       117 EB=EB/(1-V1*V1)
274           V2=(1-V1)*0.5
275           E1=EB
276       119 CONTINUE
277     C     FORCE METHOD
278           CALL FLMAT(ST,A,B,C,E,V)
279     C
280           DO 100 J=1,NEN
281           DO 100 L=1,NEN

282           M1=(NCON(I,J)-1)*NND
283           M2=(NCON(I,L) -1)*NND
284           M3=(J-1)*NND
285           M4=(L-1)*NND
286           DO 100 M=1,NND
287           DO 100 N=1,NND
288           II=M1+M
289           JJ=MHBW-M1+M2+N-M
290           I1=M3+M
291           J1=M4+N
292           IF(JJ.GT.MHBW) GO TO 100
293           SKA(II,JJ)=SKA(II,JJ)+ST(I1,J1)
```

```
294        100 CONTINUE
295            DAA=10000000.0
296            DO 510 KKN=1,MDNN
297            KNN1=(NNS+KKN-MDN)*2
298            KNN2=KNN1+MDN*2
299            KNN3=KNN1-1
300            KNN4=KNN2-1
301            KNN5=(NBW+1)/2
302            KNN6=KNN5+KNN1-KNN6
303            KNN7=KNN5+KNN3-KNN4
304            SKA(KNN1,KNN5)=SKA(KNN1,KNN5)+DAA
305            SKA(KNN2,KNN5)=SKA(KNN2,KNN5)+DAA
306            SKA(KNN3,KNN5)=SKA(KNN3,KNN5)+DAA
307            SKA(KNN4,KNN5)=SKA(KNN4,KNN5)+DAA
308            SKA(KNN2,KNN6)=SKA(KNN2,KNN6)-DAA
309            SKA(KNN4,KNN7)=SKA(KNN4,KNN7)-DAA
310        510 CONTINUE
311            NNN=NN*NND
312            JJ1=NHBW+2
313            JJ2=NHBW+1
314            DO 143 I=1,NRN
315            K=NR(I)
316            IF(U(K).EQ.0.0)GO TO 142
317            DO 142 J=1,NNN
318            KL1=K+MHBW
319            KL2=K-MHBW
320            KL3=MHBW-K+J
321            KL4=MHBW+K-J
322            DO 142 J3=1,NLOADC
323            IF((J.GT.KL2).AND.(K.GT.J))ALOAD(J,J3)=ALOAD(J,J3)-SKA(K,KL3)*U(K)
324            IF((J.GT.K).AND.(KL1.GT.J))ALOAD(J,J3)=ALOAD(J,J3)-SKA(J,KL4)*U(K)
325        142 CONTINUE
326        143 CONTINUE
327            DO 140 I=1,NRN
328            K=NR(I)
329            DO 141 J=1,NNN
330            JJ=NHBW+1+K-J
331            IF((JJ1.GT.JJ).AND.(JJ.GT.0)) SKA(J,JJ)=0.0
332        141 CONTINUE
333            DO 140 J1=1,JJ2
334            SKA(K,J1)=0.0
335            SKA(K,JJ2)=1
336            DO 140 J2=1,NLOADC
337            ALOAD(K,J2)=U(K)
338        140 CONTINUE
339            CALL  SOLVEHALF(SKA,ALOAD,NNN,NBW,NLOADC,1)
340            RETURN



341            END
342
343
344
345            SUBROUTINE   STRESSES
346            COMMON /CDATA/NEL,NN,NRN,NLOADC,NTYPE,NEN,NND,NBW,MDN,NNS
347          1,MDNA,MDNN,NREP,NC,LX,KT,WT,TL,IT,JT
348            COMMON/CEL/ELX(255),ELY(255),ELZ(255),EEE(255),VVV(255)
349            COMMON/CEST/NCON(235,4),NR(60),ALOAD(608,2),SKA(608,36),U(608)
350            DIMENSION NNEL(304,4),LNND(304,4),NP(304)
351            DIMENSION SIGMA(252,3,1)
352            DIMENSION B(3 ,8 ), D(8 ,2 ), STRESS(3 ,2 )
```

```fortran
      DIMENSION SINTER(50)
      DO 222 II=1,NEL
      DO 222 JJ=1,5
      DO 222 KK=1,NLOADC
  222 SIGMA(II,JJ,KK)=0.0
      X=0.5
      Y=0.5
      DO 204 NN1=1,NEL
      DO 205 J=1,NEN
      L1=(J-1)*NND+1
      L2=(NCON(NN1,J)-1)*NND+1
      DO 205 K=1,NND
      DO 205 L=1,NLOADC
      K1=K+L1-1
      K2=K+L2-1
      T=ALOAD (K2,L)
  205 D(K1,L)= T
      D1=ELX(NN1)
      D2=ELY(NN1)
      D3=ELZ(NN1)
      V=VVV(NN1)
      E=EEE(NN1)
      CALL STRESSMAT(B,X,Y,D1,D2,D3,E,V)
      DO  206  II=1,5
      DO  206  JJ=1,NLOADC
      S=0
      DO 206  KK=1,8
      S=S+B(II,KK)*D(KK,JJ)
  206 STRESS(II,JJ)=S
      DO  207  L=1,5
      DO  207  K=1,NLOADC
  207 SIGMA(NN1,L,K)=STRESS(L,K)
  204 CONTINUE
      DO 199 I=1,NLOADC
      WRITE (6,2055)  I
 2055 FORMAT(1H1,2X, 'LOAD CASE  ', I5/)
      WRITE (6,2050)
 2050 FORMAT (1H0, 14H DISPLACEMENTS//
     11X,'NODE NO.',10X,'X-DIRECTION',10X,'Y-DIRECTION'/)
      DO  200 J=1,NN
      J1=2*J-1
      J2=2*J
  200 WRITE (6,2031) J,ALOAD(J1,I), ALOAD(J2,I)
 2031 FORMAT (I5,2(7X,E17,6))
      WRITE (6,2032)
 2052 FORMAT(1H1,20X,'STRESS AT THE CENTROID POINT OF THE ELEMENTS'//
     1'EL.NO.',4X, 'SIGMA-X',9X,'SIGMA-Y',9X, 'SHEAR-STRESS',
     2(7X,'MAX.PR.STRESS',7X,'MIN.PR..STRESS',7X,'PR.ANGLE'/)
      DO 208 K=1,NEL
      P1= SIGMA(K,1,I)+SIGMA(K,2,I)
      P2= SIGMA(K,1,I)-SIGMA(K,2,I)
      P3=SIGMA(K,3,I)
      A= SQRT(0.25*P2*P2+P3*P3)
      PMAX= P1*0.5+A
      PMIN= P1*0.5-A
      IF(ABS(P2)-0.000001) 209,209,210
  209 A= 45
      GO TO 211
  210 A=ATAN(2*P3/P2)*90.0/3.1415925
```

```
412      211 CONTINUE
413      208 WRITE(6,2054) K,SIGMA(K,1,I),SIGMA(K,2,I), SIGMA(K,3,I),
414         1PMAX,PMIN, A
415     2054 FORMAT (I5,3X,3(E13,6,5X),F7,2)
416      199 CONTINUE
417          IPX=NC+1
418          IPY=IPX+LX
419          IPZ=IPY+LX
420          IPA=IPZ+LX
421          X1Z=ELY(IPX)
422          X2Z=ELY(IPY)
423          X3Z=ELY(IPZ)
424          X4Z=ELY(IPA)
425          X1=X1Z*0,5
426          X2=X1Z+X2Z*0,5
427          X3=X1Z+X2Z+X3Z*0,5
428          X4=X1Z+X2Z+X3Z+X4Z*0,5
429          DO 280 I=1,LX
430          IYX=NC+I
431          IYY=IYX+LX
432          IYZ=IYY+LX
433          IYA=IYZ+LX
434          Y1=SIGMA(IYX,2,1)
435          Y2=SIGMA(IYY,2,1)
436          Y3=SIGMA(IYZ,2,1)
437          Y4=SIGMA(IYA,2,1)
438          CALL CUBIC(X1,X2,X3,X4,Y1,Y2,Y3,Y4,CCC)
439          J=2*I
440          SINTER(J)=CCC
441      280 CONTINUE
442          NXY=LX-2
443          DO 282 I=1,NXY
444          IF(I.EQ.1)GO TO 285
445          IPA=LX+2-I
446          X4=-ELX(IPA)*0,5
447          IYA=IPA*2
448          GO TO 286
449      285 X4=-ELX(LX)*0,5
450          IYA=2*LX
451      286 CONTINUE
452          Y4=SINTER(IYA)
453          IPX=LX+1-I
454          IPY=IPX-1
455          IPZ=IPY-1
456          X1Z=ELX(IPX)
457          X2Z=ELX(IPY)
458          X3Z=ELX(IPZ)

459          X1=X1Z*0,5
460          X2=X1Z+X2Z*0,5
461          X3=X1Z+X2Z+X3Z*0,5
462          IYX=(LX+1-I)*2
463          IYY=IYX-2
464          IYZ=IYY-2
465          Y1=SINTER(IYX)
466          Y2=SINTER(IYY)
467          Y3=SINTER(IYZ)
468          CALL CUBIC(X1,X2,X3,X4,Y1,Y2,Y3,Y4,CCC)
469          J=(LX+1-I)*2-1
470          SINTER(J)=CCC
```

```
471          282 CONTINUE
472              X1Z=ELX(1)
473              X2Z=ELX(2)
474              X3Z=ELX(3)
475              X4Z=ELX(4)
476              X1=X1Z*0.5
477              X2=X1Z+X2Z*0.5
478              X3=X1Z+X2Z+X3Z*0.5
479              X4=X1Z+X2Z+X3Z+X4Z*0.5
480              Y1=SINTER(2)
481              Y2=SINTER(4)
482              Y3=SINTER(6)
483              Y4=SINTER(8)
484              CALL CUBIC(X1,X2,X3,X4,Y1,Y2,Y3,Y4,CCC)
485              SINTER(1)=CCC
486              DO 283 I=1,4
487              IYX=NC+1+(I-1)*LX
488              IYY=IYX+1
489              IYZ=IYY+1
490              IYA=IYZ+1
491              Y1=SIGMA(IYX,2,1)
492              Y2=SIGMA(IYY,2,1)
493              Y3=SIGMA(IYZ,2,1)
494              Y4=SIGMA(IYA,2,1)
495              CALL CUBIC(X1,X2,X3,X4,Y1,Y2,Y3,Y4,CCC)
496              J=2*LX+2+I
497              SINTER(J)=CCC
498          283 CONTINUE
499              IPX=NC+1
500              IPY=IPX+LX
501              IPZ=IPY+LX
502              IPA=IPZ+LX
503              X1Z=ELY(IPX)
504              X2Z=ELY(IPY)
505              X3Z=ELY(IPZ)
506              X4Z=ELY(IPA)
507              X1=X1Z*0.5
508              X2=X1Z+X2Z*0.5
509              X3=X1Z+X2Z+X3Z*0.5
510              X4=X1Z+X2Z+X3Z+X4Z*0.5
511              IYX=2*LX+3
512              IYY=IYX+1
513              IYZ=IYY+1
514              IYA=IYZ+1
515              Y1=SINTER(IYX)
516              Y2=SINTER(IYY)
517              Y3=SINTER(IYZ)



518              Y4=SINTER(IYA)
519              CALL CUBIC(X1,X2,X3,X4,Y1,Y2,Y3,Y4,CCC)
520              J=2*LX+2
521              SINTER(J)=CCC
522              SINTER(3)=0.0
523              SINTER(5)=0.0
524              WRITE(6,2055)
525         2055 FORMAT(1H1,'STRESS ALONG WALL-BEAM INTERFACE'///)
526              J=2*LX+1
527              DO 281 I=1,J
528              WRITE(6,2056) I,SINTER(I)
529         2056 FORMAT(I5,4X,E15.6/)
```

```
530      281 CONTINUE
531          WRITE(6,2057)
532     2057 FORMAT (////' STRESS UP WALL BOUNDARY'//)
533          DO 284 I=1,5
534          J=2*LX+1+I
535          WRITE(6,2058)I,SINTER(J)
536     2058 FORMAT(I5,4X,E15,6)
537      284 CONTINUE
538          CALL INTERP(X1,X2,X3,Y1,Y2,Y3,CCC)
539          WRITE(6,2059)CCC
540     2059 FORMAT(////(X,E15,6)
541          NREP=0
542          NAAB=1+MDN=MDNA
543          DO 240 II=NAAB,LX
544          I=(2*LX+3-2*II)
545          J=(2*LX+2-2*II)
546          IF((SINTER(I),LT,0,0),OR,(SINTER(J),LT,0,0))GO TO 241
547          GO TO 242
548      241 MDNN=MDNN+1
549      240 CONTINUE
550      242 IF (MDNN=MDNA) 243,244,244
551      243 NREP=1
552      244 MDNA=MDNN
553          IF (KT,EQ,0) GO TO 245
554          IT2=IT+LX
555          DD=ELY(IT)+ELY(IT2)
556          TD=ELZ(IT)
557          ZZ=TD*DD*DD/6
558          WRITE(6,2040)ZZ
559     2040 FORMAT(1H1,'SECTION MODULUS =',F15,1)
560          WRITE(6,2041)
561     2041 FORMAT(////' BOTTOM ELEMENT      TIE            MOMENT          BOTT
562         TOM MOM,     TOP MOM,'//)
563          DO 290 I=IT,JT
564          S1=SIGMA(I,1,1)
565          J=I+LX
566          S2=SIGMA(J,1,1)
567          AM=2*WT/(DD*TD*(S1+S2))
568          BM=WT*TL/(ZZ*(S1-S2))
569          CM=WT*TL/(ZZ*(S1+(S1-S2)/2))
570          DM=WT*TL/(ZZ*(S2+(S2-S1)/2))
571          WRITE(6,2042)I,AM,BM,CM,DM
572     2042 FORMAT(I8,F16,3,3F10,1)
573      290 CONTINUE
574      245 CONTINUE
575          RETURN
576          END


577
578
579
580          SUBROUTINE INTERP(X1,X2,X3,Y1,Y2,Y3,C)
581          B=((Y2-Y1)*(X3-X1)-(Y3-Y1)*(X2-X1))/((X2-X1)*(X3-X1)*(X2-X3))
582          A=(Y2-Y1)/(X2-X1)-B*(X2+X1)
583          C=Y1-A*X1-B*X1*X1
584          RETURN
585          END
586
587
588
```

```
589          SUBROUTINE CUBIC(X1,X2,X3,X4,Y1,Y2,Y3,Y4,D)
590          RRR=X3*X3+X1*X2-X1*X3-X2*X3
591          SSS=X4*X4+X1*X2-X1*X4-X2*X4
592          ACC=Y3-Y1-(Y2-Y1)*(X3-X1)/(X2-X1)
593          BCC=Y4-Y1-(Y2-Y1)*(X4-X1)/(X2-X1)
594          DCC=X3**3-X1**3-(X2*X2-X1*X2+X1*X1)*(X3-X1)
595          ECC=X4**3-X1**3-(X2*X2+X1*X2+X1*X1)*(X4-X1)
596          C=(BCC/SSS-ACC/RRR)/(ECC/SSS-DCC/RRR)
597          B=(ACC-C*DCC)/RRR
598          A=(Y2-Y1)/(X2-X1)-B*(X2*X2-X1*X1)/(X2-X1)-C*(X2**3-X1**3)/(X2-X1)
599          D=Y1-A*X1-B*X1*X1-C*X1**3
600          RETURN
601          END
602
603
604
605          SUBROUTINE FLMAT(S,A,B,C,EE,VV)
606          DIMENSION S(8,8)
607          V=VV
608          E=EE/(1.0-V*V)
609          W=V
610          UW1=0.5*(1.0-V)
611          U=UW1
612          AB=A*B
613          D=E*C/AB
614          F=W*U
615          G=W-U
616          Y2=B*B
617          X2=A*A
618          XU=U*X2
619          YU=U*Y2
620          DO 150 I=1,7,2
621      150 S(I,I)=D*(Y2+XU)/3.0
622          DO 151 I=2,8,2
623      151 S(I,I)= D*(X2+YU)/3.0
624          S(1,2), S(4,7), S(3,6) =D*F*AB*0.25
625          S(3,8)=S(1,2)
626          S(1,3),S(5,7)=D*(XU-2*Y2)/6.0
627          S(1,4),S(2,7),S(5,8),S(3,8)=D*G*AB*0.25
628          S(1,5),S(3,7)=-0.5*S(1,1)
629          S(1,6),S(2,5),S(3,4),S(7,8)=-S(1,2)
630          S(1,7), S(5,5) =D*(Y2-2*XU) /6.0
631          S(1,8),S(2,3),S(4,5),S(6,7)=-S(1,4)
632          S(2,4),S(6,8)=D*(X2-2*YU)/6.0
633          S(2,6),S(4,8)=-0.5*S(2,2)
634          S(2,8),S(4,6)=D*(YU-2*X2)/6.0
635          DO 152 I= 1,8



636          DO 152 J= 1,I
637      152 S(I,J)=S(J,I)
638          RETURN
639          END
640
641
642
643          SUBROUTINE STRESSMAT(G,X,Y,A,B,C,E,V)
644          DIMENSION G(3,8)
645          DO 100 I=1,3
646          DO 100 J=1,8
647      100 G(I,J)=0.0
```

```
648         E1=E   /A/B/(1.0-V*V)
649         P=(4.0-3.0*V*V)*E1
650         Q=(3.0*V*V-2.0)*E1
651         H1=V*E1
652         H2=0.5*E   /A/B/(1.0*V)
653         G2=2.0*P*Q
654         G1=P*2.0*Q
655         A2=A*G2/6.0
656         A1=A*G1/6.0
657         B2=B*G2/6.0
658         B1=B*G1/6.0
659         G(1,1)=-B2*(1.0*Y)*B1*Y
660         G(1,2)=-0.5*H1*A
661         G(1,3)=-G(1,1)
662         G(1,4)=G(1,2)
663         G(1,5)=B1*(1.0*Y)*B2*Y
664         G(1,6)=-G(1,2)
665         G(1,7)=-G(1,5)
666         G(1,8)=G(1,6)
667         G(2,1)=-0.5*H1*B
668         G(2,2)=-A2*(1.0*X)*A1*X
669         G(2,3)=-G(2,1)
670         G(2,4)=-A1*(1.0*X)*A2*X
671         G(2,5)=G(2,3)
672         G(2,6)=-G(2,4)
673         G(2,7)=G(2,1)
674         G(2,8)=-G(2,2)
675         G(3,1)=-0.5*H2*A
676         G(3,2)=-0.5*H2*B
677         G(3,3)=G(3,1)
678         G(3,4)=-G(3,2)
679         G(3,5)=-G(3,1)
680         G(3,6)=G(3,4)
681         G(3,7)=G(3,5)
682         G(3,8)=G(3,2)
683         RETURN
684         END
685
686         FINISH
```

APPENDIX B : INFILLED FRAME COMPUTER PROGRAM

SCOPE: The computer program was used to analyse infilled frame problems.

FACILITIES:
1. Concentrated loads can be applied at nodal points.

2. Non-zero displacements can be applied at nodes.

3. Generation of node and element connectivity is achieved automatically.

4. Any number of infilled frames can be connected together and frames can be left unfilled if required.

5. Either friction or no friction connections can be made on the infill-frame boundaries and separation cracking on these boundaries is automatically generated.

OUTPUT:
Printing of input data.

Element connectivity.

Displacements at nodal points.

Stresses at element centroids.

Stresses at nodal points.

Stresses on connected nodes on infill-frame boundaries.

DATA INPUT INSTRUCTIONS:

A. Problem number card (I2)

Column	Variable name	Description
1-2	NO	Problem number

B. Problem description card (10 I3)

1-3	NEL	Number of elements
4-6	NN	Number of nodes
7-9	NRN	Number of restraints or applied displacements

10-12	NLOADC	Set to 1
13-15	NTYPE	" " "
16-13	LX	Number of elements in x-direction + number of infill-frame vertical boundaries
19-21	LY	Number of elements in y-direction + number of infill-frame horizontal boundaries
22-24	INN	Set to 1
25-27	IEN	" " "
28-30	MDN	Number of nodes in x-direction

C. Element dimensions in x-direction cards (F8.2) (LX cards)

| 1-8 | DLX(I) | Horizontal dimensions of elements in order from left. Insert zero for every infill-frame boundary to indicate its position |

D. Element dimensions in y-direction cards (F8.2) (LY cards)

| 1-8 | DLY(I) | Vertical dimensions of elements in order from bottom. Insert zero for every infill-frame boundary to indicate its position |

E. Material properties card (7 F6.2)

1-6	DZ	Thickness of elements
7-12	EB	Brick or wall modulus of elasticity, E_b
13-18	VB	Brick or wall Poisson's ratio ν_b
19-24	ER	Ratio E_m/E_b, (E_m = mortar modulus of elasticity) (Set to 1 if homogeneous wall)
25-30	VR	Ratio ν_m/ν_b, (ν_m = mortar Poisson's ratio)(Set to 1 if homogeneous wall)
31-36	EC	Frame modulus of elasticity
37-42	VC	Frame Poisson's ratio

F. <u>Number of mortar elements per row cards</u> (I3) (Cards = number of rows of elements)

1-3	NER	Number of mortar elements in each horizontal row in order from bottom (Blank card if homogeneous wall) (Repeated with G cards if non homogeneous wall)

G. <u>Mortar element position cards</u> (I3) (NER cards, required only if $0 <$ NER $<$ number of columns of elements

1-3	NERP	Mortar element position, referenced to the lowest row of elements

H. <u>Number of rows of air space card</u> (I3)

1-3	K	Number of horizontal rows of air space elements

I. <u>Air space element position cards</u> (2 I3)(K cards)

1-3	L	First element of air space of row considered
4-6	M	Last element of air space of row considered

J. <u>Number of rows of beams card</u> (I3)

1-3	K	Number of horizontal rows of beam elements

K. <u>Beam element position cards</u> (2 I3) (K cards)

1-3	L	First element of beam of row considered
4-6	M	Last element of beam of row considered

L. <u>Number of columns of vertical frame members card</u> (I3)

1-3	K	Number of columns of vertical frame member elements

M. <u>Vertical frame member position cards</u> (2 I3) (K cards)

1-3	L	Bottom element of vertical frame member of column considered
4-6	M	Top element of vertical frame member of column considered

N. <u>Horizontal frame-infill boundary card</u> (4 I3)

1-3	MJX	Total number of node pairs to be connected on horizontal joints
4-6	MSX	Number of node pairs to be considered for separation
7-9	MSIX	Number of MSX node pairs with bottom node in infill
10-12	NFRX	Whether friction connection required 1 = Yes 2 = No

O. <u>Horizontal boundary node pair cards</u> (I3) (MJX cards)

1-3	NJX (I)	Bottom node number of pairs to be joined on horizontal joints. MSIX node pairs first followed by other node pairs to be considered for separation. Finally permanently connected node pairs (Frame member joints)

P. <u>Vertical frame-infill boundary card</u> (4 I3)

1-3	MJY	Total number of node pairs to be connected on vertical joints
4-6	MSY	Number of node pairs to be considered for separation
7-9	MSIY	Number of MSY node pairs with left hand node in infill
10-12	NFRY	Whether friction connection required. 1 = Yes 2 = No

Q. <u>Vertical boundary node pair cards</u> (I3) (MJY cards)

1-3	NJY(I)	Left hand node of pairs to be joined on vertical joints. MSIY node pairs first, followed by other node pairs to be considered for separation. Finally permanently connected node pairs (frame member joints)

R. <u>Number of applied loads card</u> (I3)

1-3	NALOAD	Number of applied loads

S. <u>Load information cards</u> (2 I3, F8.3) (NALOAD cards)

1-3	N1	Node number at which load is applied
4-6	N2	Direction of load, 1 = x-direction 2 = y-direction
7-14	E3	Magnitude of load

T. <u>Restraint or applied displacements cards</u> (2 I3, F10.7) (NRN cards)

    1-3   N1   Node number at which restraint or displacement
                                is applied

    4-6   N2   Direction of restraint or displacement,
                                1 = x-direction
                                2 = y-direction

    7-16   DISP   Magnitude of displacement. If restraint,
                                leave blank

```
      1          LIST LP
      2          PROGRAM (G2PN)
      3          EXTENDED DATA
      4          INPUT 5 =CR0
      5          OUTPUT 6 = LP0
      6          USE 1=ED1
      7          USE 8=ED2
      8          COMPRESS INTEGER AND LOGICAL
      9          END
     10   C
     11   C
     12
     13
     14
     15          MASTER  FEMSA
     16          COMMON /CDATA/NEL,NN,NRN,NLOADC,NTYPE,NEN,NND,NBW,MDN,NNS
     17         1,MDNA,MDNN,NREP,NC,LX,MJX,MJY,MSX,MSY,MS1X,MS1Y,NFRX,NFRY
     18          COMMON/CEL/ELX(520),ELY(520),ELZ(520),EEE(520),VVV(520)
     19          COMMON/CEST/NCON(540,4),NR(95),ALOAD(1500,2),U(1500)
     20         1,NJX(110),NJY(110)
     21        1 READ (5,2000) NO
     22     2000 FORMAT (I2)
     23          IF (NO.EQ.0) GO TO 2
     24          WRITE (6,2081)   NO
     25     2081 FORMAT (1H1,40X,'PROBLEM NO.=',I2//)
     26          CALL   SETUP
     27      299 CONTINUE
     28          CALL   ASSEMBLE
     29          CALL   STRESSES
     30          IF(NREP.EQ.1)GOTO299
     31          GO TO  1
     32        2 STOP
     33          END
     34   C
     35   C
     36
     37   C
     38   C
     39   C
     40
     41
     42
     43




     44
     45
     46
     47          SUBROUTINE  SETUP
     48          COMMON /CDATA/NEL,NN,NRN,NLOADC,NTYPE,NEN,NND,NBW,MDN,NNS
     49         1,MDNA,MDNN,NREP,NC,LX,MJX,MJY,MSX,MSY,MS1X,MS1Y,NFRX,NFRY
     50          COMMON/CEL/ELX(520),ELY(520),ELZ(520),EEE(520),VVV(520)
     51          COMMON/CEST/NCON(540,4),NR(95),ALOAD(1500,2),U(1500)
     52         1,NJX(110),NJY(110)
     53          DIMENSION DLX(50),DLY(50)
     54          READ(5,2001)NEL,NN,NRN,NLOADC,NTYPE,LX,LY,INN,IEN,MDN
     55     2001 FORMAT( 10I3)
     56          DO 900 I=1,LX
     57          READ (5,9000) DLX(I)
```

```
58    9000 FORMAT (F8.2)
59     900 CONTINUE
60         DO 901 I=1,LY
61         READ (5,9001) DLY(I)
62    9001 FORMAT (F8.2)
63     901 CONTINUE
64         JTH=LX*LY
65         KTH=1
66         K=1
67      50 IYTH=(KTH-1)/LX+1
68         IXTH=KTH-LX*(IYTH-1)
69         DLXT=DLX(IXTH)
70         DLYT=DLY(IYTH)
71         IF(DLXT.EQ.0.0)GOTO51
72         IF(DLYT.EQ.0.0)GOTO51
73         NCON(K,1)=((LX+1)*KTH-1)/LX
74         NCON(K,2)=NCON(K,1)+1
75         NCON(K,3)=NCON(K,2)+MDN
76         NCON(K,4)=NCON(K,1)+MDN
77         K=K+1
78      51 KTH=KTH+1
79         IF(KTH.EQ.JTH+1)GOTO52
80         GOTO50
81      52 J=1
82         LXTH=LX
83         DO921K=1,LXTH
84         DLXT=DLX(K)
85         IF(DLXT.EQ.0.0)GOTO922
86         DLX(J)=DLXT
87         J=J+1
88         GOTO921
89     922 LX=LX-1
90     921 CONTINUE
91         J=1
92         LYTH=LY
93         DO923K=1,LYTH
94         DLYT=DLY(K)
95         IF(DLYT.EQ.0.0)GOTO924
96         DLY(J)=DLYT
97         J=J+1
98         GOTO923
99     924 LY=LY-1
100    923 CONTINUE
101        READ(5,9002)DZ,EB,VB,ER,VR,EC,VC
102   9002 FORMAT(7F6.2)
103        DO 903 I=1,LY
104        DO 904 J=1,LX
105        K=(I-1)*LX+J
106        ELX(K)=DLX(J)
107        ELZ(K)=DZ
108        EEE(K)=EB
109        VVV(K)=VB
110    904 ELY(K)=DLY(I)
111        READ (5,9003) NER
112   9003 FORMAT (I5)
113        IF (NER.EQ.0) GO TO 903
114        IF (LX-NER) 906,906,905
115    905 DO 908 J=1,NER
116        READ (5,9004) NERP
```

```
117      9004 FORMAT (I3)
118           K=(I-1)*LX+NERP
119           EEE(K)=ER*EB
120           VVV(K)=VR*VB
121       908 CONTINUE
122           GO TO 903
123       906 DO 910 J=1,LX
124           K=(I-1)*LX+J
125           EEE(K)=ER*EB
126           VVV(K)=VR*VB
127       910 CONTINUE
128       903 CONTINUE
129           READ(5,9005)K
130      9005 FORMAT(I5)
131           IF (K.EQ.0) GO TO 916
132           DO 912 I=1,K
133           READ(5,9006)L,M
134      9006 FORMAT(3I3)
135           DO 913 J=L,M
136       913 EEE(J)=0.000001
137       912 CONTINUE
138       916 CONTINUE
139           READ(5,9005)K
140           DO 914 I=1,K
141           READ(5,9006)L,M
142           DO 915 J=L,M
143           EEE(J)=EC
144       915 VVV(J)=VC
145       914 CONTINUE
146           READ(5,9005)K
147           DO917I=1,K
148           READ(5,9006)L,M
149           DO918J=L,M,LX
150           EEE(J)=EC
151       918 VVV(J)=VC
152       917 CONTINUE
153           READ(5,9007)MJX,MSX,MS1X,NFRX
154           DO919I=1,MJX
155       919 READ(5,9005)NJX(I)
156           READ(5,9007)MJY,MSY,MS1Y,NFRY
157           DO920I=1,MJY
158       920 READ(5,9005)NJY(I)
159           NEN=4
160           NND=2
161      9007 FORMAT(4I3)
162
163           WRITE (6,2004)
```

```
164      2004 FORMAT(35X,'FINITE ELEMENT  2-D  ANALYSIS'//)
165           WRITE (6,2005) NEL,NN,NRN,NLOADC
166      2005 FORMAT(5X,'NO OF RECTANGULAR ELEMENTS            ',I5/
167          1 5X,'NO OF NODES                           ',I5/
168          2 5X,'NO OF RESTRAINTS                      ',I5/
169          3 5X,'NO OF APPLIED LOAD CASES              ',I5/)
170           IF (NTYPE-1)54,54,55
171        54 WRITE (6,2006)
172           GO TO 56
173        55 WRITE (6,2007)
174        56 CONTINUE
175      2006 FORMAT (5X,' PLANE STRESS'//)
```

```
176      2007 FORMAT (5X,' PLANE STRAIN'//)
177           IF(NFRX.EQ.2)GOTO70
178           WRITE(6,2020)
179      2020 FORMAT(5X,' SHEAR CONNECTION ON HORIZONTAL INFILL BOUNDARIES'/)
180           GOTO71
181       70 WRITE(6,2021)
182      2021 FORMAT(5X,' NO SHEAR CONNECTION ON HORIZONTAL INFILL BOUNDARIES'/)
183       71 IF(NFRY.EQ.2)GOTO72
184           WRITE(6,2022)
185      2022 FORMAT(5X,' SHEAR CONNECTION ON VERTICAL INFILL BOUNDARIES'//)
186           GOTO73
187       72 WRITE(6,2023)
188      2023 FORMAT(5X,' NO SHEAR CONNECTION ON VERTICAL INFILL BOUNDARIES'//)
189       73 CONTINUE
190           WRITE(6,2008)
191      2008 FORMAT(/10X,'CONNECTIVITY AND DIMENSIONS OF RECTANGULAR
192          1ELEMENTS'//5X,'EL.NO',4(5X,'NODE'),10X,'X',10X, 'Y',10X,
193          2'T',10X,'E',10X,
194          3'V'/ 16X,'1',8X,'2',8X,'3',8X,'4'/)
195           NNN=2*NN
196           DO  57 I=1,NEL
197           WRITE (6,2009) I,(NCON(I,J),J=1,4),ELX(I),ELY(I),ELZ(I),EEE(I),
198          2VVV(I)
199       57 CONTINUE
200      2009 FORMAT (I9   ,4(I9),/X,5(F11,6))
201           DO 60 I=1,NNN
202           DO 60 J=1,NLOADC
203           U(I)=0.0
204       60 ALOAD(I,J)=0
205           WRITE (6,2010)
206      2010 FORMAT (1H1,5X,'APPLIED LOAD'///)
207           DO 58 I=1,NLOADC
208           READ (5,2100) NALOAD
209      2100 FORMAT (I3)
210           WRITE (6,2200) I
211      2200 FORMAT(/' LOAD CASE ',I5//5X,'NODE NO,',5X,'SENSE',
212          15X, 'MAGNITUDE'/)
213           DO 58 J=1,NALOAD
214           READ(5,2011)N1,N2,ES
215      2011 FORMAT ( 2I3, F8 ,2 )
216           L=(N1-1)*2+N2
217           ALOAD(L,I)=ES
218       58 WRITE (6,2012) N1,N2,ALOAD(L,I)
219      2012 FORMAT(2I10,9X,F10,5)
220           WRITE (6,2013)
221      2013 FORMAT(1H1,5X,'RESTRAINED NODES'// 5X,'NODE NO,',5X,'SENSE'/)
222           K=0

223           DO 59 I=1,NRN
224           READ (5,2014) N1,N2,DISP
225           WRITE (6,2015)N1,N2,DISP
226           L=(N1-1)*2+N2
227           K=K+1
228           NR(K)=L
229           U(L)=DISP
230       59 CONTINUE
231      2014 FORMAT(2I3,F10,7)
232      2015 FORMAT(2I10,F20,7)
233           NEN1=NEN-1
234           NBW2= 0
```

```
235            DO 61 I=1,NEL
236            DO 61 J=1,NEN1
237            JJ=J+1
238            DO 61 K=JJ,NEN
239            NBW1=NCON(I,J)-NCON(I,K)
240            IF(NBW1)62,62,63
241         62 NBW1=-NBW1
242         63 IF(NBW1-NBW2) 61,61,64
243         64 NBW2=NBW1
244         61 CONTINUE
245            NBW=(NBW2+1)*NND*2-1
246            WRITE(6,2016)NBW
247       2016 FORMAT(//' BAND WIDTH = ', I2//)
248            NN2=2*NN
249            DO 69 I=1,NN2
250         69 ALOAD(I,2)=ALOAD(I,1)
251            MDNA=MDN
252            MDNN=MDN
253            RETURN
254            END
255
256
257
258
259
260
261
262
263
264            SUBROUTINE ASSEMBLE
265            COMMON /CDATA/NEL,NN,NRN,NLOADC,NTYPE,NEN,NND,NBW,MDN,NNS
266           1,MDNA,MDNN,NREP,NC,LX,MJX,MJY,MSX,MSY,MS1X,MS1Y,NFRX,NFRY
267            COMMON/CEL/ELX(520),ELY(520),ELZ(520),EEE(520),VVV(520)
268            COMMON/CEST/NCON(520,4),NR(95),ALOAD(1500,2),U(1500)
269           1,NJX(110),NJY(110)
270            COMMON/CSKA/S(2200)
271            DIMENSION ST(8,8)
272            DIMENSION RLOAD(1500)
273            DAA=10000000.0
274            NNN=NN*NND
275            DO 2082 JC=1,NLOADC
276            DO 2083 II=1,NNN
277       2083 RLOAD(II)=ALOAD(II,2)
278
279            REWIND 1
280            NHBW=(NBW+1)/2
281            NB=NHBW/NND+1
282            MHBW=NHBW-1
283            NNN=NN*NND
284            LMAX=2200
285            LEQPB=LMAX/NHBW
286            LNPBL=LEQPB/NND
287            NEQPB=LNPBL
288            MUMBL=(NN-1)/LNPBL+1
289      C
290      C     FORM STIFFNESS MATRIX
291      C
292            DO 3110 III=1,MUMBL
293            DO 3154 MN=1,LMAX
```

```
294   5154 S(MM)=0.0
295        ISTART=(III-1)*NEQPB*NND
296        ICOUNT=NEQPB*NND
297        IF(III.EQ.MUMBL)ICOUNT=NNN-(III-1)*NEQPB*NND
298        N1=ISTART+1
299        N2=ISTART+ICOUNT
300        JSTART=(III-1)*NEQPB
301        JCOUNT=NEQPB
302        IF(III.EQ.MUMBL)JCOUNT=NN-(III-1)*NEQPB
303        NN1=JSTART+1
304        NN2=JSTART+JCOUNT
305        NN1=NN1-NB
306        NN2=NN2+NB
307        DO 5211 JJJ=1,NEL
308        KTEST=0
309        DO 3111 L=1,NEN
310        IF((NCON(JJJ,L).GT.NN2).OR.(NCON(JJJ,L).LT.NN1))GO TO 3111
311        DO 3111 J=1,NEN
312        IF((NCON(JJJ,J).GT.NN2).OR.(NCON(JJJ,J).LT.NN1))GO TO 3111
313        M1=(NCON(JJJ,J)-1)*NND
314        M2=(NCON(JJJ,L)-1)*NND
315        M3=(J-1)*NND
316        M4=(L-1)*NND
317        IF(KTEST)3220,3220,3221
318   3220 CONTINUE
319        V=VVV(JJJ)
320        E=EEE(JJJ)
321        A=ELX(JJJ)
322        B=ELY(JJJ)
323        C=ELZ(JJJ)
324        CALL FLMAT(ST,A,B,C,E,V)
325        KTEST=1
326   3221 CONTINUE
327        DO 3111 N=1,NND
328        DO 3111 M=1,NND
329        JJ=M2+N
330        IF(JJ.LT.N1)GO TO 3111
331        IF(JJ.GT.N2)GO TO 3111
332        JJ=JJ-N1+1
333        IF((M1+M).GT.JJ)GO TO 3111
334        I1=M3+M
335        J1=M4+N
336        II=JJ-M1-M+1
337        IF(II.GT.NHBW)GO TO 3111
338        KK=II+(IJ-1)*NHBW
339        S(KK)=S(KK)+ST(I1,J1)
340   3111 CONTINUE


341   5211 CONTINUE
342   C
343   C    PUT RESTRAINTS
344   C    EQUAL DISPLACEMENTS
345        DO515J=1,MJX
346        IF(NJX(J).LE.0)GOTO515
347        KNN1=NJX(J)*2
348        KNN2=KNN1+MDN*2
349        KNN3=KNN1-1
350        KNN4=KNN2-1
351        KNN5=(NBW+1)/2
352        KNN6=KNN5+KNN1-KNN6
```

```
353        KNN7=KNN5+KNN5-KNN4
354        LN1=(KNN1-N1)*NHBW+1
355        LN2=(KNN2-N1)*NHBW+1
356        LN3=(KNN3-N1)*NHBW+1
357        LN4=(KNN4-N1)*NHBW+1
358        LN6=LN2+NHBW-KNN6
359        LN7=LN4+NHBW-KNN7
360        IF((KNN1.GE.N1).AND.(KNN1.LE.N2))S(LN1)=S(LN1)+DAA
361        IF((KNN2.GE.N1).AND.(KNN2.LE.N2))S(LN2)=S(LN2)+DAA
362        IF((KNN2.GE.N1).AND.(KNN2.LE.N2))S(LN6)=S(LN6)+DAA
363        IF((J.LE.MSX).AND.(NFRX.EQ.2))GOTO313
364        IF((KNN3.GE.N1).AND.(KNN3.LE.N2))S(LN3)=S(LN3)+DAA
365        IF((KNN4.GE.N1).AND.(KNN4.LE.N2))S(LN4)=S(LN4)+DAA
366        IF((KNN4.GE.N1).AND.(KNN4.LE.N2))S(LN7)=S(LN7)+DAA
367    313 CONTINUE
368        DO314J=1,MJY
369        IF(NJY(J).LE.0)GOTO314
370        KNN1=NJY(J)*2
371        KNN2=KNN1+2
372        KNN3=KNN1-1
373        KNN4=KNN2-1
374        KNN5=(NBW+1)/2
375        KNN6=KNN5+KNN1-KNN6
376        KNN7=KNN5+KNN5-KNN4
377        LN1=(KNN1-N1)*NHBW+1
378        LN2=(KNN2-N1)*NHBW+1
379        LN3=(KNN3-N1)*NHBW+1
380        LN4=(KNN4-N1)*NHBW+1
381        LN6=LN2+NHBW-KNN6
382        LN7=LN4+NHBW-KNN7
383        IF((KNN3.GE.N1).AND.(KNN3.LE.N2))S(LN3)=S(LN3)+DAA
384        IF((KNN4.GE.N1).AND.(KNN4.LE.N2))S(LN4)=S(LN4)+DAA
385        IF((KNN4.GE.N1).AND.(KNN4.LE.N2))S(LN7)=S(LN7)+DAA
386        IF((J.LE.MSY).AND.(NFRY.EQ.2))GOTO314
387        IF((KNN1.GE.N1).AND.(KNN1.LE.N2))S(LN1)=S(LN1)+DAA
388        IF((KNN2.GE.N1).AND.(KNN2.LE.N2))S(LN2)=S(LN2)+DAA
389        IF((KNN2.GE.N1).AND.(KNN2.LE.N2))S(LN6)=S(LN6)+DAA
390    314 CONTINUE
391  C
392        LCHECK=(N2-N1+1)*NHBW
393        DO 3115 KKK=1,NRN
394        KR=NR(KKK)
395        RLOAD(KR)=U(KR)
396        LC2=(N2-N1)*NHBW+1
397        KR2=KR
398        KR1=KR
399        NC=KR-N1+1

400        IF(KR.GT.N2)GO TO 3115
401        IF(KR-N1)3118,3117,3117
402   3117 LC=(KR-N1)*NHBW+1
403        LR=LC
404        S(LC)=1.0
405        DO 3119 NJ=2,NHBW
406        LC=LC+1
407        KR1=KR1-1
408        IF(KR1.LE.0)GO TO 3119
409        RLOAD(KR1)=RLOAD(KR1)-S(LC)*U(KR)
410   3119 S(LC)=0.0
411        DO 3120 NI=1,MHBW
```

```
412          KR2=KR2+1
413          LR=LR+NHBW+1
414          IF(LR.GT.(LC2+MHBW))GO TO 3120
415          RLOAD(KR2)=RLOAD(KR2)-S(LR)*U(KR)
416          S(LR)=0.0
417    3120 CONTINUE
418          GO TO 3115
419    3118 IF((N1-KR).GT.MHBW)GO TO 3115
420          LCC=N1-KR+1
421          MC=NHBW-N1+KR
422          DO 3122 MI=1,MC
423          IF(LCC.GT.LCHECK)GO TO 3122
424          KR3=(LCC-1)/NHBW+N1
425          IF(KR3.GE.N1)RLOAD(KR3)=RLOAD(KR3)-S(LCC)*U(KR)
426          S(LCC)=0.0
427          LCC=LCC+NHBW+1
428    3122 CONTINUE
429    3115 CONTINUE
430    C
431    C     WRITE STIFFNESS MATRIX INTO TAPE
432    C
433          L1=1
434          L2=NHBW
435          DO 3130 N=1,ICOUNT
436          WRITE(1) (S(I),I=L1,L2)
437          L1=L1+NHBW
438    3130 L2=L2+NHBW
439    3110 CONTINUE
440          CALL SOLVE(NNN,NHBW,RLOAD)
441
442          DO 2084 II=1,NNN
443    2084 ALOAD(II,JC)=RLOAD(II)
444    2082 CONTINUE
445          RETURN
446          END
447
448
449          SUBROUTINE SOLVE(NN,MM,R)
450          COMMON/CSKA/A(2200)
451          DIMENSION ND(200),F(520),X(2304),ALT(1)
452          DIMENSION R(NN)
453
454          NR=NN-1
455          NM=NN-MM
456          NN1=NN+1
457          MM1=MM+1
458          NC=2300/MM
```

```
459          NW=NC*MM
460          NREC1=(NN+NC-2)/NC-1
461
462    C     DECOMPOSITION OF BAND MATRIX
463    C
464          DO 110 J=1,MM
465    110  ND(J)=(J*(J+1))/2
466    C
467    C     SET UP FIRST TRIANGULAR BLOCK IN A
468    C
469          REWIND 1
470          REWIND 8
```

```
471              DO 150 N=1,MM
472              LC1=ND(N)-N+1
473              LC2=LC1+MM-1
474         150  READ(1)(A(I),I=LC1,LC2)
475              NX=0
476              NTRACK=1
477              NUMX=0
478              DO 200 N=1,NR
479       C
480       C      TRIANGLE IS SIMULTANEOUSLY REDUCED AND SHIFTED
481       C      PIVOTS AND MULTIPLIERS ARE TRANSFERRED TO X
482       C
483              MR=MINO(MM,NN1-N)
484              JJ=NX*MM+1
485              NX=NX+1
486              PIVOT=A(1)
487              X(JJ)=PIVOT
488              DO 150 J=2,MR
489              L=ND(J)
490         150  F(J)=A(L)
491              DO 160 J=2,MR
492              C=F(J)/PIVOT
493              JJ=JJ+1
494              X(JJ)=C
495              L=ND(J)
496              L1=ND(J-1)+1
497              DO 160 I=2,J
498              L=L-1
499              L1=L1-1
500         160  A(L1)=A(L)-C*F(I)
501              IF(N-NM)191,191,190
502       C
503       C      STORE NEXT COLUMN
504       C
505         191  READ(1)(A(I),I=LC1,LC2)
506         190  IF(NX-NC)200,201,201
507       C
508       C      'NC'REDUCED ROWS ARE WRITTEN ON 'NBUFF' DISK TRACKS
509       C
510         201  WRITE(8)(X(LX),LX=1,NW)
511              NUMX=NUMX+NW
512              NX=0
513         200  CONTINUE
514              JJ=NX*MM+1
515              X(JJ)=A(1)
516              WRITE(8)(X(LX),LX=1,JJ)
517              NUMX=NUMX+JJ



518       C
519       C
520       C      FORWARD REDUCTION
521       C
522         220  NTRACK=0
523              REWIND 8
524              NX=NC
525              DO 240 N=1,NR
526              MR=MINO(MM,NN1-N)
527              IF(NX-NC)250,229,269
528         229  IF(NUMX-NW)228,231,231
529         228  NW=NUMX
```

```
530.      251 READ(8)(X(LX),LX=1,NW)
531          NUMX=NUMX-NW
532          NX=0
533      250 JJ=NX*MM+1
534          NX=NX+1
535          C=R(N)
536          R(N)=C/X(JJ)
537          L1=N+1
538          L2=L1+MR-2
539          DO 240 I=L1,L2
540          JJ=JJ+1
541      240 R(I)=R(I)-C*X(JJ)
542          JJ=NX*MM+1
543          ALAST=X(JJ)
544          ALT(1)=ALAST
545          IF(NX-NC)235,232,232
546      232 READ(8)(ALT(LX),LX=1,1)
547      233 R(NN)=R(NN)/ALAST
548    C
549    C      BACK SUBSTITUTION
550    C
551          NW=NC*MM
552          BACKSPACE 8
553          IF(NX-NC)300,301,301
554      301 BACKSPACE 8
555          GO TO 312
556      300 NW=JJ
557      312 READ(8) (X(LX),LX=1,NW)
558          NW=NC*MM
559          NX=NN-NREC1*NC-1
560          DO 260 L=2,NN
561          N=NN1-L
562          MR=MINO(MM,L)
563          NX=NX-1
564          IF(NX)251,250,250
565      251 NTRACK=NTRACK-NBUFF
566          BACKSPACE 8
567          BACKSPACE 8
568          NW=NC*MM
569          READ(8)(X(LX),LX=1,NW)
570          NX=NC-1
571      250 JJ=NX*MM+1
572          L1=N+1
573          L2=L1+MR-2
574          DO 260 I=L1,L2
575          JJ=JJ+1
576      260 R(N)=R(N)-X(JJ)*R(I)


577          RETURN
578          END
579
580
581          SUBROUTINE   STRESSES
582          COMMON /CDATA/NEL,NN,NRN,NLOADC,NTYPE,NEN,NND,NBW,MDN,NNS
583         1,MDNA,MDNN,NREP,NC,LX,MJX,MJY,MSX,MSY,MS1X,MS1Y,NFRX,NFRY
584          COMMON/CEL/ELX(520),ELY(520),ELZ(520),EEE(520),VVV(520)
585          COMMON/CEST/NCON(520,4),NR(95),ALOAD(1500,2),U(1500)
586         1,NJX(110),NJY(110)
587          DIMENSION SIGMA(750,3,1)
588          DIMENSION B(3,8),D(8,1),STRESS(3,1)
```

```
589         DIMENSION NNEL(750,4),LNNO(750,4),NP(750)
590         DO 222 II=1,NEL
591         DO 222 JJ=1,5
592         DO 222 KK=1,NLOADC
593     222 SIGMA(II,JJ,KK)=0.0
594         X=0.5
595         Y=0.5
596         DO 204 NN1=1,NEL
597         DO 205 J=1,NEN
598         L1=(J-1)*NND+1
599         L2=(NCON(NN1,J)-1)*NND+1
600         DO 205 K=1,NND
601         DO 205 L=1,NLOADC
602         K1=K+L1-1
603         K2=K+L2-1
604         T=ALOAD (K2,L)
605     205 D(K1,L)= T
606         D1=ELX(NN1)
607         D2=ELY(NN1)
608         D3=ELZ(NN1)
609         V=VVV(NN1)
610         E=EEE(NN1)
611         CALL STRESSMAT(B,X,Y,D1,D2,D3,E,V)
612         DO  206  II=1,5
613         DO  206  JJ=1,NLOADC
614         S=0
615         DO 206  KK=1,8
616         S=S+B(II,KK)*D(KK,JJ)
617     206 STRESS(II,JJ)=S
618         DO  207  L=1,5
619         DO  207  K=1,NLOADC
620     207 SIGMA(NN1,L,K)=STRESS(L,K)
621     204 CONTINUE
622         DO 199 I=1,NLOADC
623         WRITE (6,2033)  I
624    2033 FORMAT(1H1,2X, 'LOAD CASE ', I3/)
625         WRITE (6,2050)
626    2050 FORMAT (1H0, 14H DISPLACEMENTS//
627        11X,'NODE NO.',10X,'X-DIRECTION',10X,'Y-DIRECTION'/)
628         DO  200 J=1,NN
629         J1=2*J-1
630         J2=2*J
631     200 WRITE (6,2051) J,ALOAD(J1,I), ALOAD(J2,I)
632    2051 FORMAT (I5,2(7X,E15,6))
633         WRITE (6,2052)
634    2052 FORMAT(1H1,20X,'STRESS AT THE CENTROID POINT OF THE ELEMENTS'//
635        1'EL.NO.',4X, 'SIGMA-X',9X,'SIGMA-Y',9X, 'SHEAR-STRESS',


636        2/X,'MAX.PR.STRESS'/X,'MIN.PR..STRESS',7X,'PR.ANGLE'/)
637         DO 208 K=1,NEL
638         P1= SIGMA(K,1,I)+SIGMA(K,2,I)
639         P2= SIGMA(K,1,I)-SIGMA(K,2,I)
640         P3=SIGMA(K,3,I)
641         A= SQRT(0.25*P2*P2+P3*P3)
642         PMAX= P1*0.5+A
643         PMIN= P1*0.5-A
644         IF(ABS(P2)-0.0000001) 209,209,210
645     209 A= 45
646         GO TO 211
647     210 A=ATAN(2*P3/P2)*90.0/3.14159265
```

```
648       211 CONTINUE
649       205 WRITE(6,2054) K,SIGMA(K,1,I),SIGMA(K,2,I), SIGMA(K,3,I),
650          1PMAX,PMIN, A
651      2054 FORMAT (I5,5X,5(E12,6,5X),F7,2)
652       199 CONTINUE
653           DO230I=1,NN
654           L=1
655           DO251J=1,NEL
656           DO251K=1,NEN
657           IF(NCON(J,K).NE.I)GOTO251
658           NNEL(I,L)=J
659           LNNO(I,L)=K
660           NP(I)=L
661           L=L+1
662       251 CONTINUE
663       250 CONTINUE
664           DO252II=1,NN
665           DO252JJ=1,3
666       252 SIGMA(II,JJ,1)=0,0
667           DO255I=1,NN
668           NCOUNT=NP(I)
669           DO234JJJ=1,NCOUNT
670           NN1=NNEL(I,JJJ)
671           NN2=LNNO(I,JJJ)
672           X=0,0
673           Y=0,0
674           IF((NN2.EQ.2).OR.(NN2.EQ.3))X=1,0
675           IF((NN2.EQ.3).OR.(NN2.EQ.4))Y=1,0
676           DO235J=1,NEN
677           L1=(J-1)*NND+1
678           L2=(NCON(NN1,J)-1)*NND+1
679           DO235K=1,NND
680           K1=K+L1-1
681           K2=K+L2-1
682           T=ALOAD(K2,1)
683       235 D(K1,1)=T
684           D1=ELX(NN1)
685           D2=ELY(NN1)
686           D3=ELZ(NN1)
687           V=VVV(NN1)
688           E=EEE(NN1)
689           CALL STRESSMAT(B,X,Y,D1,D2,D3,E,V)
690           DO236II=1,3
691           S=0,0
692           DO236KK=1,8
693           S=S+B(II,KK)*D(KK,1)
694       236 STRESS(II,1)=S


695           DO237L=1,3
696       237 SIGMA(I,L,1)=STRESS(L,1)/NCOUNT+SIGMA(I,L,1)
697       234 CONTINUE
698       233 CONTINUE
699           WRITE(6,9021)
700      9021 FORMAT(1H1,20X,'STRESS AT THE NODAL POINTS OF ELEMENTS'//
701          12X,'NODE NO,',5X,'SIGMA-X',11X,'SIGMA-Y',11X,'SHEAR-STRESS'/)
702           DO238K=1,NN
703           WRITE(6,9022)K,SIGMA(K,1,1),SIGMA(K,2,1),SIGMA(K,3,1)
704      9022 FORMAT(I5,5X,3(E15,6,5X))
705       238 CONTINUE
706           NREP=0
```

```
707         WRITE(6,2040)
708    2040 FORMAT(1H1,'  STRESSES ON JOINED NODES'///'  HORIZONTAL JOINTS'//
709        1'  NODE NO,    SIGMA-Y'/)
710         DO240I=1,MSX
711         NSA=NJX(I)
712         IF(NSA.LE.0)GOTO240
713         IF(I.LE.MS1X)GOTO241
714         NSA=NSA+MDN
715    241  J=NSA
716    242  WRITE(6,2041)J,SIGMA(J,2,1)
717    2041 FORMAT(I5,E18,6)
718         IF(SIGMA(J,2,1).LE.0,0)GOTO251
719         NREP=1
720         NSA=0
721    251  CONTINUE
722    253  NJX(I)=NSA
723         IF(I.LE.MS1X)GOTO254
724         NJX(I)=NJX(I)-MDN
725    254  CONTINUE
726    240  CONTINUE
727         WRITE(6,2043)
728    2043 FORMAT('  VERTICAL JOINTS'//'  NODE NO,    SIGMA-X'/)
729         DO255I=1,MSY
730         NSA=NJY(I)
731         IF(NSA.LE.0)GOTO255
732         IF(I.LE.MS1Y)GOTO256
733         NSA=NSA+1
734    256  J=NSA
735    257  WRITE(6,2041)J,SIGMA(J,1,1)
736         IF(SIGMA(J,1,1).LE.0,0)GOTO259
737         NREP=1
738         NSA=0
739    259  CONTINUE
740    260  NJY(I)=NSA
741         IF(I.LE.MS1Y)GOTO262
742         NJY(I)=NJY(I)-1
743    262  CONTINUE
744    255  CONTINUE
745         RETURN
746         END
747  C
748  C
749
750
751
752         SUBROUTINE FLMAT(S,A,B,C,EE,VV)
753         DIMENSION S(8,8)


754         V=VV
755         E=EE/(1.0-V*V)
756         W=V
757         UW1=0.5*(1.0-V)
758         U=UW1
759         AB=A*B
760         D=E*C/AB
761         F=W+U
762         G=W-U
763         Y2=B*B
764         X2=A*A
765         XU=U*X2
```

```
766            YU=U*Y2
767            DO 150 I=1,7,2
768     150 S(I,I)=D*(Y2+XU)/3.0
769            DO 151 I=2,8,2
770     151 S(I,I)=D*(X2+YU)/3.0
771            S(1,2), S(4,7), S(3,6) =D*F*AB*0.25
772            S(3,8)=S(1,2)
773            S(1,3),S(5,7)=D*(XU-2*Y2)/6.0
774            S(1,4),S(2,7),S(5,8),S(3,8)=D*G*AB*0.25
775            S(1,5),S(3,7)=-0.5*S(1,1)
776            S(1,6),S(2,5),S(3,4),S(7,8)=-S(1,2)
777            S(1,7), S(3,5) =D*(Y2-2*XU) /6.0
778            S(1,8),S(2,3),S(4,3),S(6,7)=-S(1,4)
779            S(2,4),S(6,8)=D*(X2-2*YU)/6.0
780            S(2,6),S(4,8)=-0.5*S(2,2)
781            S(2,8),S(4,6)=D*(YU-2*X2)/6.0
782            DO 152 I= 1,8
783            DO 152 J= 1,I
784     152 S(I,J)=S(J,I)
785            RETURN
786            END
787
788
789
790
791
792
793
794            SUBROUTINE STRESSMAT(G,X,Y,A,B,C,E,V)
795            DIMENSION G(3,8)
796            DO 100 I=1,3
797            DO 100 J=1,8
798     100 G(I,J)=0.0
799            E1=E  /A/B/(1.0-V*V)
800            P=(4.0-3.0*V*V)*E1
801            Q=(3.0*V*V-2.0)*E1
802            H1=V*E1
803            H2=0.5*E  /A/B/(1.0+V)
804            G2=2.0*P+Q
805            G1=P+2.0*Q
806            A2=A*G2/6.0
807            A1=A*G1/6.0
808            B2=B*G2/6.0
809            B1=B*G1/6.0
810            G(1,1)=-B2*(1.0-Y)-B1*Y
811            G(1,2)=-0.5*H1*A
812            G(1,3)=-G(1,1)
```

```
813            G(1,4)=G(1,2)
814            G(1,5)=B1*(1.0-Y)+B2*Y
815            G(1,6)=-G(1,2)
816            G(1,7)=-G(1,5)
817            G(1,8)=G(1,6)
818            G(2,1)=-0.5*H1*B
819            G(2,2)=-A2*(1.0-X)-A1*X
820            G(2,3)=-G(2,1)
821            G(2,4)=-A1*(1.0-X)-A2*X
822            G(2,5)=G(2,3)
823            G(2,6)=-G(2,4)
824            G(2,7)=G(2,1)
```

```
825        G(2,8)=-G(2,2)
826        G(3,1)=-0.5*H2*A
827        G(3,2)=-0.5*H2*B
828        G(3,3)=G(3,1)
829        G(3,4)=-G(3,2)
830        G(3,5)=-G(3,1)
831        G(3,6)=G(3,4)
832        G(3,7)=G(3,5)
833        G(3,8)=G(3,2)
834        RETURN
835        END
836        FINISH
```